COMPOSITE METAL POLYMER (CMP) FOR NON-STICK IMPROVEMENTS IN CHP PLANTS

KME-715

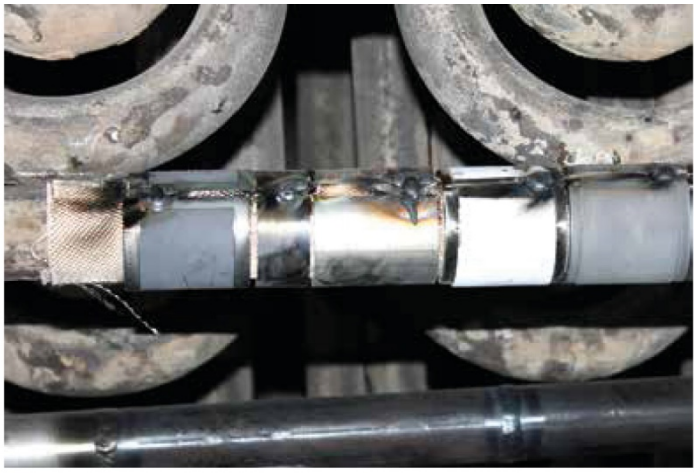

CONSORTIUM MATERIALS TECHNOLOGY
for thermal energy processes

KME
CONSORTIUM MATERIALS TECHNOLOGY
for thermal energy processes

Composite Metal Polymer (CMP) for non-stick improvements in CHP plants

KME-715

MATTI HUHTAKANGAS, MH ENGINEERING AB

RAGNA ELGER, SWEREA KIMAB AB
LEYLA WICKSTRÖM, SWEREA KIMAB AB
RIKARD NORLING, SWEREA KIMAB AB

ISBN 978-91-7673-094-2 | © 2018 ENERGIFORSK

Energiforsk AB | Phone: 08-677 25 30 | E-mail: kontakt@energiforsk.se | www.energiforsk.se

Preface

The project has been performed within the framework of the materials technology research programme KME, Consortium materials technology for thermal energy processes, period 2014-2018. The consortium is at the forefront of developing material technology to create maximum efficiency for energy conversion of renewable fuels and waste. KME has its sights firmly set on continuing to raise the efficiency of long-term sustainable energy as well as ensuring international industrial competitiveness.

KME was established 1997 and is a multi-cliental group of companies over the entire value chain, including stakeholders from the material producers, manufacturers of systems and components for energy conversion and energy industry (utilities), that are interested in materials technology research. In the current programme stage, eight industrial companies and 14 energy companies participate in the consortium. The consortium is managed by Energiforsk.

The programme shall contribute to increasing knowledge within materials technology and process technology development to forward the development of thermal energy processes for efficient utilisation of renewable fuels and waste in power and heat production. The KME goals are to bring about cost-effective materials solutions for improved fuel flexibility, improved operating flexibility, increased availability and power production with low environmental impact.

KME's activities are characterised by long term industry and demand driven research and constitutes an important part of the effort to promote the development of new energy technology with the aim to create value and an economic, environmentally friendly and long term sustainable energy society.

The industry has participated in the project through own investment (60 %) and the Swedish Energy Agency has financed the academic partners (40 %).

Bertil Wahlund, Energiforsk

Abstract

To reduce the amount of deposits in a heat- and power plant, a new concept of a composite surface layer already evaluated in the pulp and paper industry was examined.

The project examined a surface layer consisting of a thermally sprayed layer of a nickel-base material and a top coating with expected good release properties. While the nickel-base material was common for all samples, ten different top coatings were tested. The samples were exposed in wear tests and in plant exposures. As the top coatings had different temperature characteristics, different top coatings were exposed in different positions in the plant.

The wear tests indicate that wear at room temperature leaves a reasonable share of top coating on the surface of the samples. For the polymeric materials, the share was 50-60% after 10 h wear testing.

In furnace exposures, the PTFE-based top coating exposed in lower temperature areas shows the best behaviour in terms of coverage after exposure. No high temperature exposed top coatings could be detected after exposure. In the low-temperature areas, the amount of deposit was generally low. If the samples exposed in the low-temperature areas were compared with reference samples or surrounding tubes, no difference in deposit amount could be observed after exposure. In the high temperature regions, where the amount of deposit is much higher, there were signs that possibly the graphite based material had somewhat less deposit. Unfortunately, these samples were not photographed before demounting and the reduced amount is only an indication.

It is suggested that further research should be focused towards other top coatings especially in the high temperature areas where the deposit amount is substantial. Also, larger areas in the plant are suggested to be coated to visualise possible differences in the flow pattern and also to reduce the effect of edge effects.

Sammanfattning

Kraft- och värmeproduktion med biobränsle, returträ och olika slags avfall medför ofta kraftiga avlagringar på ytor i kraftvärmeverken. Det gör att värmeöverförande ytor blir mindre effektiva och mindre el och värme produceras i pannan. Det gör också att problemen med korrosion under beläggningarna ökar och att mer underhåll behövs jämfört med om inga avlagringar bildades. Om ytskiktet försvårade att avlagringar fick fäste, skulle det kunna minska mängden avlagringar. För energibolagen skulle detta ge ökad el- och värmeeffektivitet, högre tillgänglighet för pannan, ökad bränsleflexibilitet, och lägre underhållskostnader.

Målet med arbetet var att göra en vetenskaplig studie av egenskaperna hos en ny metall-polymer-komposit (CMP) baserad på ett termiskt sprutat skikt av en nickelbas-legering med ett toppskikt med goda släppningsegenskaper för avlagringen och beständighet vid förhöjda temperaturer.

I projektet har CMP med olika toppskikt exponerats i biobränsleeldade kraftvärmeverk. Proverna har exponerats en eller två säsonger. Dessutom har prover exponerats i nötningstester och i några försök på lab. Toppskikten av polymermaterialhar undersökts i detalj. Undersökningar har gjorts visuellt samt med elektronmikroskopi kombinerat med energidispersiv röntgenanalys (SEM/EDS).

Av de undersökta toppskikten med polymer, visade toppskiktet med PTFE (teflon) bäst resultat avseende slitage och täckningsgrad efter exponering. Dessa prover exponerades i economiser och elektrostatiskt filter. Materialen med polysiloxane (silikon) visade olika beteende i olika positioner. Det fanns ingen signifikant skillnad i avlagringsmängd mellan de exponerade proverna och omkringliggande material. En anledning kan vara att det bildades litet beläggning i de valda positionerna i pannorna. Ett undantag var prover i panna i Västhamnsverket, där proverna visade mycket mer beläggning efter exponering än omkringliggande tuber. Det kan dock ha andra orsaker som gasflöden eller att exponeringstemperaturen var litet annorlunda på proverna jämfört omkringliggande tuber.

Resultaten visar att ett kompositskikt kan klara påfrestningarna vid exponering, och att toppskiktet till ganska stor del kan finnas kvar, men att effekten avseende mängd beläggning bör utredas vidare. Vid en sådan undersökning, är det önskvärt att en större area beläggs och att beläggning görs direkt på ytorna i pannan.

Sökord: Biobränsleeldade kraftvärmeverk; Fältexponeringar; Beläggningar; Non-stick; Avlagring

Summary

Combined heat- and power production using biomass, refuse wood or other waste, often implies a large amount of deposits on the surfaces in the CHP plant. The deposits might result in inefficient heat transfer of the heat-transferring surfaces, corrosion due to deposits and a need for soot blowing. These problems would be reduced if a surface layer with good non-stick, erosion and corrosion properties was added on the surfaces. For the energy companies this could result in better heat-transfer, increased heat- and power production, increased fuel flexibility, increased plant availability and reduced maintenance costs.

The aim of the work was to examine the behaviour of a new polymer-composite material (CMP) with a thermally sprayed nickel-base layer applied on surfaces of the plant and a top coating of a material with good thermal and non-stick properties.

The project included exposure of a CMP layer with a number of different top coatings in biomass fired power plants. The samples were exposed for one or two seasons. The polymeric top coatings were examined and analysed in detail. Some additional laboratory exposures and wear tests were performed. The detailed analysis was performed with scanning electron microscope combined with energy dispersive X-ray diffraction (SEM/EDS).

Among the three materials with a polymeric top coating, the material with PTFE (teflon) showed the best adherence to the nickel base layer in the field and wear exposures. This coating was exposed in the economiser and ESP cone. The materials with polysiloxane (silicone) showed different behaviour in different positions. There was no significant difference in amount of deposits between the exposed samples and the surrounding tubes in the CHP plant. A reason may be that the amount of deposit was low in the exposure positions. One exception was the samples exposed in the furnace at Västhamnsverket, where more deposit was observed on the samples compared with surrounding material. The reason might be e. g. gas flow patterns or different temperatures on tack-welded samples compared to the surrounding tubes.

The results show that a CMP layer could have reasonable coverage with remaining top coating after exposure, but that the effect on deposit formation has to be further examined. If further examined, larger areas are requested as well as a coating applied directly on the surfaces of the plant.

Key words: Biomass fuelled combined heat and power plant; Field tests; Coating; Non-stick; Deposit

List of contents

1 Introduction

1.1 BACKGROUND

Combined heat- and power production using biomass, refuse wood or other difficult fuel, often implies a large amount of deposits on the surfaces in the CHP plant. The deposit amount depends on the chemical complexity of the fuel and its alkali content, primarily the content of potassium [1]. Numerous combinations of low temperature melts may also occur from elements such as Cl, K, Na, Pb and Zn. The deposits might result in inefficient heat transfer in the heat-transferring surfaces, corrosion due to deposits on both cooled and un-cooled surfaces and a need for soot blowing. These problems would diminish if a surface layer with good non-stick, erosion and corrosion properties was added on the surfaces. For the energy companies this could result in better heat-transfer, increased heat- and power production, increased fuel flexibility, increased plant availability and reduced maintenance costs [2]-[6].

The negative consequences of boiler fouling for the maintenance work can be illustrated by Figure 1 showing an example from Öresundskraft, Västhamnsverken. Before furnace maintenance work can be started, the slag hanging at especially the fuel inlets needs to be removed, as it may fall down. The cleaning work is quite spectacular and dangerous as can be seen from the illustration. The photo is quite typical for furnace fouling in boilers burning "difficult" biomass, which in this case is wood pellets having a high content of alkali metals. At this boiler it is normally found at the revision periods that large parts of the furnace walls are covered with a slag layer of a few centimeters and some larger lumps scattered all-over.

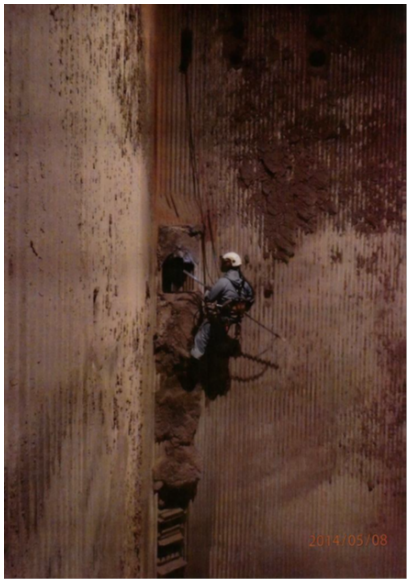

Figure 1. Cleaning of the furnace walls performed at Västhamnsverken.

The aim of the work was to examine the behaviour of a new polymer-composite material (CMP) with a nickel-base layer that is sputtered on surfaces of the plant and a top coating of a polymeric material with good thermal, corrosion, erosion- and non-stick properties. The expression non-stick refers in this application to the ability of a material to repel deposits. A good non-stick ability will result in a surface that is more

repellent than worse non-stick ability. An image of a CMP material before exposure is shown in Figure 2.

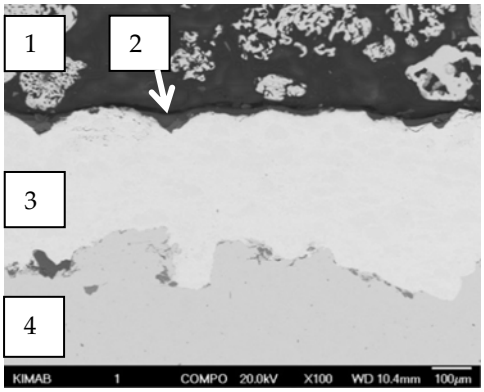

Figure 2. Image of the cross-section of a mounted sample before exposure. (1) Mounting media (2) Polymer top coating (3) Sputtered Nickel-base layer (4) Base material (carbon steel).

The metal part in the CMP-coating could be a metal or – if very high erosion resistance is needed – a cermet. In the project, the used nickel-base had a chromium content of approximately 20 wt-% and the possibility to form precipitates of a hard phase at exposure. The nickel-base material in this project was added by HVOF. The surface of the base material was prepared to get an optimal attachment of the sputtered metal layer.

The top coating used on the CMP material candidates of the project were applied as a paint with several components: One component (solute 1) with major task to reduce the adherence of deposits, one component (solute 2) that acts as a binder between the particles of solute 1 together and also attach the top coating to the base material. The last component is a solvent added to get an easily applicable liquid. The top coating can be painted onto the metal part of the CMP coating. A pigment is also added to the mixture. After painting, the material is cured at a temperature that is dependent on the top coating characteristics and the solvent evaporates leaving a thin layer of solid coating. There are other possibilities, for example chemical vapour deposition (CVD) of Si, but such candidates were excluded from the project due to the application procedure.

The project included exposure of a number of chosen materials in field tests. The materials either had a polymeric top coating or another top coating such as boron nitride or graphite-based top coatings. The sprayed nickel base layer was common for all materials. The samples with the polymeric top coating were examined and analysed in detail. The exposures were primarily performed in field tests, but some additional laboratory exposures and wear tests were performed. The detailed analysis was performed with scanning electron microscope combined with energy dispersive X-ray diffraction (SEM/EDS).

1.2 DESCRIPTION OF THE RESEARCH FIELD

Within the paper industry, CMP based on carbide containing thermally sprayed metal coatings and polymers has been used for more than 20 years [7]. The primary use has been for the steam heated dryer cylinders. Different coating systems have been tested in this environment [8][9]. Compared to boilers, the chemical environment is quite different and depending on position the temperature is lower. A special advantage of

thermal spray compared to overlay welding is that it can be reapplied numerous times without risk of thermal cracking.

Possible problem areas in the CHP plant where CMP could be considered are the furnace walls and evaporator panels, the first and - if the temperature is suitable - the second superheater, as well as the economiser. Deposits on these parts decrease the boiler efficiency and increase the risk of deposit-induced corrosion and erosion from excessive need of soot-blowing. Partial blocking of the flue gas paths increases the flue gas velocity locally and causes erosion. Hygroscopic deposits give down-time corrosion, which contributes to the overall material loss but also attacks the oxide layer intended to protect against high temperature corrosion.

The incoming water temperature to the economiser is limited by low temperature corrosion, i.e. dew-point corrosion from sulphuric and hydrochloric acids. Increased corrosion resistance would allow lowering the temperature limit, which would give higher electrical efficiency. Sometimes this applies to air preheaters and fuel dryers as well.

Other surfaces where deposit may cause corrosion or other types of problems include: fan blades where unbalance can cause bearing failure and fire may be caused by friction heat, if the deposits contain unburned fuel; components in electrostatic precipitator (ESP) filters, where the filtering effect may be lowered causing increased particle emissions; ash release cones of textile and ESP filters, where extensive deposit build-up gives increased pressure drop over the boiler decreasing its efficiency and increased risk of secondary combustion causing damages.

1.3 RESEARCH TASK

Although the use of CMP is new to boiler technology, thermally sprayed metal coatings with hard phase precipitates to give high erosion resistance have been used and investigated for several decades [10]-[13]. The challenges in boilers are several. The polymer part of the composite must withstand the temperature and chemical environment. Recently fluoropolymers have been developed with a temperature capability of 450 °C [14] . The metallic part must withstand corrosion and provide erosion protection for the polymer and corrosion protection for the underlying metal substrate. There shall be no or limited chemical interaction between the polymer and the metallic parts. For example, hypothetically at high temperature the polymer could cause carburisation of the metal accelerating its own breakdown. Further fluoropolymers might release hydro-fluoric acid during breakdown, which in its turn could cause reduced protective properties of the oxide layer and resulting corrosion. Investigating these possible mechanisms will provide a better understanding of them providing a basis for further material development aiming at widening the possible area of use for CMP.

1.4 GOAL

The overall scientific goal of the project is to obtain a broad scientific understanding of the properties and breakdown mechanisms of a CMP in a boiler environment. One goal of this project, which is an initial study since the field of research is new, is to provide input for future studies where some of the identified mechanisms will be studied in-depth aiming at giving comprehensive explanations of the ongoing corrosion mechanisms.

Specific Scientific Goals were:

1. To investigate how to obtain a certain "equilibrium" polymer-to-metal area ratio during abrasive wear or erosion and to explain why it is achieved, as well as to establish a criteria for a minimum ratio that results in a significant improvement of the non-stick properties.

2. To investigate the high temperature capability of the CMP and partially explain the corrosion/failure mechanism active at the upper temperature limit.

3. To investigate the influence on fouling during field service with respect to amount and adhesion.

4. To investigate the corrosion behaviour and partially explain the ongoing corrosion mechanisms, when exposed to high temperature corrosion during field service.

5. To investigate the corrosion behaviour and partially explain the ongoing corrosion mechanisms, when exposed to low temperature corrosion during field service.

1.5 PROJECT ORGANISATION

The project consists of five Activities:

1. Literature study to find a polymer with a good combination of high temperature resistance and non-stick properties.

2. Laboratory investigation of the degradation of the CMP during abrasive wear and erosion.

3. Laboratory investigation of the temperature capability of the polymer when being part of a CMP during exposure in humid atmosphere.

4. Field exposure of CMP at boiler areas susceptible to high temperature corrosion and post-exposure investigation of the samples.

5. Field exposure of CMP at boiler areas susceptible to low temperature corrosion and post-exposure investigation of the samples.

The applying company MH Engineering was responsible for the literature study of Activity 1, producing the test materials for Activities 2-5, and inserting/inspecting/removing the test materials during the field test of Activities 4-5, as well as on-site evaluation of material/fouling behaviour. They have cooperated with Alu-Releco Oy to get access to the necessary technology with relation to the polymer part of the CMP material.

The field exposures of Activities 4 and 5 have been performed both at Västhamnsverket in Helsingborg belonging to Öresundskraft, which is fired with wood pellets having a high content of alkali metals, and at Avedöre, a straw-fired boiler belonging to Ørsted. Exposures were made at areas susceptible to high temperature (Activity 4) and low temperature (Activity 5) corrosion. At Västhamnsverket testing was performed in furnace parts with fouling issues, at a lower temperature superheater, in the economiser area and at the cones of the electrostatic precipitator (ESP) filter. At Avedöre, the exposures were made in the superheater and economiser areas.

The co-applicant Swerea KIMAB was responsible for performing Activities 2-3 and the post-exposure evaluation related to Activities 4-5. The tool used in the project was primarily SEM-EDS.

Participating companies and their representatives, as well as the project financing:

MH Engineering: Matti Huhtakangas
In-kind contribution 1 017 kkr.

Swerea KIMAB AB: Ragna Elger, Rikard Norling, Leyla Wickström
Research budget 944 kkr.

Öresundskraft, Västhamnsverket: Henrik Wangsell & Fredrik Joelsson
In-kind contribution 250 kkr.

Ørsted (formerly DONG Energy): Søren Aakjaer Jensen
In-kind contribution 150 kkr.

Reference group:

Bo Jönsson, Sandvik Heating Technology
Pamela Henderson, Vattenfall AB

2 Experimental

The materials were prepared according to the procedure: Degreasing of the base metal – abrasive blasting to SA 21/2 – Surface treatment with Al_2O_3 to optimal profile – Thermal spray (HVOF) with CorEr™ - Application of non-stick material (top coating) – Tempering of the non-stick material at material-specific temperature. For the wear tests, carbon steel was used as substrate, while the base material varied for the samples exposed in the commercial plants was carbon steel for low-temperature positions and high temperature steel grades for the superheater positions. The procedure used for the preparation was identical for all prepared samples.

In contrary to commercially exposed samples, wear test samples were exposed at room temperature. All materials are listed in Table 1. The samples exposed at Västhamnsverket were tack-welded onto the furnace walls and thus partly cooled during exposure, whereas the materials in Avedöre were not cooled.

Table 1. Coating materials exposed in the project

No	Supplier Material name	Type	T_{max} [°C]
1	ALU-Releco, Finland, AR-107/102 PTFE	PTFE	250
2	ALU-Releco, Finland, AR-150	Ceramic material	400
3	Diamant Metallplastic, DE Dichtol HTR	Not specified	550
4	FMP Coatings Canada	Boron nitride-silicate	Not available
5	FMP Coatings, Canada	Al phosphate/Boron nitride	Not available
6	Millidyne, Finland Avalon non-stick	Polysiloxane	250
7	Millidyne, Finland MDC-HT1	Not clear	650
8	Aremco, USA CP4020 S1	Silicone	590
9	Aremco,USA Pyropaint 634BN	Boron nitride	850
10	Aremco, USA Pyropaint 634 GR	Graphite based	1200

Metallographic preparation of the as received samples and the wear test samples (10 h) was carried out by mounting the samples in conductive media followed by diamond polishing to 1μm (materials 1 and 8) or 0.25 μm (material 6 as recieved), before examination in SEM/EDS. The samples that were exposed in the commercial plants were dry sectioned and then further sectioned by dry methods as well as dry grinded

to P4000. For field test samples, smaller pieces were dry cut from the tubes, followed by mounting in conductive media. To remove any deformation from the initial cutting process, approximately 3-4 mm of the mounted sample was removed by dry cutting along the flat side of the mount using precision cutting equipment. Prior to SEM/EDS analysis, the samples were dry ground to P2500 SiC to avoid any chlorides to dissolve. The samples analysed by SEM/EDS in cross section are presented in Table 2.

Table 2. Samples for SEM/EDS analysis in cross section after field exposure at Västhamnsverket and Avedöre.

Material No.	Type	Positions analysed Västhamnsverket (Öresundskraft)	Positions analysed Avedöre (Ørsted)
1	PTFE	Economizer (Sample 3.1 2016) (Sample 4.1 2017) ESP Cone (Sample 2.1 2016) (Sample 1.1 2017)	Nil
2	Ceramic	ESP Cone (Sample 1.2, 2017)	Position C (Eco 2) (sample 3.2, 2017)
3	Not specified	ESP Cone (Sample 1.3, 2017)	Position B (SH 1 LT) (Sample 7.3, 2017) Position C (Eco 2) (sample 3.3, 2017)
4	Boron nitride	Not included/analysed	Position A (SH-HT) (sample 9.4, 2017) Position B (SH 1 LT) (sample 7.4, 2017) Position C (Eco2) (sample 4.4, 2017)
5	Not clear	SH-HT (Sample 9.5 2017) (Sample 10.9 2017) (Sample 10.10 2017)	Not included
6	Polysiloxane	Economizer (Sample 3.6 2016) (Sample 4.6 2017) ESP Cone (Sample 2.6 2016) (Sample 1.6 2017)	Not included
7	Not clear	Not included/analysed	Position A (SH-HT) (sample 9.7, 2017) Position B (SH 1 LT) (sample 8.7, 2017)
8	Silicone or glass?	SH-LT (sample 5.8, 2016)	Position B (SH 1 LT) (sample 8.8, 2017) Position C (Eco2) (sample 4.8, 2017)
9	Boron nitride?	SH-HT (Sample 10.9, 2017)	Position A (SH-HT) (sample 10.9, 2017)
10	Graphite based	SH-HT (Sample 10.10, 2017)	Position A (SH-HT) (sample 10.10, 2017)

2.1 WEAR TESTING

Wear tests were carried out in a abrasive wear test drum at Swerea KIMAB. The wear tests were performed for three different exposure times (30 min, 2 h and 10 h). The samples were photographed during short stops at total wear test times of 30 min (all samples), 2 h (samples exposed for 2 and 10 h), 4 h, 6 h and 10 h (samples exposed for 10 h). Anti-corrosive agent was added to the test to avoid corrosion of the underlying substrate. All materials were included in the 10 h wear test, while material 10 was excluded for the shorter exposure times due to very low adhesion to the substrate. Pre-rolled gravel from Arlanda was used in the wear tests.

The hardness was measured using a hardness tester, Q10, used for micro Vickers measurement with a load of 50 g. The hardness was measured for the base material (carbon steel) and for the sputtered nickel-rich layer of one unexposed laboratory sample of material 8. These two layers were identical for all prepared laboratory samples.

2.2 WETTING ANGLE MEASUREMENT BY DROPLET TEST

The wetting angle was measured with a PG-X Measuring Head with PGX Software 3.4 (FIBRO System AB (www.fibro.se)) using deionised water and a defined droplet size of 7 μL. In the test, the droplet is placed on the surface of a sample. The image of the droplet was analysed and the wetting angle was given by the program. A sketch of the definition of the wetting angle is shown in Figure 3. As shown, a water repellent material will result in a larger wetting angle than a less repellent one.

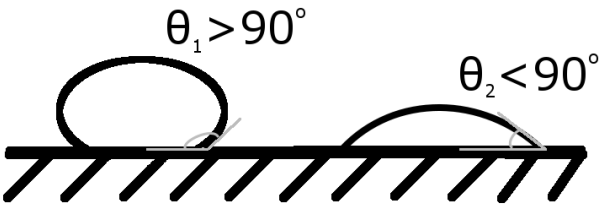

Figure 3. Examples of the wetting angle for a water repellent (left) and a less water repellent (right) material.

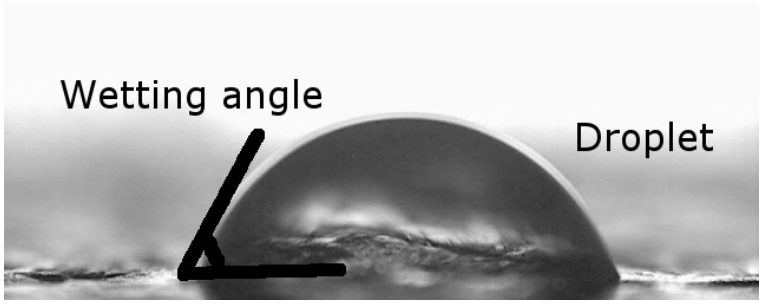

Figure 4. Typical droplet on material 1 after wear test 10 h, before water wash.

For each material, the wetting angle was measured for 10 different positions evenly spaced on the surface and at least 5 mm distance from the edges. After application, the

droplet was allowed to stabilise for at least 5 min on the surface before wetting angle measurement. The wetting angle was measured 10 times for each droplet to avoid fluctuations during measurement. Only materials with polymer top layer (materials 1, 6 and 8) were included in the droplet tests. The tests were carried out on as received samples and on the samples from the wear tests with total exposure times of 30 min, 120 min and 600 min. The wear test samples were carefully cleaned with water before the measurements. Note that unique samples were analysed for the different exposure times.

2.3 LABORATORY EXPOSURES OF MATERIAL 1

Laboratory exposures were performed in a horizontal tube furnace with an inner quartz tube with an inner diameter of approx. 42 mm. Exposures were performed for single specimens of material 1 in a mixture of N_2/21% O_2 humidified at room temperature (approx. 3 vol-% H_2O). The gases were supplied from the central gas system and wetted by bubbling through a water filled bottle. The exposures were performed with a total gas flow of approximately 250mL/min at three different temperatures: 400°C, 500°C and 600°C for 168 h hot dwell time. One initial exposure from room temperature up to 400°C with subsequent heating after a period of 2 h to 600°C with temperature ramp 10K/min was also performed. Temperature calibration was performed according to standard ISO 17245. The samples were placed into and taken out of the furnace at a temperature below 100°C. The specimens were exposed in alumina boats baked at 1000°C for 24h before exposure.

To evaluate the composition of the gas in a qualitative manner, a mass spectrometer was attached to the outlet of the furnace. The background signal was measured after overnight gas flow through the set-up and subtracted from the analysed results. The measurement used for the isothermal exposures was a measurement only including selected peaks. For the ramped initial exposure also a scan between 0 and 100 atomic mass units (amu) was included in order to identify any peaks from the fluorine lists the mass numbers included in the data sampling with selected peaks as well as their possible origin.

Table 3. The mass numbers included in the analysis in the mass spectrometer and suggested origins

	Mass number	Constituent/origin
Expected peaks of the background	14	N
	16	O
	18	H_2O
	28	N_2, CO
	32	O_2
	40	Ar
	44	CO_2
Peaks expected from PTFE	19	F
	31	CF
	50	CF_2
	69	CF_3
	88	CF_4

2.4 FIELD EXPOSURES

2.4.1 Västhamnsverket/Öresundskraft

Västhamnsverket is a pulverised fuel plant where firing was performed with biopellets during the exposure time. The field exposures at Västhamnsverket were performed during the firing seasons 2015/16 (in total 2928 h) and 2016/17. Firing was performed, the steam and in some instances gas temperatures for 2015/16 are included as well as the ID of the exposed and the analysed samples. A sketch with the indicated sample exposure positions is shown in Figure 5. Also, the flue gas recirculation fan wheel was applied with material 1 as top coating in 2013 and examined the years 2014-2017.

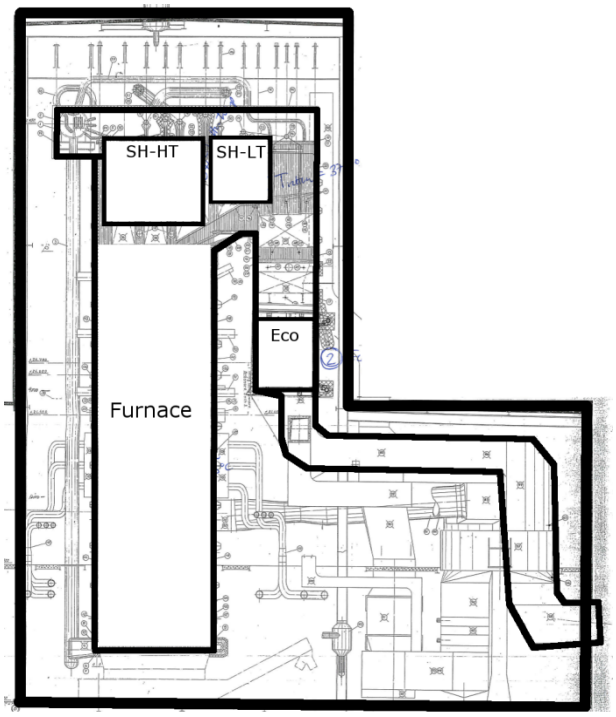

Figure 5. Image of Västhamnsverket. Note that the ESP cone is not included, and located next to the outlet to the lower right in the image

Table 4. Temperatures at the exposure positions of Västhamnsverket during the firing season 2015/16 (20th Nov 2015-20th Mar 2016). The samples are named as follows: (position)-(material number)

Position	Water/steam temperature (°C)	Approximate temperature for gas phase (°C)	Samples exposed	Samples analysed
ESP Cone	n.a.	180-200	2.1,2.2,2.3,2.6 (2016) 1.1,1.2,1.3,1.6 (2017)	2.1,2.6 (2016) 1.1,1.2,1.3,1.6 (2017)
Economiser	250	370	3.1,3.6 (2016) 4.1,4.6 (2017)	3.1,3.6 (2016) 4.1,4.6 (2017)
Furnace , water walls	520	850	No samples analysed	No samples analysed
SH-LT (ÖHIb)	370	na	5.8	5.8 (2016)
SH-HT (ÖHII, 2017)	490	na	9.4,9.5 10.9,10.10	9.5 (2017) 10.9,10.10 (2017)
SH-HT (ÖHIII, 2016)	520	na	No samples analysed	No samples analysed

2.4.2 Ørsted /Avedöre

The boiler at Avedøreværket used as host for this project is a once-through straw-fired boiler with grate. The samples in Avedöre were exposed for one firing season – 2016-10-01 to 2017-05-17, approximately 5500 h. Only samples intended for examination in 2017 were analysed. In addition to the exposed samples, the reference material 253MA was exposed. A sketch with the indicated sample exposure positions is shown in Figure 6.

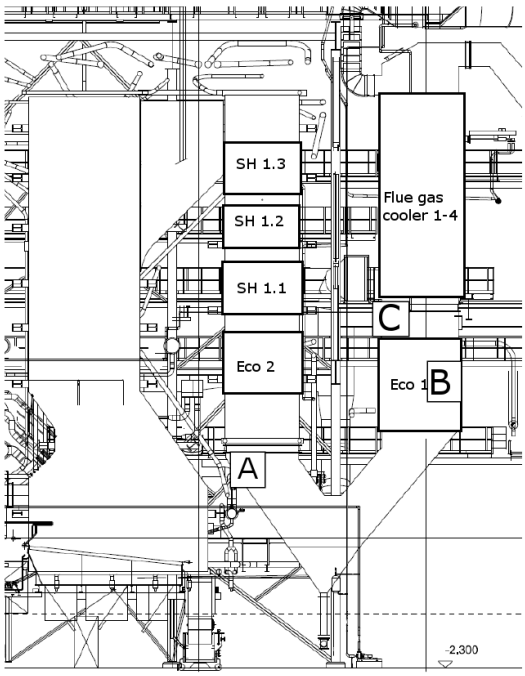

Figure 6.Image of Ørsted /Avedöre.The sample positions are indicated by letters A-C-

Table 5. Materials exposed in Ørsted /Avedöre including aproximate exposure temperatures.

Position	Approximate temperature for gas phase (°C)	Samples exposed	Samples analysed	Remarks
Position A (SH-HT)	475-535	9.4, 9.7 10.9, 10.10 11.4,11.7 12.9, 12.10 Ref	9.4,9.7 10.9,10.10 Ref	
Position B (SH1-LT)	Not measured	5.3, 5.4 6.7,6.8 7.3,7.4 8.7, 8.8 Ref	7.3, 7.4 8.7, 8.8 Ref	Soot blower exposed
Position C (ECO 1)	225-275	1.1, 1.3 2.4, 2.8 3.1, 3.3 4.4, 4.8 Ref	3.1 (Material 2) 3.3 4.4, 4.8 Ref	

3 Results

3.1 HARDNESS MEASUREMENTS

For the laboratory prepared sample of unexposed material 8, hardness for the substrate carbon steel was on average 150 HV0.05 within the sample and with little variation. For the sputtered nickel-rich layer of CorEr™, the hardness values varied within the sample from 487 HV 0.05 to 1084 HV 0.05 with an average of 780 HV 0.05. The base material and the sputtered nickel rich layer were identical for all lab exposed samples.

3.2 WEAR TEST

The samples exposed for 10 h in wear tests were photographed after 30-60-120-240-360 and 600 min exposure in the wear test. The photographs of material 1 are shown in Figure 7. The images include a reference sample with the sputtered layer of nickel-base material only to the left, and an unexposed sample including the top coat to the right. The exposed sample is shown in the center position. In the images, it is observed that the outer layer is worn gradually. Also, the wear is uneven, with more wear to the left of the sample. As the gravel is rotated in the same direction throughout the test, the uneven wear is expected. All materials showed wear. If all the photographs of each exposed material are compared, a top coat coverage of 25-50 % is approximated for almost all materials. An exception is material 10 as almost no top coat is left after only 30 min of exposure. Photographs of all samples exposed in the 10 h wear exposure are given in Appendix A.

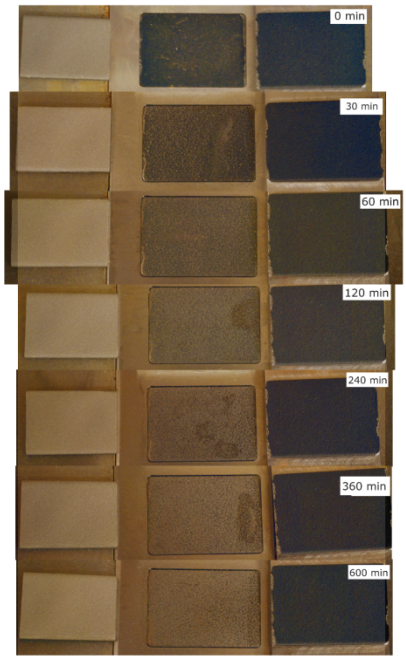

Figure 7. Image after wear test on material 1 after exposure time indicated in the figure. To the left of each sample, a sample without the top coat is shown and to the right the unexposed material. As light might change between the different exposure times, the middle samples should primarily be compared within the unexposed samples to the right.

3.2.1 Cross sections of materials 1, 6 and 8 before and after wear testing

3.2.1.1 Before wear testing

SEM images of the cross sections before wear testing are shown in Figure 8 - Figure 10 for materials 1, 6 and 8. For material 1, fluorine was analysed in the top coating at levels of 15-35 wt-% using SEM/EDS, consistent with the applied PTFE-layer. For materials 6 and 8, the top coat showed clear enrichment of Si and O that is in agreement with the given top coat material polysiloxane for material 6 and silicone or glass for material 8. Particles of silicon oxide and aluminium oxide were often observed in the boundary between the base material and the sputtered nickel base layer (indicated in Figure 8). This was due to the initial preparation method of the samples and will not be further discussed.

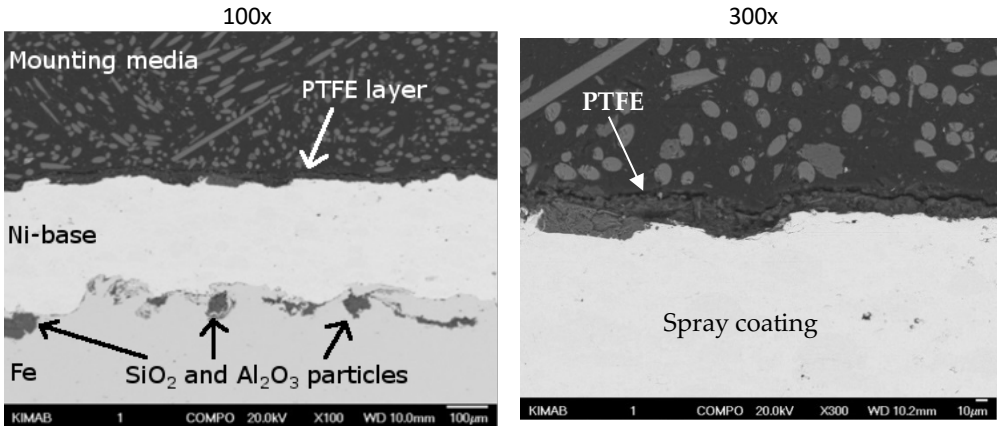

Figure 8. SEM images of as received material 1 (Alu-Releco, PTFE) in cross section at two different magnifications. Base material (carbon steel), spray coating (nickel base) and top coating (PTFE layer) are indicated in the figures. Scale bar is 100 µm at 100x magnification and 10 µm at 300x.

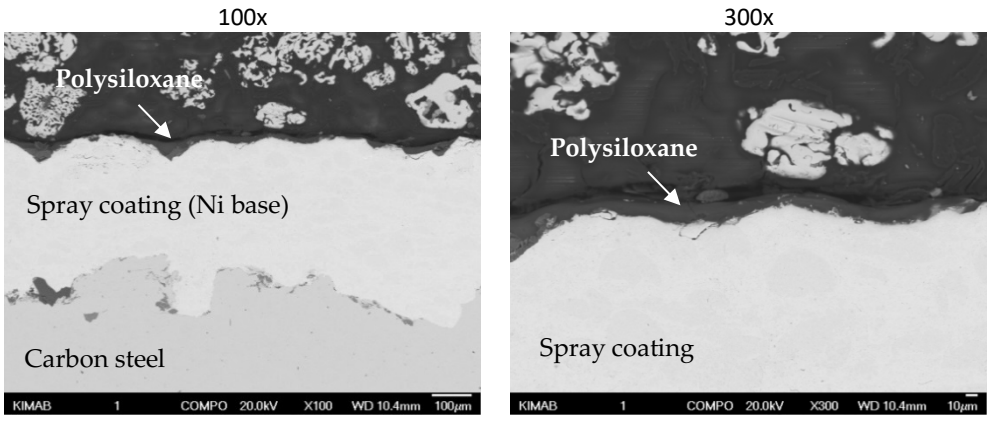

Figure 9. SEM images of as received material 6 (Millidyne, polysiloxane) in cross section at two different magnifications. Base material (carbon steel), spray coating and top coating are indicated in the figures. Scale bar is 100 µm at 100x magnification and 10 µm at 300x.

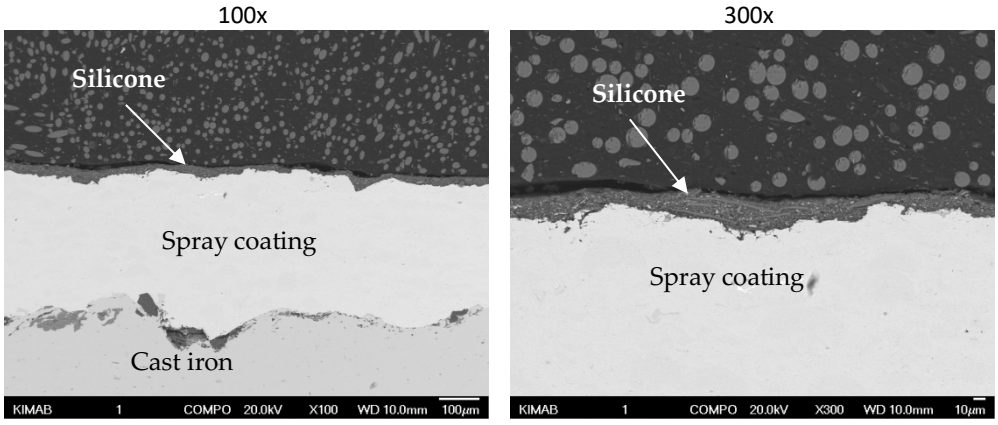

Figure 10. SEM images of as received material 8 (Aremco, Silicone) in cross section at two different magnifications. Base material (carbon steel), spray coating and top coating are indicated in the figures. Scale bar is 100 µm at 100x magnification and 10 µm at 300x

After wear testing – 30 min, 2h and 10h wear testing

For material 1, quite good adhesion of the polymer was observed after 30 min (80-90% surface coverage). After 2 h for material 1, there was quite significant crevice formation between the sample and the mounting media. In regions with crevice formation, the polymer appeared to have partly attached itself to the mounting media but still being partly adherent to the sample. In those cases, it was assumed that the polymer adhesion to the sample surface had been adequate until it was partly removed during the hot mounting process. The adhesion of the top layer was estimated to approximately 80%. After 10 h, adequate adhesion of the polymer was observed for material 1 (≈ 60-70%). There was occasional (small) crevice formation between the sample and mount. In these locations, no top coating was observed, but it was not clear whether this was due to the mounting procedure or a consequence of the wear testing (or if the coating somehow could have been removed during the grinding procedure). SEM images with the corresponding elemental map of fluorine are shown in Figure 11 - Figure 13.

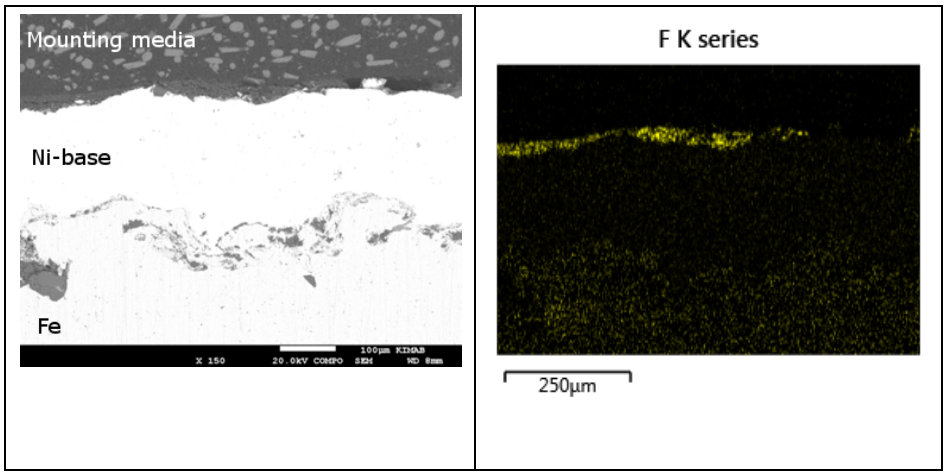

Figure 11. Material 1, 30 min wear testing: Back-scattered SEM image and the corresponding EDS elemental map of F at 150x magnification. F is clearly observed on top of the nickel coating. The fluorine signal in the base material is an artefact. The scale bar in the SEM image is 100 µm.

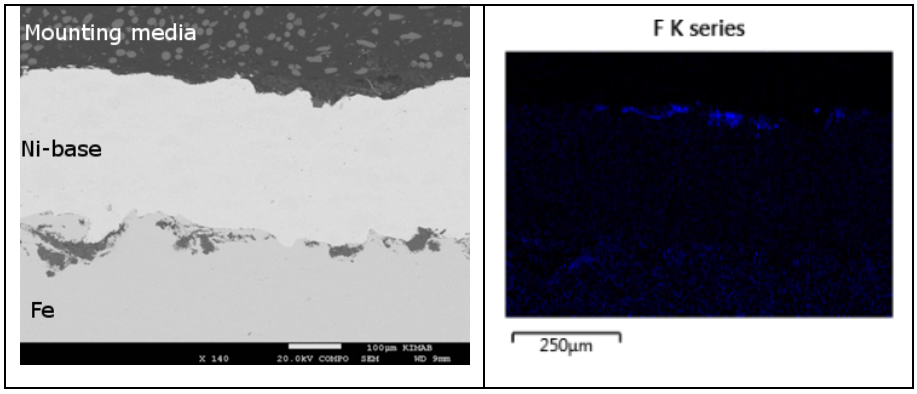

Figure 12. Material 1 after 2 h wear testing: Back-scattered SEM image and the corresponding EDS elemental map of F at 140x magnification. A distinct F-layer was detected on top of the nickel-base material, indicating presence of PTFE polymer. The scale bar in the SEM image is 100 µm.

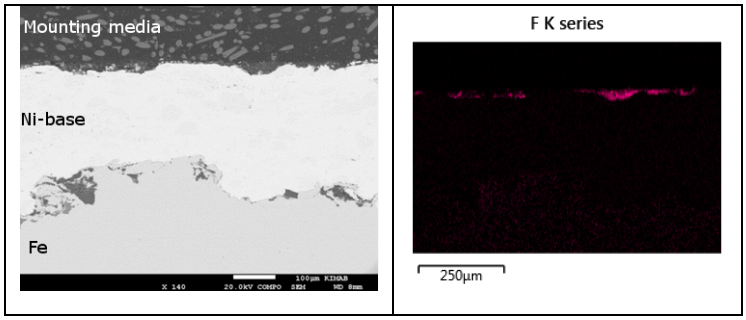

Figure 13. Material 1 after 10 h wear testing: Back-scattered SEM image and the corresponding EDS elemental map of F at 140x magnification. A distinct F-layer was detected on top of the nickel-base material, indicating presence of PTFE polymer.The scale bar in the SEM image is 100 µm.

After 30 min wear testing material 6 showed less uniform adhesion of the top coating compared to material 1 (50-60%). Less homogeneous coverage was observed towards the middle of the specimen compared to nearer the edges. This is probably just an effect of the exposure method. There was occasional crevice formation between the specimen and mounting media. Reduction in adhesion after 2 h wear testing in comparison to after 30 min wear testing was observed (≈50% adhesion). After 10 h wear testing, approximately half of the examined surface was covered by the top coating (≈50%). Quite large crevice was present between the mount and sample and there was alternatingly polymer present where there was crevice and alternatingly not. Hence, crevice formation may not necessarily have caused the coating to detach from the sample surface. Backscattered images of material 6 after the wear test, and the corresponding EDS elemental maps of Si and O are shown in Figure 14- Figure 17.

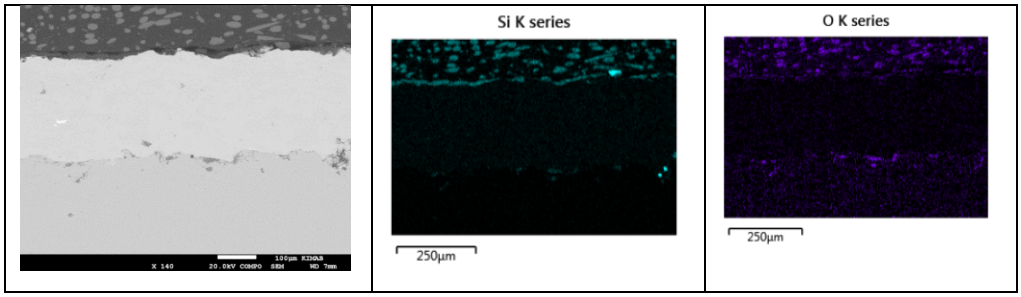

Figure 14. Back-scattered SEM image of material 6 after 30 min wear testing. In the SEM image, the scale bar is 100µm at 140x magnification. Also included are elemental maps of Si and O observed in the top coating. Distinct Si layer with a more diffuse O layer indicating polysiloxane coating are observed in the elemental maps.

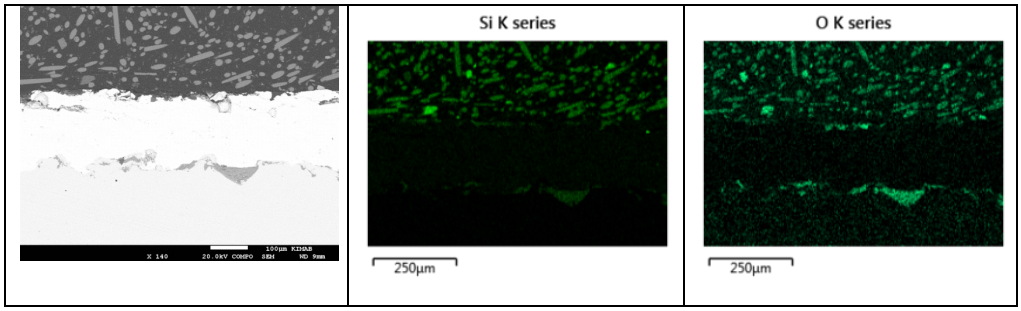

Figure 15. Back-scattered SEM image of material 6 after 2 h wear testing. In the SEM image, the scale bar is 100µm at 140x magnification. Also included are EDS elemental maps of Si and O. Hardly any Si or O was detected on the surface of the sample, indicating little coverage of the polysiloxane coating in this location.

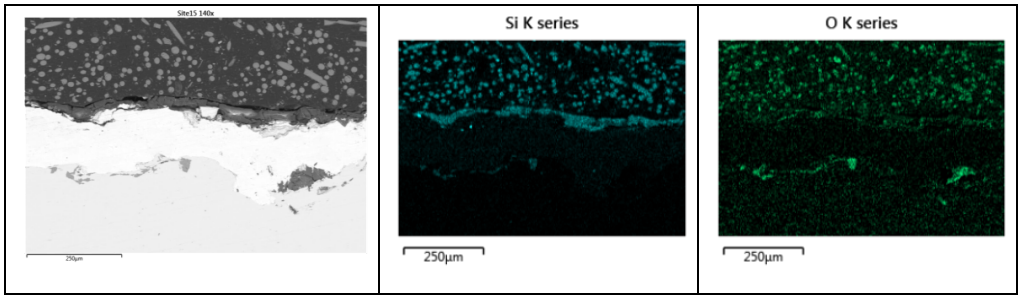

Figure 16. Back-scattered SEM image of material 6 after 2 h wear testing. Scale bar is 250µm at 140x magnification. Also included are EDS elemental maps of Si and O observed in the top coating. Distinct Si layer together with a bit more diffuse O layer was detected, indicating presence of polysiloxane layer.

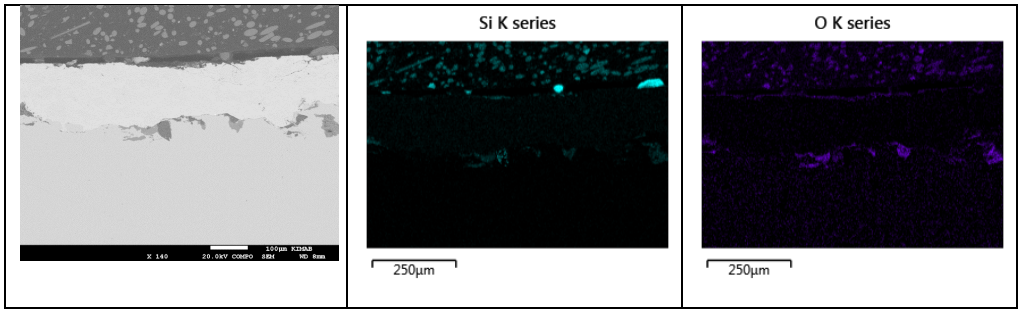

Figure 17. Backscattered image of material 6 after 10 h wear testing. The scale bar is 100µm at 140x magnification. Corresponding elemental maps of Si and O indicate only a slight presence of polysiloxane layer.

After 30 min wear testing of material 8, generally very good adhesion (≈ 90%) of the coating (silicone) was noted. There was occasional crevice formation between the sample and mounting media, which did not appear to have influenced the attachment of the top coating. After 2 h wear testing, material 8 showed app. 70% adhesion of top coating (silicone). Occasional crevice formation was observed between the sample and mount. In these locations, no top coating was observed, but it was not clear whether this was due to the mounting procedure or a consequence of the wear test. After 10 h wear testing of material 8, approximately half the examined surface (≈50%) exhibited top coating. Hardly any crevice between the sample and mount was observed. In Figure 18 - Figure 20, the backscattered image of material 8 after 30 min, 2 h and 10 h wear test is shown along with corresponding elemental maps of Si, Al and O.

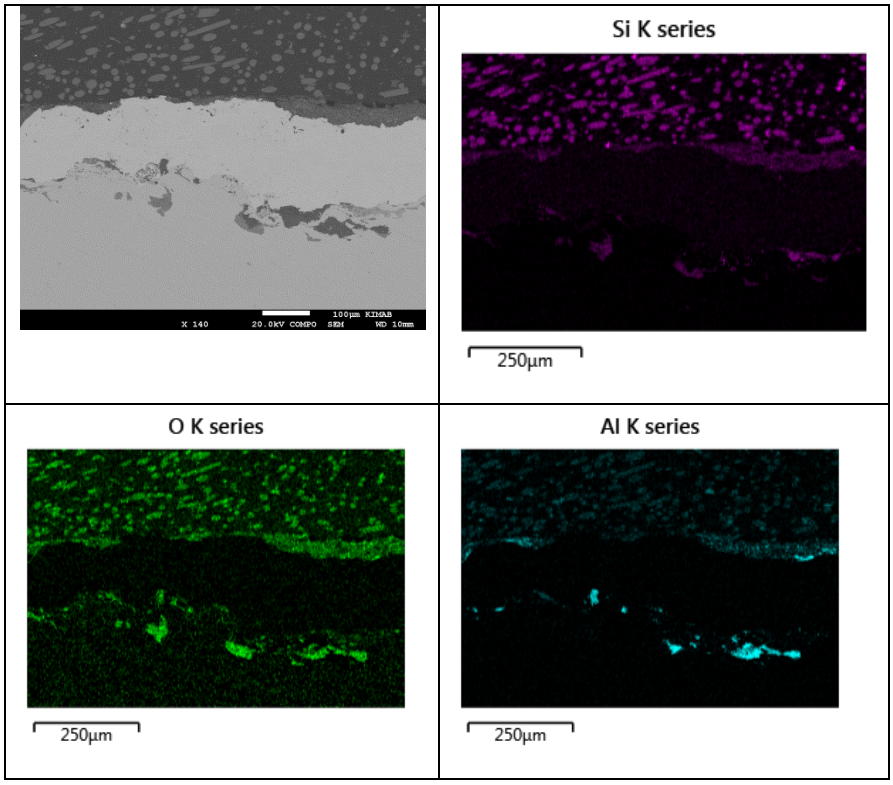

Figure 18. Back-scattered SEM image of material 8 after 30 min wear testing. Al, Si and O are detected on the surface. Scale bar in SEM image is 100 µm at 140x magnification

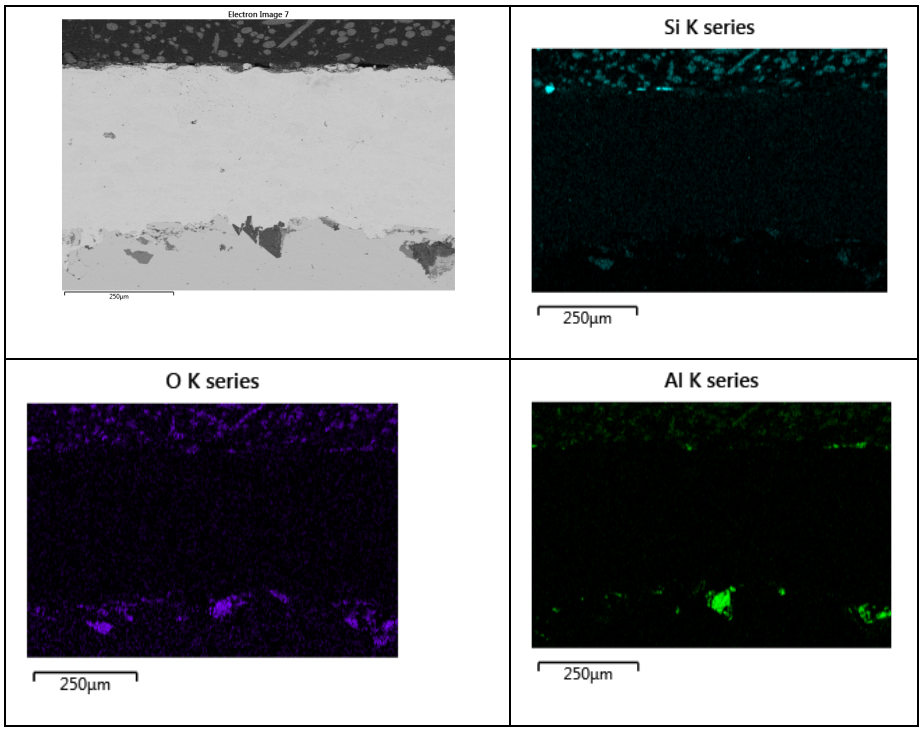

Figure 19. Back-scattered image of material 8 after 2 h wear testing. The scale bar in SEM image is 250µm at 140x magnification. Hardly any Si layer was detected, indicating little presence of the silicone top coating. The scale bar in SEM image is 250 µm.

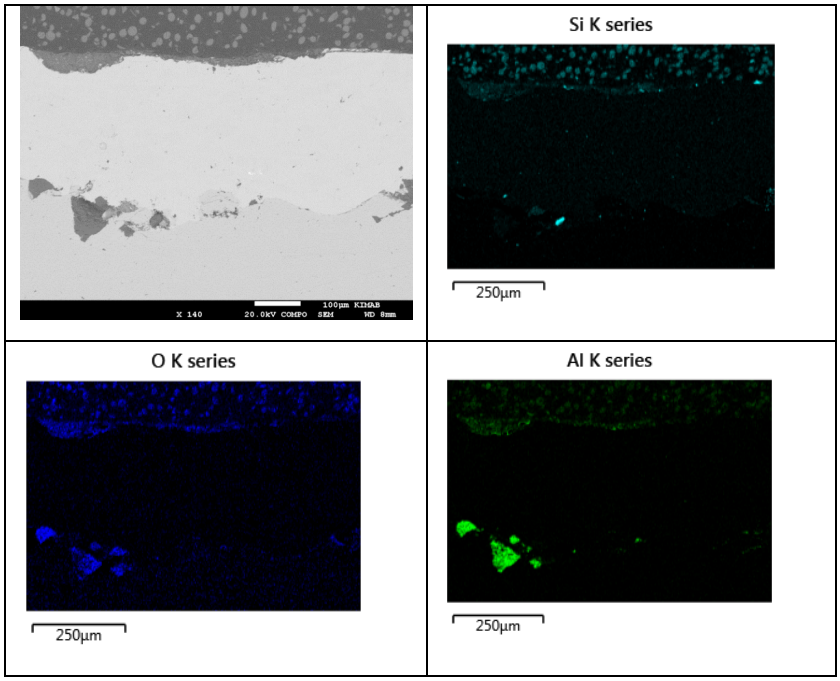

Figure 20. Back-scattered image of material 8 after 10 h wear testing. The SEM scale bar is 100µm at 140x magnification. In the corresponding elemental maps, a layer enriched in Si and O is observed.

As shown, all examined materials (1, 6, 8) show some coverage of the top coating after the wear test for 10 h. A qualitative estimation in terms of surface coverage/adhesion of the top coating over the examined surface was carried out for each material (Figure 21).

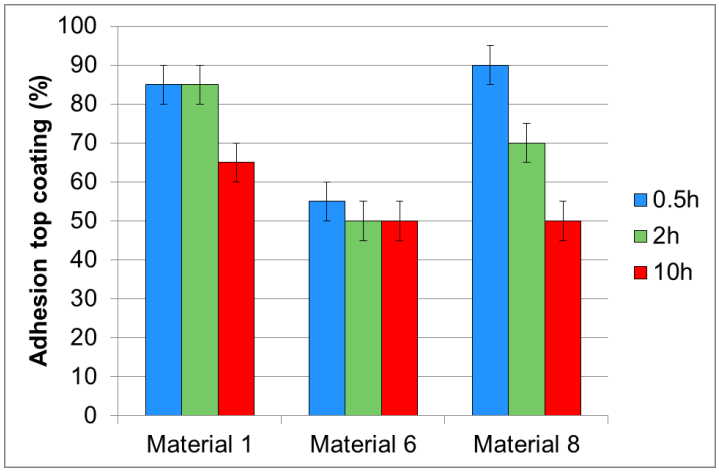

Figure 21. Qualitative estimation of top coating coverage (polymer) of examined surface for material 1, 6 and 8 after wear testing for 0.5, 2 and 10h.

3.3 DROPLET TESTS ON SAMPLES EXPOSED IN WEAR TESTING

The wear of the sample surfaces shows non-uniform distribution. The reason is that the gravel in the test is rotated in the same direction throughout the test and some positions will show more wear than others. In the droplet test, as-recieved material 6 shows very different results depending on position of the droplet on the surface. In some positions, the droplet shows some water repellent ability, while the droplet in other positions flows out onto the surface. The other as-recieved materials (materials 1 and 8) displayed more homogeneous results.

All results from the droplet tests are included in Figure 22. As shown, the samples examined as received displayed smaller wetting angles that the samples exposed at different time spans in the wear tests. No clear trend that corresponded to longer wear test exposure could be identified for materials 1 and 6. For material 8, a slightly smaller wetting angle was observed if the sample exposed for 30 minutes is compared with the sample exposed for 600 min. The sample exposed as-recieved displayed a lower wetting angle than the samples exposed in the wear tests.

The effect of the cleaning procedure before droplet tests was examined. The result indicated that degreasing with acetone resulted in a larger wetting angle, as opposed to the expected effect of degreasing the samples. After acetone cleaning of the as-received samples, results showed less variation. As no effect on Teflon is supposed after acetone cleaning, there might be other constituents in the sputtered layer that are affected by acetone. Thus, the other samples were not degreased. It is suggested that the cleaning procedure could be further examined in future work.

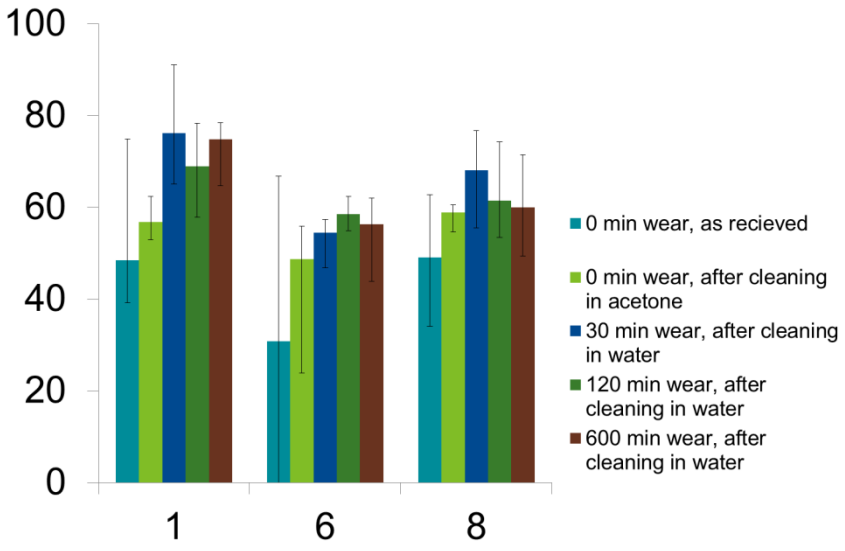

Figure 22. The wetting angle after droplet tests on the exposed samples versus the material numbers. The indicated time spans refer to time of exposure in the wear test.

3.4 LABORATORY EXPOSURES

Material 1 (AluReleco, PTFE) was examined as delivered and after isothermal exposures and after the ramped exposure 400-600°C. Fluorine signal was detected in some spots on the sample exposed at 500°C, while the fluorine no fluorine was detected after exposure at 400°C or 600°C. A close-up of the outer part of the sample after exposure at 500°C is shown in Figure 23.

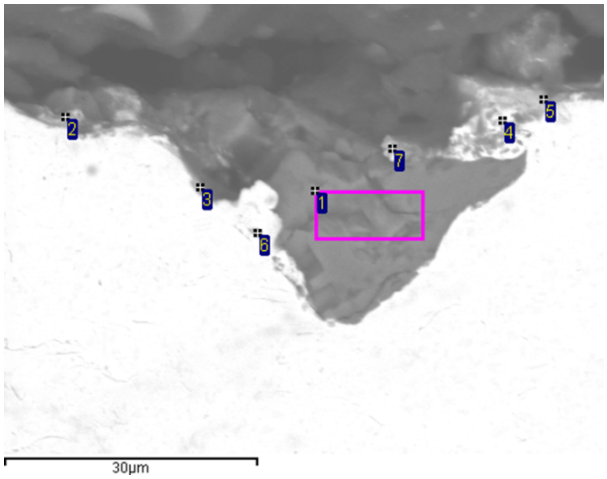

Figure 23. Back-scattered image of material 1 after isothermal exposure at 500°C. Fluorine was detected in spectra 4 and 5. Scale bar at 30 µm.

The mass spectrometer measurements showed no peaks at the mass numbers of the. As the layer is very thin, this is not unexpected. However, in the initial exposure, where temperature was gradually increased to 600°C, the ion current for CO_2 shows a peak after reaching 600°C that gradually disappears within less than an hour. It is suggested that CO_2 is formed during the degradation of the PTFE layer. In Figure 24, the ion current measured by the mass spectrometer is shown for the exposure performed with a temperature ramp from 400 to 600°C. The time where temperature rise is initiated is denoted t0. In the enlargement to the right, a clear increase in the signal at 44 atomic units (corresponding to the atomic weight of carbon dioxide) is noted. The CO_2 signal starts to increase after approximately 5 minutes, corresponding to 450°C with the present temperature ramp (10 °C/min). The signal is back at the initial level after another 30 minutes. In the exposure, 600°C was reached after 20 min The two isothermal exposures performed at 400°C and 600°C show no change in CO_2 peak during exposure. A plausible explanation is a different data sampling procedure that unfortunately showed less sensitivity.

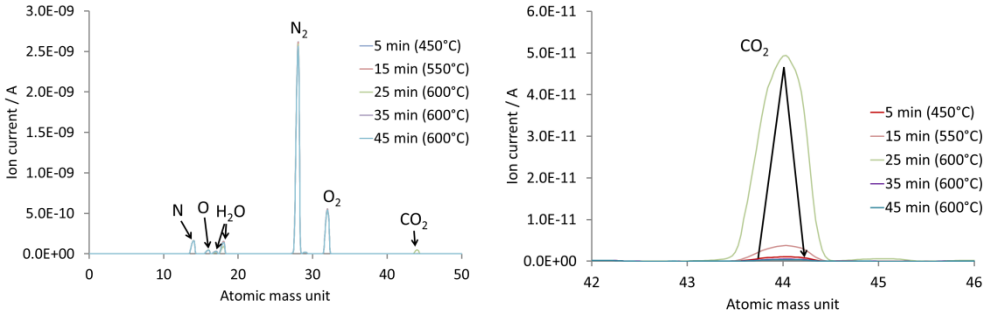

Figure 24. Ion current versus atomic mass for a sample heated from 400°C to 600°C. The time indicated refers to time from start of heat-up from 400°C to 600°C. 600°C is reached after 20 minutes The images show the signal during heat-up to and at 600°C with possible species origin indicated in the image. Left: Signals in the interval 0-50 AMU. Right: Signal in the interval 42-46 AMU. The arrow indicates increasing time.

3.5 PLANT EXPOSURES

3.5.1 Öresundskraft/Västhamnsverket

Furnace

The amount of deposit varied with location, as the northern wall displayed more deposit than the eastern wall. The samples which had been tack welded onto the furnace walls also displayed clearly more deposit than surrounding tubes, as shown in Figure 25. According to the furnace owner, the material generally used in the furnace was carbon steel St.45.8. The reason for the uneven deposit distribution might be temperature difference of the tack welded samples compared to surrounding material or geometric factors influencing the gas flow in the specific area. No analysis of the samples was performed in SEM/EDS.

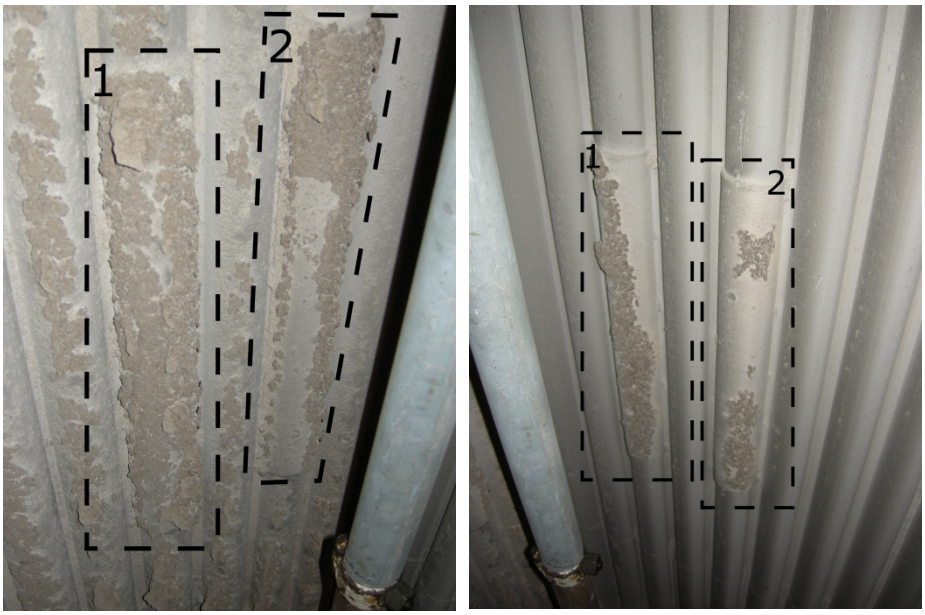

Figure 25. Images from inside of furnace. Material welded onto the northern wall (left) and material welded onto the eastern wall (right). Panels labelled 1 are spray coated with material 2 and 4, whereas panels labelled 2 are spray coated with material 5, 9 and 10.

SH-HT

The high temperature superheater (SH-HT) samples were only analysed after the second season. Images of the samples before sectioning are given in Figure 26-Figure 27.

Figure 26. Material 4 (left part of tube) and material 5 (right part of tube) after exposure in the superheater (SH-HT). Removed from site in 2017.

Figure 27. Material 10 (left part of tube) and material 9 (right part of tube) after exposure in the superheater (SH-HT). Removed from site in 2017.

Cross-sections of material 5 are shown in Figure 28-Figure 29. The top coating of Al-phosphate could not be observed in the analysis. Instead, a thick deposit layer with somewhat elevated level of oxygen close to the metal surface is shown. In Figure 29, it is shown that nickel and chromium is observed with oxygen in a band close to the metal surface. This could indicate a non-protective oxide layer on the nickel-base layer of the CMP.

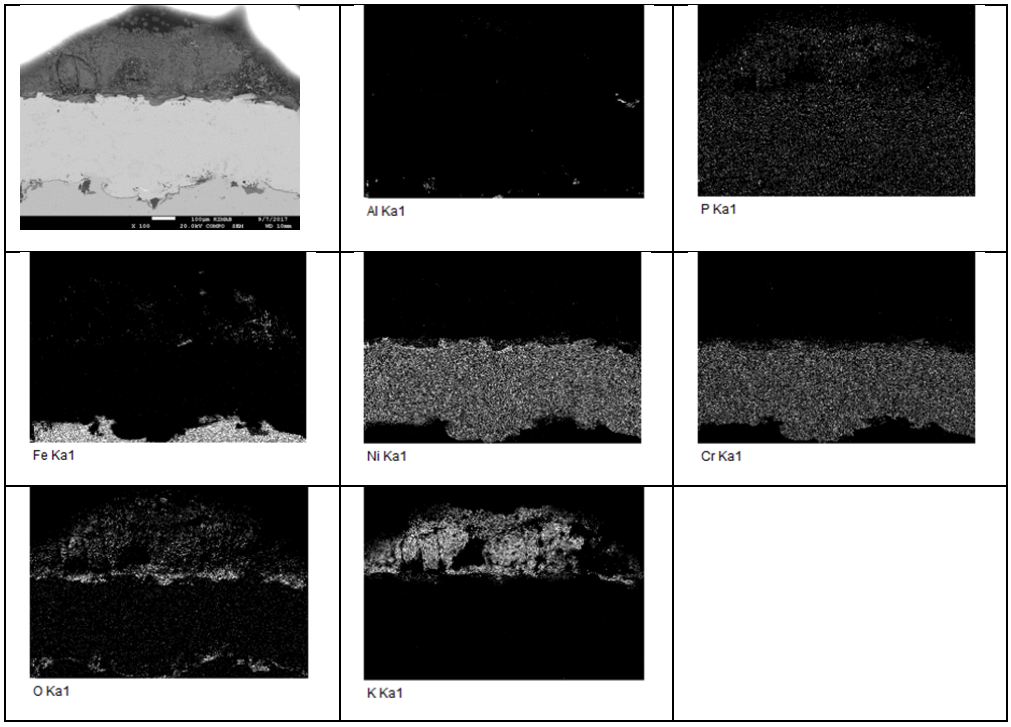

Figure 28. EDS analysis results of material 5 after exposure at Västhamnsverket in the superheater (SH-HT). Sample removed from site in 2017. Scale bar in the SEM image is 100 µm.

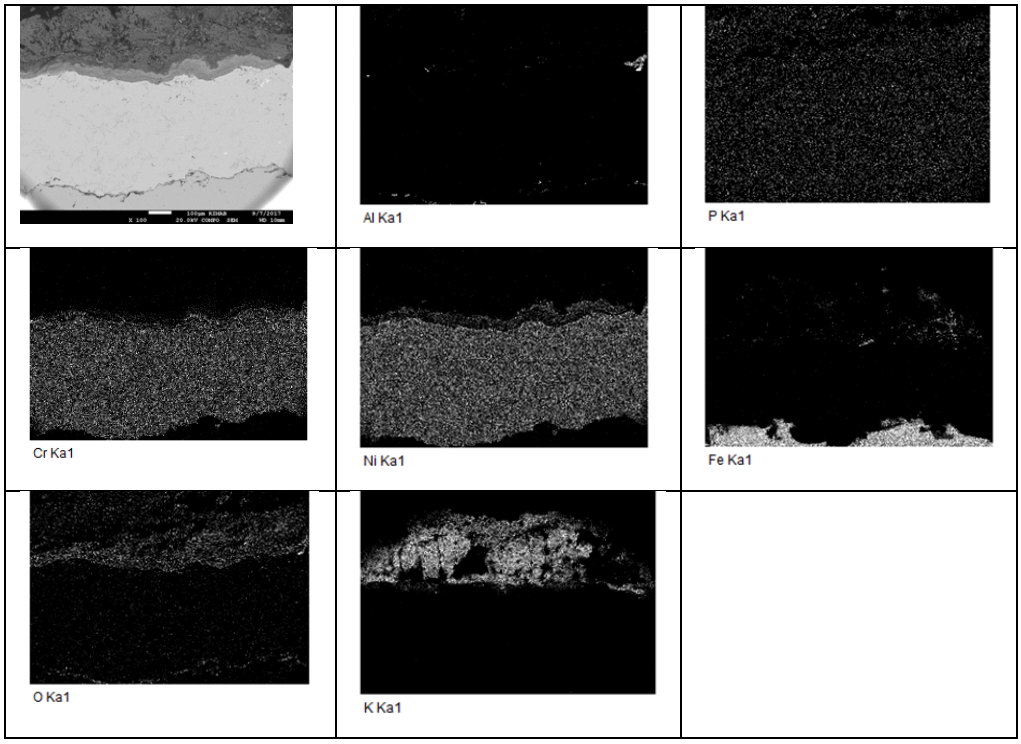

Figure 29. EDS analysis results of material 5 after exposure at Västhamnsverket in the superheater (SH-HT). Sample removed from site in 2017. Scale bar in the SEM image is 100 µm.

Material 9 also showed a thick deposit layer (Figure 30-Figure 32). In some instances, the CMP layer had detached from the base material. No increased signal for boron or nitrogen could be detected at the CMP surface. A slight increase in the oxygen signal was observed at the CMP surface, indicating an oxide layer. At the base-metal/CMP interface, areas with elevated oxygen content were observed together with Al or Si and are probably a result of the initial surface treatment of the base metal. Interesting to note is the increase in oxygen signal in the interface between CMP and base metal in Figure 32. Even though particles of SiO_2 and Al_2O_3 are expected in the interface, the signal from Al and Si do not form a continuous layer as the oxygen signal. This might indicate an initial corrosion attack and initiation of CMP detachment. Material 9 was not examined before exposure.

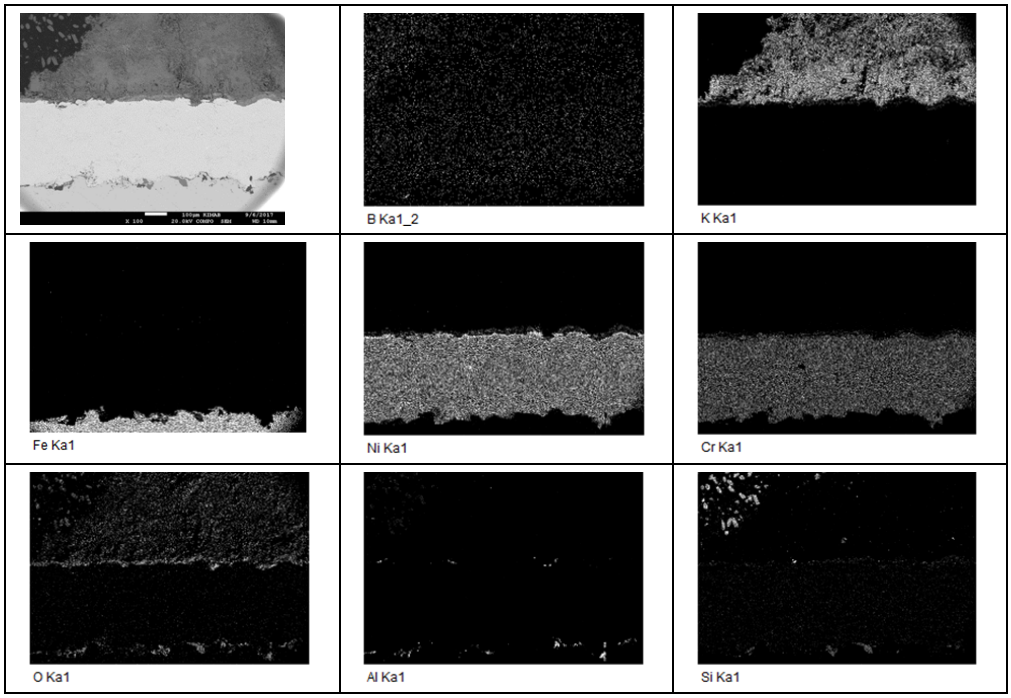

Figure 30. EDS analysis results of material 9 after exposure at Västhamnsverket in the superheater (SH-HT). Sample removed from site in 2017. Scale bar in the SEM image is 100 µm.

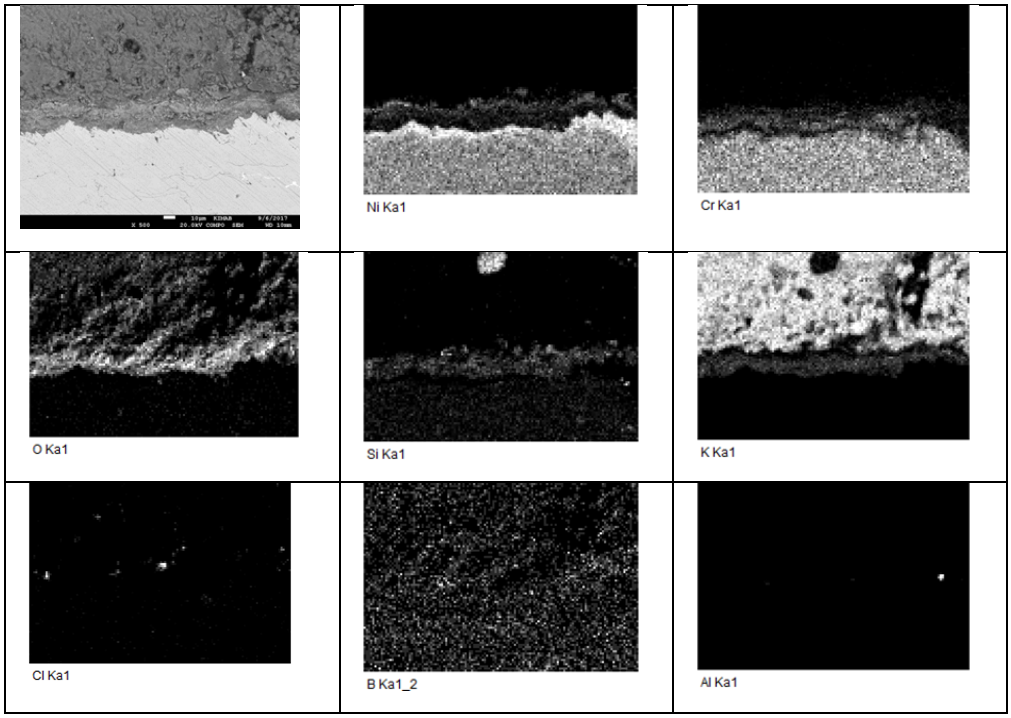

Figure 31. EDS analysis results of material 9 after exposure at Västhamnsverket in the superheater (SH-HT). Sample removed from site in 2017. Scale bar in the SEM image is 10 µm.

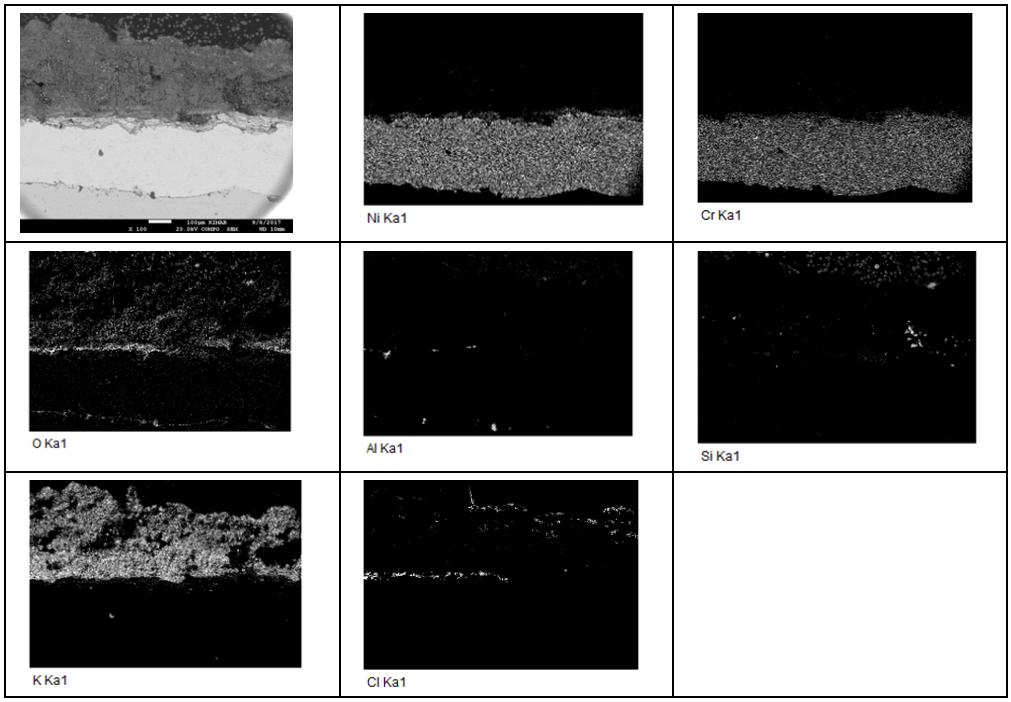

Figure 32. EDS analysis results of material 9 after exposure at Västhamnsverket in the superheater (SH-HT). Sample removed from site in 2017. Scale bar in the SEM image is 100 µm.

The graphite based Material 10 showed good adhesion of the CMP layer, but there was no elevated carbon signal at the deposit/CMP interface. The amount of deposit varied over the cross-section as shown in the images in Figure 33. A layered oxide structure with Ni and Cr was observed at the surface, with no significant increase in carbon signal at the interface between deposit and CMP layer (Figure 34). It is suggested that the layer was too thin to be observed by SEM/EDS.

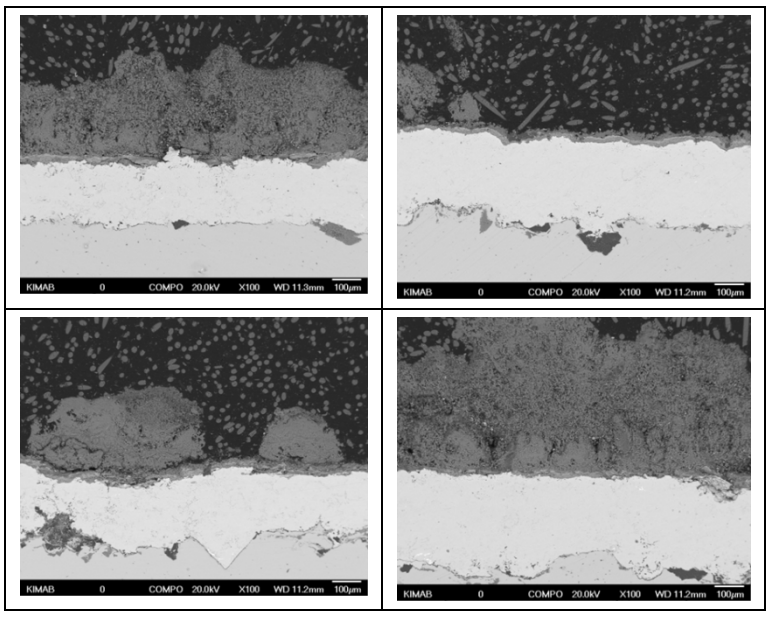

Figure 33. SEM images of material 10 after exposure at Västhamnsverket in the superheater (SH-HT). Sample removed from site in 2017. Scale bar is 100 µm at 100x magnification.

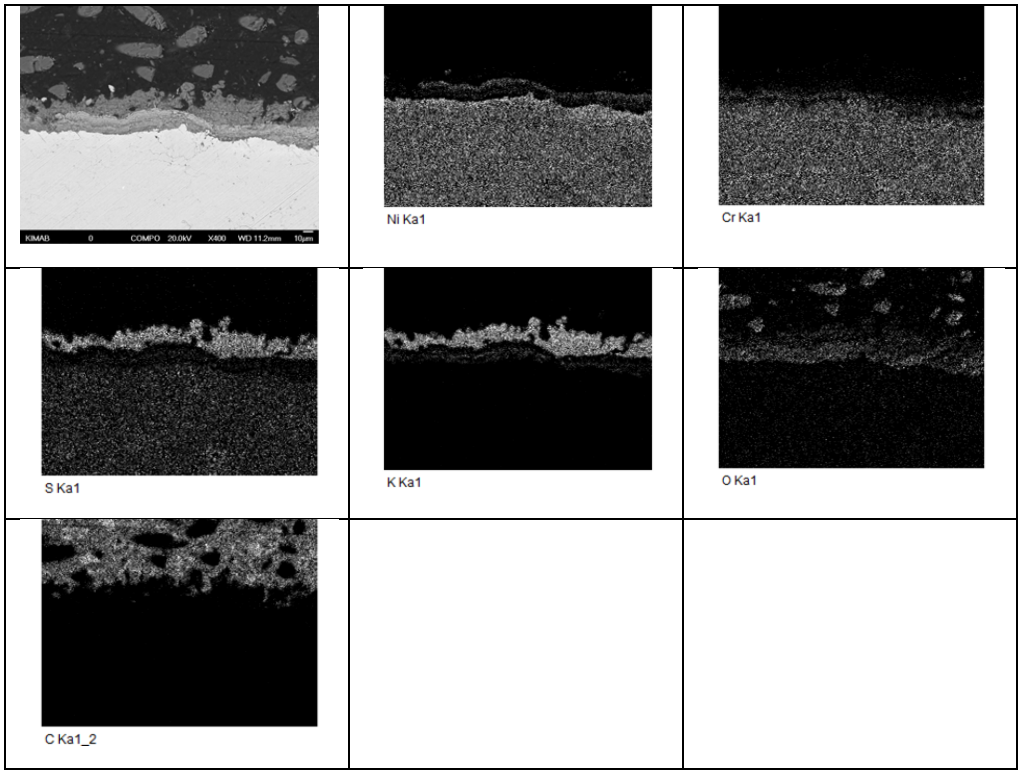

Figure 34. EDS analysis results of material 10 after exposure at Västhamnsverket in the superheater (SH-HT). Sample removed from site in 2017. Scale bar in the SEM image is 10 µm.

In summary, no top coating from materials 5, 9 or 10 could be detected. Material 10 showed areas with very little deposit. This might be due to a good release ability of the top coating, but may also depend on different handling of different samples during demounting of the samples from the superheater area.

SH-LT

Material 8, which in the wear test exposures showed presence of Al and Si in the coated layer was examined after exposure in the SH-LT region. A complicating factor is that the expected deposit layer in a CHP plant is often rich in K, Ca, Si and O due to deposits from the flue gas. Thus, it may be hard to distinguish the coating from the expected deposit. After exposure during the first season, coating could only be identified occasionally in deep pits of the sprayed metal layer. Rather, most areas where Si, O and Al were observed, also showed presence of potassium (K) or zinc. As K was not present in the analysis after wear test exposures, a probable explanation is that K originates from the environment and that the larger share of the surface layers observed in Figure 35 - Figure 36 is deposit formed during exposure in the flue gas environment. As shown, the deposit layer (indicated in the images) shows presence of K, O and Si. The Si and K are suggested to originate from the environment. However, in some deep pits, the composite metal polymer surface appears to be intact. An example is shown in Figure 37, where no K or Ca was detected in a small part of the surface layer where Si and O were observed.

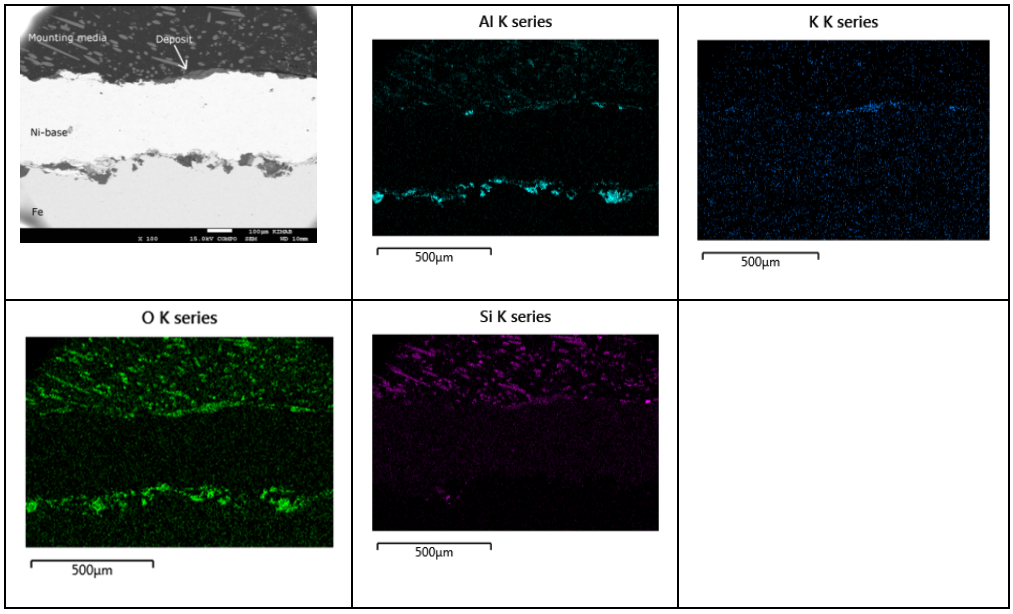

Figure 35. Back-scattered SEM image of material 8 after exposure in the superheater region (SH-LT). Sample removed 2016. Scale bar in the SEM image is 100µm at 100x magnification.

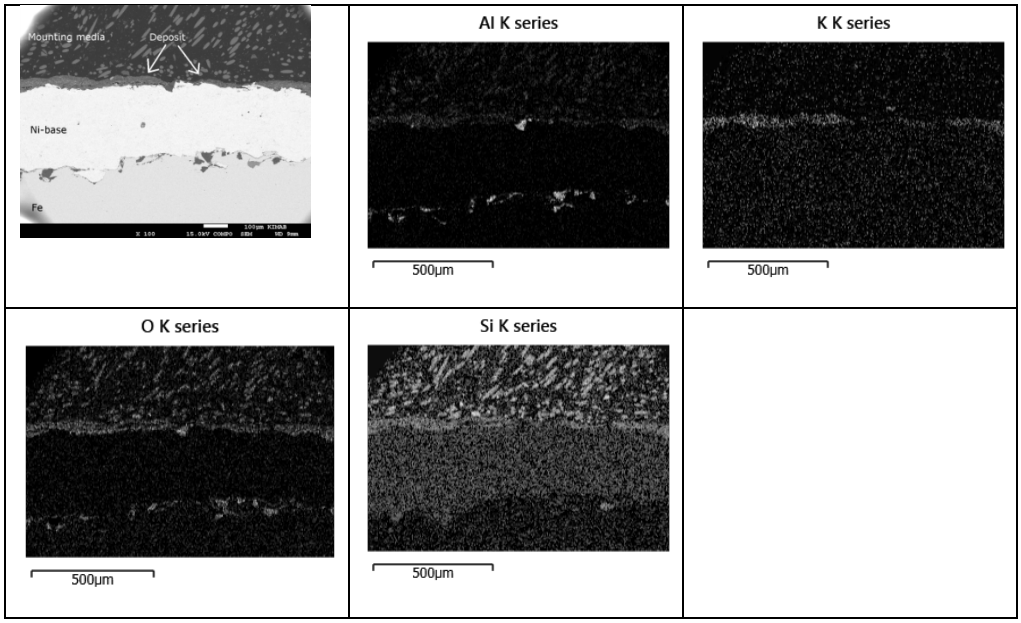

Figure 36. Backscattered image of material 8 after exposure in the SH-LT region at Västhamnsverket, sample removed 2016. The deposit is indicated in the SEM image. EDS elemental maps of Si, O, Al and K are included. The scale bar in the SEM image is at 100µm at 100 x magnification.

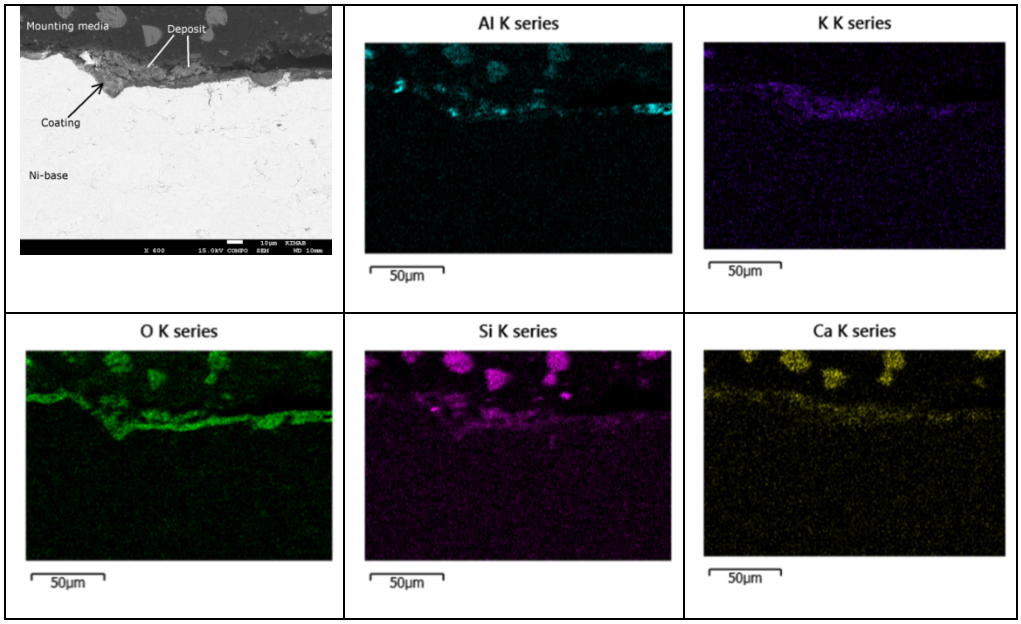

Figure 37. Backscattered image of material 8 after exposure in the SH-LT region at Västhamnsverket, sample removed 2016. The deposit is indicated in the SEM image as well as a small area with coating. EDS elemental maps of Si, O, Al, Ca and K are included. The scale bar in the SEM image is at 10µm at 600 x magnification.

Economizer

In the economiser area, material 1 and 6 were exposed. There was no apparent difference in amount of deposit formation between the samples and the surrounding tubes (Figure 38).

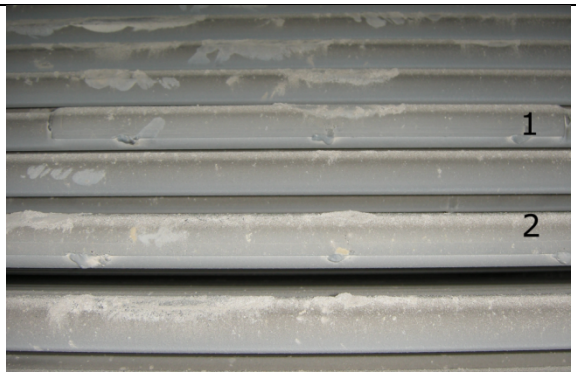

Figure 38. The tack-welded tubes in the economizer at Västhamnsverket. The tube named 1 was removed from the site in 2016 and the one named 2 in 2017.

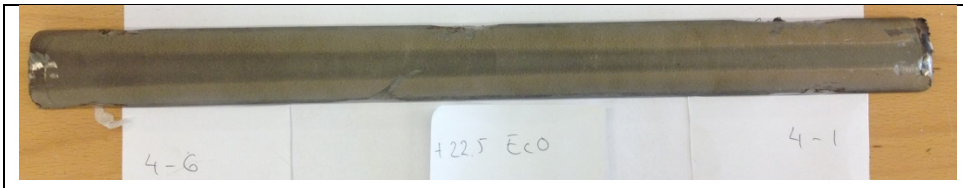

Figure 39. Material 6 (left part of tube) and material 1 (right part of tube) after exposure in the economizer. Tube removed from site in 2017.

For material 1 removed in 2016 (Figure 40), there was generally good adhesion/coverage of the PTFE layer. Good adhesion was also observed for material 1

removed in 2017, where the top coating was observed on most part of the surface (Figure 41). In most regions where the top coating was observed, the F-layer was still detected although with varying uniformity along the examined surface. More deposit including K and Cl was observed on the samples exposed for two firing seasons (removed in 2017). No pronounced difference in coverage of the PTFE layer was observed between the samples.

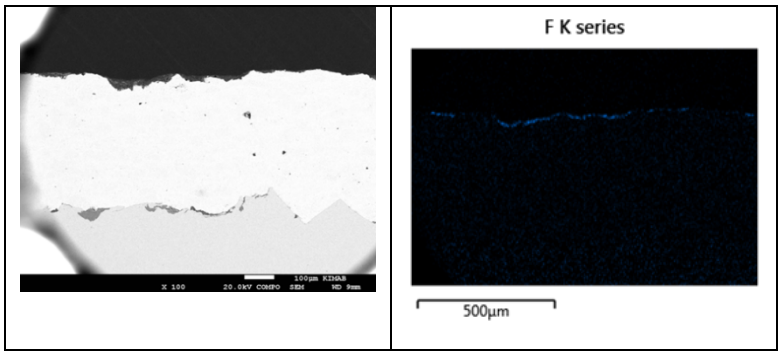

Figure 40. SEM images of material 1 after exposure at Västhamnsverket in the economizer. Sample removed from site in 2016. Scale bar is 100 µm at 100x magnification.

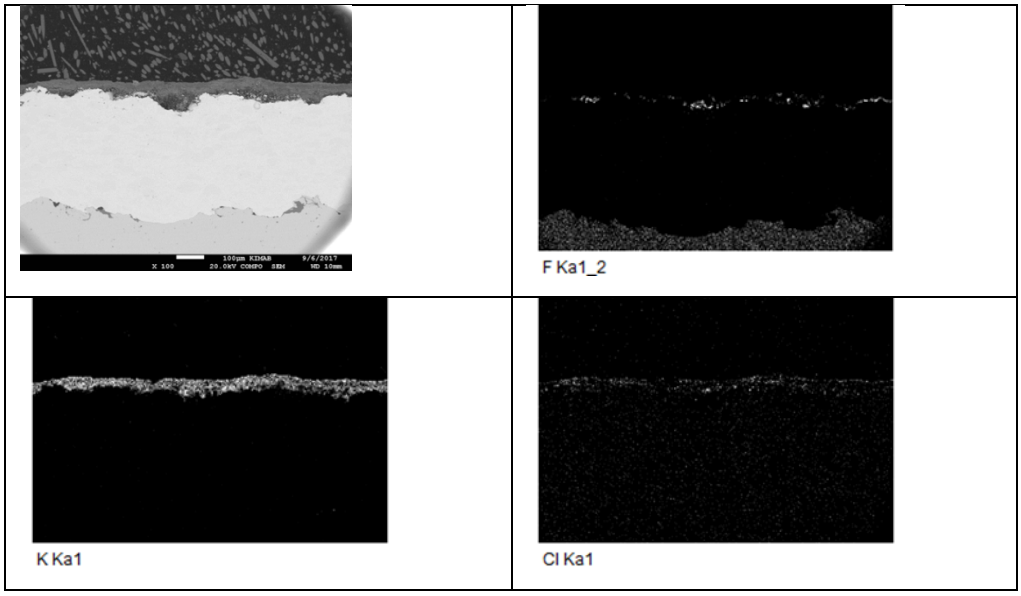

Figure 41. EDS analysis results of material 1 after exposure at Västhamnsverket in the economizer. Sample removed from site in 2017. Scale bar in SEM image is 100 µm. The fluorine signal in the carbon steel is an artefact.

For material 6 removed in 2016, there was quite poor coverage, with the coating being either very thin or missing (Figure 42- Figure 43). The coating showed varied thickness and was sometimes quite thin on as received sample as well. Presence of deposit from the flue gas may have shielded any signal from the coating and made it difficult to compare the top coating coverage between the two samples. Thus EDS signal from K is included to image the parts of the deposit possibly originating from the flue gas. It cannot be excluded that K has been incorporated in the top coating. For the material removed in 2017, there was only sporadic detection of Si (Figure 44-Figure 45)

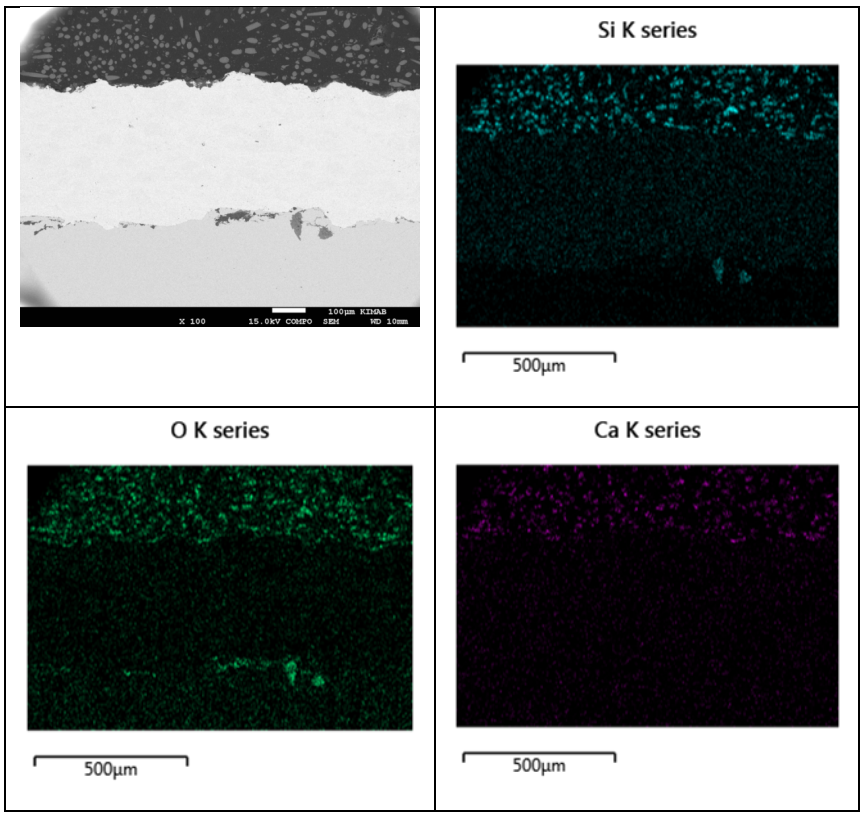

Figure 42. SEM images of material 6 after exposure at Västhamnsverket in the economizer. Sample removed from site in 2016. Scale bar at 100x magnification is 100 µm. EDS analysis for O and Si included to image that the coating is absent. Ca included as reference for deposit originating from exposure.

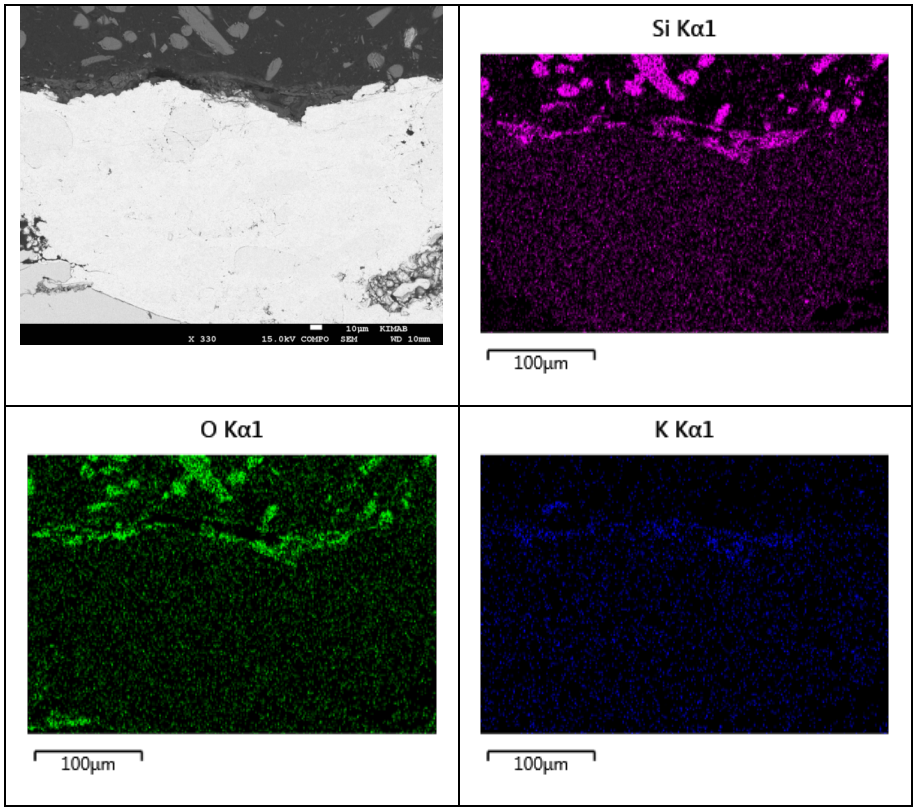

Figure 43. SEM images of material 6 after exposure at Västhamnsverket in the economizer. Sample removed from site in 2016. Scale bar at 330x magnification is 10 µm. EDS analysis for O and Si included to image that the coating is absent. K included as reference for deposit originating from exposure.

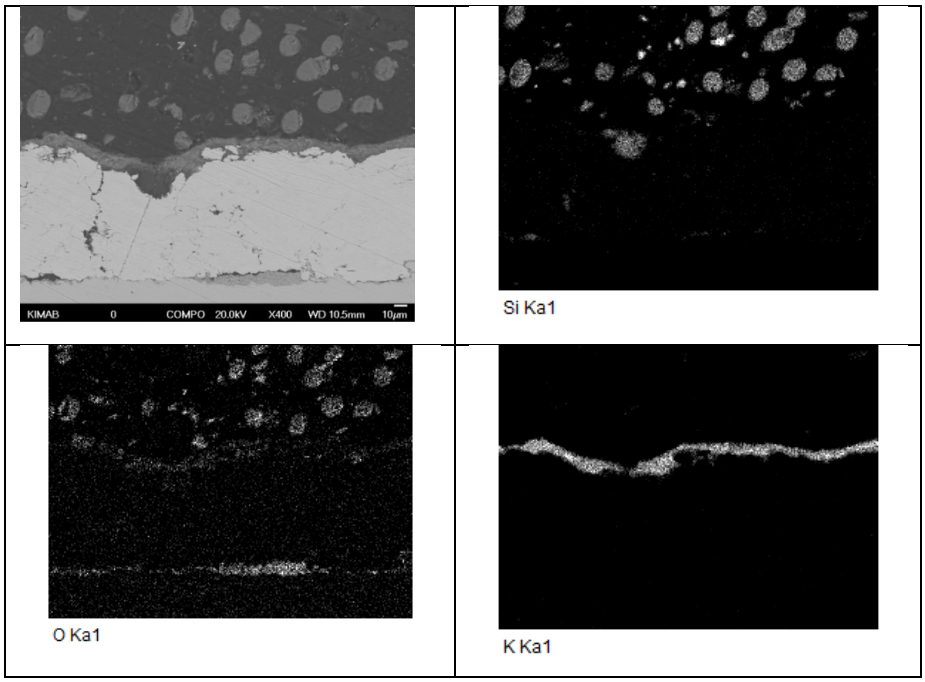

Figure 44. SEM images of material 6 after exposure at Västhamnsverket in the economizer. Sample removed from site in 2017. Scale bar at 400x magnification is 10 µm. EDS analysis for O and Si included to image the coating. K included as reference for deposit originating from exposure. The top coating is absent in present images.

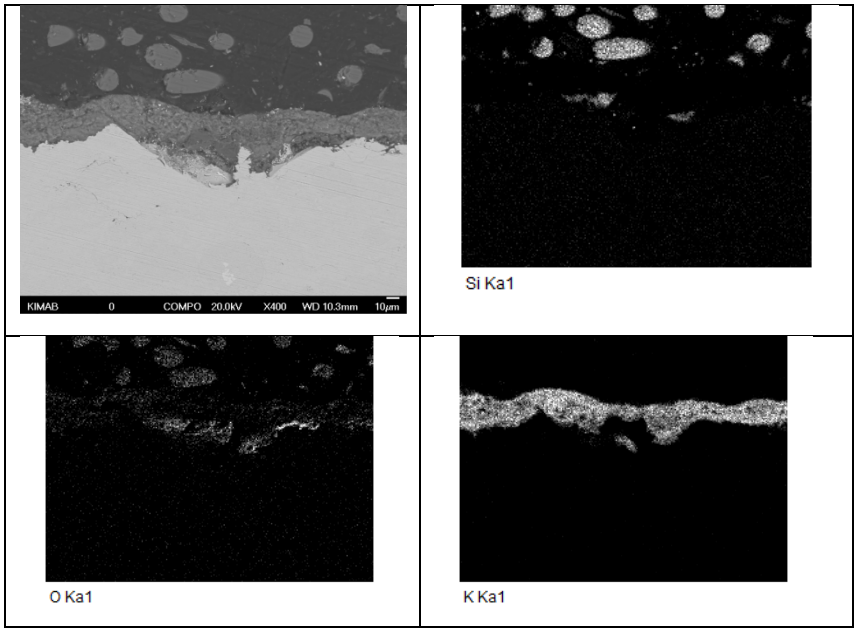

Figure 45. SEM images of material 6 after exposure at Västhamnsverket in the economizer. Sample removed from site in 2017. Scale bar at 400x magnification is 10 µm. EDS analysis of O and Si are included to image that the top coating is absent. K included as reference for areas of deposit originating from the exposure.

ESP Cone

In the ESP Cone, the deposit layer was observed to be very loosely adherent by visual inspection and slight brushing (Figure 46-Figure 47).

Figure 46. Photographs showing the position of the samples in the electrostatic filter (arrowed, left) and the two sample panels removed from their position (right). While the panel marked ”1” was brushed slightly after removal, the deposits of the samples are clearly observed in the panel marked ”2”.

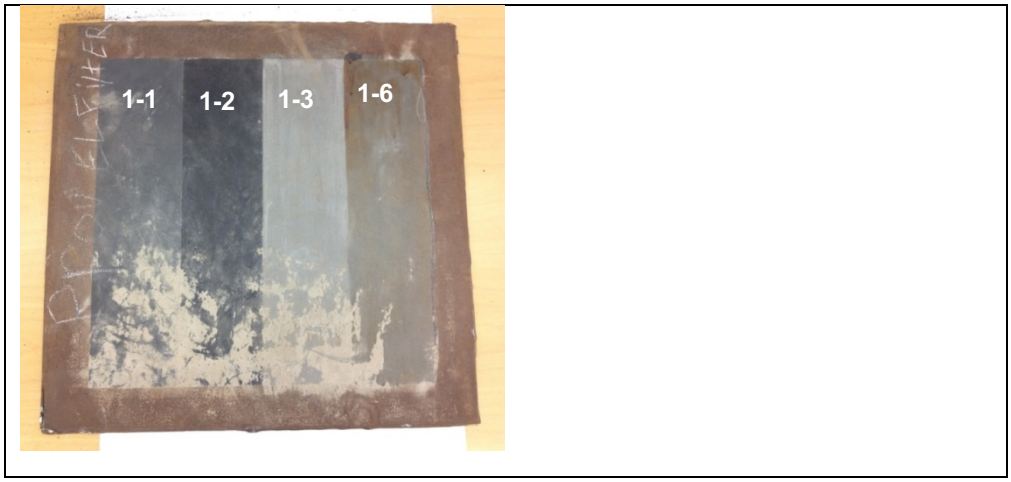

Figure 47. Material (from left) 1, 2, 3 and 6 after exposure in the ESP cone. Plate removed from site in 2017.

For material 1 removed in 2016, good adherence of the PTFE layer was detected (Figure 48-Figure 49). Similarly good adhesion of the top coating was observed for the material removed in 2017, although it was missing in some regions (Figure 50-Figure 51). The amount of deposit was very low on the samples as discussed above.

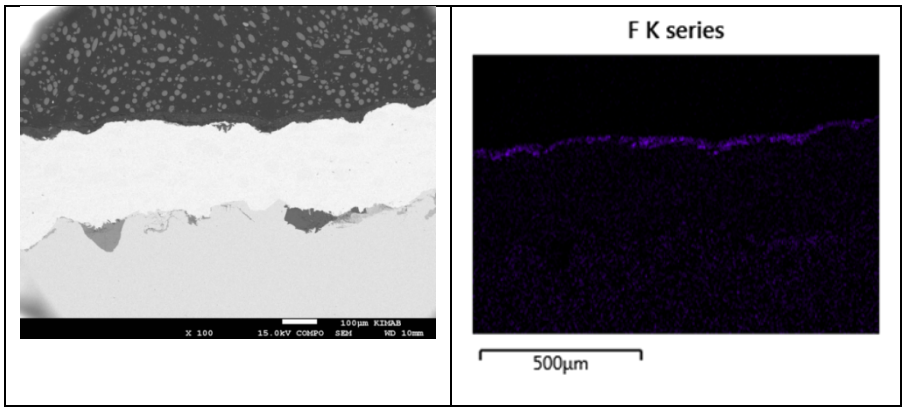

Figure 48. SEM images of material 1 after exposure at Västhamnsverket in the ESP cone. Sample removed from site in 2016.Scale bar at 100x magnification is 100 µm. EDS analysis of fluorine included to the right.

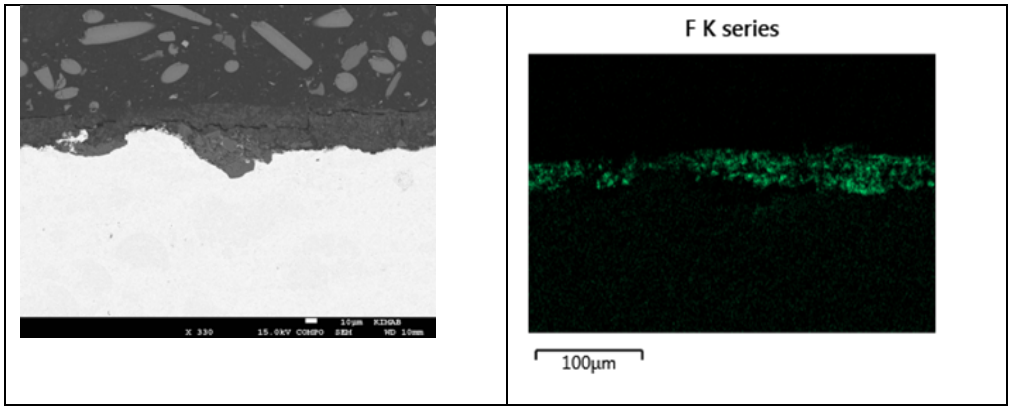

Figure 49. SEM image at 330x magnification and EDS analysis of F of material 1 after exposure at Västhamnsverket in the ESP cone. Sample removed from site in 2016. Scale bar in SEM image is 10 µm.

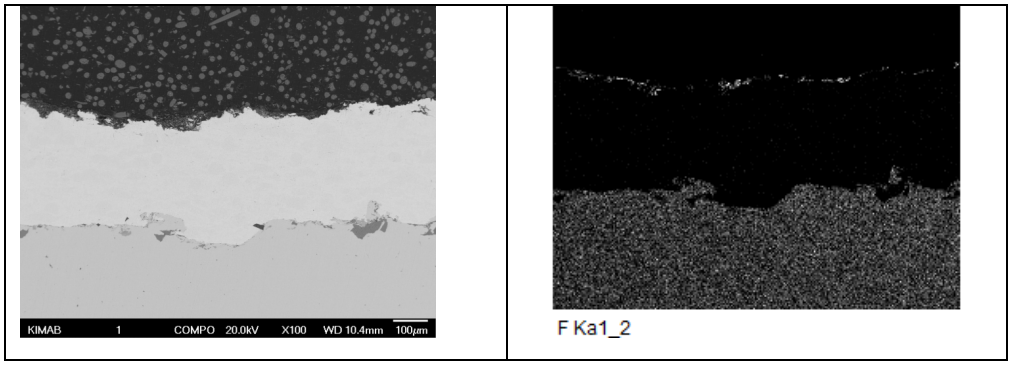

Figure 50. SEM image at 100x magnification and EDS analysis of F of material 1 after exposure at Västhamnsverket in the ESP cone. Sample removed from site in 2017. The fluorine signal detected in the base material is an artefact. Scale bar in SEM image is 100 µm.

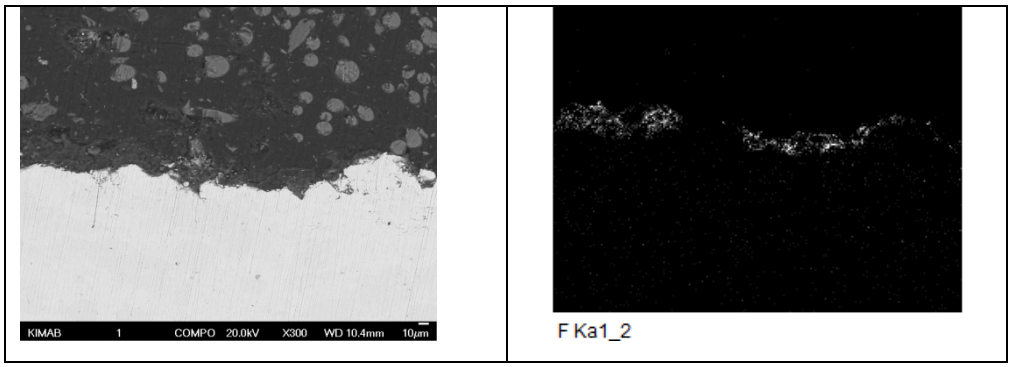

Figure 51. SEM image at 300x magnification and EDS analysis of F of material 1 after exposure at Västhamnsverket in the ESP cone. Sample removed from site in 2017. Scale bar in SEM image is 10 µm.

Good adhesion of the polysiloxane coating was observed for material 6 removed in 2016 (Figure 52-Figure 53). Fairly good silicone coverage, although somewhat reduced, was recorded on the sample removed in 2017 (Figure 54-Figure 55). As shown in the EDS analyses, very little deposit from the flue gas was observed on the samples. This is suggested to be due to loosely adherent deposit layers.

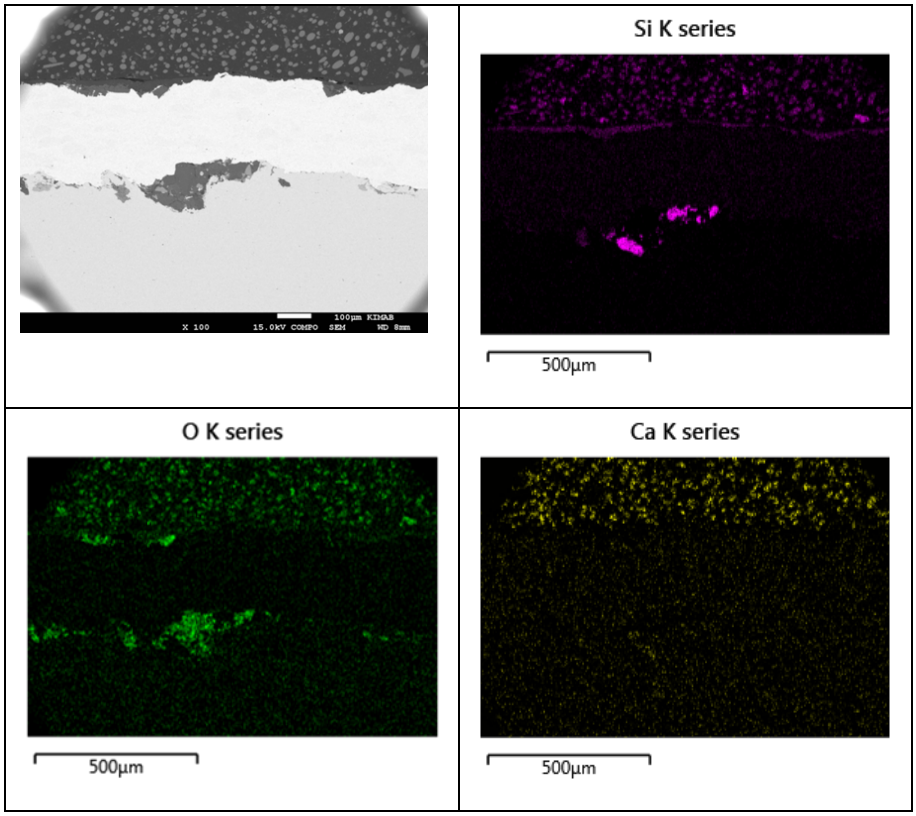

Figure 52. EDS analysis of material 6 exposed in the ESP Cone at Västhamnsverket. Sample removed from site in 2016. Scale bar in SEM image 100µm.

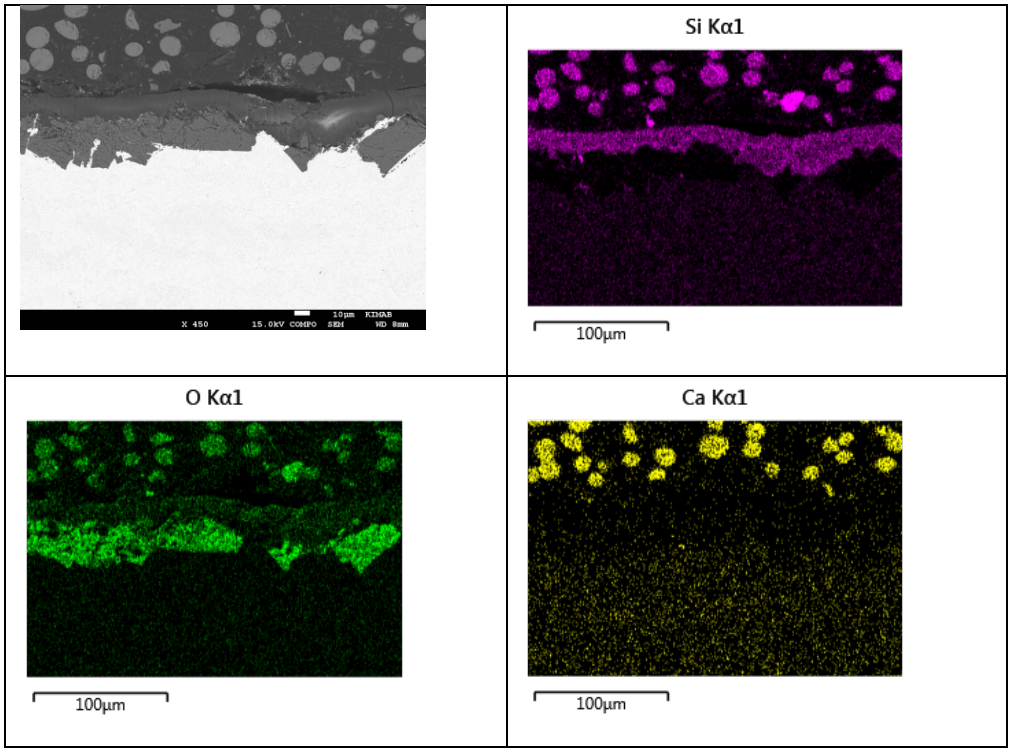

Figure 53. EDS analysis of material 6 exposed in the ESP cone at Västhamnsverket. The sample was removed from the site in 2016. The scale bar in the SEM image is 10 µm.

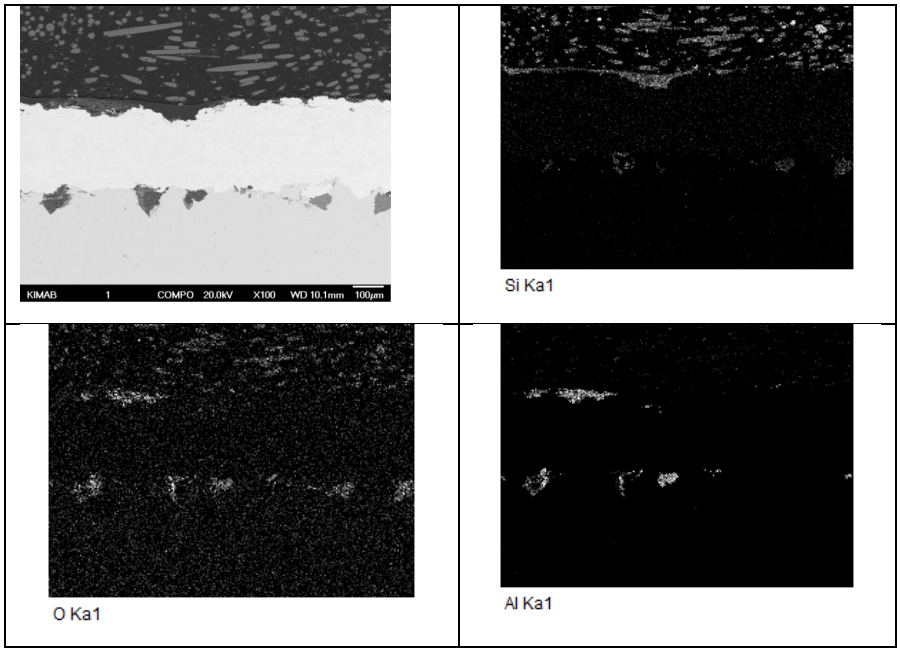

Figure 54. EDS analysis of material 6 exposed in the ESP cone at Västhamnsverket. The sample was removed from the site in 2017. The scale bar in the SEM image is 100 µm. No deposit layer including Ca or K could be identified in the analysis.

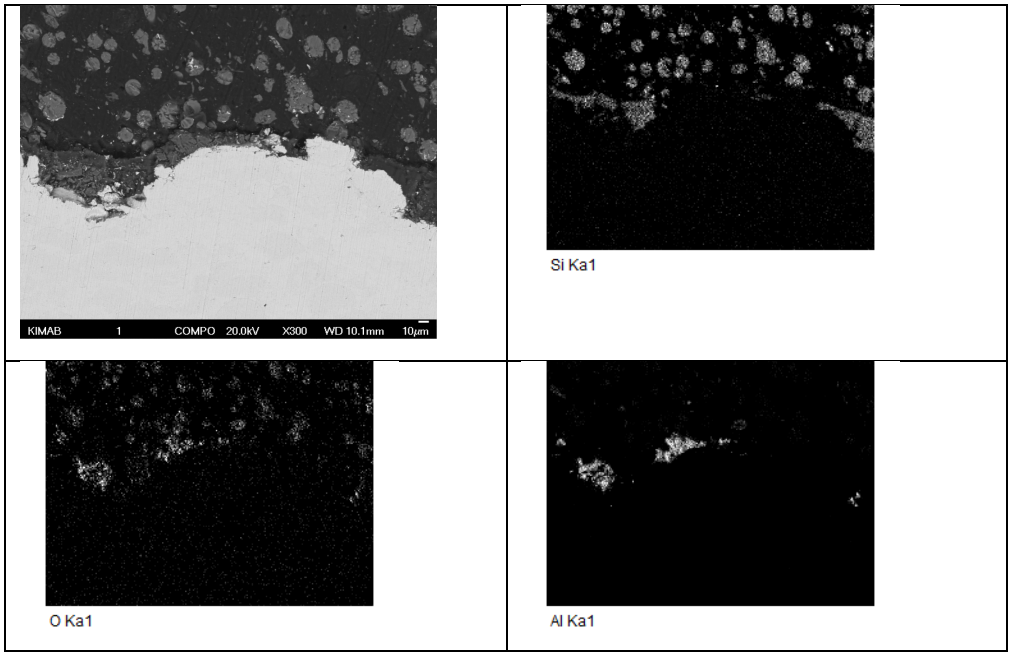

Figure 55. EDS analysis of material 6 exposed in the ESP cone at Västhamnsverket. The sample was removed from the site in 2017. The scale bar in the SEM image is 100 µm. No deposit layer including Ca or K could be identified in the analysis. The scale bar in the SEM image is 10 µm.

The flue gas recirculation fan wheel

The flue gas recirculation fan was originally sprayed with the polymeric material 1 as top coating in 2013 (Figure 56) At inspection in 2014, 2015 and 2017, the fan was photographed (Figure 57-Figure 59). As shown, the amount of deposit on the wheel is small and the sprayed coating is still visible after 4 years of operation. The maintenance

was performed only once the first firing season compared to once a week before the application. No data are known regarding maintenance the following firing seasons.

Figure 56. The flue gas fan after application of CMP in 2013

Figure 57. The flue gas fan at inspection 2014

Figure 58. The flue gas fan at inspection 2015

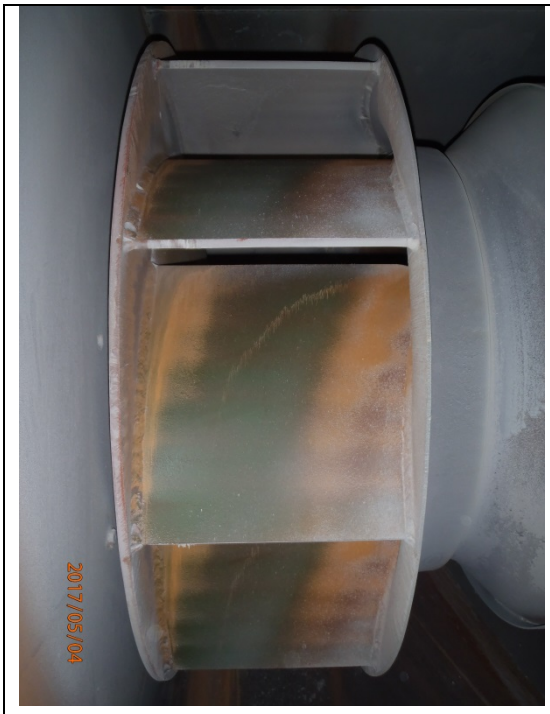

Figure 59. The flue gas fan at inspection 2017

3.5.2 Ørsted /Avedöre

SH-HT (Position A)

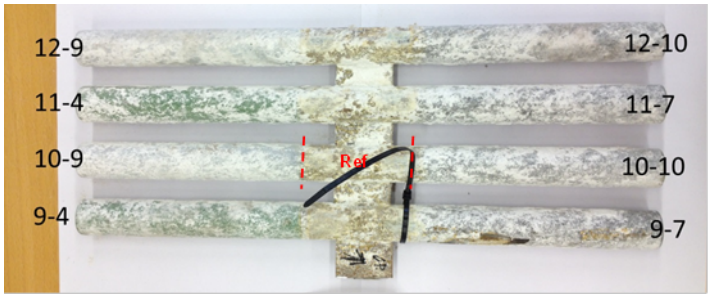

Figure 60. Photographs of tubes coated with material 4, 7, 9 and 10 (as highlighted in picture) after exposure at Ørsted /Avedöre in the superheater (SH-HT). Tubes were removed from site in 2017. Reference sample was taken from non-coated region within dashed lines. Metallographic examination was carried out for the reference sample and samples 9-4, 9-7, 10-9 and 10-10.

An image of the exposed materials 4, 7, 9 and 10 from position A is shown in Figure 60. By visual inspection, no difference in amount of deposit could be observed. The reference sample showed presence of K, P and S in the deposit layer. Also some oxide was observed, given by the signal of O and Fe (Figure 61). Material 4 was a boron-nitride silicate and material 9 a boron-nitride. For material 4, the silicon signal after exposure was more pronounced than for the reference material (Figure 61-Figure 62). However, in both cases, a distinct potassium layer was observed on the surface. For material 4, it is suggested that potassium might have interacted with the silicate layer. Boron could not be distinguished. For material 9, no top coating with boron nitride

could be observed after exposure (Figure 63). One reason might be a very thin top coating. As no unexposed material was analysed, no clear conclusions could be drawn regarding the expected appearance. Material 10 used a graphite based top coating. The graphite based top coating was not possible to detect in SEM/EDS.

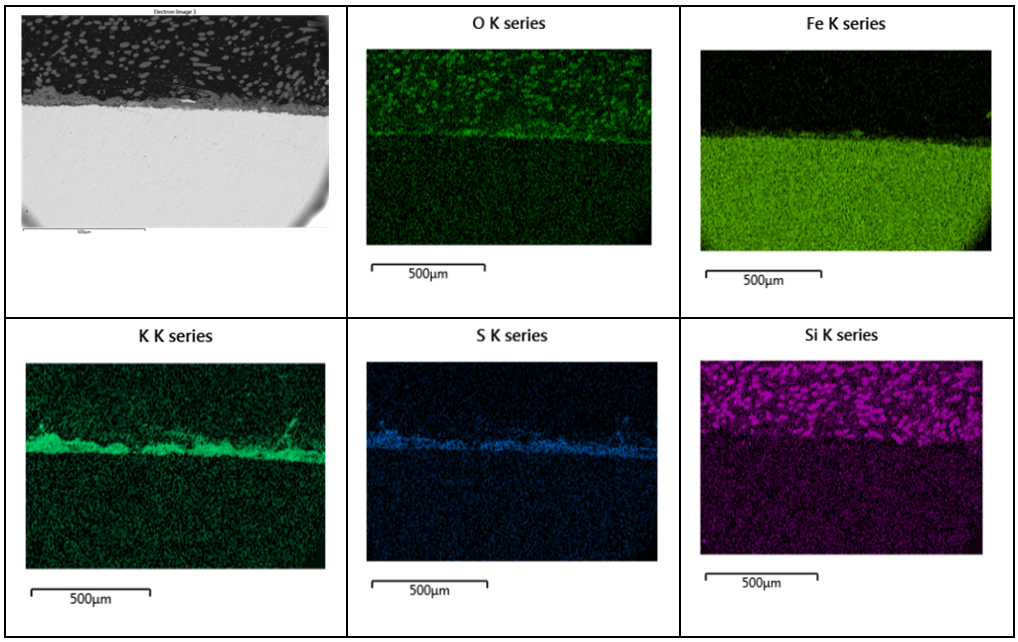

Figure 61. EDS analysis results of carbon steel reference sample after exposure at Ørsted /Avedöre in position A (SH-HT). Sample removed from site in 2017. Scale bar in SEM image is 500 µm.

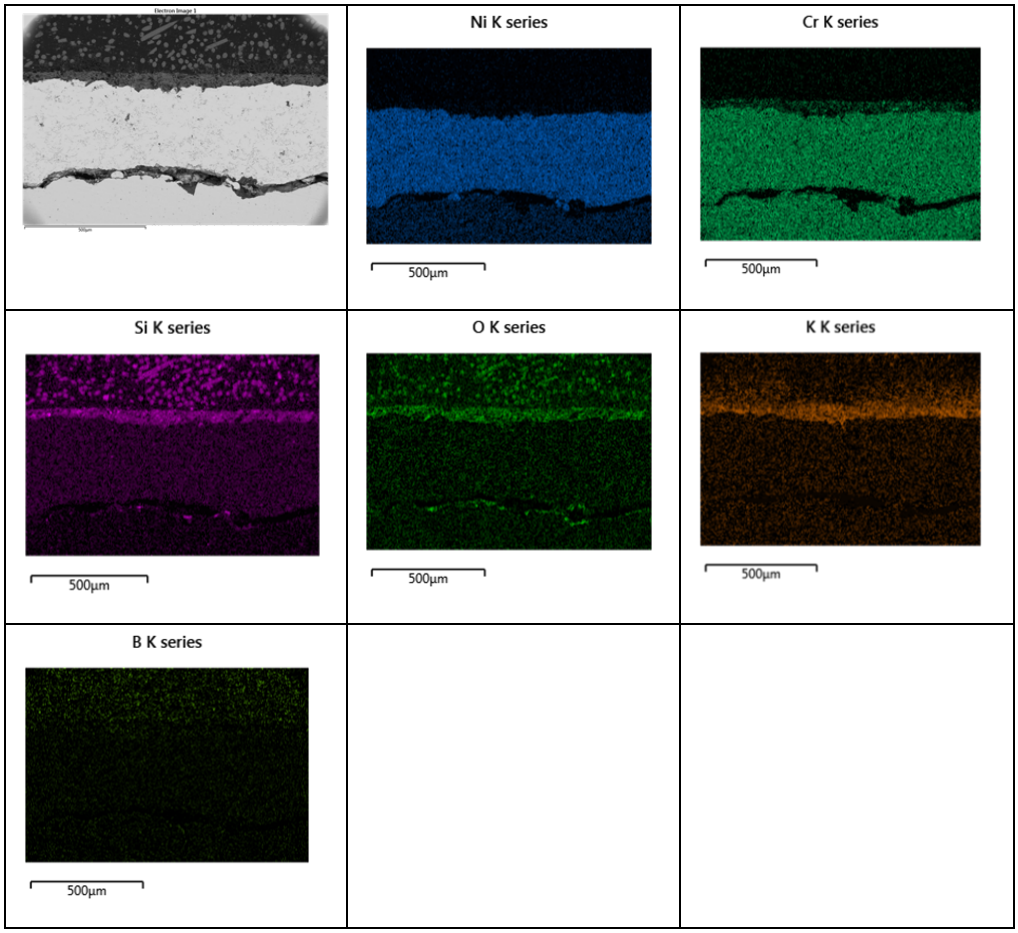

Figure 62. EDS analysis results of material 4 after exposure at D Ørsted /Avedöre in position A (SH-HT). Sample removed from site in 2017. Scale bar in SEM image is 500 µm.

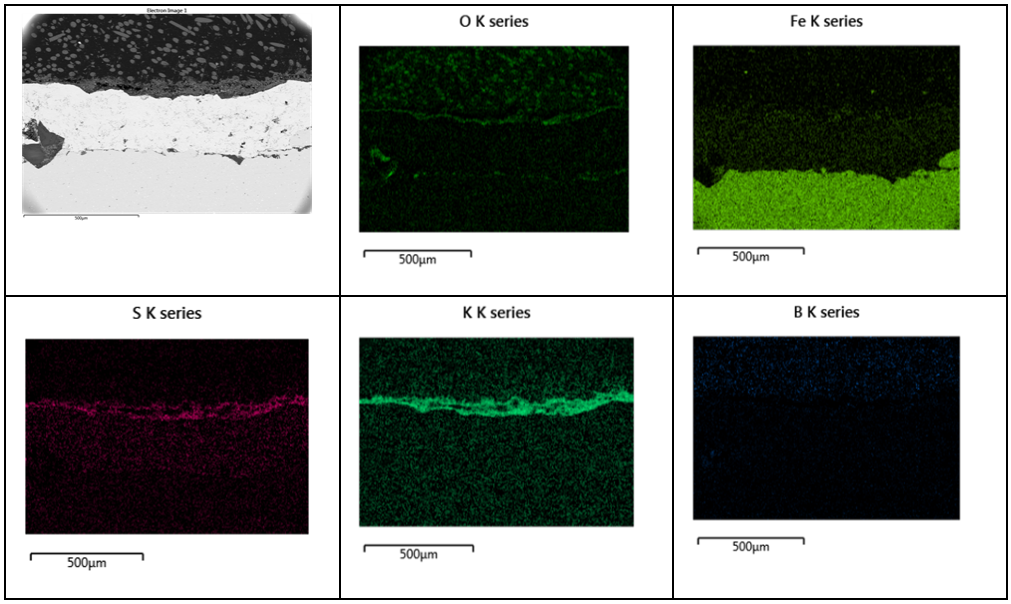

Figure 63. EDS analysis results of material 9 after exposure at Ørsted /Avedöre in the superheater (SH-HT). Sample removed from site in 2017. Scale bar in SEM image is 500 µm.

SH-1-LT (Position B)

A photograph of the sample mounted in position B before exposure is given in Figure 64. After exposure (Figure 65), position B in Avedöre shows approximately equal amount of deposit on the sprayed areas as on the middle, reference areas. As only one firing season was included in the project, only material 8, sample 8-8, and a reference were examined in detail.

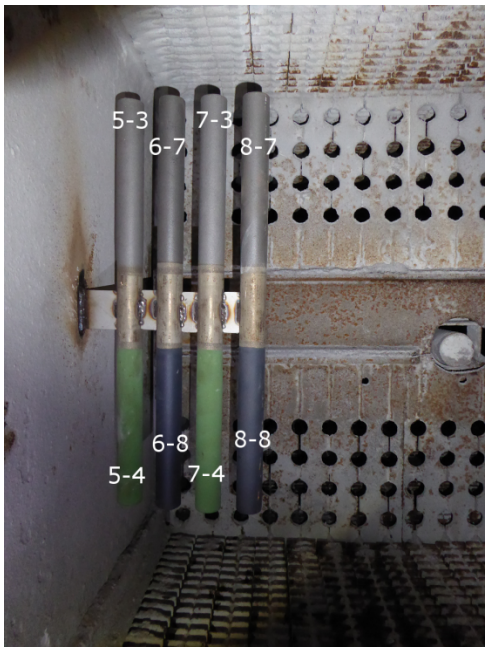

Figure 64. Image of the samples before exposure in position B (SH-1-LT) in Avedøre. The sample numbers are indicated in the image.

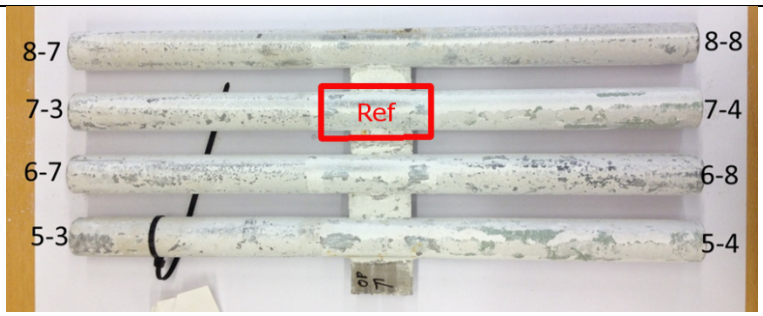

Figure 65. Photographs of the samples after exposure at Ørsted /Avedöre in the superheater (SH-1-LT). The tubes were removed from the site in 2017. A reference sample (indicated) was taken from the middle non-coated region.

If the signal for Si is compared between material 8 and the reference (Figure 66 - Figure 67), the Si signal at the metal surface might be somewhat more distinct on material 8 (Figure 66). This indicates possible presence of the silicone layer on the test sample. A deposit layer rich in K/S/O/Cl was detected at the surface of both samples. Following sample preparation, there was occasional large crevice between the sample of material 8 and the mount, but there was still good adherence of the silicone layer.

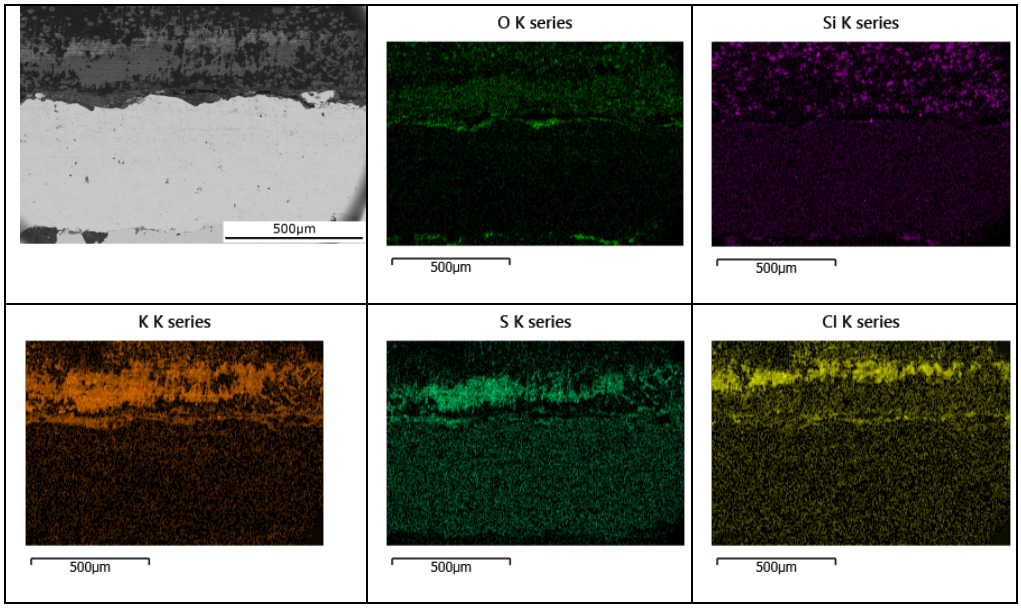

Figure 66. Back-scattered image of material 8 exposed in position B in Avedöre. EDS analysis included for given elements. The sample was removed from the site in 2017.

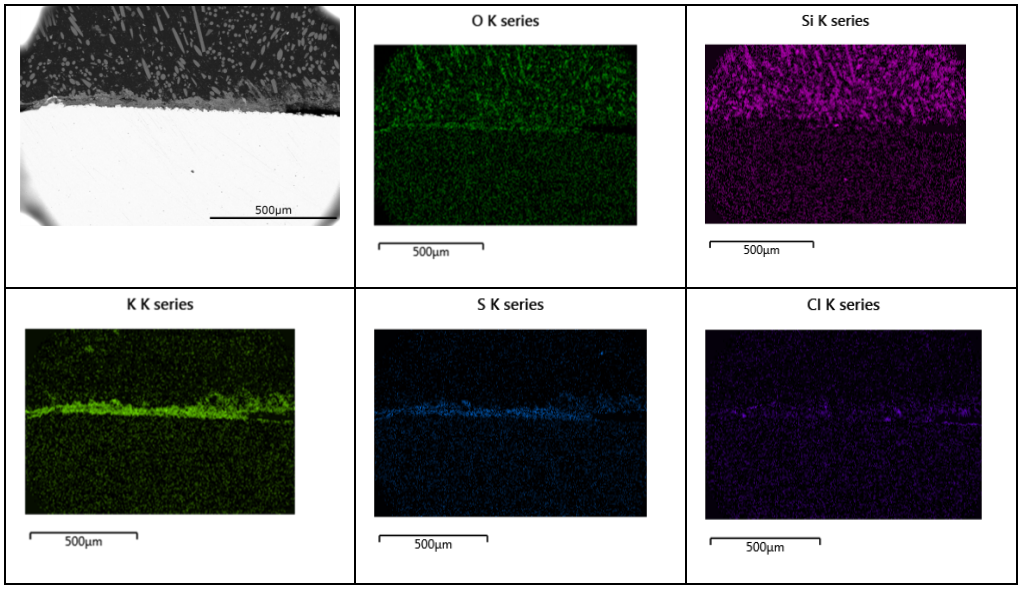

Figure 67. Back-scattered image and EDS analysis of reference sample from position B in Avedöre. EDS analysis included for given elements. The sample was removed from the site in 2017.

Economiser (Position C)

An image of the unexposed and the exposed samples of position C are shown in Figure 68and Figure 69. The amount of deposit on coated and un-coated areas of the uncooled samples was approximately equal after the exposure in position C.

Figure 68. Photograph of the samples mounted in position C in Avedöre before exposure. Sample ID indicated in the image. The scale bar is approximate.

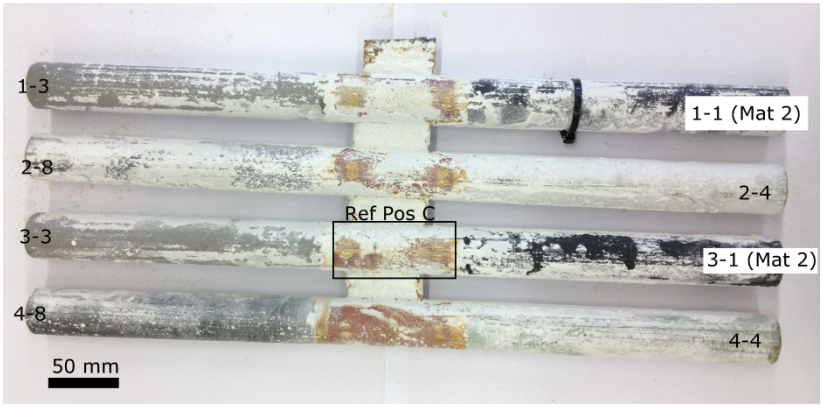

Figure 69. Photograph of the coated tubes with sample ID noted in the image after exposure at Ørsted /Avedöre in position C. The tubes were removed from the site in 2017. The reference sample was taken from the indicated area. Note that material 2 was exposed as samples 3.1 and 1.1

For material 8, the coverage after exposure was good for the coating after exposure. Some examples are given in Figure 70-Figure 72. A deposit layer was observed including K/Cl/Ca/S/O and some Si, which made the analysis a little more uncertain regarding origin of the Si. EDS analysis of the non-coated carbon steel reference material was included for comparison.

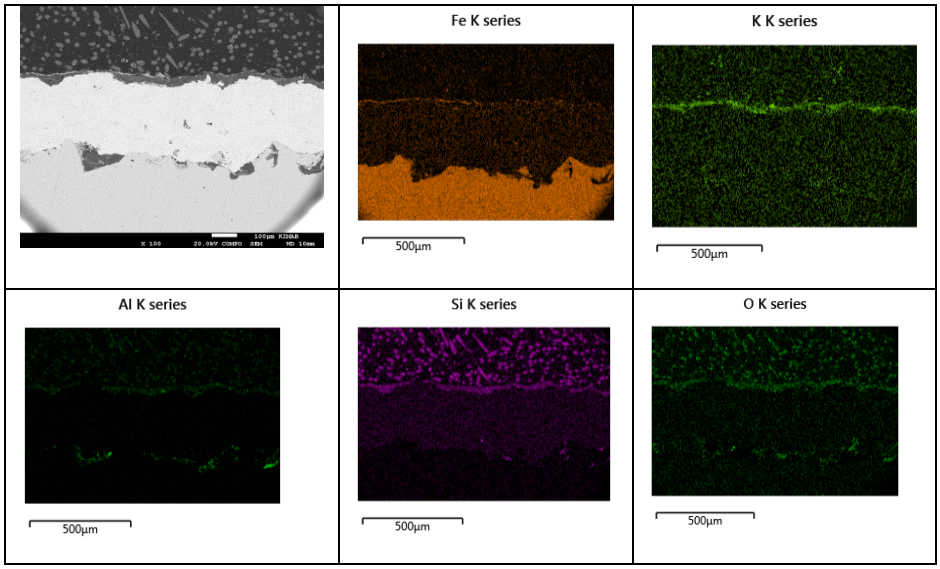

Figure 70. Back-scattered image and EDS analysis of material 8 after exposure in Position C in Avedöre. The scale bar in the SEM image is 100µm.

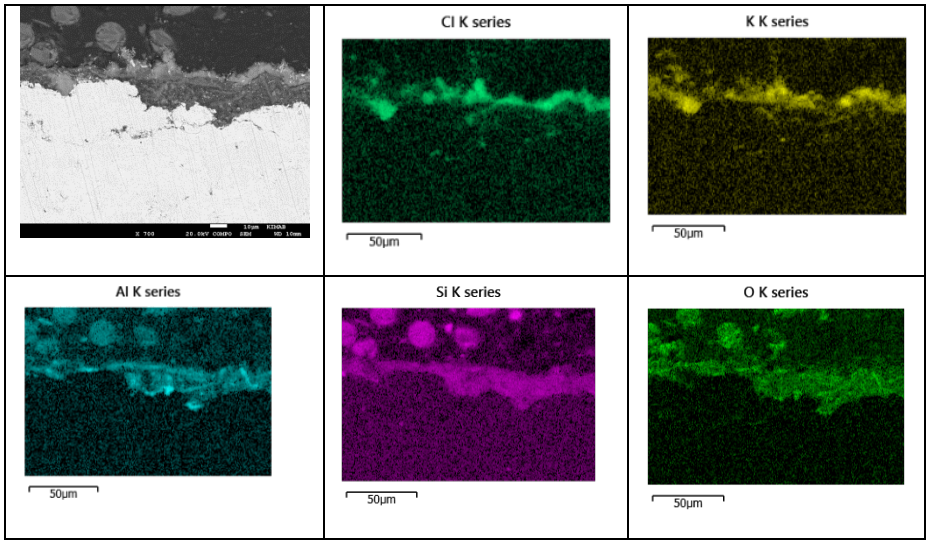

Figure 71. Back-scattered image at 700x magnification and EDS analysis of material 8 after exposure in Position C in Avedöre. The scale bar in the SEM image is 10µm.

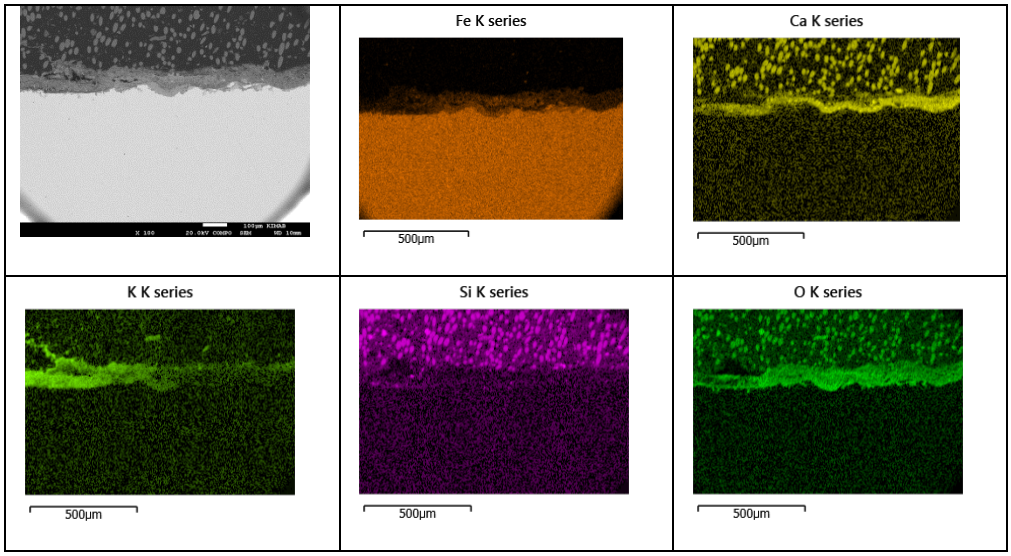

Figure 72. Back-scattered image and EDS analysis of the reference material (carbon steel) after exposure in position C in Avedöre. The sample was removed from the site in 2017. The scale bar in the SEM image is 100µm.

4 Analysis of the results

The wear test is a preliminary test to choose candidates that are more or less prone to degradation by wear. In the wear tests, all materials showed some degradation of the outer top coating. Material 10, which is a graphite base paint, showed almost no top coating after only 30 minutes wear test. A non-optimised heat treatment could not be excluded. The polymer top coatings were also examined by droplet tests. These tests did not give any significant results, to a high extent dependent on the different degree of wear at different parts of the samples. This caused a large spread in the results. To compare the wear test and use these results for ranking of materials at exposure in a furnace is not easy. In the furnace, erosion by particles is expected to be the more severe process. Also the tests were performed with water as liquid and at room temperature. In the furnace, the samples will be exposed to high temperatures and to deposits with substances such as sulphates and chlorides that may have other wetting characteristics than water. Even so, the wear test showed what candidates that had a good behaviour at room temperature and which had not.

The laboratory exposures performed at 400 and 600°C for material 1 (AluReleco, PTFE) shows no clearly identified layer of PTFE after the exposures. For the sample exposed at 500°C, fluorine could be occasionally detected in partly shadowed areas on the surface of the sample. This might indicate sample surface variation regarding the coverage or surface topology between different areas of a sample. No fluorine components were observed in the mass spectrometer measurements. However, in the exposure where the temperature was gradually increased to 600°C, the ion current for CO_2 shows a peak starting at 450°C that gradually disappears within less than an hour. It is suggested that CO_2 is formed during the degradation of the PTFE layer. Comparing these results with a CHP plant, it is suggested that material 1 could be used at slightly higher temperatures than the given max temperature (250°C) for shorter time periods.

The analysis method using SEM/EDS was straight-forward for material 1, as this material was made with fluorine in the top coating. This element is normally not observed in deposits of a CHP plant and the surface layer could be easy distinguished. For the materials using polysiloxane (materials 6 and 8), the analysis was not quite as simple. Silicon is often observed in deposits of CHP plants. Thus, a combination of silicon with either potassium, calcium or chlorine was used to identify areas where silicon was probably part of a deposit layer. It could not be excluded that the top coating, is still present, but that the deposit elements have been incorporated by for example mechanical damage and multiple cracks in the top coating.

The samples of materials 4, 5, 9 and 10 that were exposed in high-temperature areas showed no clear top coating layer after exposure in neither Västhamnsverket nor Avedöre. However, as these materials were not examined before exposure, no conclusions regarding the possibility to observe the top coating by SEM/EDS could be drawn. A slight decrease in amount of deposit was observed on the graphite based material 10. However, the difference could be due to handling of the samples during demounting. No photographs before demounting were taken.

The plant exposed samples of materials 1 and 6 have been exposed in low-temperature regions (ESP Cone and Economiser, Västhamnsverket), while material 8 has been

exposed at higher temperatures (SH-LT, Västhamnsverket; SH-1-LT (Position B) and Economiser (Position C) in Avedöre).

For the samples exposed in the economizer at Västhamnsverket, material 1 showed good coverage of the top coating after exposure, while material 6 showed quite poor coverage. The amount of deposits in the area was generally low and they were loosely adherent. There was no obvious difference between the amount of deposits on the samples compared to surrounding material.

For the samples exposed in the ESP cone at Västhamnsverket, material 1 showed good adherence, but in some regions the top coating was missing. Material 6 showed in general fairly good coverage. There was no obvious difference in deposit formation on surrounding areas compared with the coated areas of the panels.

Material 8 was exposed in Västhamnsverket (SH-LT) and in Avedöre (SH-1-LT (Positions B) and Economiser (Position C)). At Västhamnsverket, material 8 showed intermediate adhesion with almost no or missing top coating in others. In position B in Avedöre, good adhesion was observed for material 8. The amount of deposit was compared between material 8 and the reference material. If all images are observed, no clear difference could be observed regarding the amount of deposit on material 8 compared with the reference material. In the economizer region (position C), very good coverage of material 8 was observed. The amount of deposit was very low both on reference material and on material 8.

The flue gas recirculation fan at Västhamnsverket had the polymeric material 1 applied as top coating in 2013. At inspections in 2014, 2015 and 2017 it was seen that the amount of deposit on the wheel was small and the coating was still visible after 4 years of operation. During the first firing season after the application maintenance was performed only once compared to once a week before the application. No data are known regarding maintenance the following firing seasons.

The aim of the project was to test some candidate coating materials to reduce the amount of deposits in different areas of a CHP plant. Even though one of the materials showed very good adherence (material 1), there was generally no clear difference in amount of deposits compared to surrounding areas. Also, in some positions, not much deposit was formed during exposure. An exception was the furnace area at Västhamnsverket. For the samples with non-polymeric top coating exposed in the furnace at Västhamnsverket, more deposit was observed on the exposed samples compared to surrounding tubes in the furnace. The reason for the uneven deposit distribution might be temperature difference of the tack welded samples compared to surrounding material or geometric factors influencing the gas flow in the specific area.

After the project was finished, but shortly before completing this report, some promising observations were reported with respect to the behaviour of some CMP coatings at Västhamnsverket. These observations are reported in Appendix D. They were taken into account when the conclusions of the following section were drawn.

5 Conclusions

The examined top coatings have not shown a reduced deposit formation in the examined lower temperature areas of the two CHP plants at Avedöre or Västhamnsverket. However, not much deposit was formed at all in these exposure areas during the testing. This makes it difficult to determine if there would have been a non-stick effect if the deposit formation had been greater.

For the high temperature areas, material 10 may show reduced deposit formation, but results are uncertain due to lack of a photograph before demounting of the samples.

No top coating could be detected by SEM/EDS on the samples exposed in the superheater areas position A (Avedöre) or SH-HT (Västhamnsverket). This could possibly imply that only little or no top coatings were present after exposure. However, at least some coating of material 4 exposed in the superheater areas position A (Avedöre) remained, as could be observed by its visible green colour.

The PTFE based material (material 1) showed very good coverage in both wear tests performed for 10 h and in furnace exposures.

The graphite based material (material 10) had very poor adherence when exposed in the wear tests.

The flue gas recirculation fan at Västhamnsverket showed substantially less deposit build-up and an exceptional decrease in required maintenance after being coated with material 1.

The lower part of the furnaces walls at Västhamnsverket benefited greatly from the non-stick properties resulting from being coated with material 3. This was shown by the time for cleaning by sand blasting during revision stops being decreased from 5 days to 2 days and by the corresponding sand consumption being decreased from 12 to 5 tonnes.

From the project results a general conclusion can be drawn that some CMP coatings at certain boiler positions may result in substantial savings in need of maintenance from the achieved non-stick properties. However, this must be verified on a case-to-case basis.

6 Goal fulfilment

Specific Scientific Goals were:

1. To investigate how to obtain a certain "equilibrium" polymer-to-metal area ratio during abrasive wear or erosion and to explain why it is achieved, as well as to establish a criteria for a minimum ratio that results in a significant improvement of the non-stick properties.

The surface of the base material was prepared to obtain a high amount of peaks before the application of the Ni-base material. The parameters of the grit blasting were varied within the project. The spray parameters were varied and those appearing to be optimal for the application of the Ni-base layer were chosen for preparation of the exposed samples. All materials of the project, were included in the wear tests and showed similar results regarding coverage of the top coating after 10 h of exposure. Regarding the coverage, the rate of top coating wear decreased after the initial period. For materials with polymeric top coating, the coverage after 10 h was at least 50 %, which is believed to give significant contribution to the non-stick properties.

2. To investigate the high temperature capability of the CMP and partially explain the corrosion/failure mechanism active at the upper temperature limit.

The fluoropolymeric CMP was examined in laboratory tests and showed release of carbon dioxide at approximately 450°C. This is regarded to be due to the break-down of the polymeric layer. Regarding the metal part of the CMP, the metal part appeared to be unaffected by the break-down of the polymer. For the furnace exposed materials, no corrosion in the Ni-base material was observed. Also, the metal part of CMP showed only delamination from the base materials in very few of the examined samples, and only in SH-HT position A in Ørsted /Avedöre.

3. To investigate the influence on fouling during field service with respect to amount and adhesion.

The amount of deposit was compared between the samples and the surrounding areas by visual inspection. In the lower temperature areas, no clear difference could be observed between the samples and the surrounding areas. In some high temperature areas, the samples showed more deposit than surrounding tubes. This may however have different reasons such as gas flow in the furnace, temperature variation and geometric issues.

4. To investigate the corrosion behaviour and partially explain the ongoing corrosion mechanisms, when exposed to high temperature corrosion during field service.

Some oxide formation was observed on the samples exposed in position A in Avedöre. However, the Ni-base layer appeared to be intact in almost all examined samples.

5. To investigate the corrosion behaviour and partially explain the ongoing corrosion mechanisms, when exposed to low temperature corrosion during field service.

No low temperature corrosion was observed on the polymeric CMP candidates. However, it may have been that the boiler test areas were not subject to dew point corrosion.

Considering the motivations above, the scientific goals are considered to be fulfilled.

7 Suggestions for future research work

As the amount of deposits is much higher in the high temperature areas, it is suggested that further research is focused on these parts of the furnace. New materials are suggested to be tested as none of the examined top coating candidates could be observed by SEM/EDS after the exposure. Also other application methods might be an alternative to increase the adhesion of the top coating to the nickel-base layer.

For future work, it is important to ensure field tests with sample temperatures and gas flows equal to surrounding areas. This is especially important for the high-temperature areas as the present approach introduced possible differences in temperature and gas flow on the samples. An increase in deposit amount was also observed on the samples, compared to surrounding areas. To achieve equal temperature and equal gas flow, one suggestion is that larger areas of the plant are given the CMP layer. There might be other suggestions to solve this issue.

8 Literature references

[1] Herstad Svärd S, Åmand L-E, Bowalli J, Öhlin J, Steenari B-M, Pettersson J, Svensson J-E, Karlsson S, Larsson E, Johansson L-G, Davidsson K, Bäfver L , Almark M, "Frame work - Measures for simultaneous minimization of alkali related operating problems, Phase 3", Värmeforsk report no. 1167, Stockholm, 2011.

[2] Andersson P, "Deposit induced corrosion in biofuel combustion" , Ph.D. thesis, Chalmers, Gothenburg, 2004.

[3] Hjörnhede A, Henderson P, "The effect of cleaning on materials wastage in biomass and waste fired power plants", Värmeforsk report no. 970, Stockholm, 2006.

[4] Hjörnhede A, Westberg S-B, Henderson P, Wetterström J, Jonasson A, "Evaluation of tube shielding", Värmeforsk report no. 1031, Stockholm, 2007.

[5] Norling R, Hjörnhede A, Mattsson M, "Long term testing of materials for tube shielding, stage 2", Värmeforsk report no. 1215, Stockholm, 2012.

[6] Davidsson K, Johansson I, Stålenheim A, Boman K, "Cleaning methods for combustion facilities that use difficult fuels", Stockolm, Värmeforsk project no. A12-210, in press, Stockholm 2014.

[7] Personal communication with Matti Huhtakangas

[8] Piltonen, P., Stoor, T., Niinimäki, J., "On-site evaluation method for the non-stick properties of paper machine drying cylinder materials – A description of the methodology and two case studies", Measurement, Vol. 46, 2013, pp. 1061-1064.

[9] Urbanski, J., "Teflon covers solve starch build-up problem on Flambeau dryer cylinders", Pulp and Paper, vol. 64 (2), 1990, pp. 89-90.

[10] Wang B-Q, Geng G Q, Levy A V, "Erosion-corrosion of thermal spray coatings", Surface and Coatings Technology, Vol. 43-44, 1990, p. 859-874.

[11] Wang B-Q, Geng G Q, Levy A V, "*Erosion-corrosion of thermal spray coatings*", Surface and Coatings Technology, Vol. 43-44, 1990, p. 859-874.

[12] Wang B-Q, Shui Z R, "*Hot erosion behaviour of carbide–metal composite coatings*", Journal of Materials Processing Technology, Vol. 143-144, 2003, p. 87-92.

[13] Hjörnhede A, "Erosion-corrosion resistance and adhesion of laser and thermally deposited coatings in fluidised beds", Ph.D. thesis, Chalmers, Gothenburg, 2004.

[14] Alu-Releco OY, Pettri Narko, personal communication, 2014.

9 Appendices

Appendix A Images after all wear tests.

Appendix B SEM/EDS results after wear tests

Appendix C. SEM/EDS results after field exposures

Appendix A. Images after all wear tests

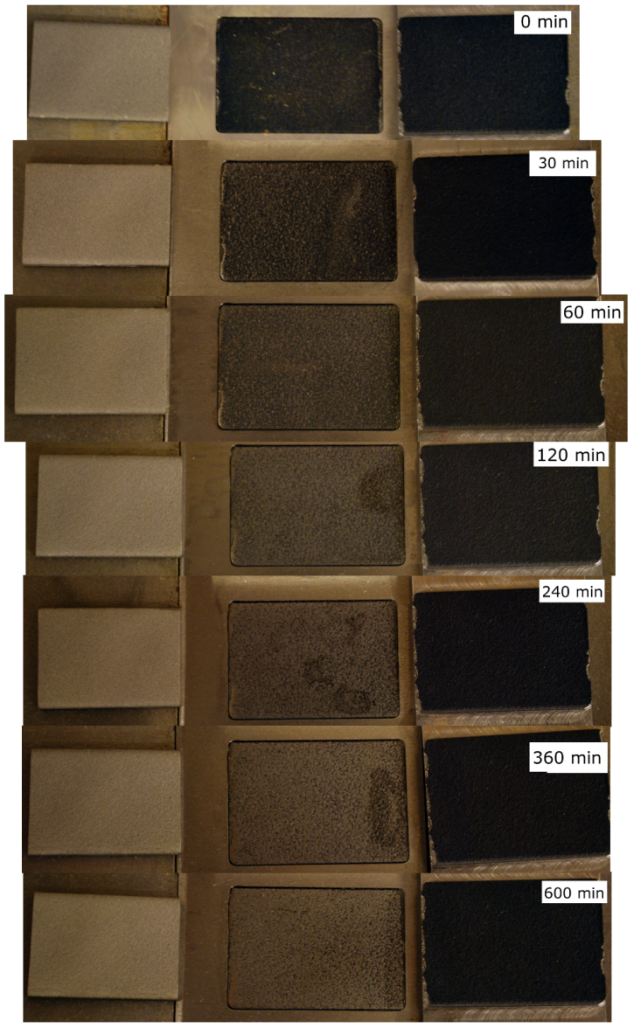

Material 1

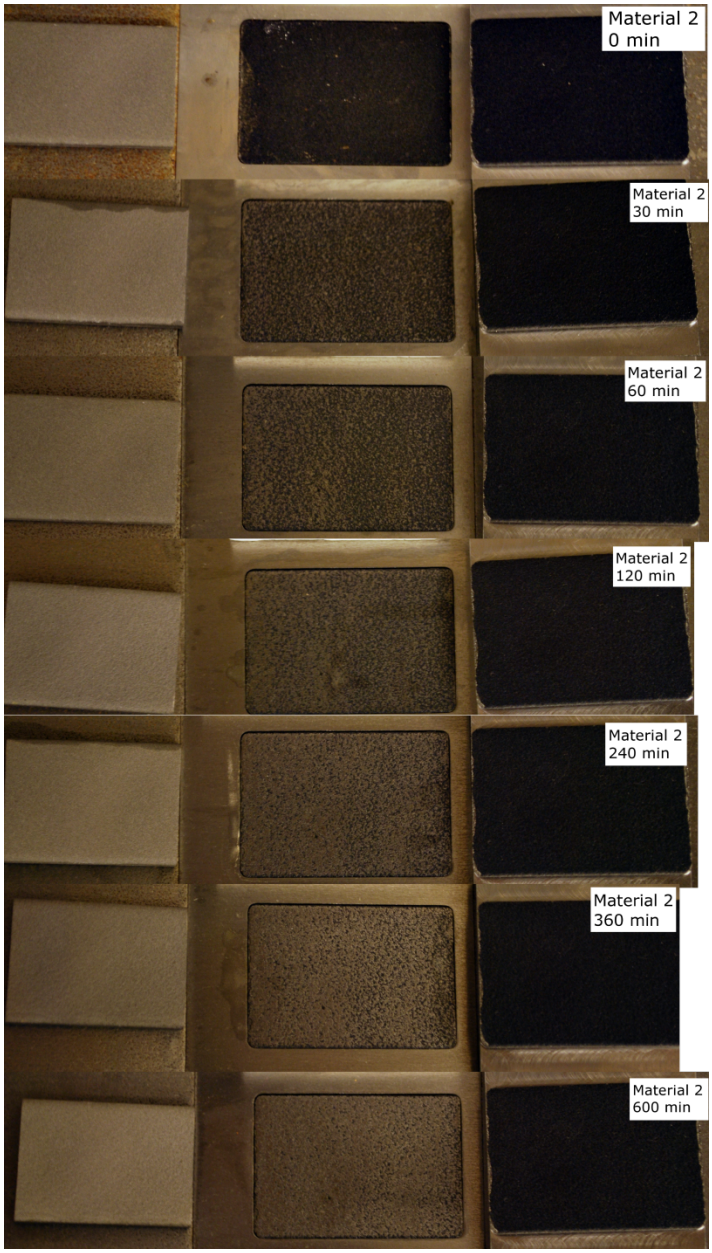
Material 2
0 min
Material 2
30 min
Material 2
60 min
Material 2
120 min
Material 2
240 min
Material 2
360 min
Material 2
600 min

Material 2

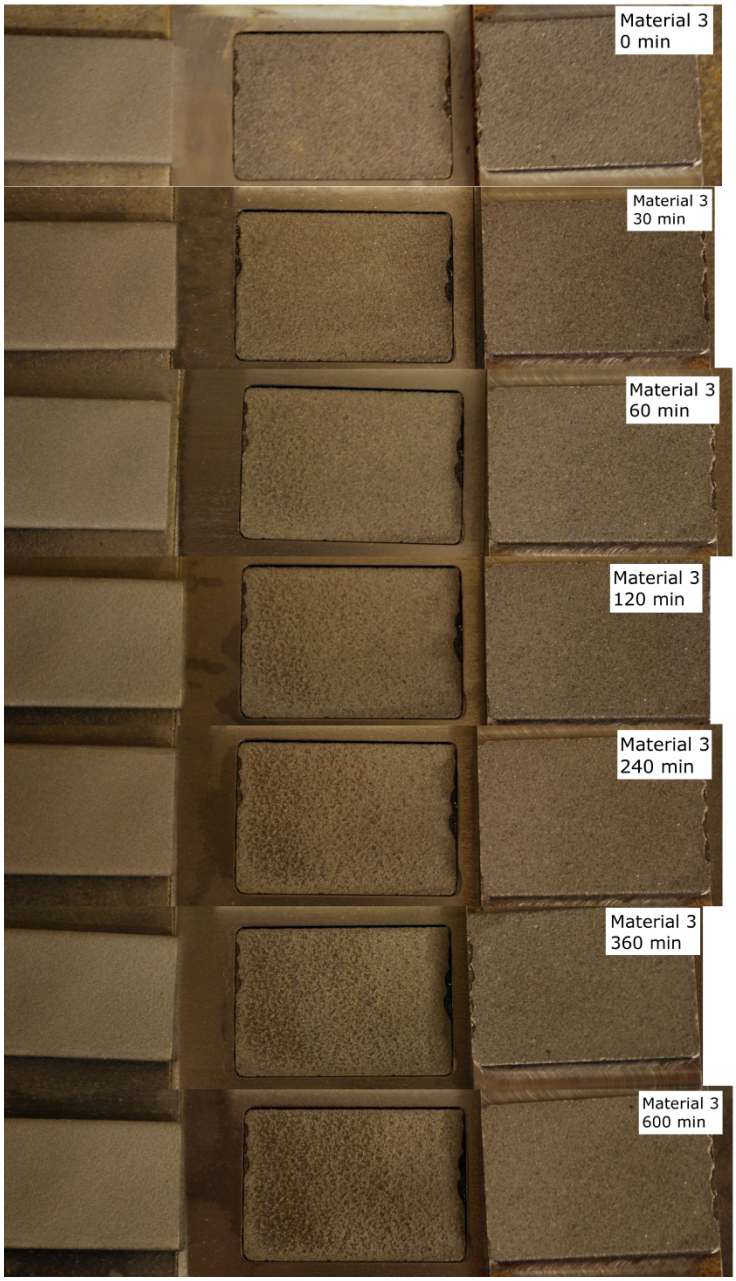
Material 3
0 min
Material 3
30 min
Material 3
60 min
Material 3
120 min
Material 3
240 min
Material 3
360 min
Material 3
600 min

Material 3.

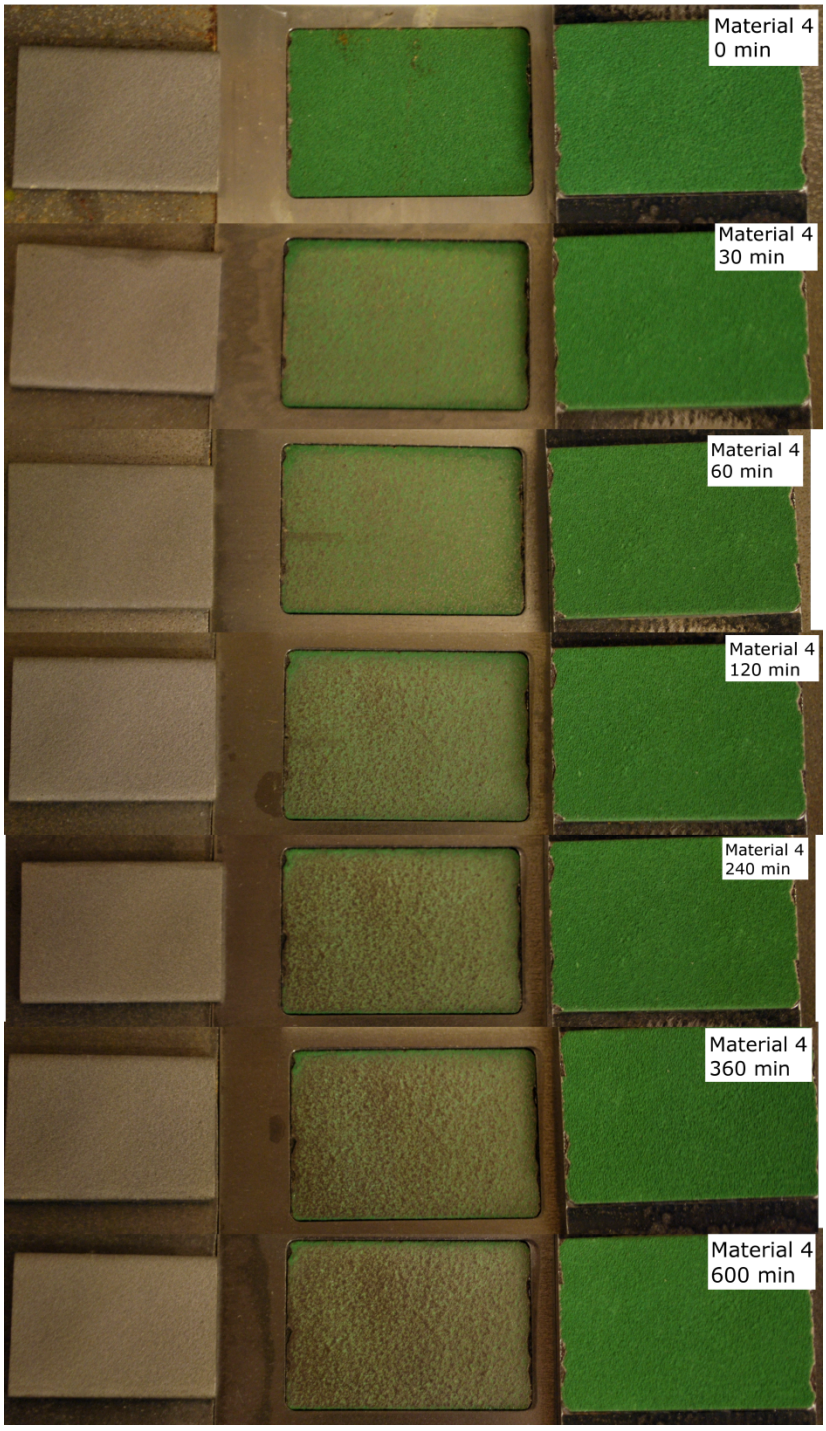
Material 4
0 min
Material 4
30 min
Material 4
60 min
Material 4
120 min
Material 4
240 min
Material 4
360 min
Material 4
600 min

Material 4

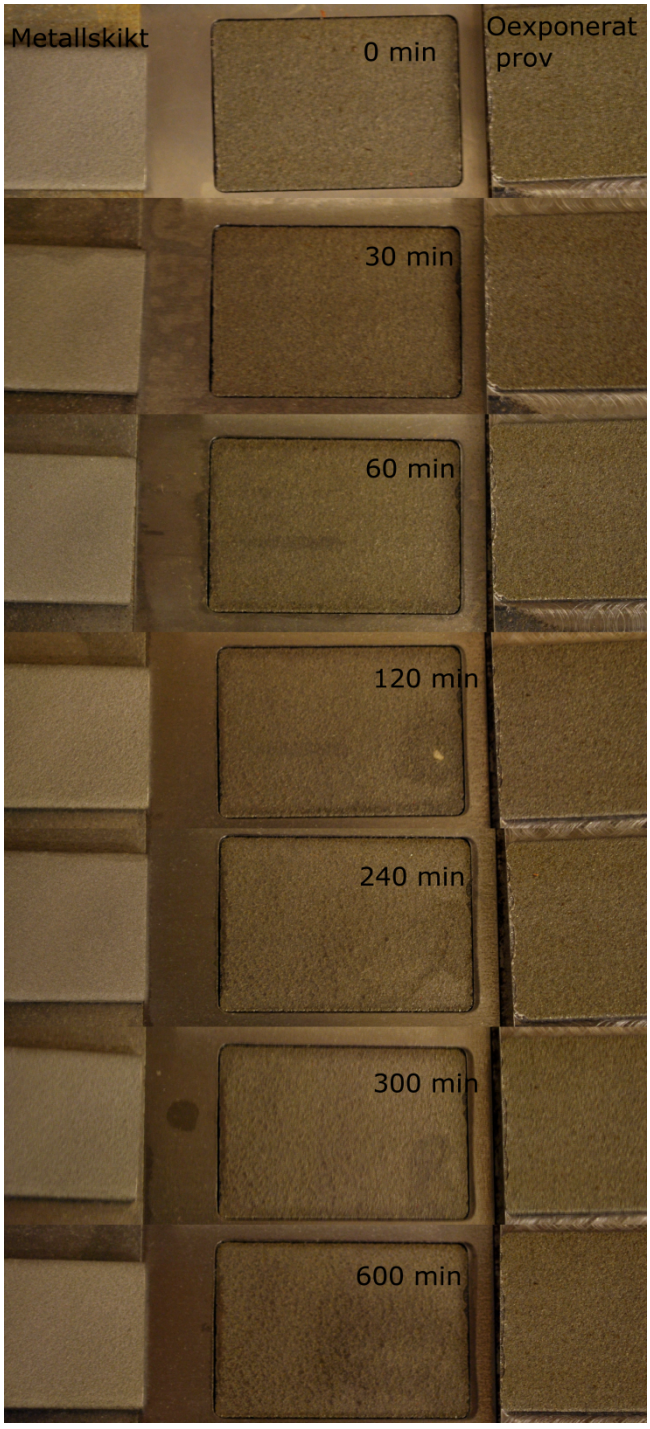
Metallskikt
0 min
Oexponerat prov
30 min
60 min
120 min
240 min
300 min
600 min

Material 6

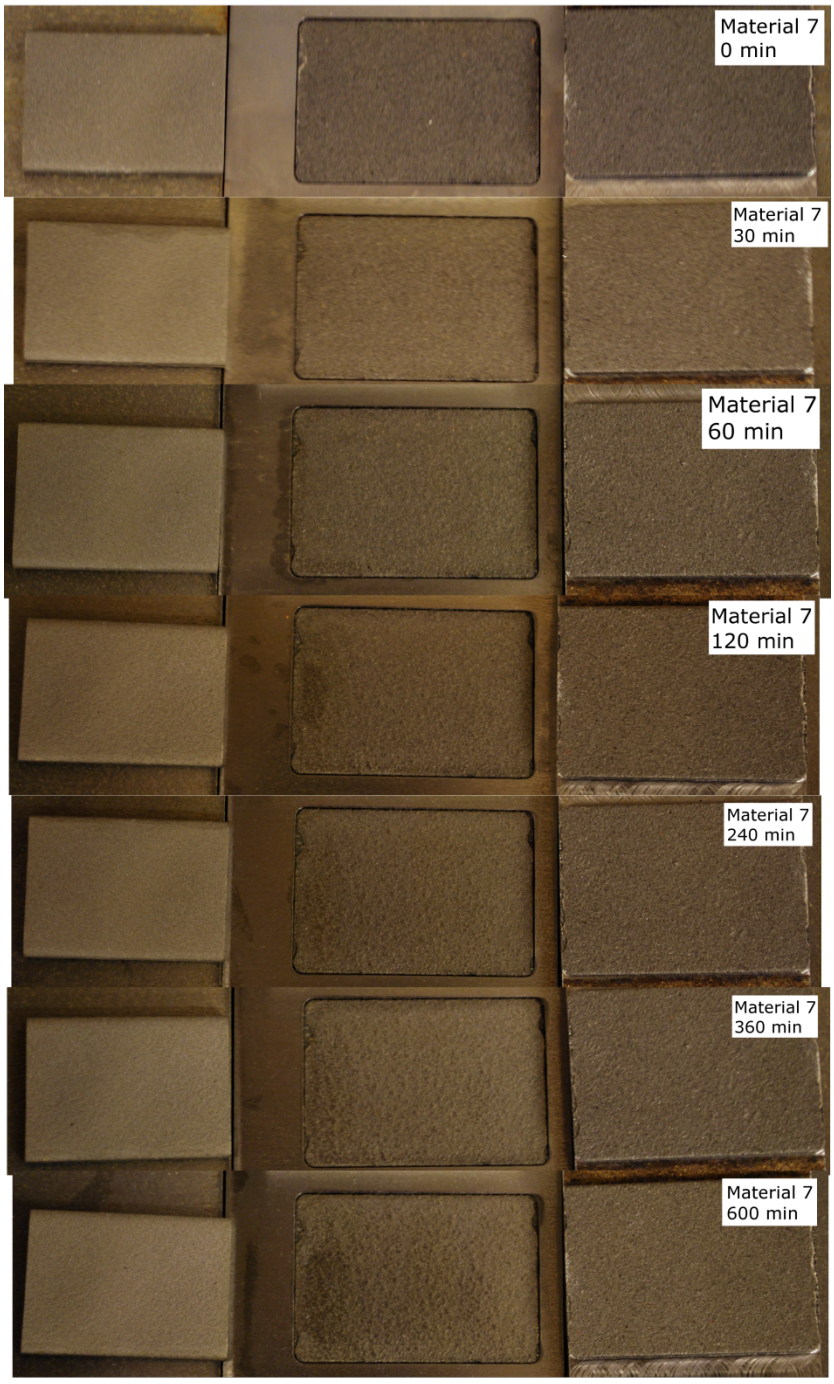
Material 7
0 min
Material 7
30 min
Material 7
60 min
Material 7
120 min
Material 7
240 min
Material 7
360 min
Material 7
600 min

Material 7

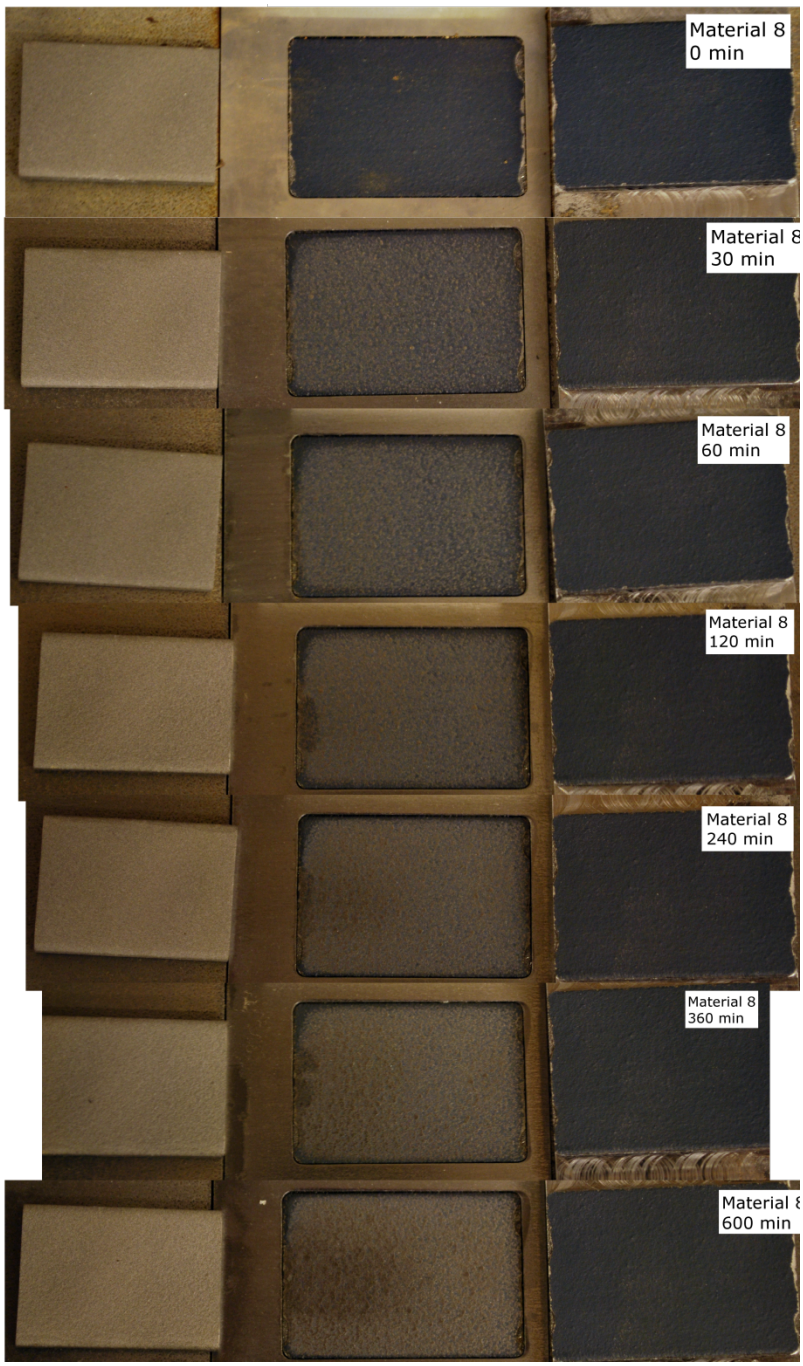
Material 8
0 min
Material 8
30 min
Material 8
60 min
Material 8
120 min
Material 8
240 min
Material 8
360 min
Material 8
600 min

Material 8

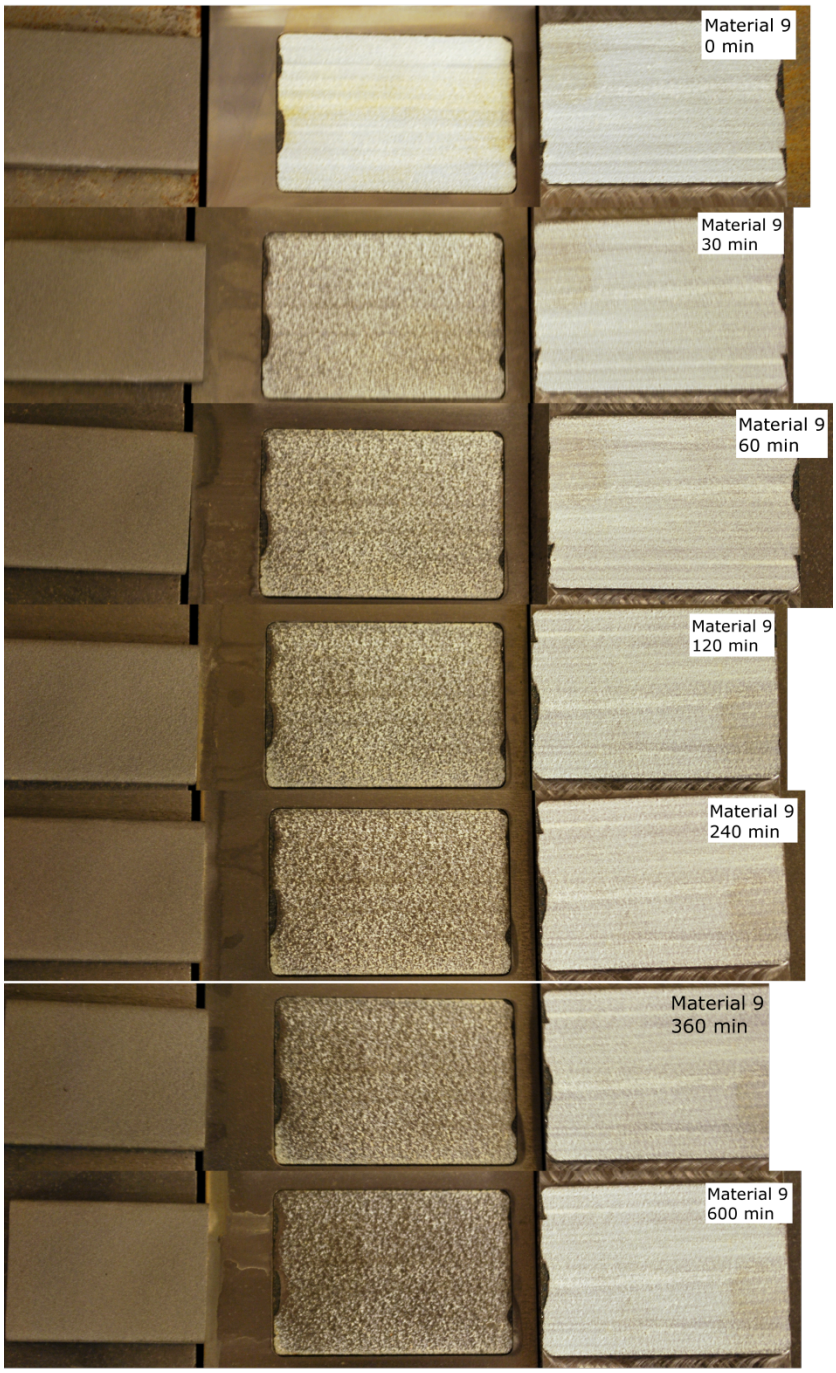
Material 9
0 min
Material 9
30 min
Material 9
60 min
Material 9
120 min
Material 9
240 min
Material 9
360 min
Material 9
600 min

Material 9

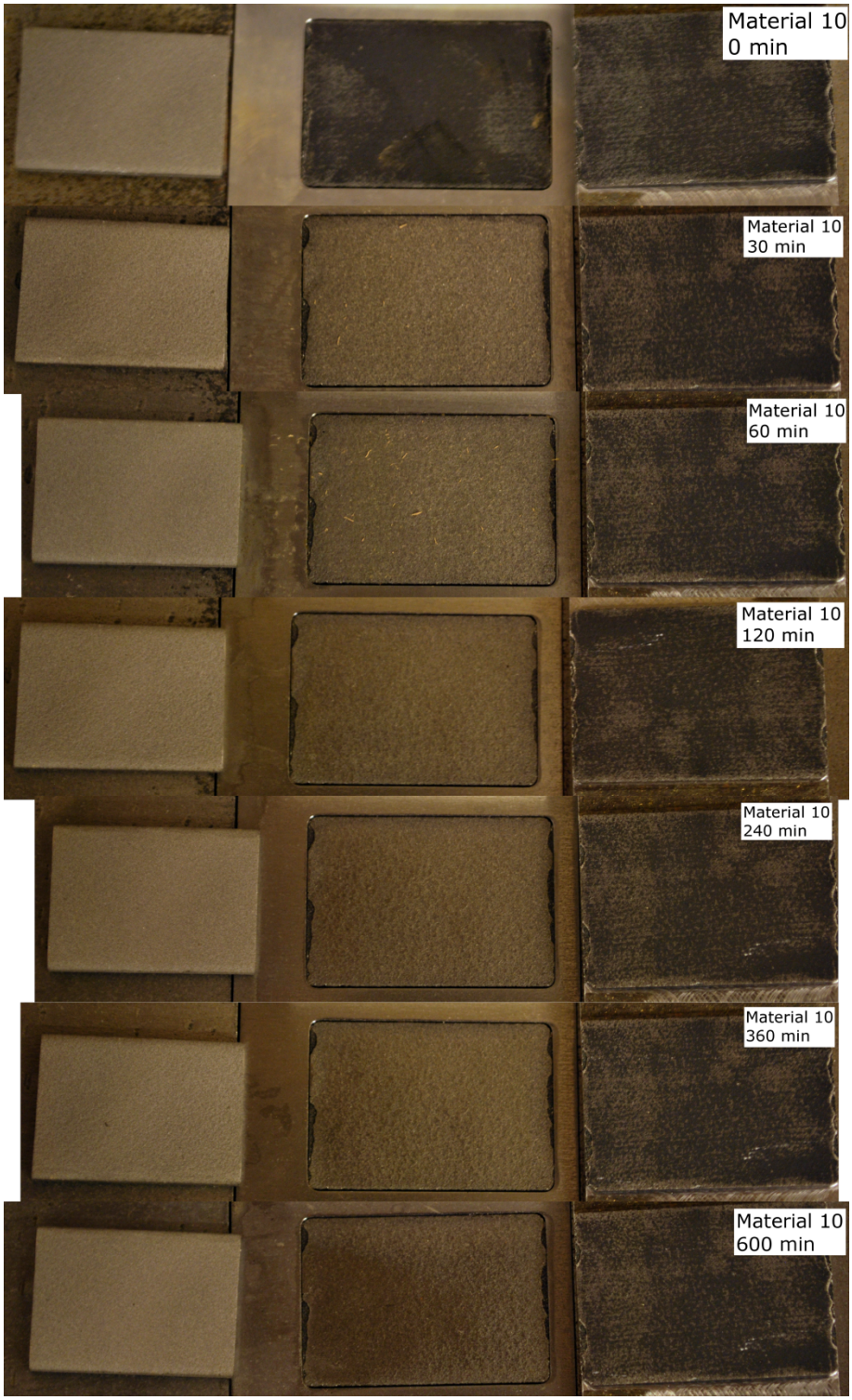
Material 10
0 min
Material 10
30 min
Material 10
60 min
Material 10
120 min
Material 10
240 min
Material 10
360 min
Material 10
600 min

Material 10

Appendix B. SEM/EDS results from wear tests

30 min wear testing, material 1

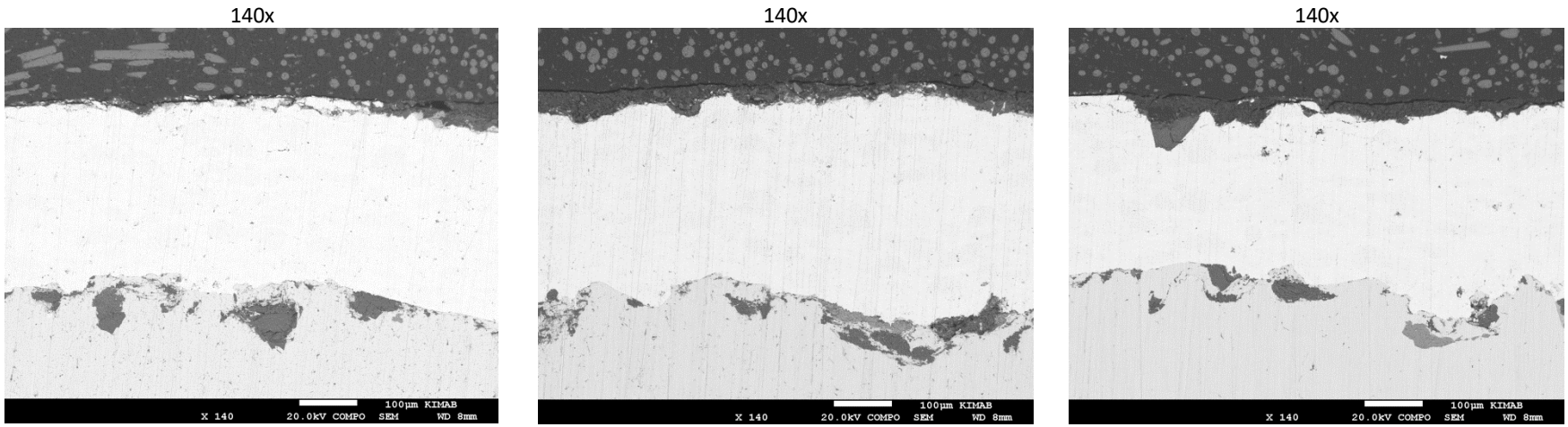

Figure 73. SEM images of material 1 after 30 min wear testing. Scale bar is 100 µm at 140x magnification.

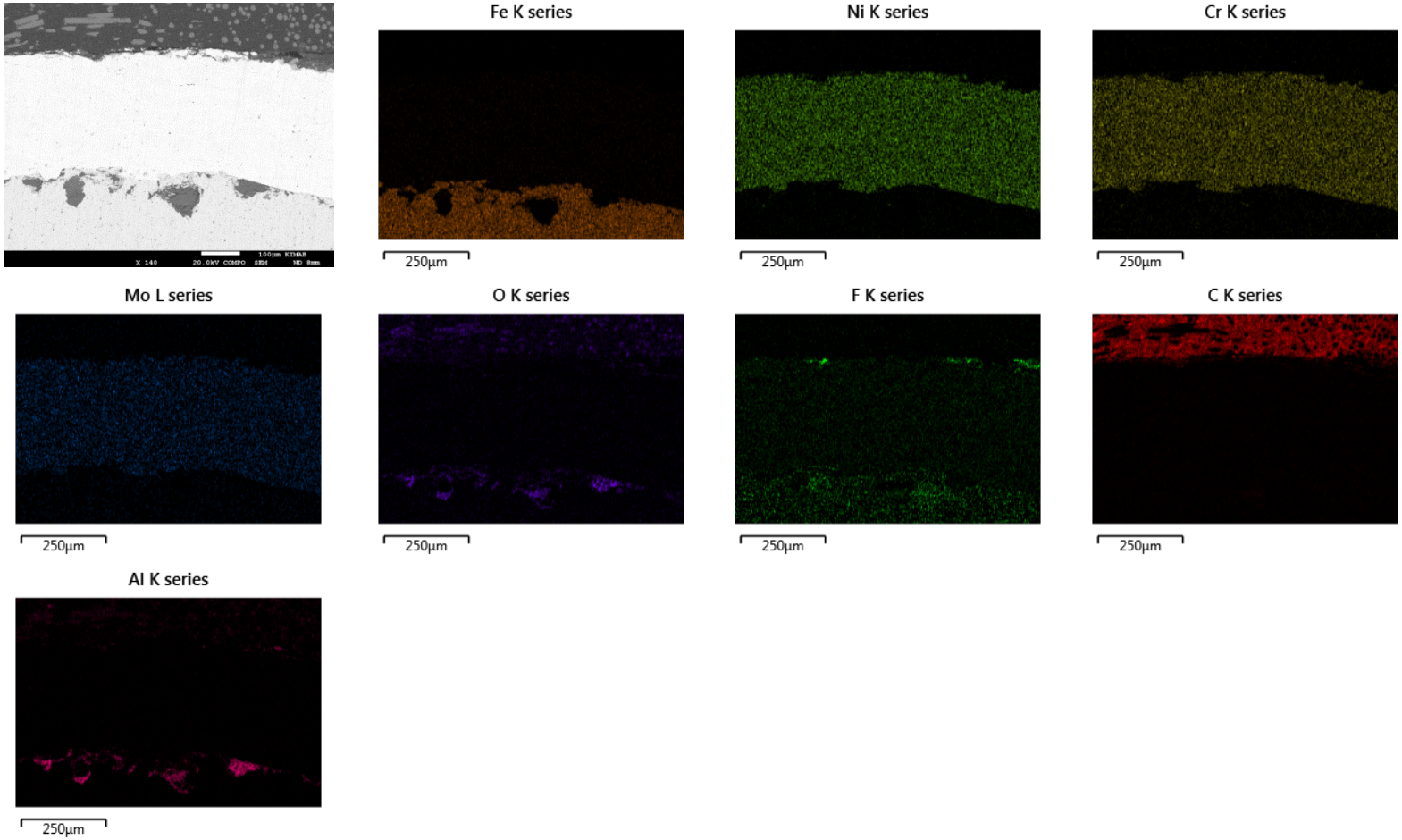

Figure 74. EDS analysis of material 1 after 30 min wear testing. Scale bar in SEM image is 100 µm.

30 min wear testing, material 6

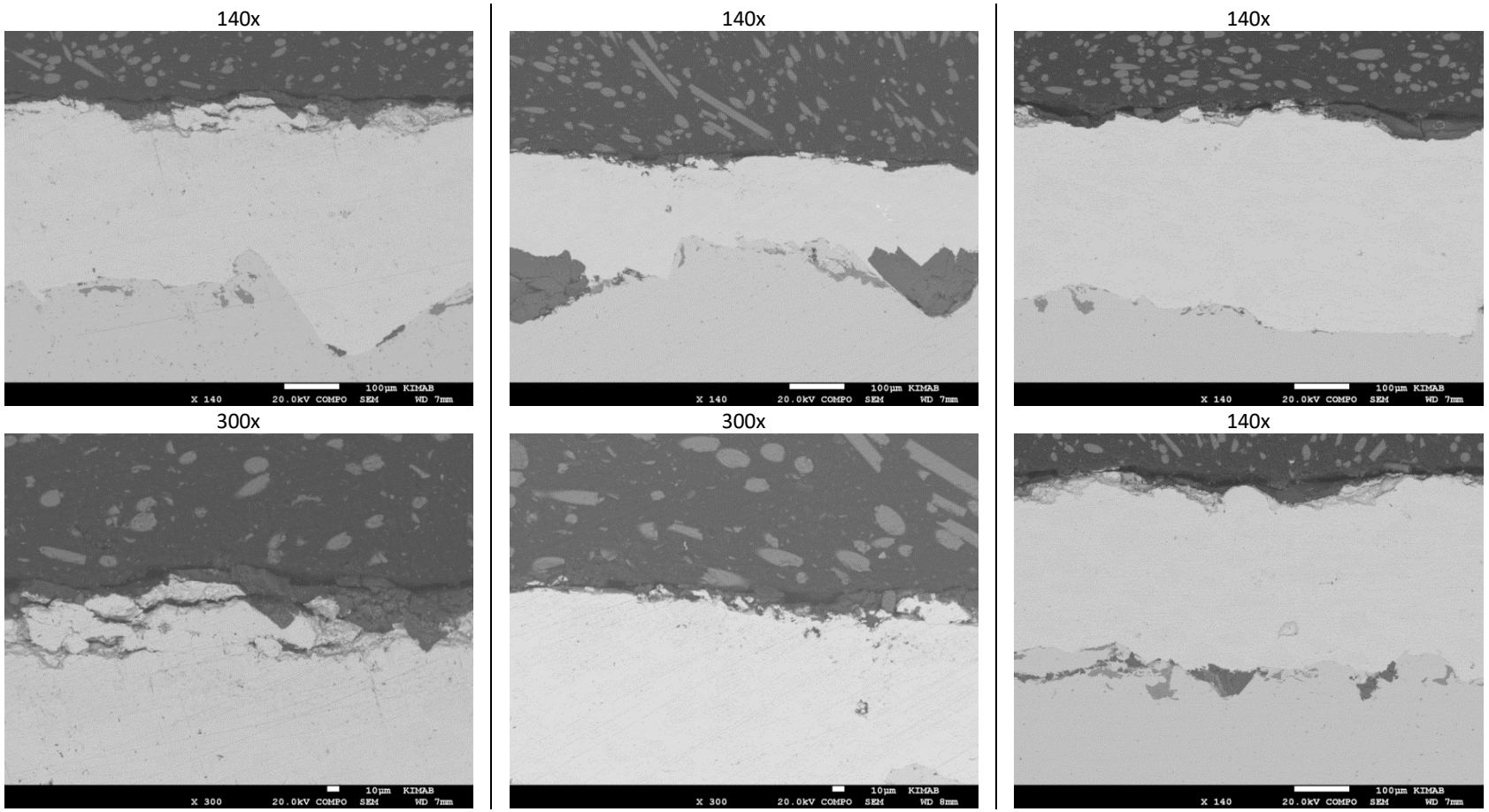

Figure 75. SEM images of material 6 after 30 min wear testing. Scale bar is 100 µm at 140x magnification and 10 µm at 300x.

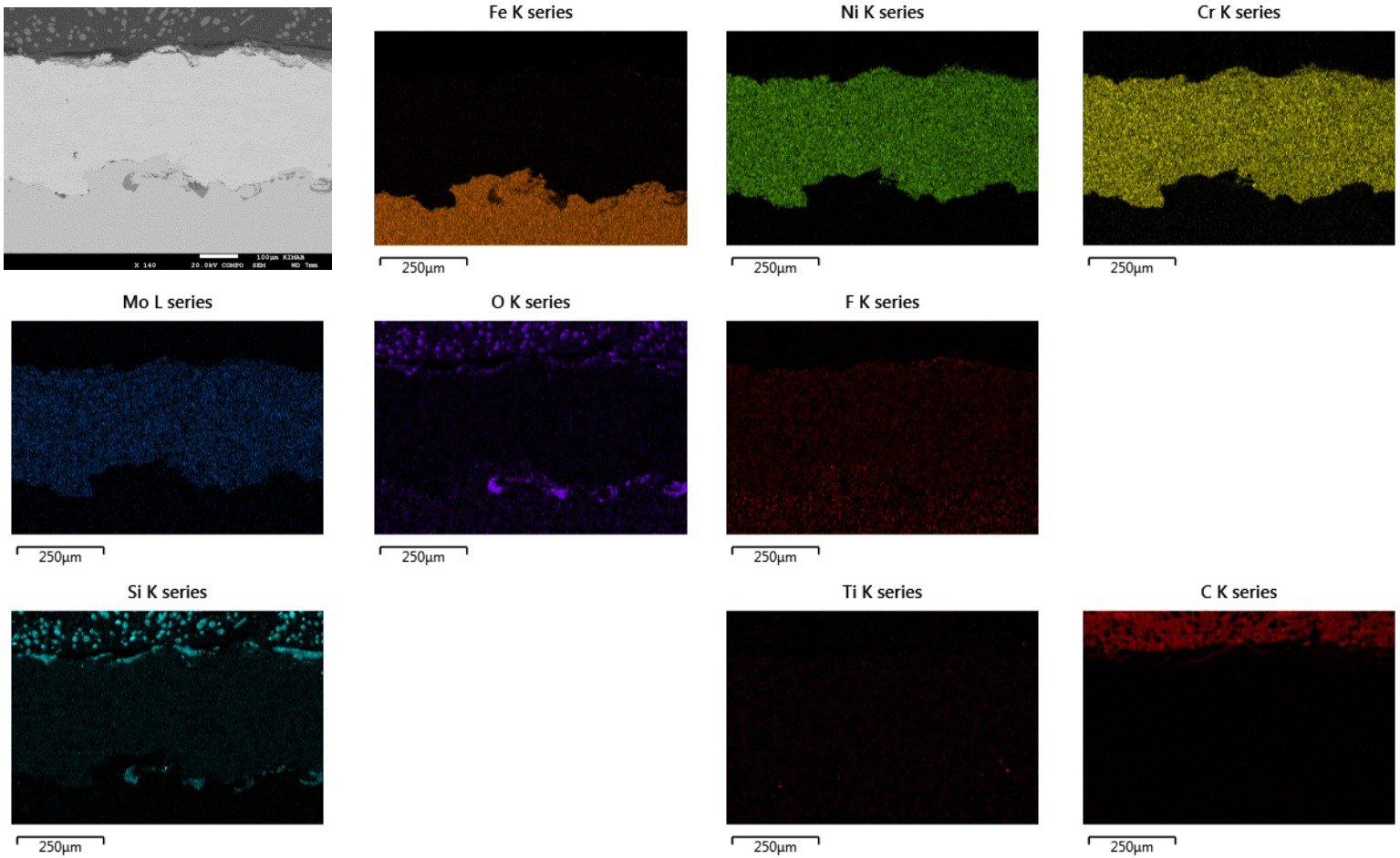

Figure 76. EDS analysis of material 6 after 30 min wear testing. Scale bar in SEM image is 100 µm.

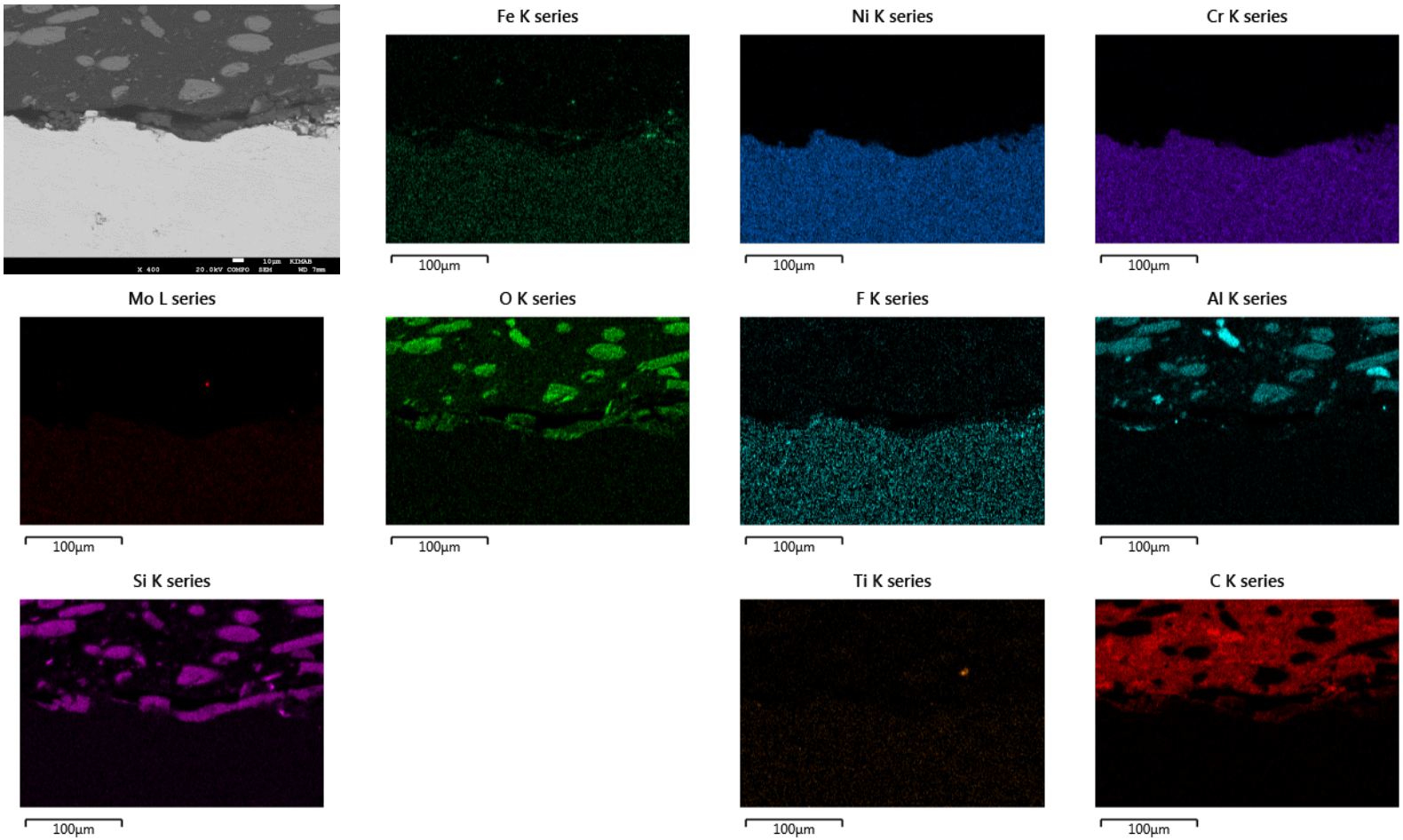

Figure 77. EDS analysis of material 6 after 30 min wear testing. Scale bar in SEM image is 10 µm.

30 min wear testing, material 8

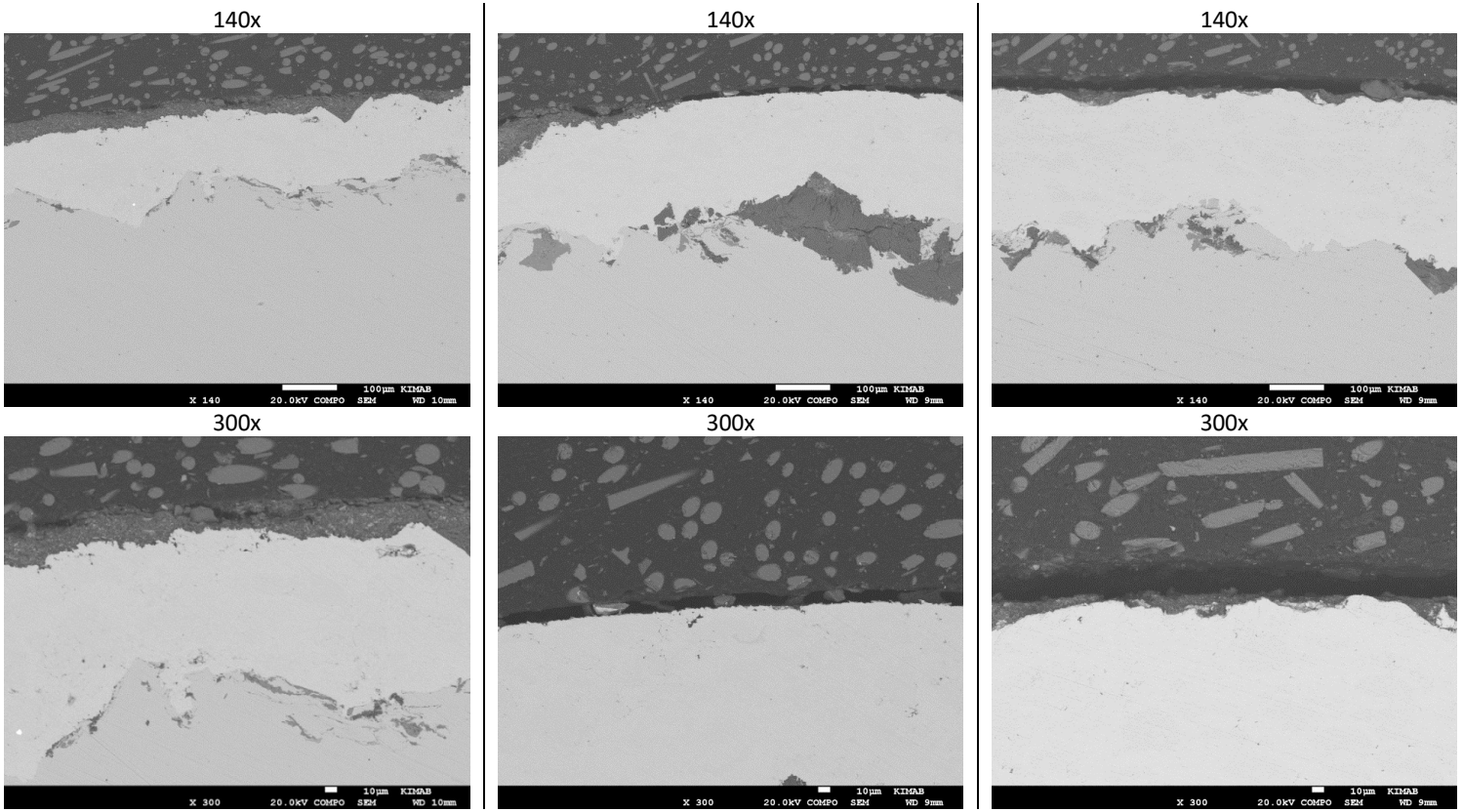

Figure 78. SEM images of material 8 after 30 min wear testing. Scale bar is 100 µm at 140x magnification and 10 µm at 300x.

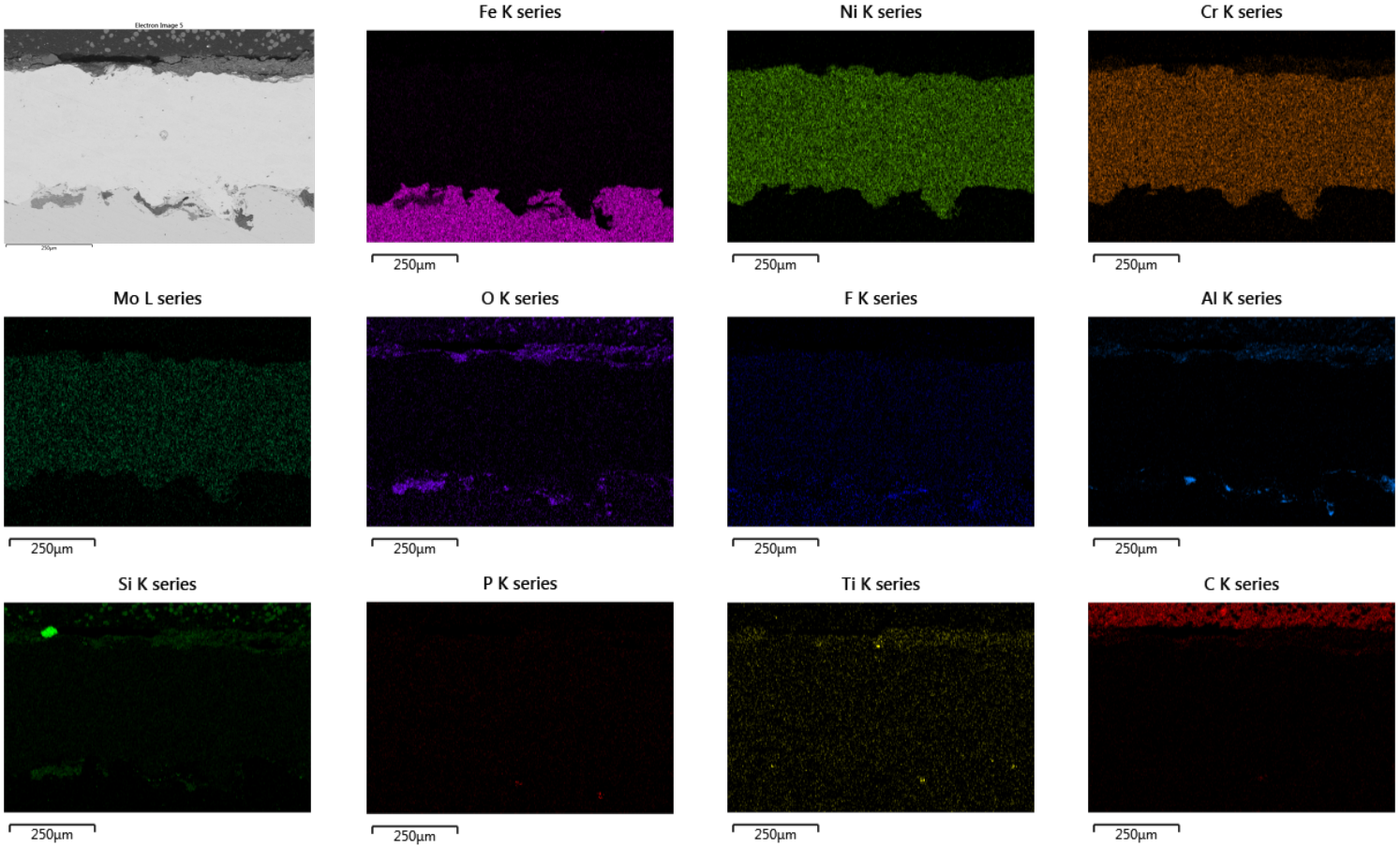

Figure 79. EDS analysis of material 8 after 30 min wear testing. Scale bar in SEM image is 250 µm.

2h wear testing, material 1

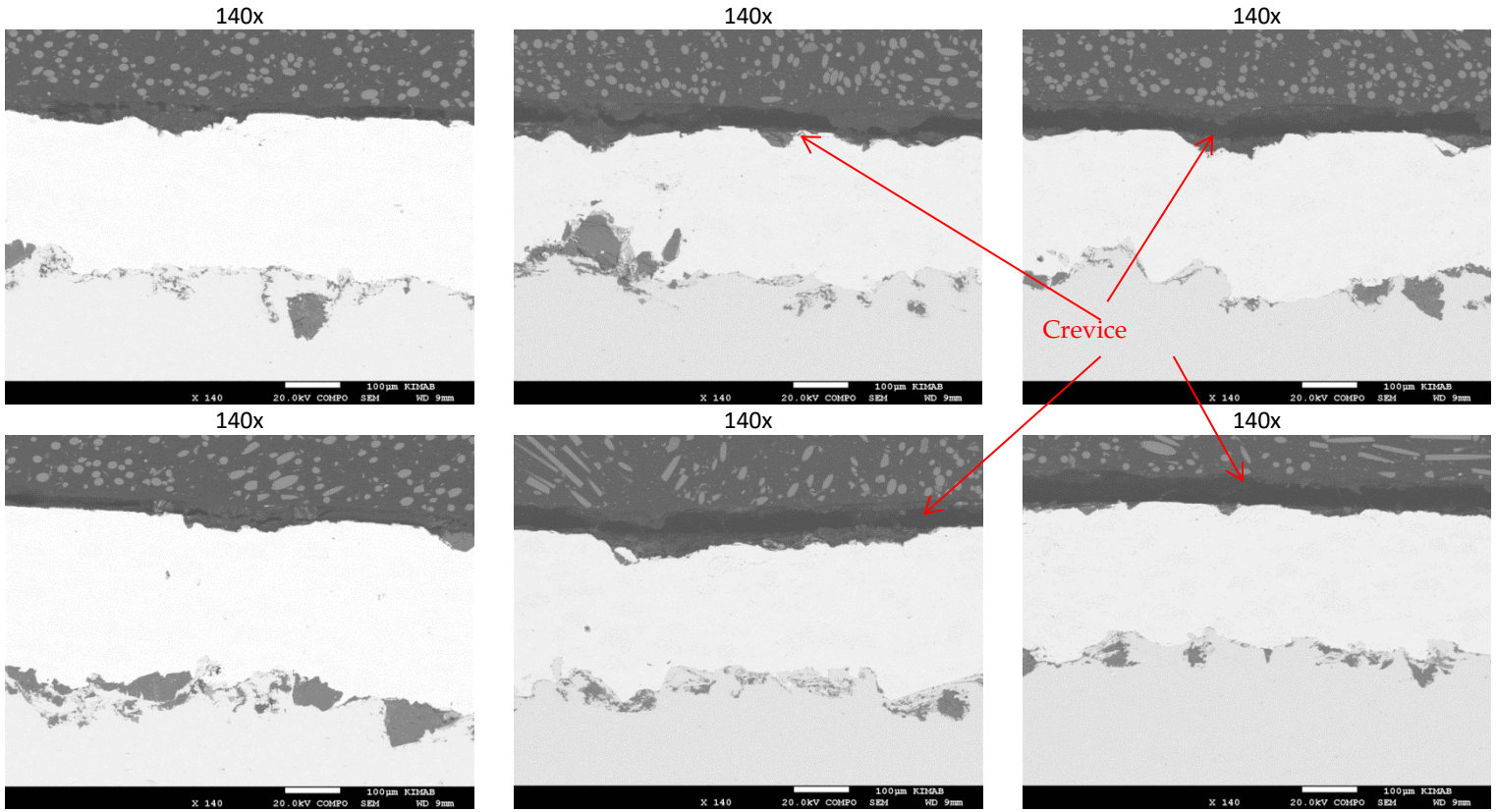

Figure 80. SEM images of material 1 after 2 h wear testing. Scale bar is 100 µm at 140x magnification.

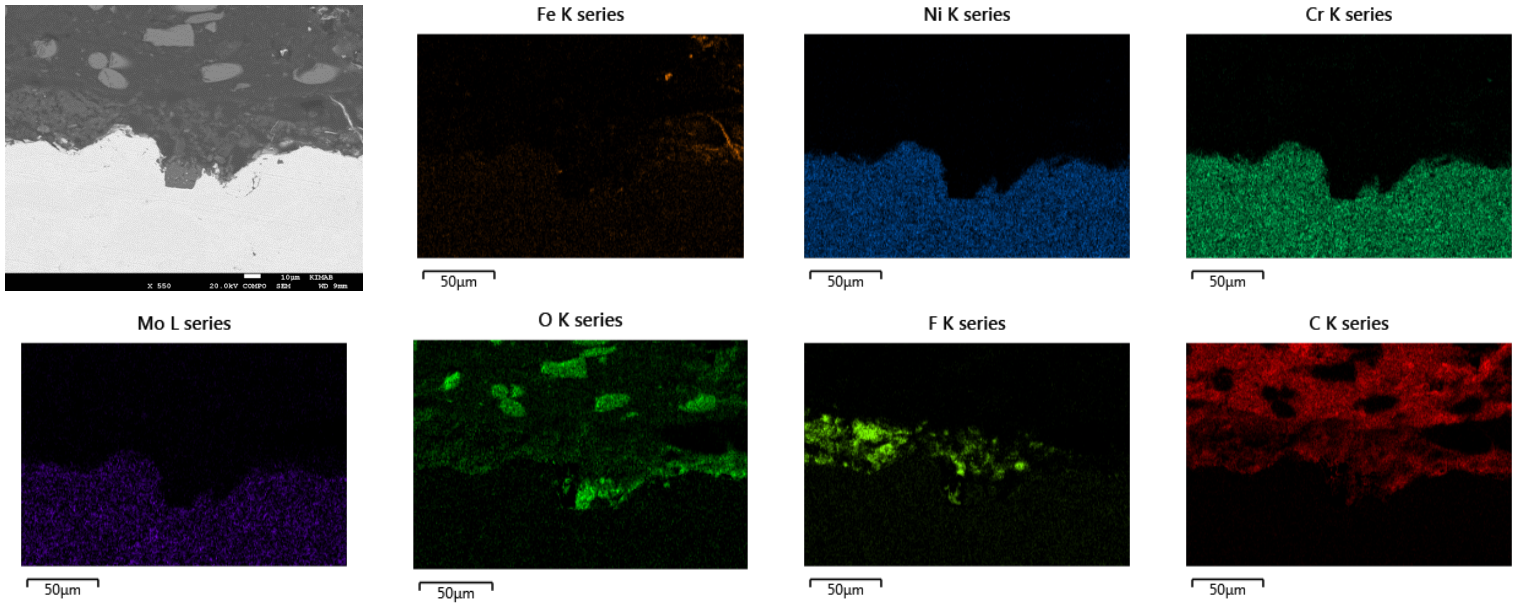

Figure 81. EDS analysis of material 1 after 2 h wear testing. Scale bar in SEM image is 10 µm.

2h wear testing, material 6

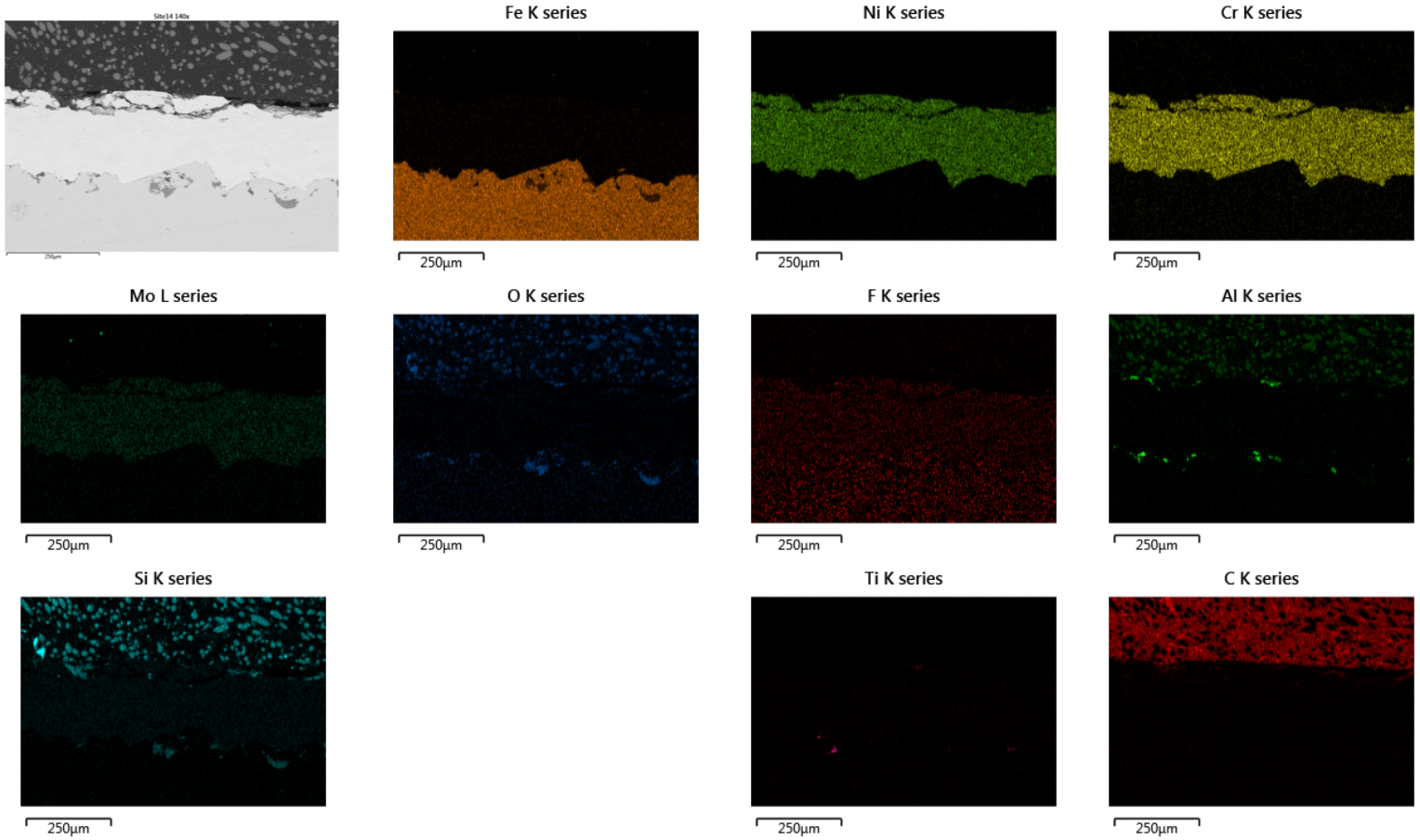

Figure 82. EDS analysis of material 6 after 2 h wear testing. Scale bar in SEM image is 250 µm.

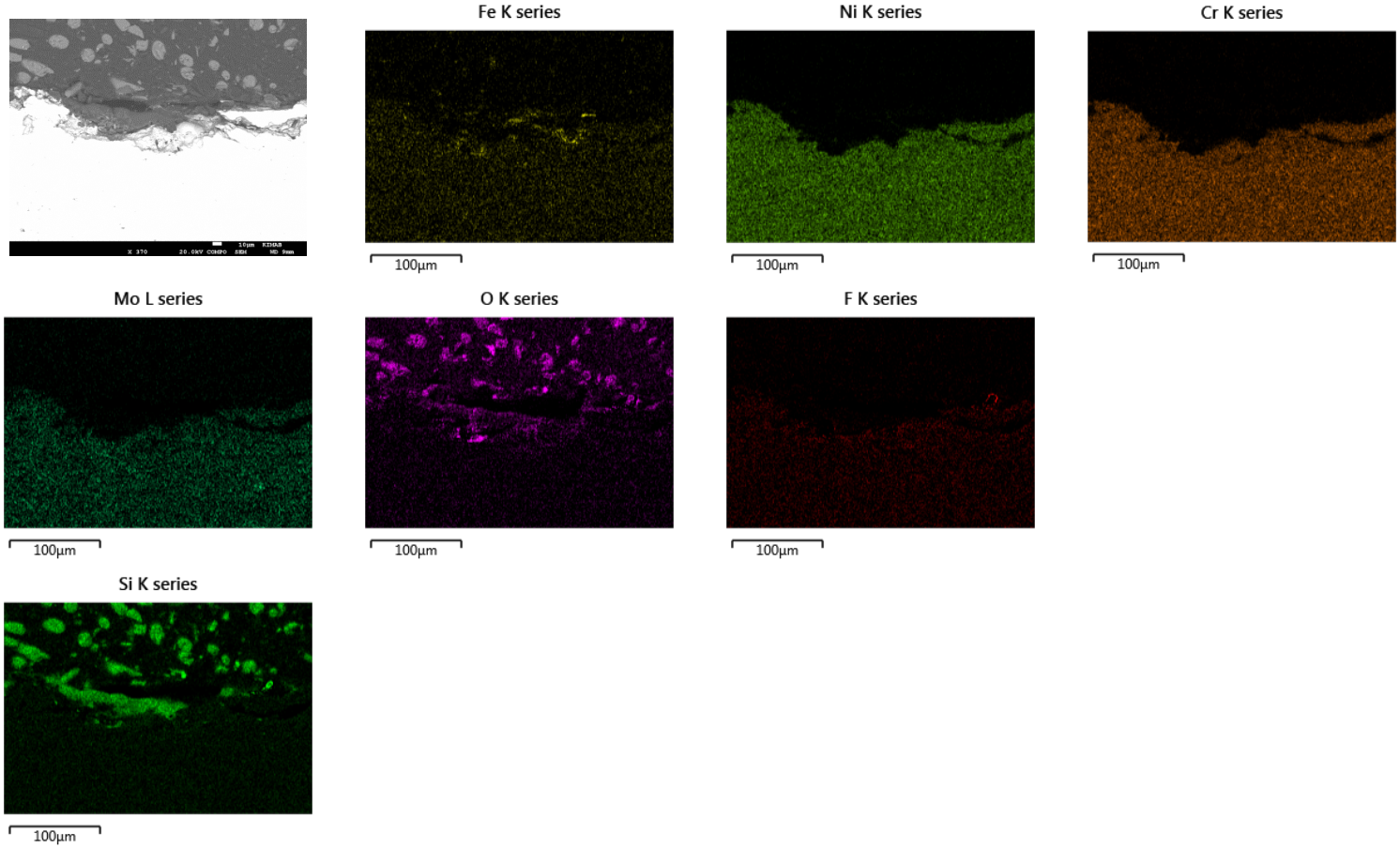

Figure 83. EDS analysis of material 6 after 2 h wear testing. Scale bar in SEM image is 10 µm.

2h wear testing, material 8

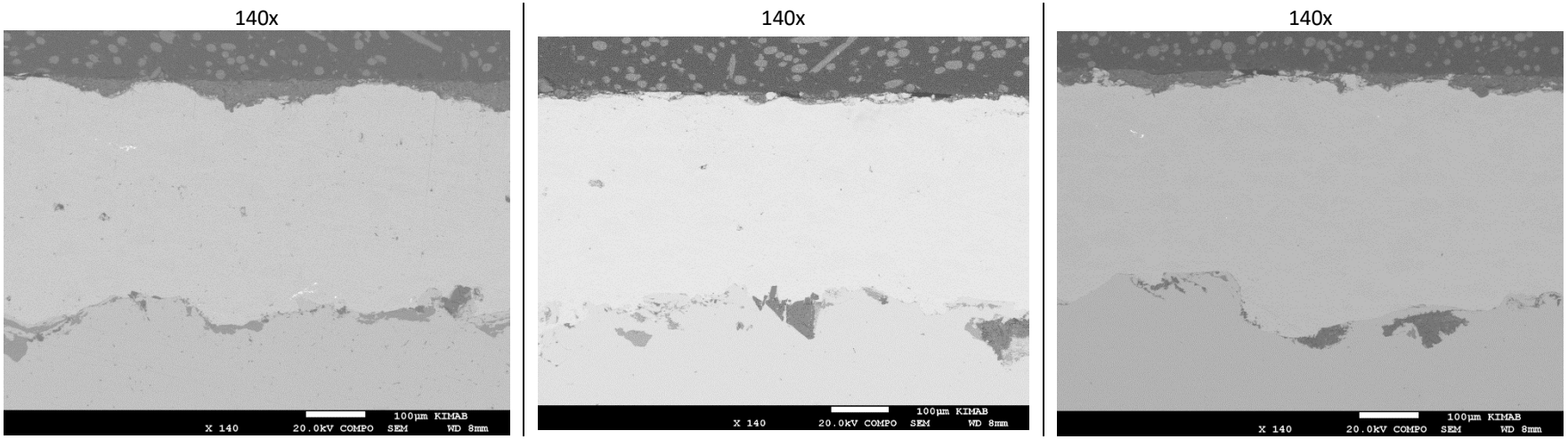

Figure 84. SEM images of material 8 after 2 h wear testing. Scale bar is 100 µm at 140x magnification.

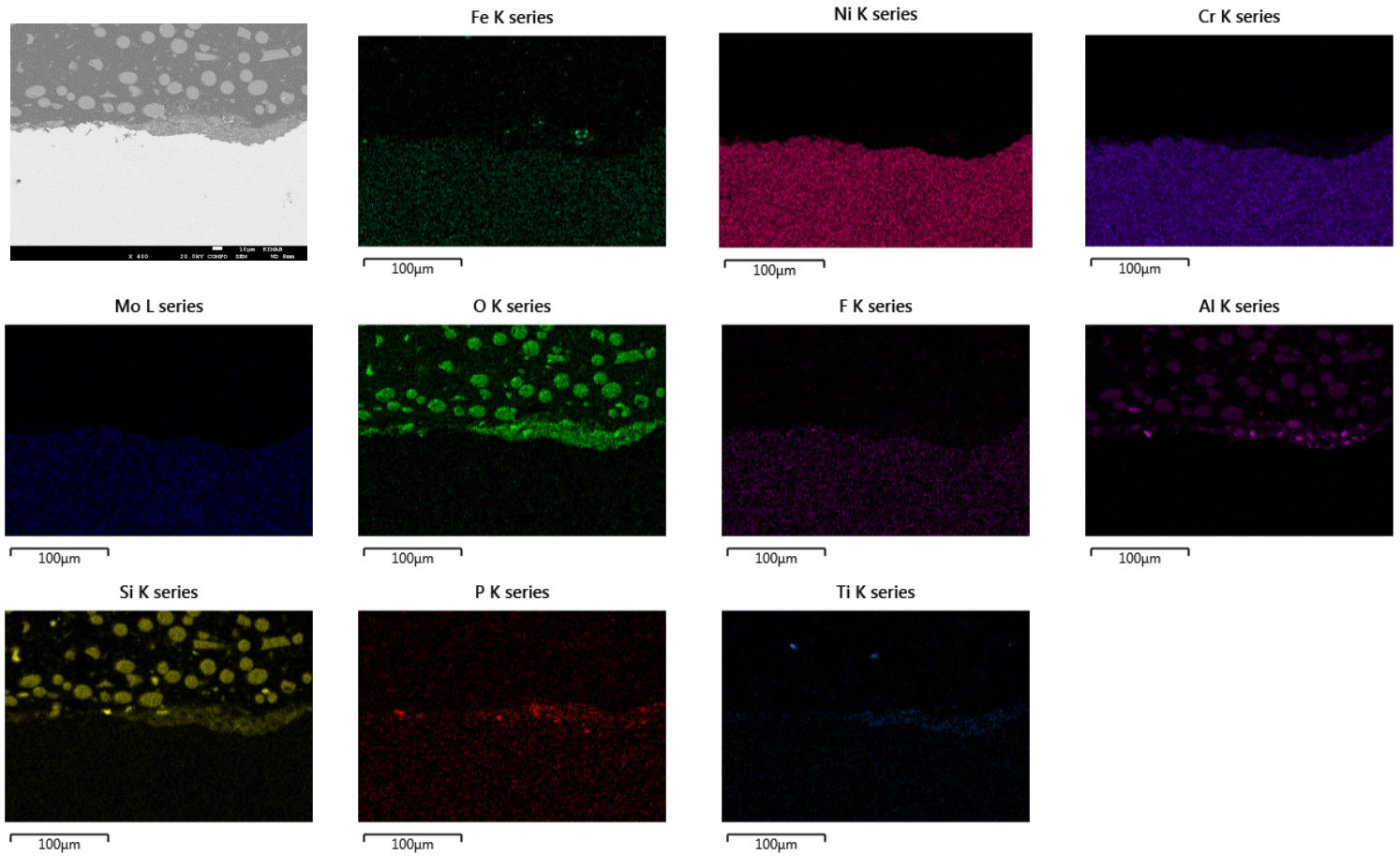

Figure 85. EDS analysis results of of material 8 after 2 h wear testing. Scale bar in SEM image is 10 µm.

10h wear testing, material 1

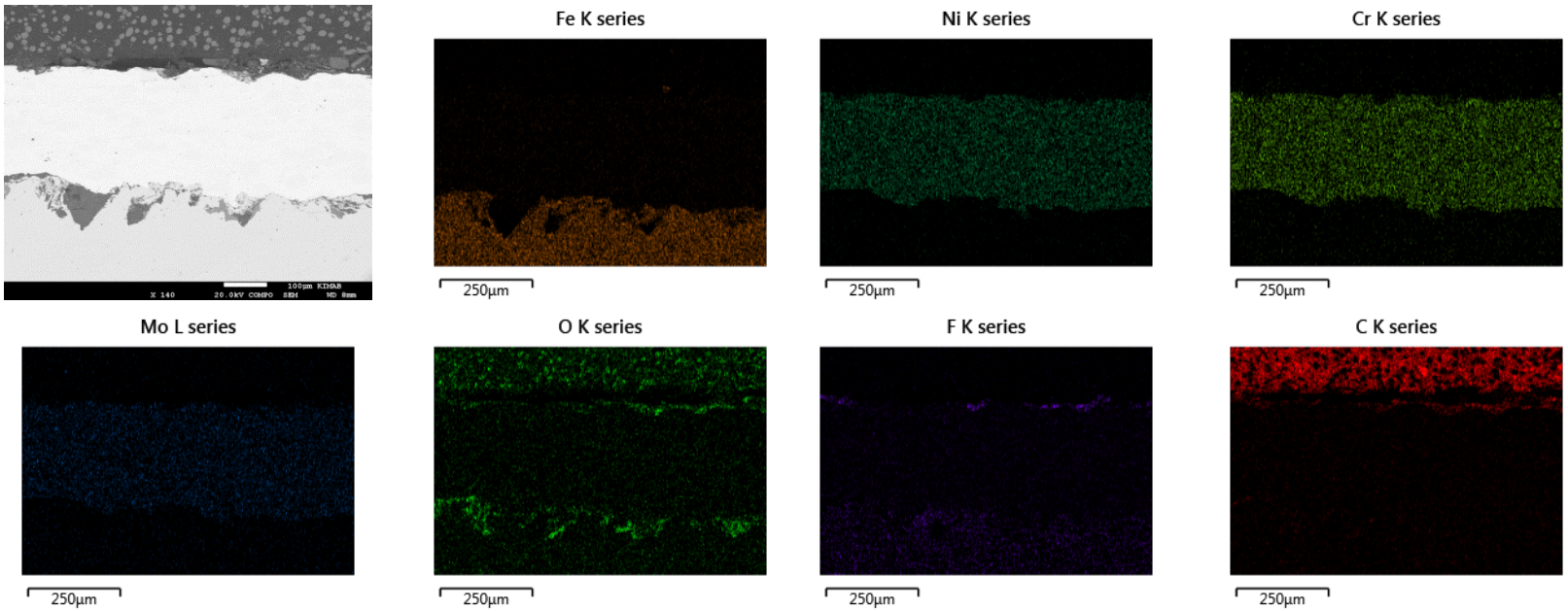

Figure 86. EDS analysis results of material 1 after 10 h wear testing. Scale bar in SEM image is 100 µm.

10h wear testing, material 6

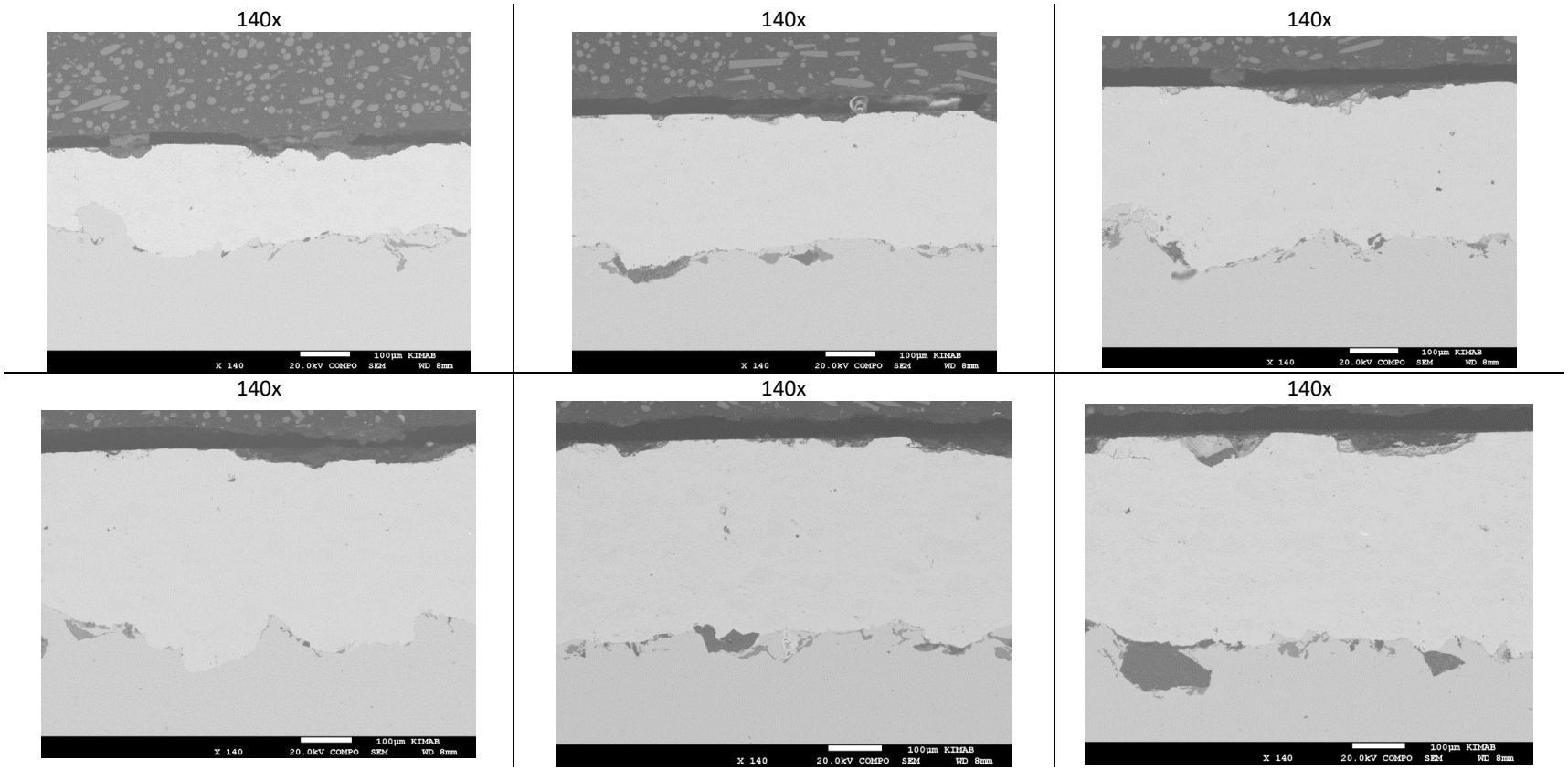

Figure 87. SEM images of material 6 after 10 h wear testing. Scale bar is 100 µm at 140x magnification.

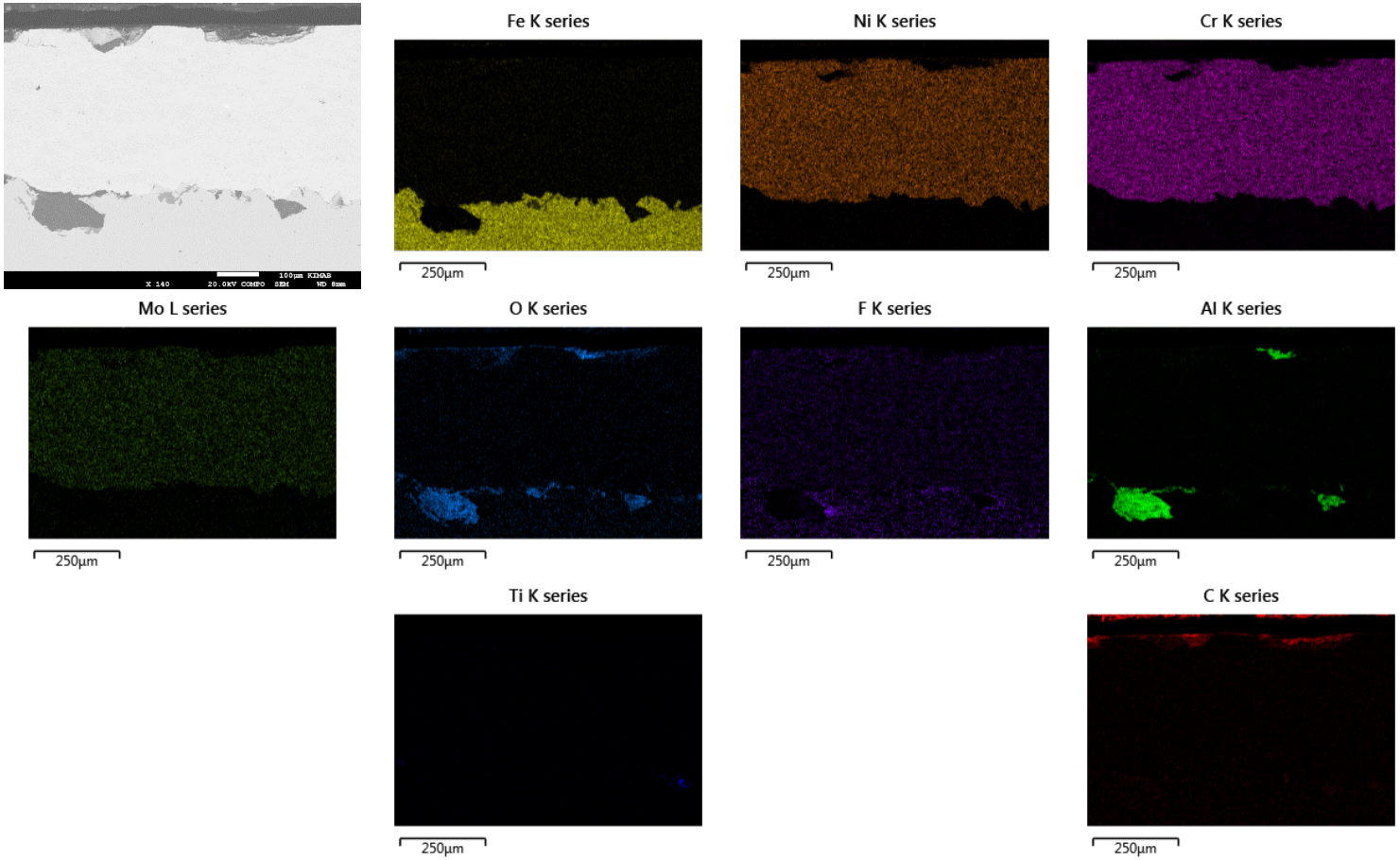

Figure 88. EDS analysis results of material 6 after 10 h wear testing. Scale bar in SEM image is 100 µm.

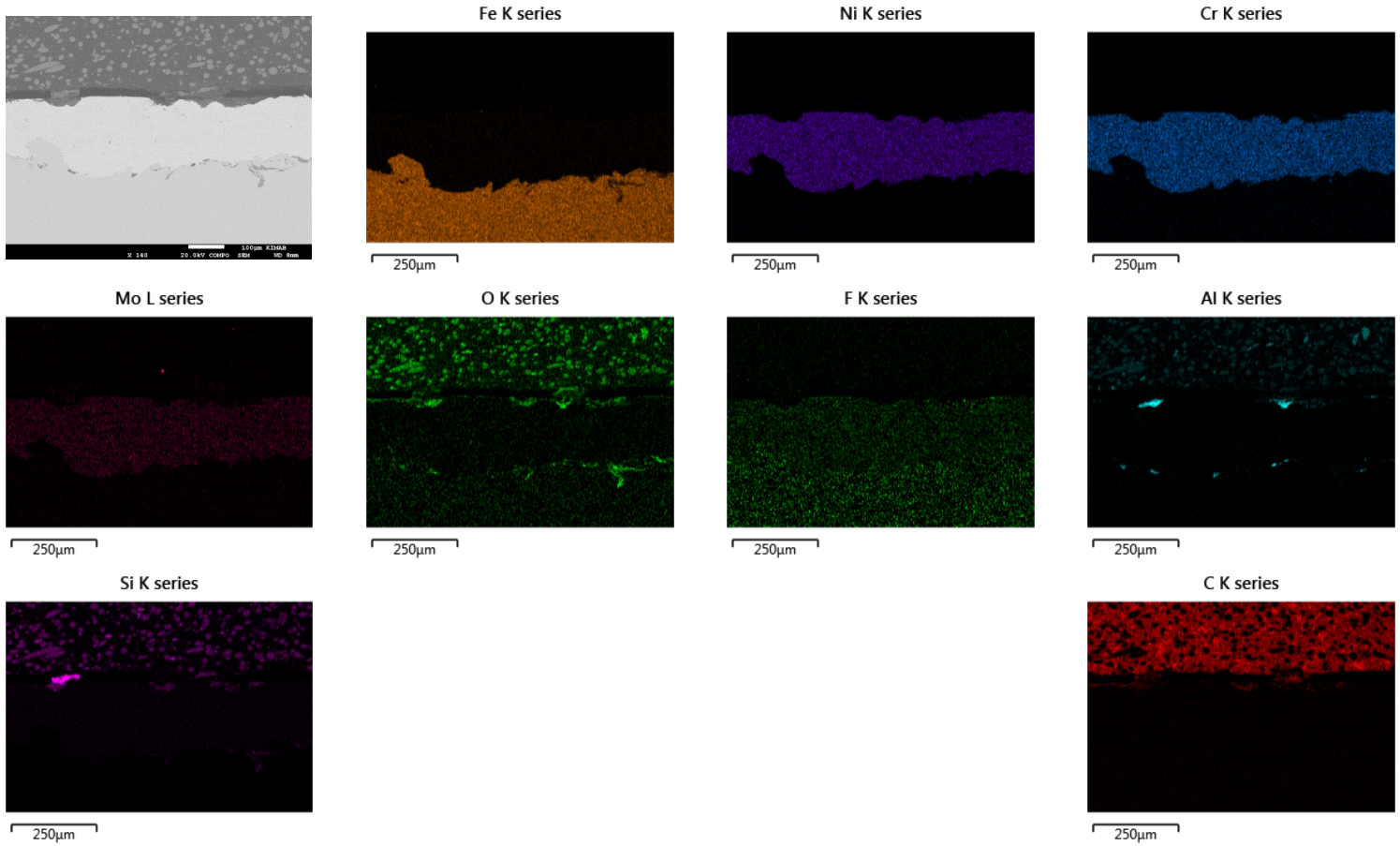

Figure 89. EDS analysis results of material 6 after 10 h wear testing. Scale bar in SEM image is 100 µm.

10h wear testing, material 8

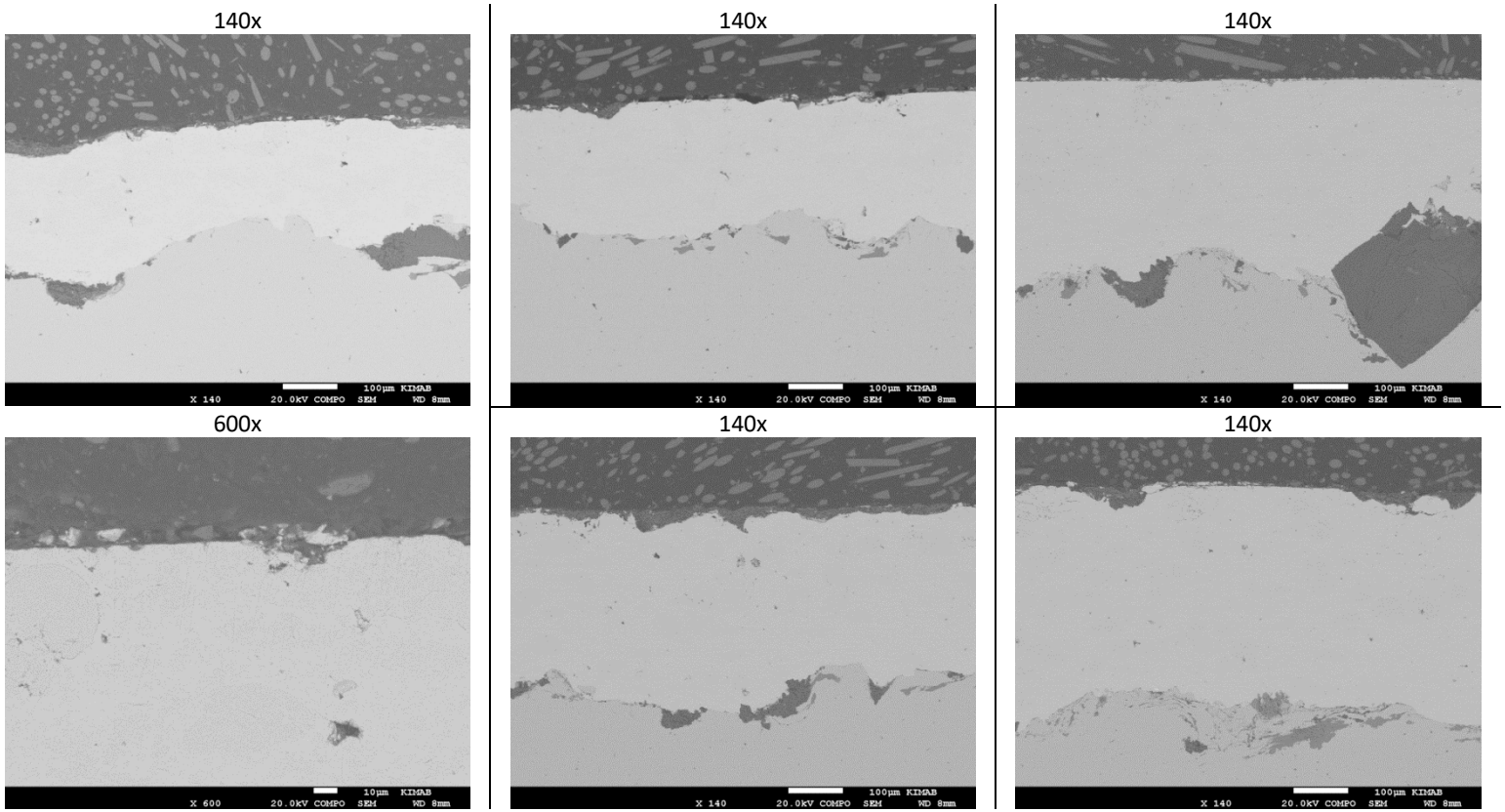

Figure 90. SEM images of material 8 after 10 h wear testing. Scale bar is 100 µm at 140x magnification and 10 µm at 600x.

Appendix C. SEM/EDS results from field exposures

Öresundskraft

SH-HT

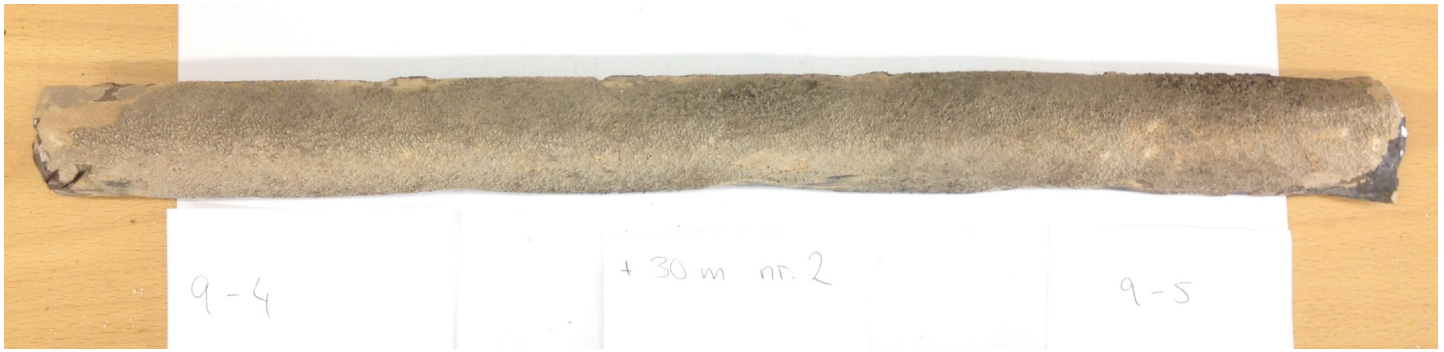

Figure 91. Material 4 (left part of tube) and material 5 (right part of tube) after exposure in the superheater (SH-HT). Removed from site in 2017.

Figure 92. Material 10 (left part of tube) and material 9 (right part of tube) after exposure in the superheater (SH-HT). Removed from site in 2017.

9-5_+30m_nr2 (FMP, Al-phosphate) (Mat 5)

FMP, Al-phosphate (Mat 5), (9-5_+30m_nr2) (sample removed in 2017)

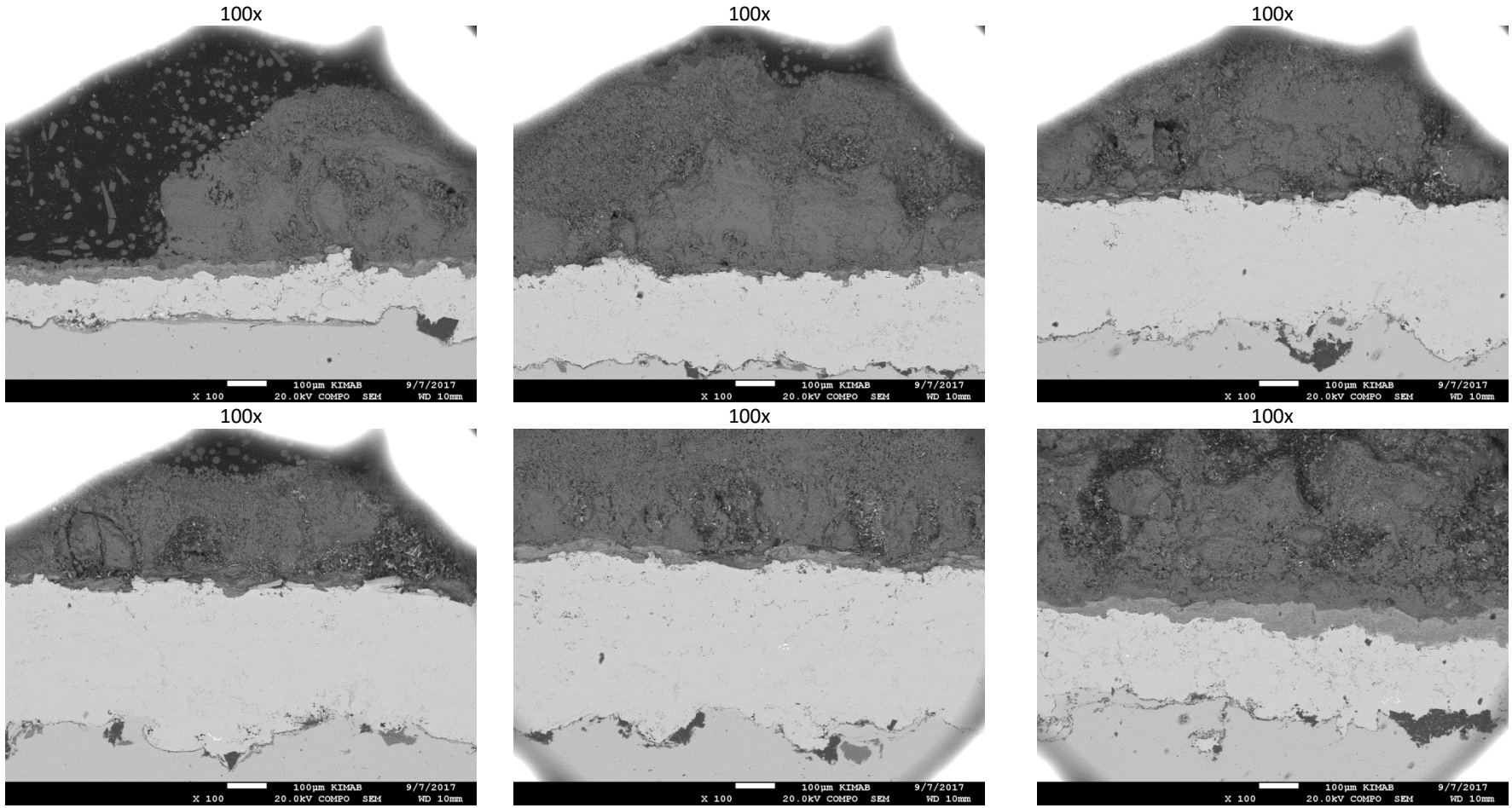

Figure 93. SEM images of material 5 after exposure at Västhamnsverket in the superheater (SH-HT). Sample removed from site in 2017. Scale bar is 100 µm at 100x magnification.

9-5_+30m_nr2 (FMP, Al-phosphate) (Mat 5)

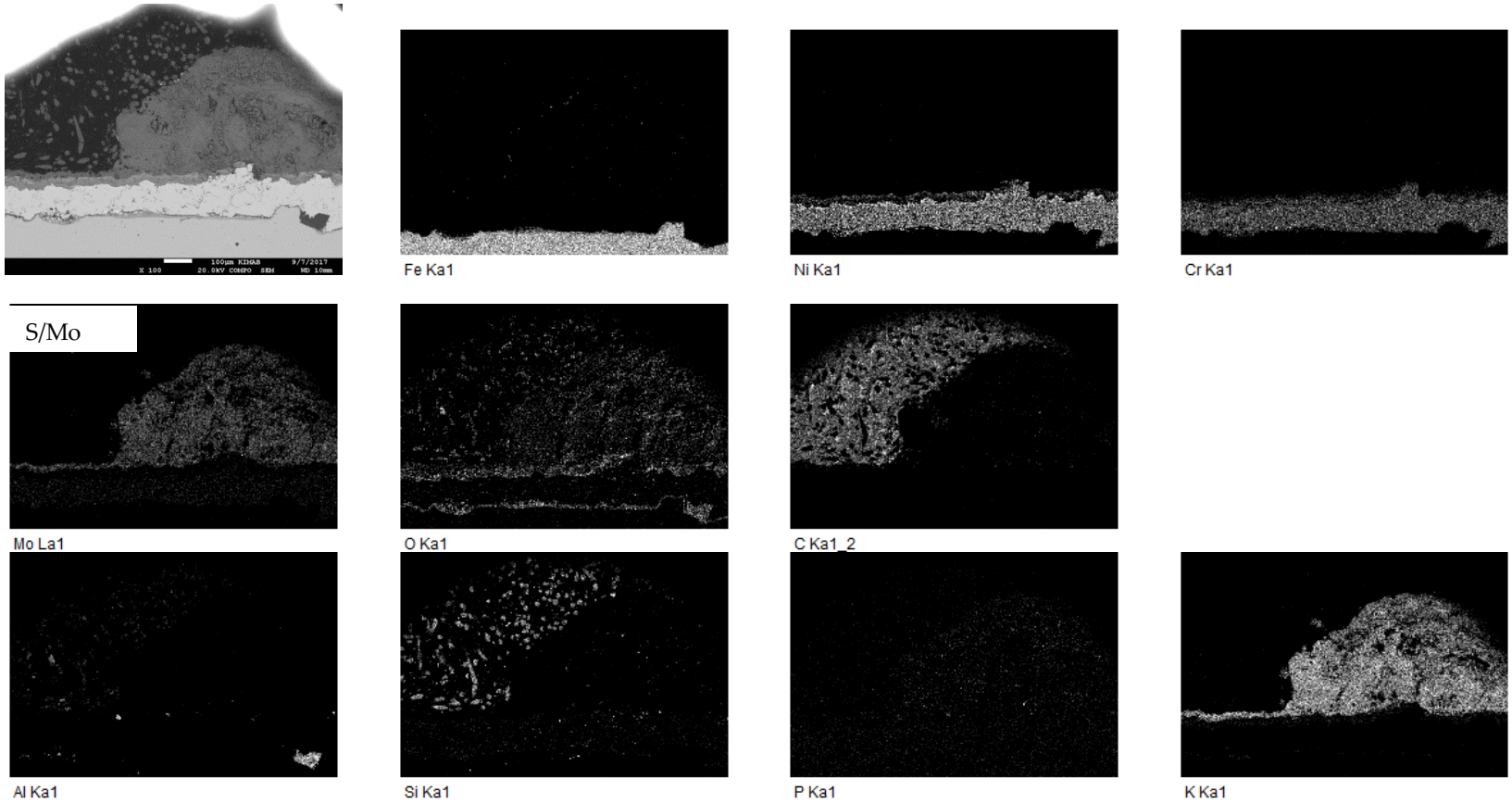

Figure 94. EDS analysis results of material 5 after exposure at Västhamnsverket in the superheater (SH-HT). Sample removed from site in 2017. Scale bar in the SEM image is 100 µm. The S and Mo maps were identical due to an overlap.

9-5_+30m_nr2 (FMP, Al-phosphate) (Mat 5)

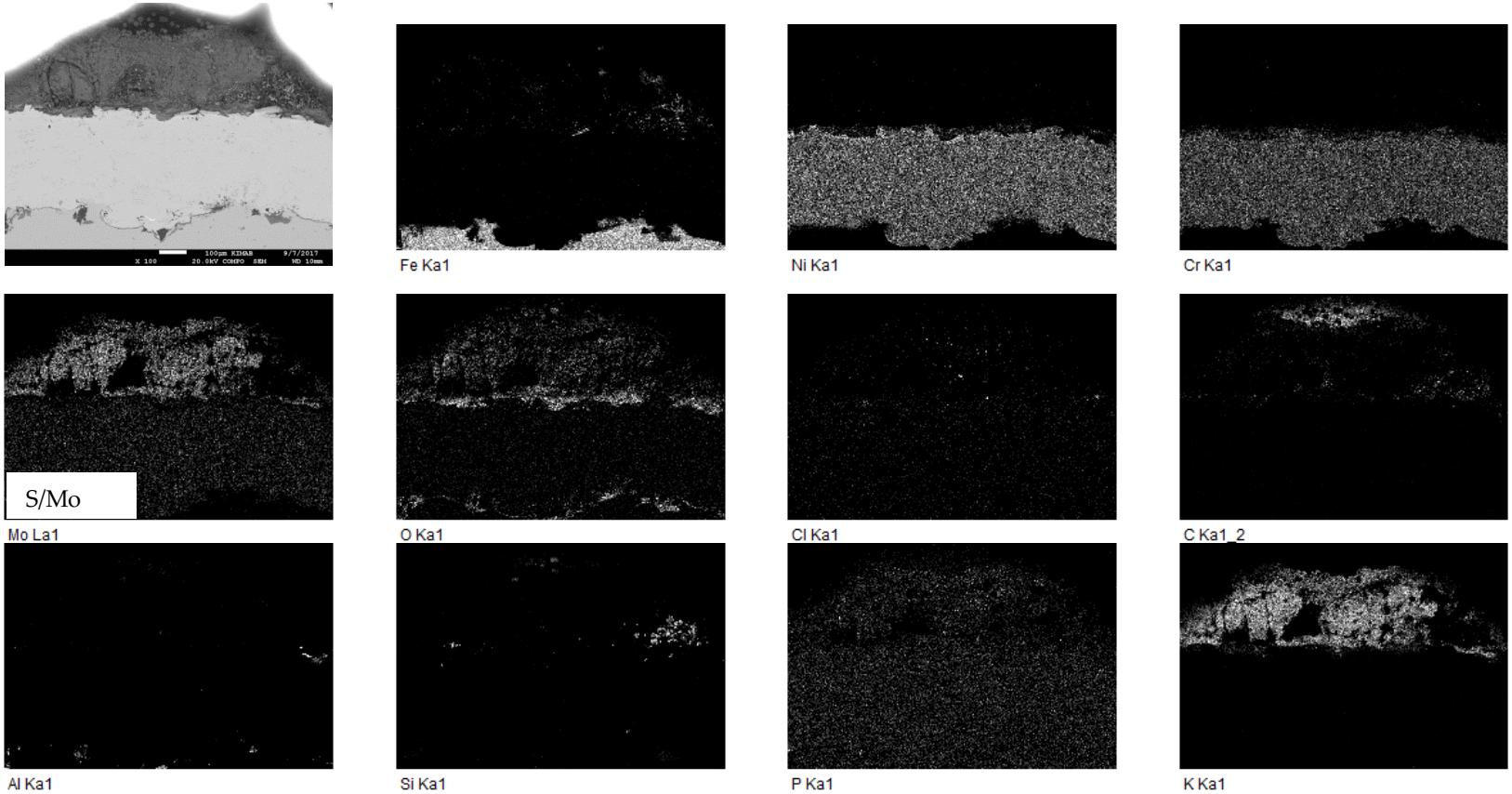

Figure 95. EDS analysis results of material 5 after exposure at Västhamnsverket in the superheater (SH-HT). Sample removed from site in 2017. Scale bar in the SEM image is 100 µm. The S and Mo maps were identical due to an overlap.

9-5_+30m_nr2 (FMP, Al-phosphate) (Mat 5)

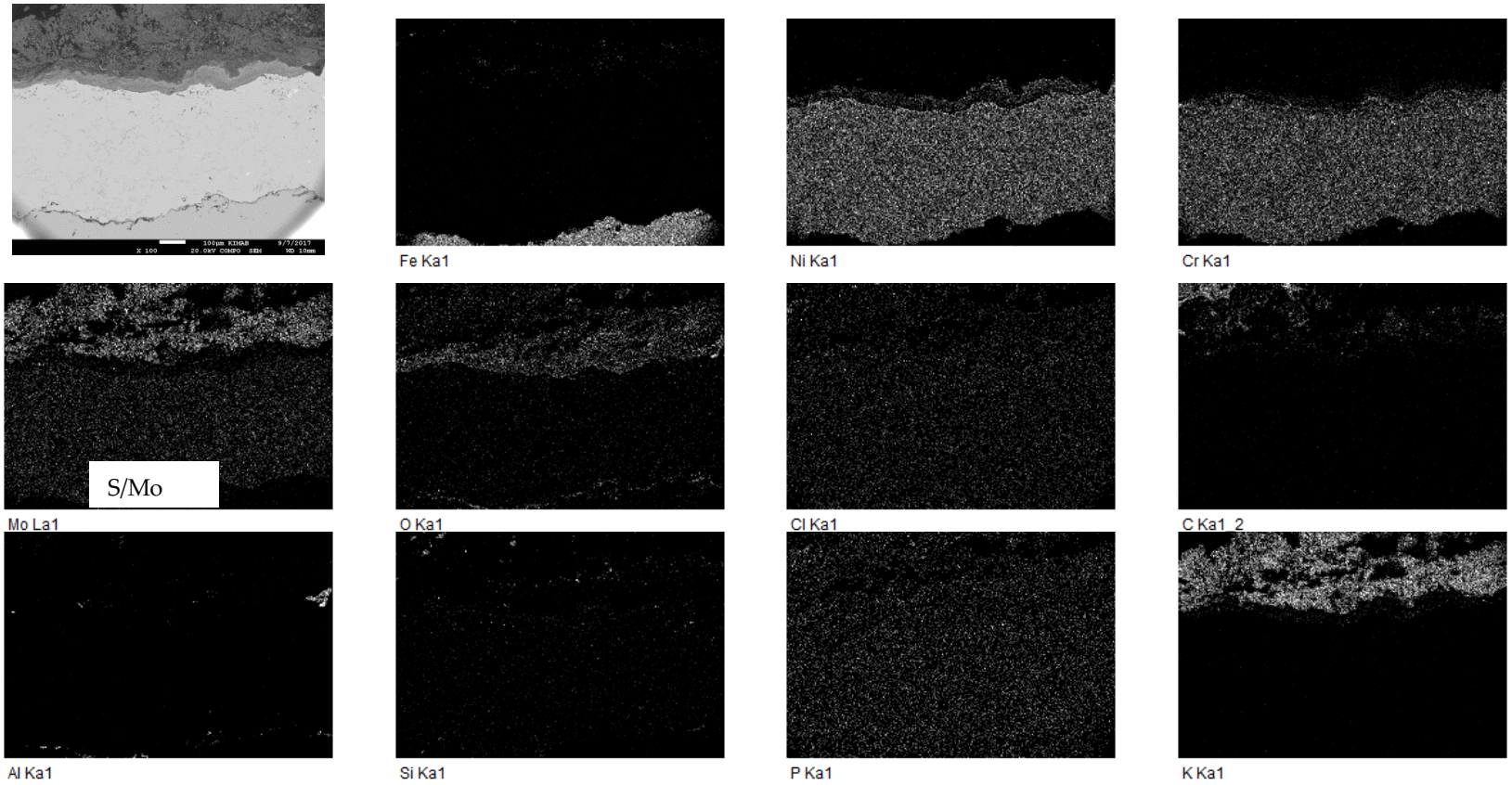

Figure 96. EDS analysis results of material 5 after exposure at Västhamnsverket in the superheater (SH-HT). Sample removed from site in 2017. Scale bar in the SEM image is 100 µm. The S and Mo maps were identical due to an overlap.

Aremco (BN) (Mat 9), (10-9_+30m nr 1) (sample removed in 2017)

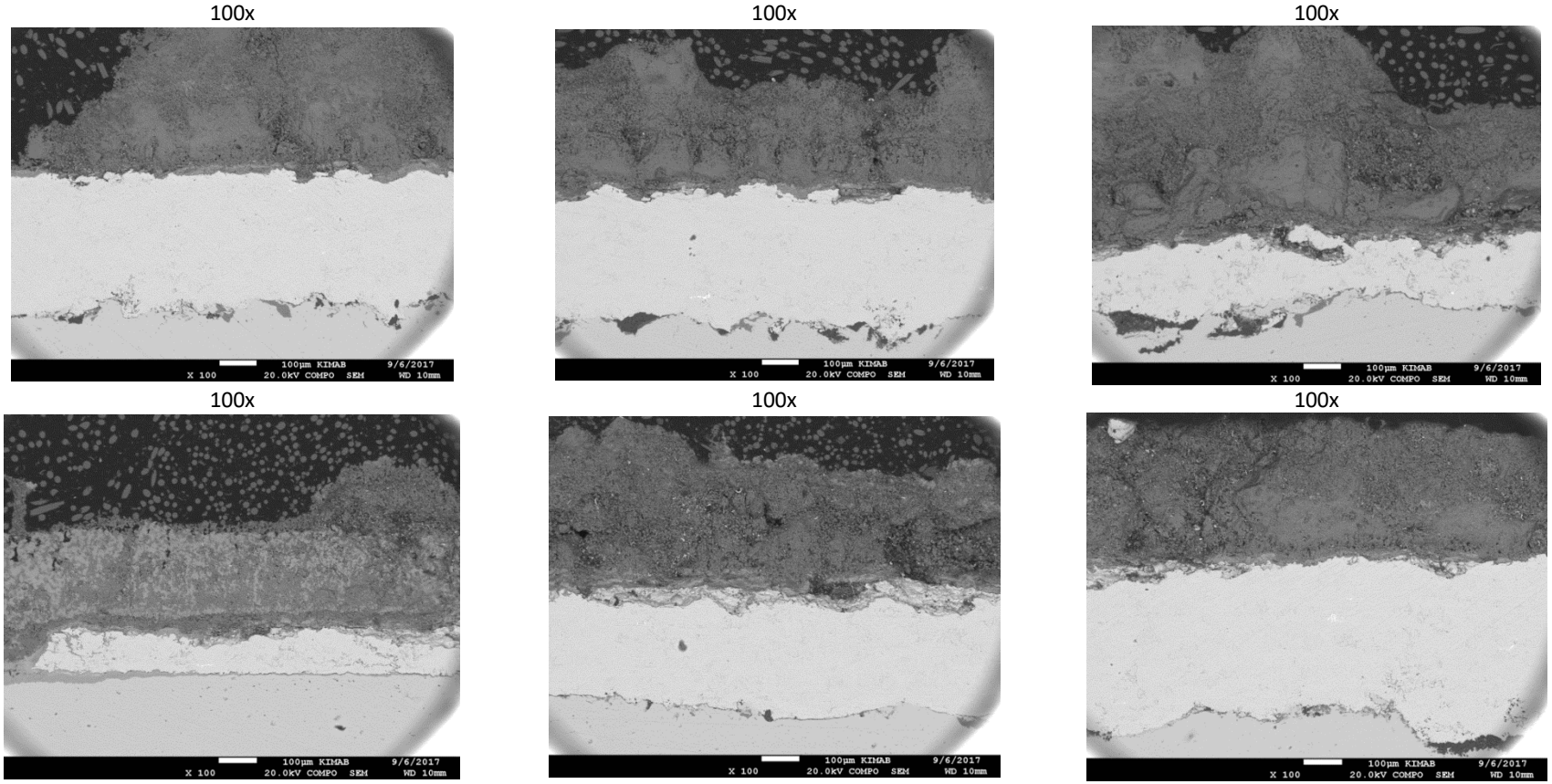

Figure 97. SEM images of material 9 after exposure at Västhamnsverket in the superheater (SH-HT). Sample removed from site in 2017. Scale bar is 100 µm at 100x magnification.

10-9_+30m nr 1__Aremco (BN) (Mat 9)

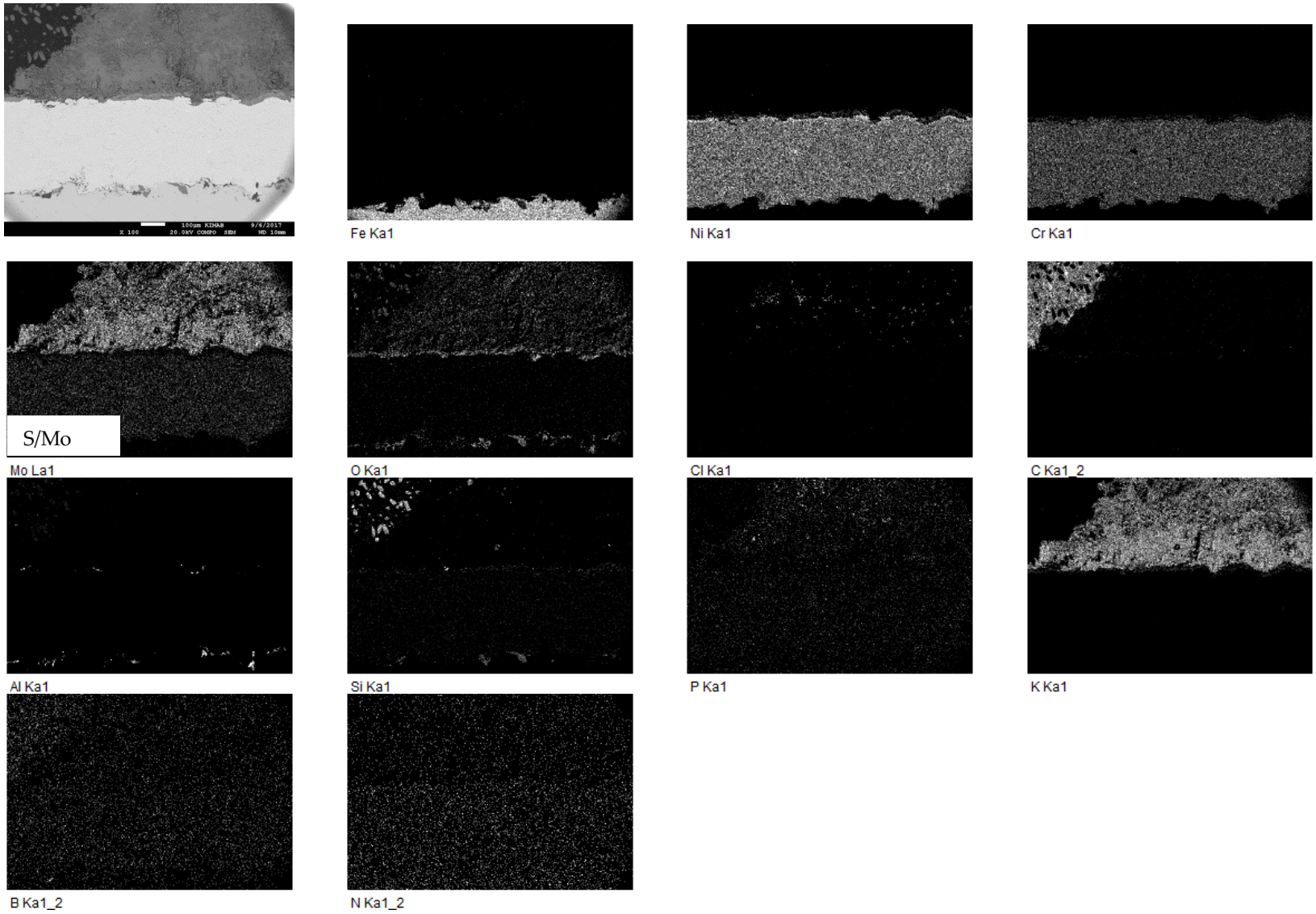

Figure 98. EDS analysis results of material 9 after exposure at Västhamnsverket in the superheater (SH-HT). Sample removed from site in 2017. Scale bar in the SEM image is 100 µm. The S and Mo maps were identical due to an overlap.

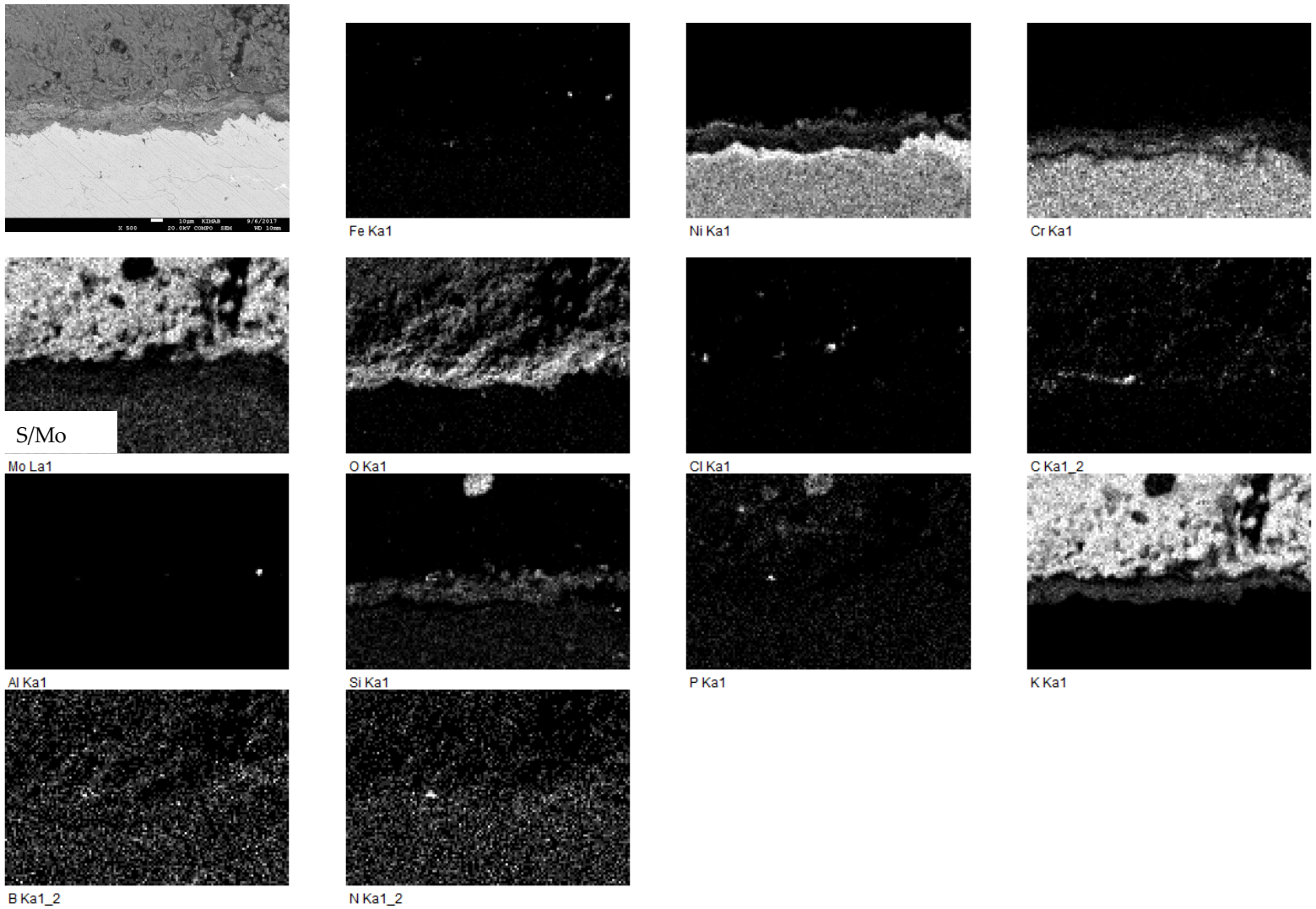

Figure 99. EDS analysis results of material 9 after exposure at Västhamnsverket in the superheater (SH-HT). Sample removed from site in 2017. Scale bar in the SEM image is 10 µm. The S and Mo maps were identical due to an overlap.

10-9_+30m nr 1__Aremco (BN) (Mat 9)

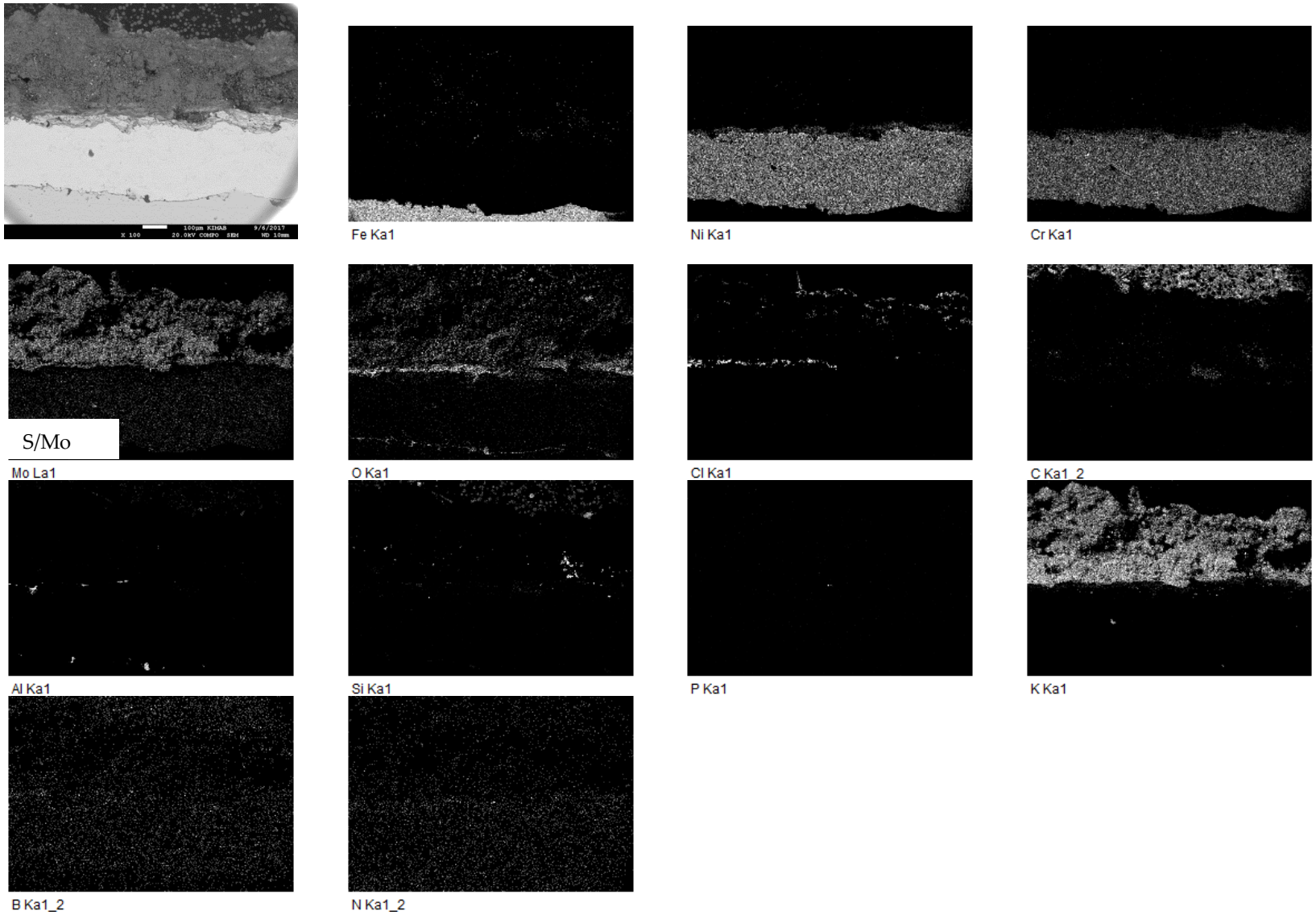

Figure 100. EDS analysis results of material 9 after exposure at Västhamnsverket in the superheater (SH-HT). Sample removed from site in 2017. Scale bar in the SEM image is 100 µm. The S and Mo maps were identical due to an overlap.

Aremco grå (Graphite), (Mat 10) (10-10_+30m_nr1) (sample removed in 2017)

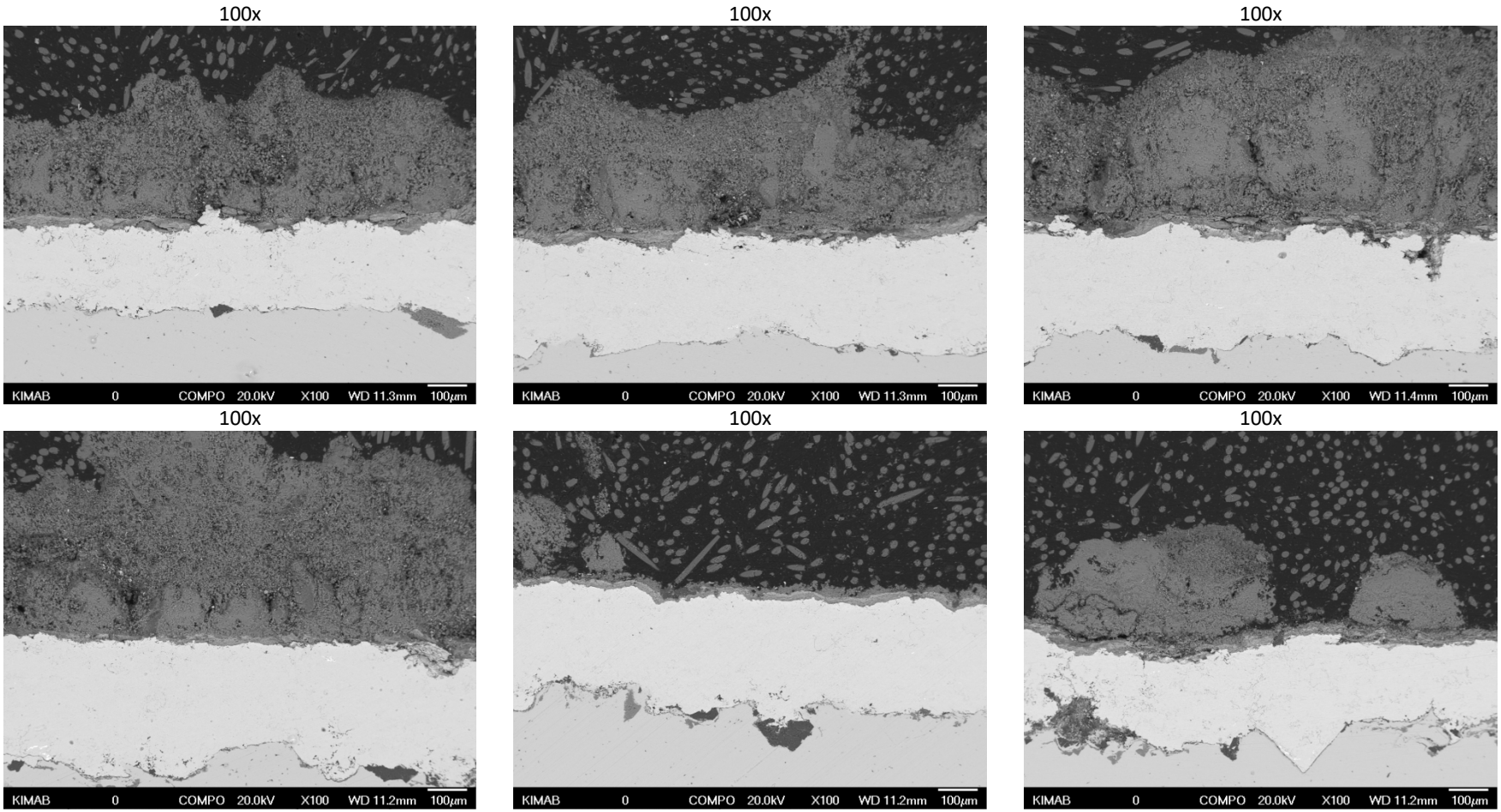

Figure 101. SEM images of material 10 after exposure at Västhamnsverket in the superheater (SH-HT). Sample removed from site in 2017. Scale bar is 100 µm at 100x magnification.

10-10_+30mnr1__Aremco grå (Graphite) (Mat 10)

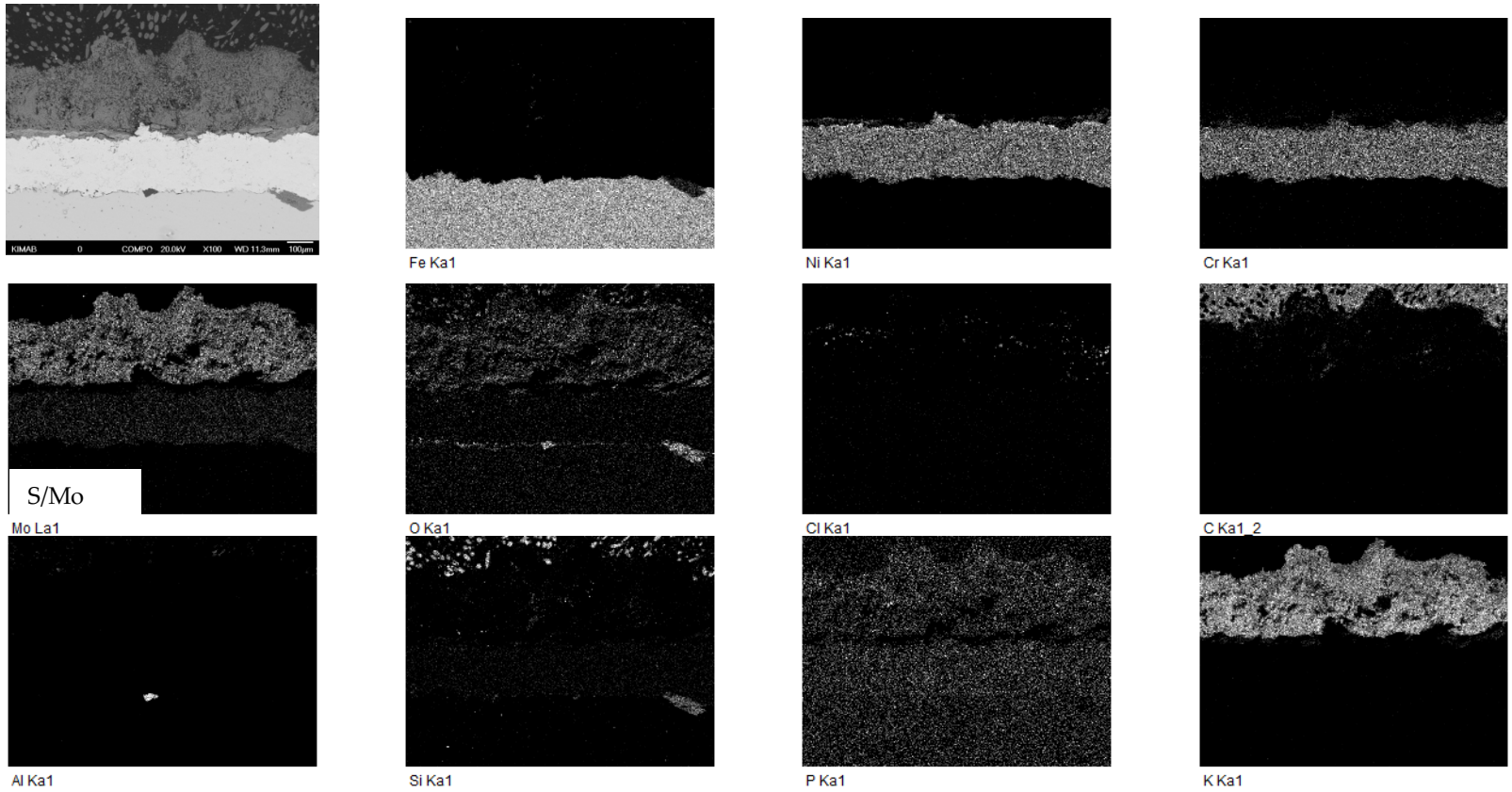

Figure 102. EDS analysis results of material 10 after exposure at Västhamnsverket in the superheater (SH-HT). Sample removed from site in 2017. Scale bar in the SEM image is 100 µm. The S and Mo maps were identical due to an overlap.

10-10_+30mnr1__Aremco grå (Graphite) (Mat 10)

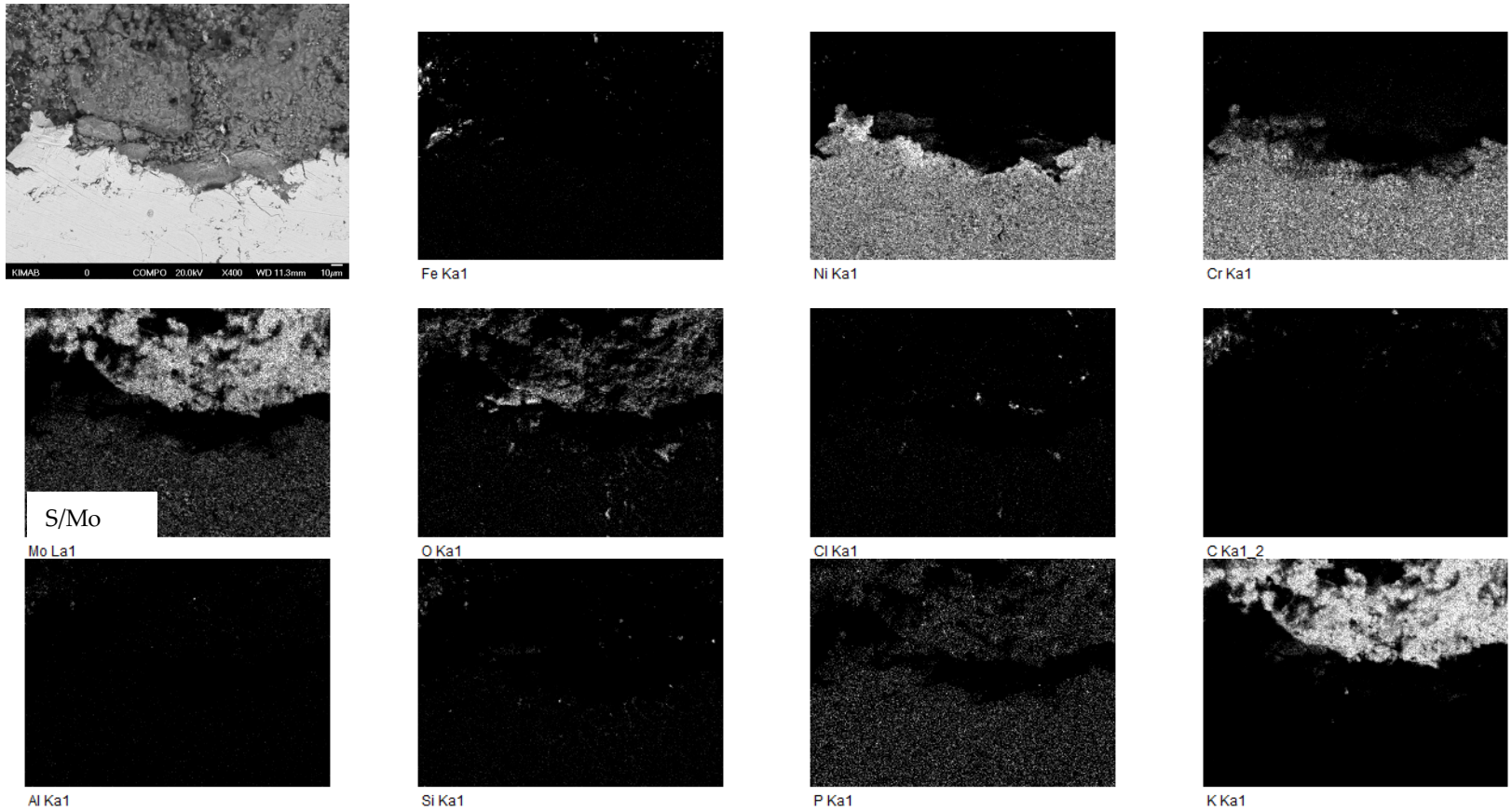

Figure 103. EDS analysis results of material 10 after exposure at Västhamnsverket in the superheater (SH-HT). Sample removed from site in 2017. Scale bar in the SEM image is 10 µm. The S and Mo maps were identical due to an overlap.

10-10_+30mnr1__Aremco grå (Graphite) (Mat 10)

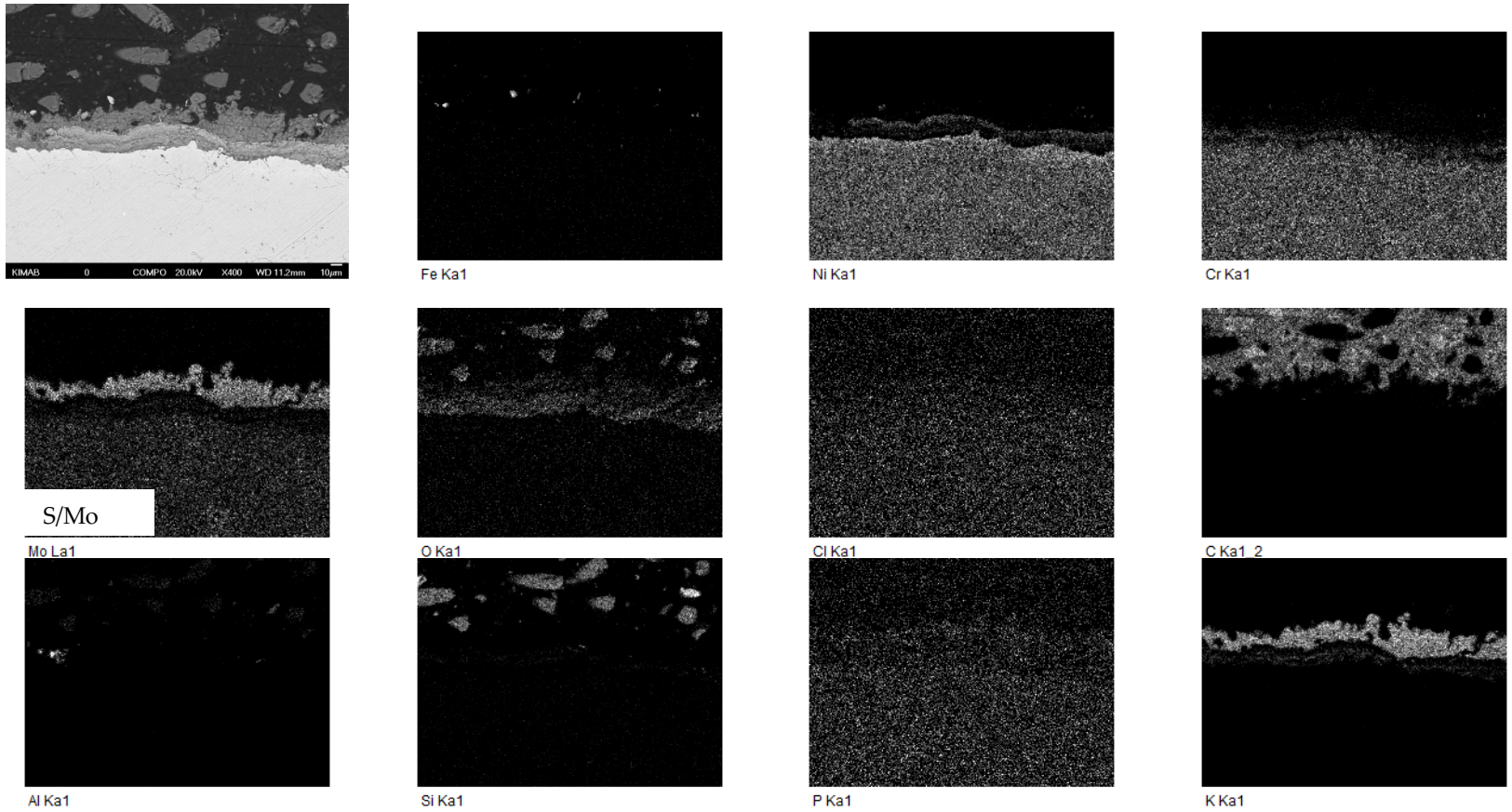

Figure 104. EDS analysis results of material 10 after exposure at Västhamnsverket in the superheater (SH-HT). Sample removed from site in 2017. Scale bar in the SEM image is 10 µm. The S and Mo maps were identical due to an overlap.

SH-LT

Aremco, Silicone, vasthamnsverket, Mat 8 (5.8), 2016

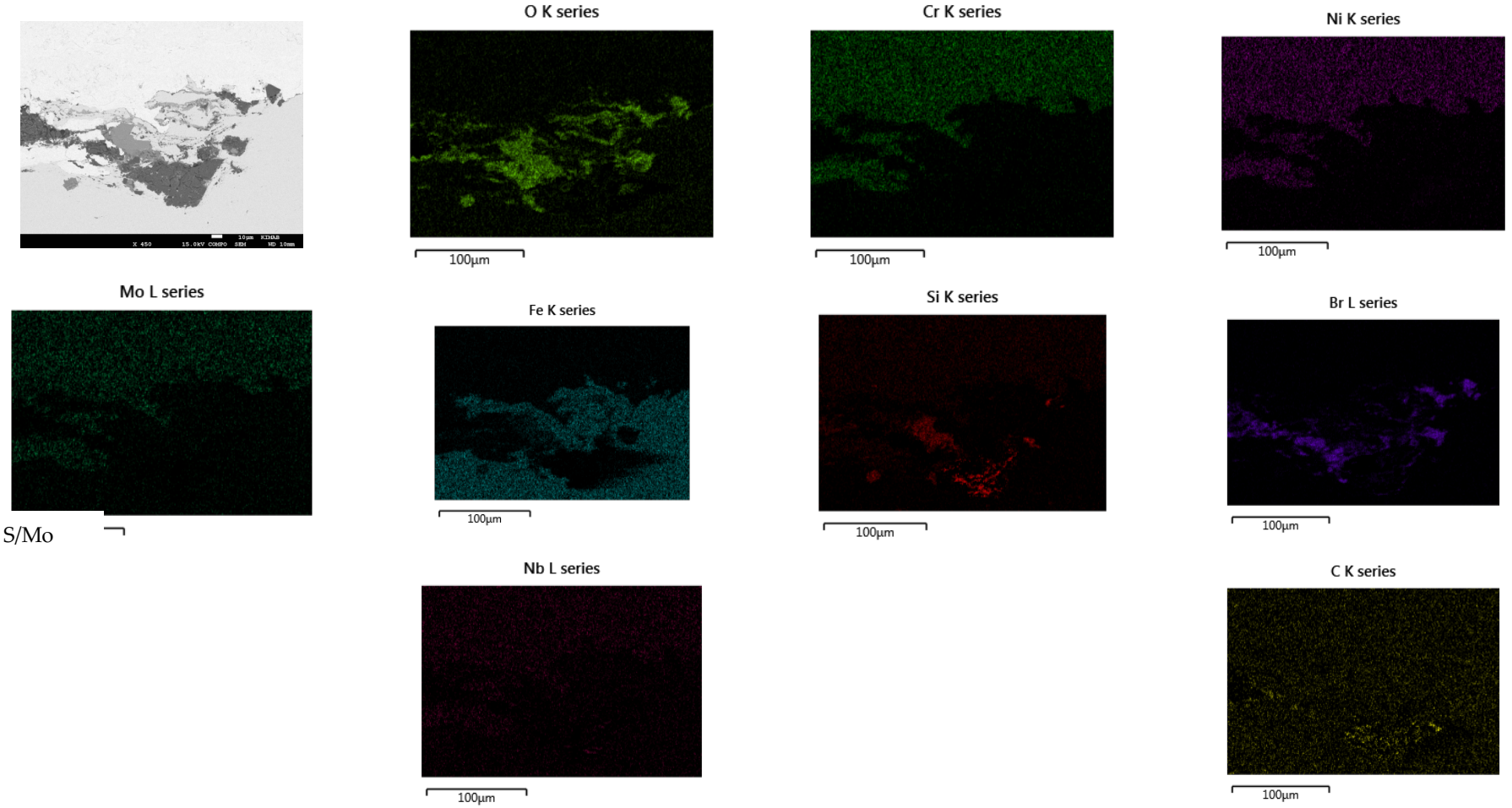

Figure 105. EDS analysis results of material 8 after exposure at Västhamnsverket in the superheater (SH-LT). Sample removed from site in 2016. Scale bar in the SEM image is 10 µm. The S and Mo maps were identical due to an overlap.

ESP Cone

ALU-Releco (ceramic) (Mat 2) (sample removed in 2017)

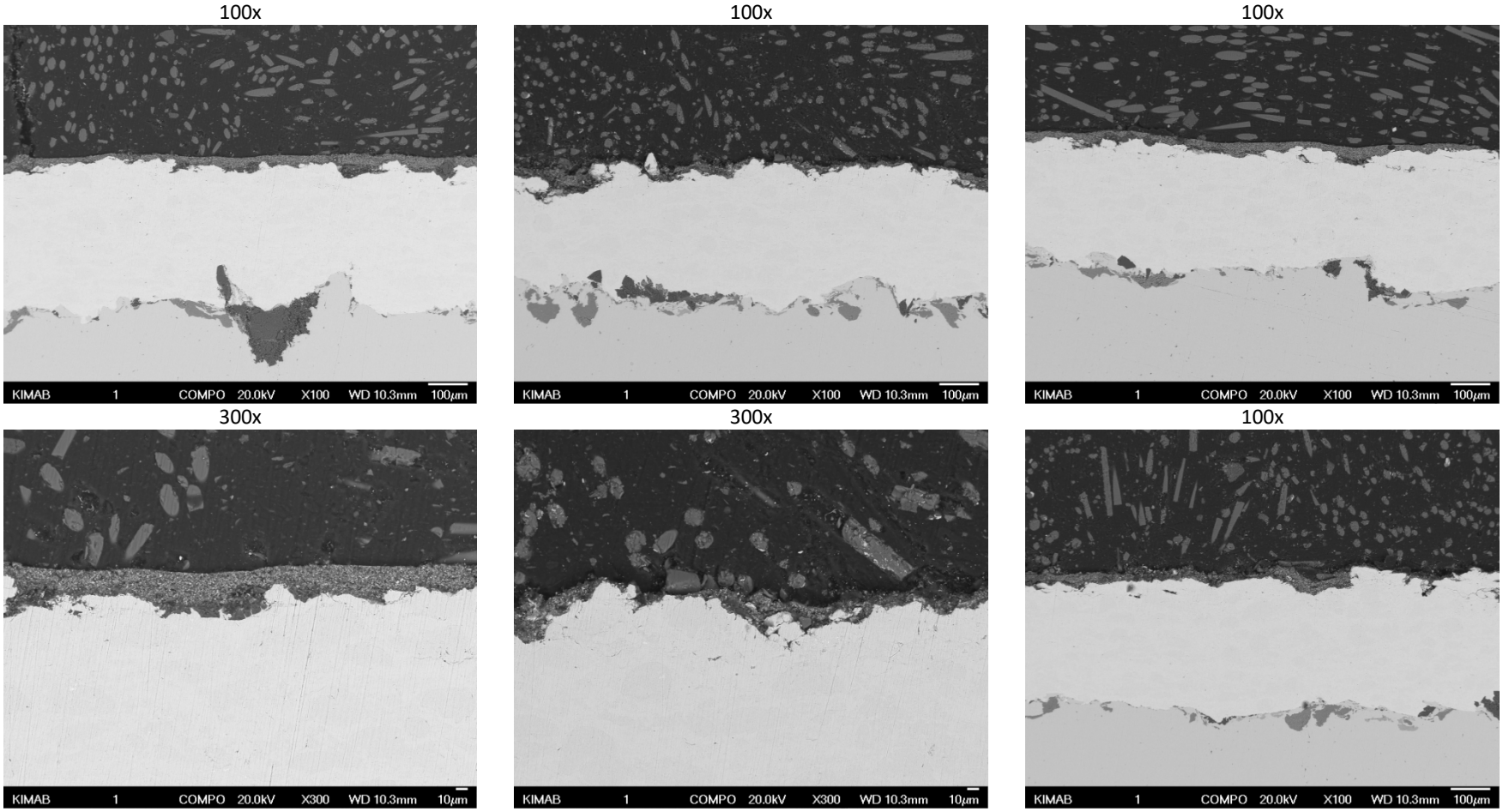

Figure 106. SEM images of material 2 after exposure at Västhamnsverket in the ESP Cone. Sample removed from site in 2017. Scale bar is 100 µm at 100x magnification and 10 µm at 300x

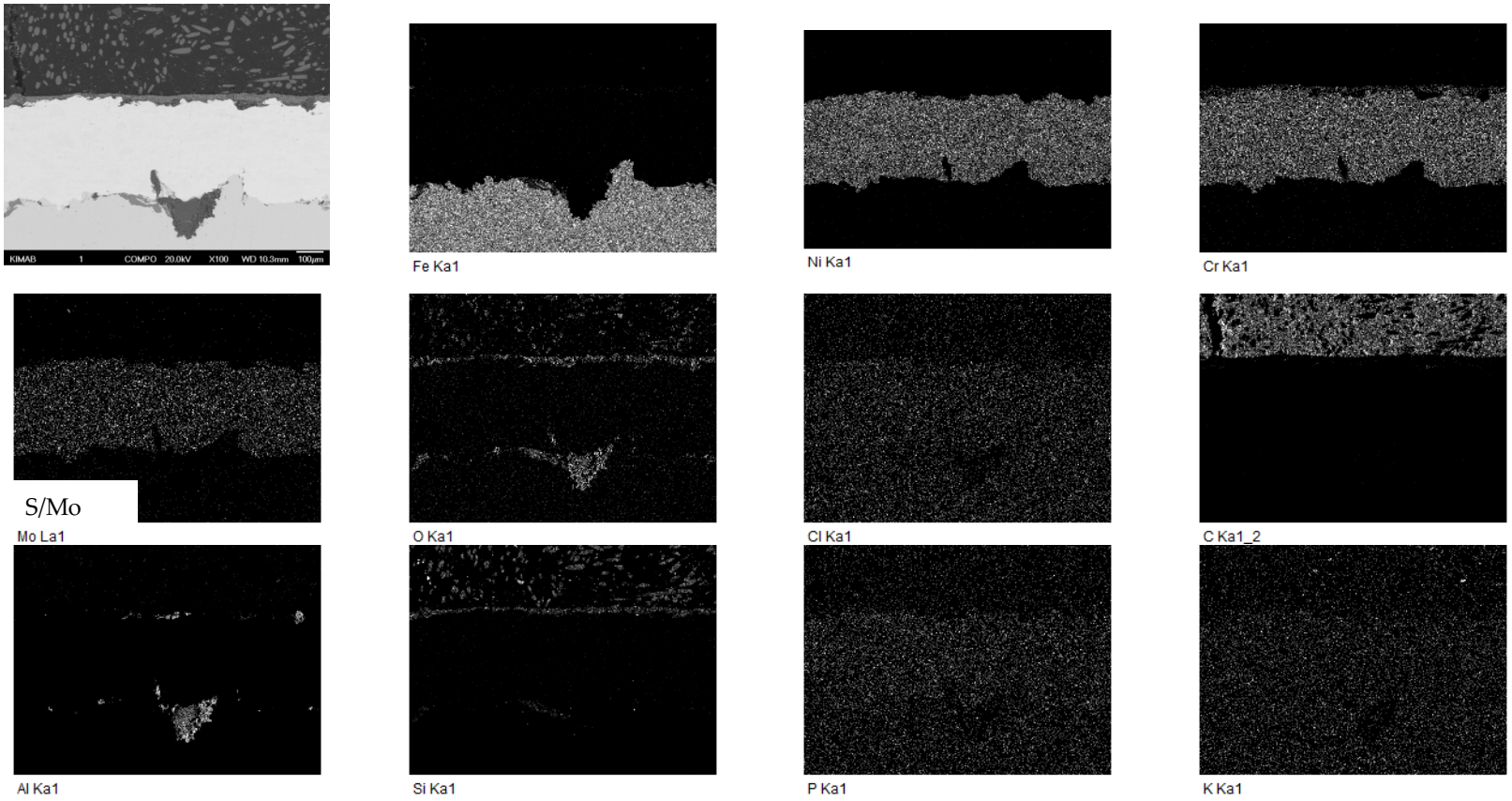

Figure 107. EDS analysis results of material 2 after exposure at Västhamnsverket in the ESP Cone. Sample removed from site in 2017. Scale bar in the SEM image is 100 µm. The S and Mo maps were identical due to an overlap.

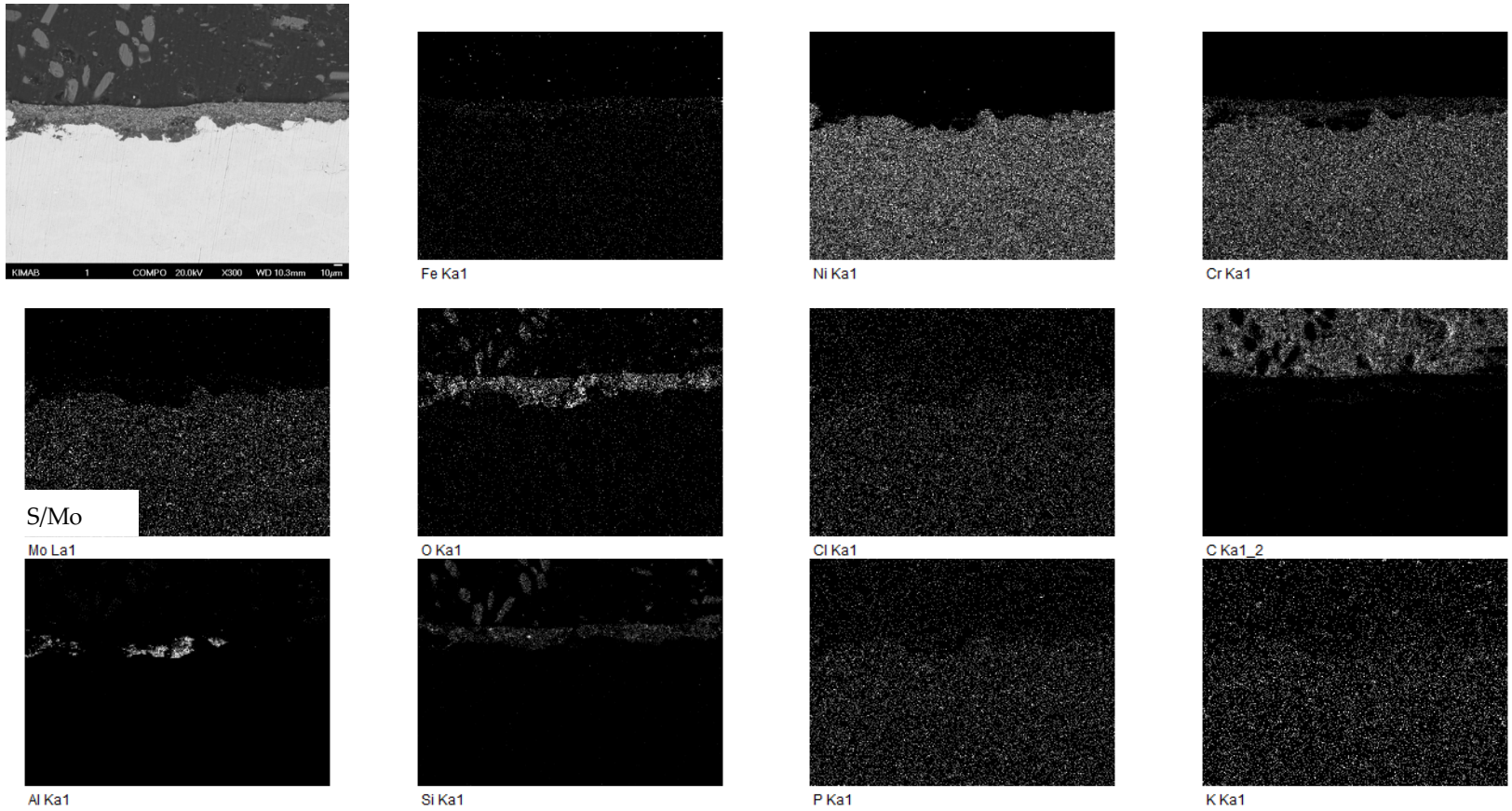

Figure 108. EDS analysis results of material 2 after exposure at Västhamnsverket in the ESP Cone. Sample removed from site in 2017. Scale bar in the SEM image is 10 µm. The S and Mo maps were identical due to an overlap.

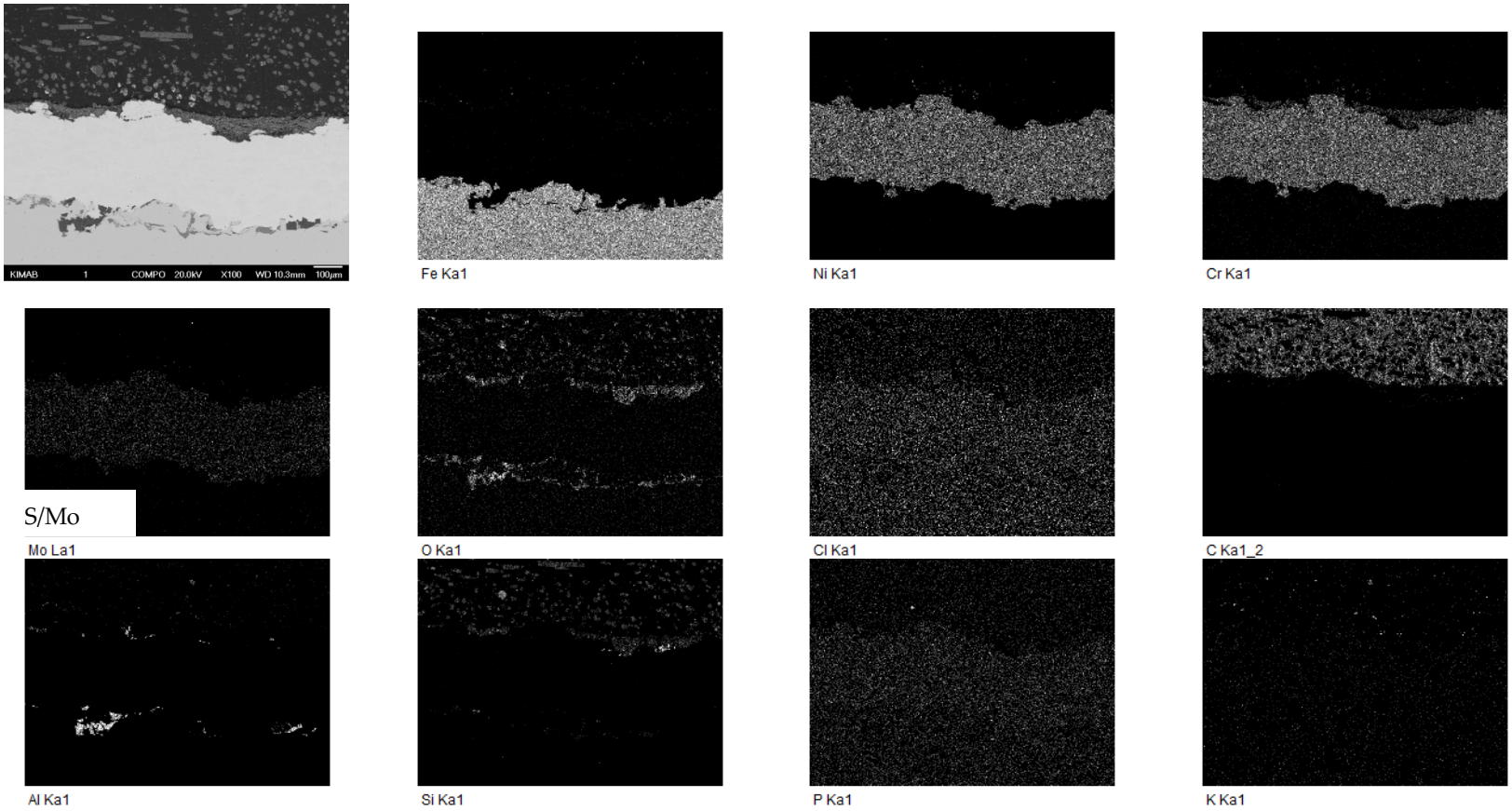

Figure 109. EDS analysis results of material 2 after exposure at Västhamnsverket in the ESP Cone. Sample removed from site in 2017. Scale bar in the SEM image is 100 µm. The S and Mo maps were identical due to overlap.

Diamant Metallplastic, Dichtol HTR (Mat 3) (sample removed in 2017)

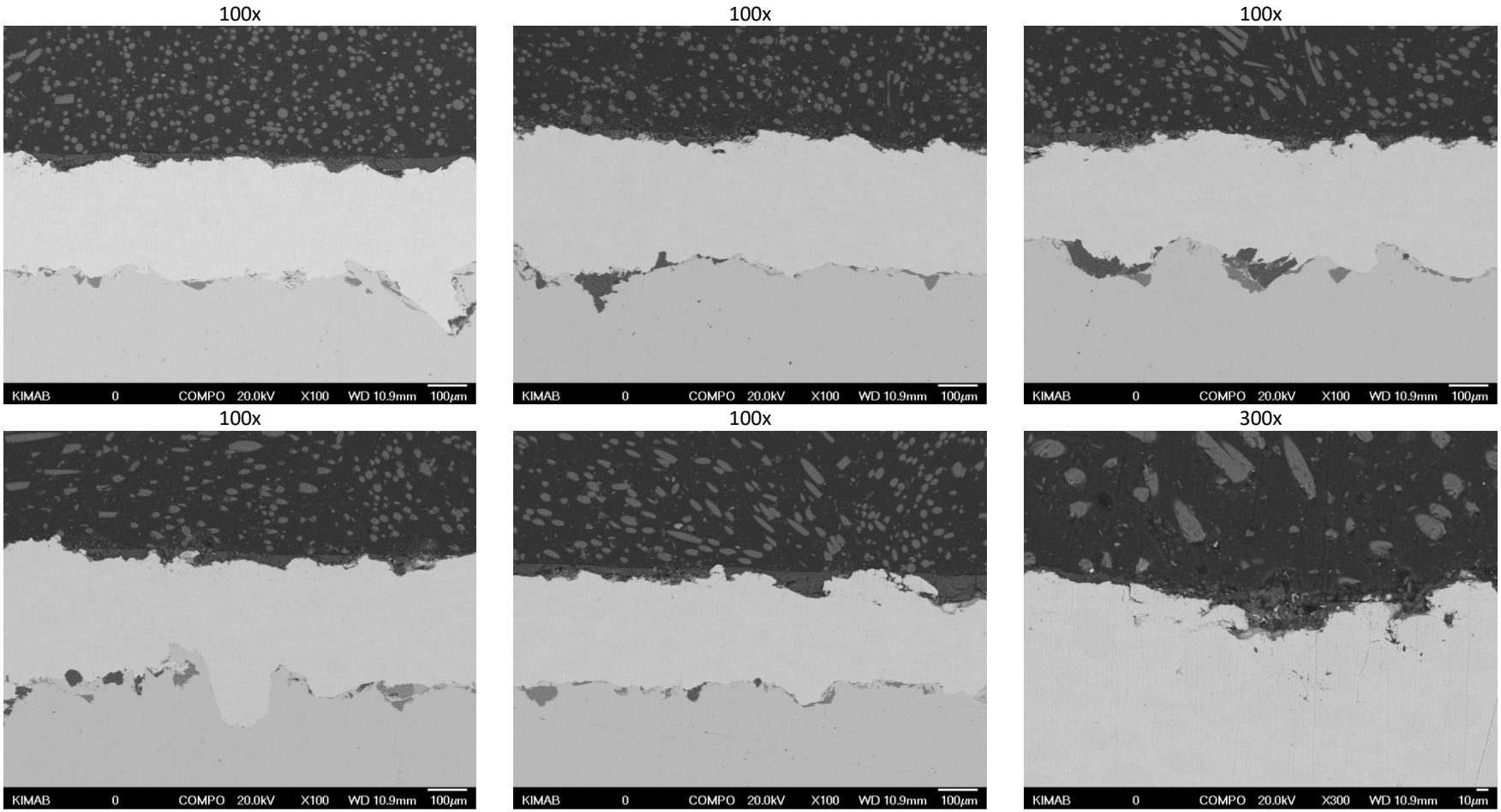

Figure 110. SEM images of material 3 after exposure at Västhamnsverket in the ESP Cone. Sample removed from site in 2017. Scale bar is 100 µm at 100x magnification and 10 µm at 300x.

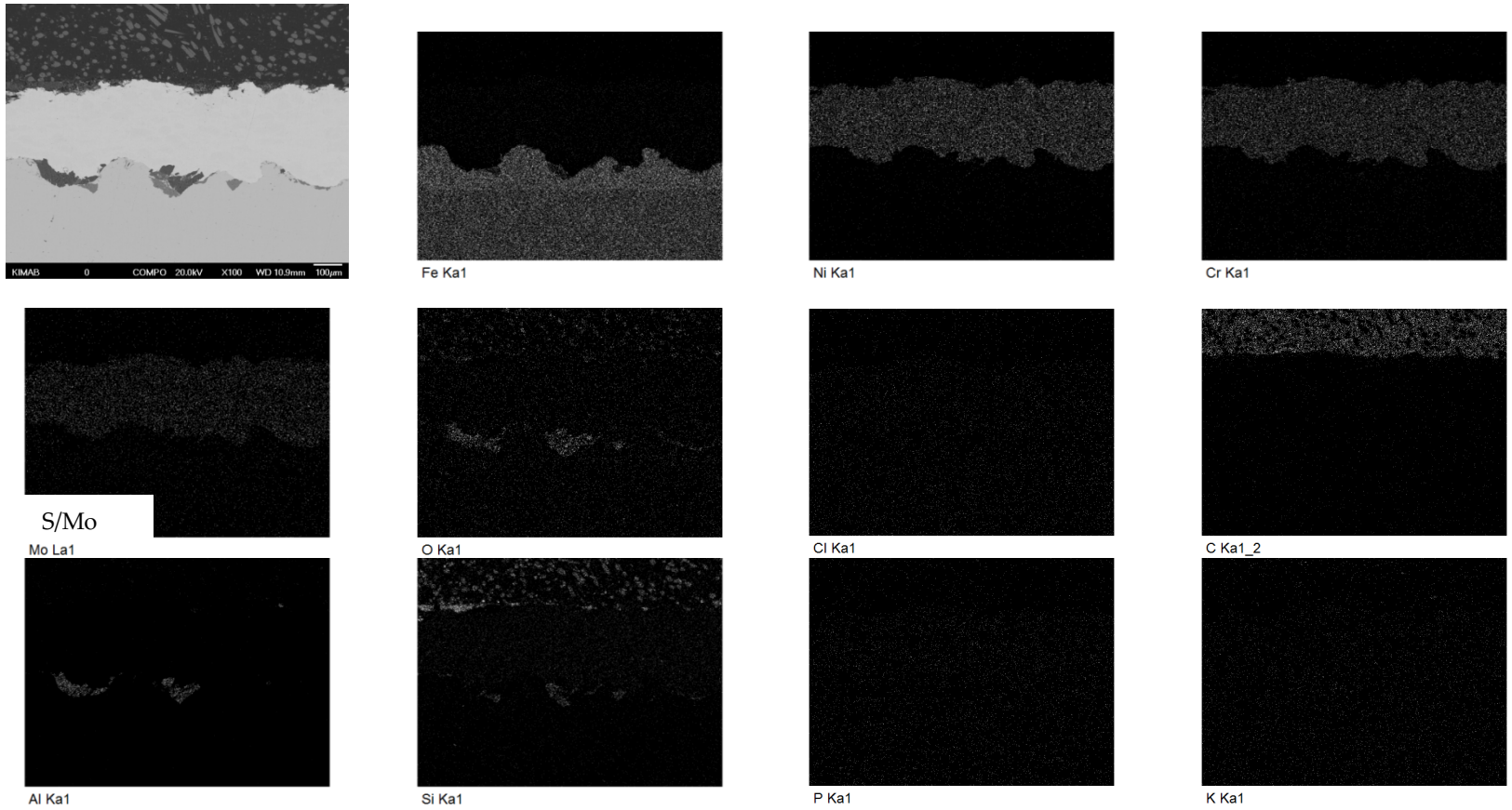

Figure 111. EDS analysis results of material 2 after exposure at Västhamnsverket in the ESP Cone. Sample removed from site in 2017. Scale bar in the SEM image is 100 µm. The S and Mo maps were identical due to overlap.

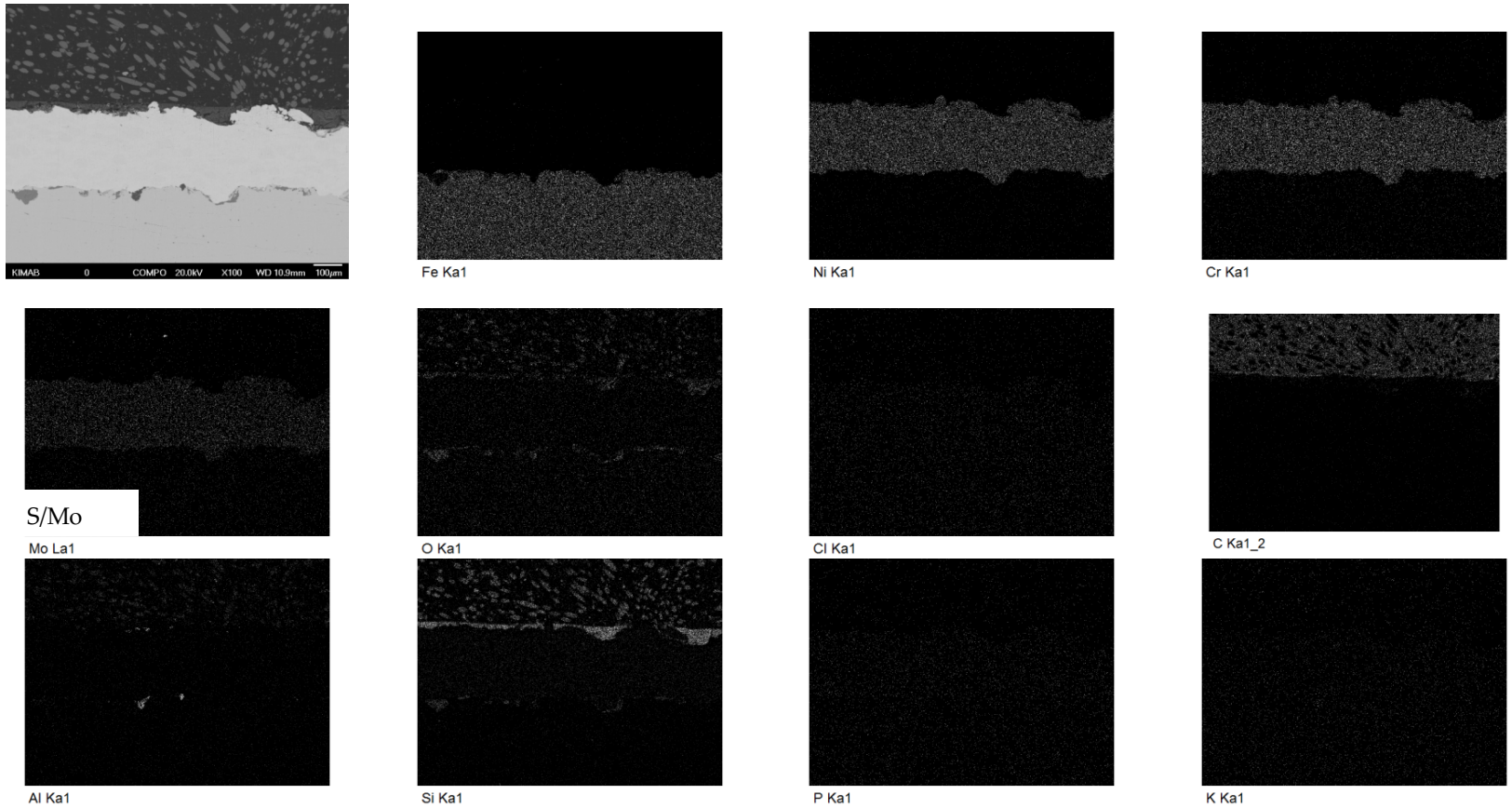

Figure 112. EDS analysis results of material 2 after exposure at Västhamnsverket in the ESP Cone. Sample removed from site in 2017. Scale bar in the SEM image is 100 µm. The S and Mo maps were identical due to overlap.

Ørsted Avedøre

SH-HT

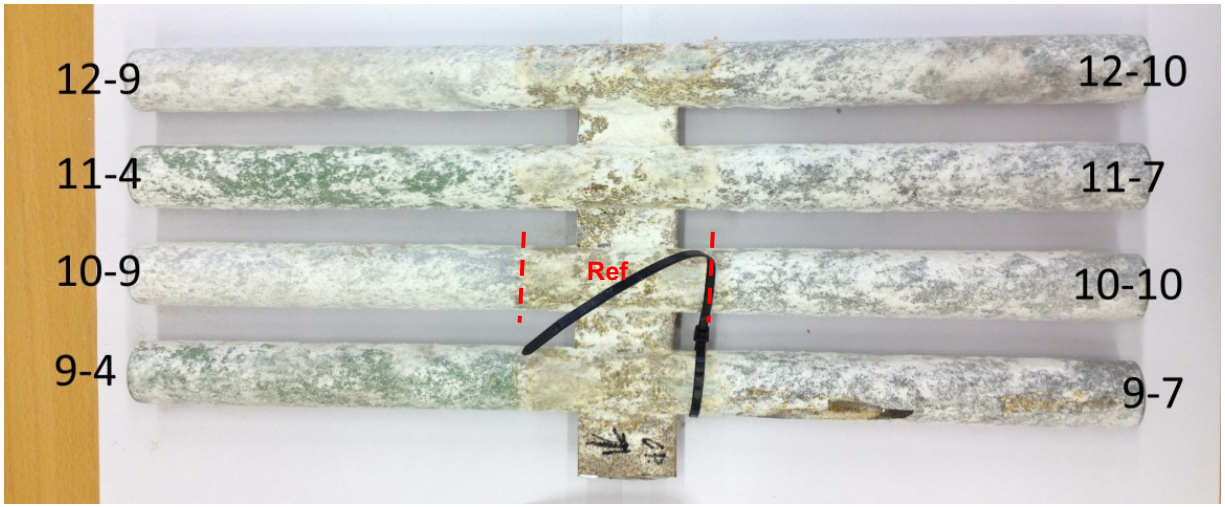

Figure 113. Photographs of tubes coated with material 4, 7, 9 and 10 (as highlighted in picture) after exposure at Ørsted Avedøre in the superheater (SH-HT). Tubes were removed from site in 2017. Reference sample was taken from non-coated region within dashed lines. Metallographic examination was carried out for the reference sample and samples 9-4, 9-7, 10-9 and 10-10.

Carbon steel reference (sample removed 2017), (SH HT)

Carbon steel reference (sample removed in 2017)

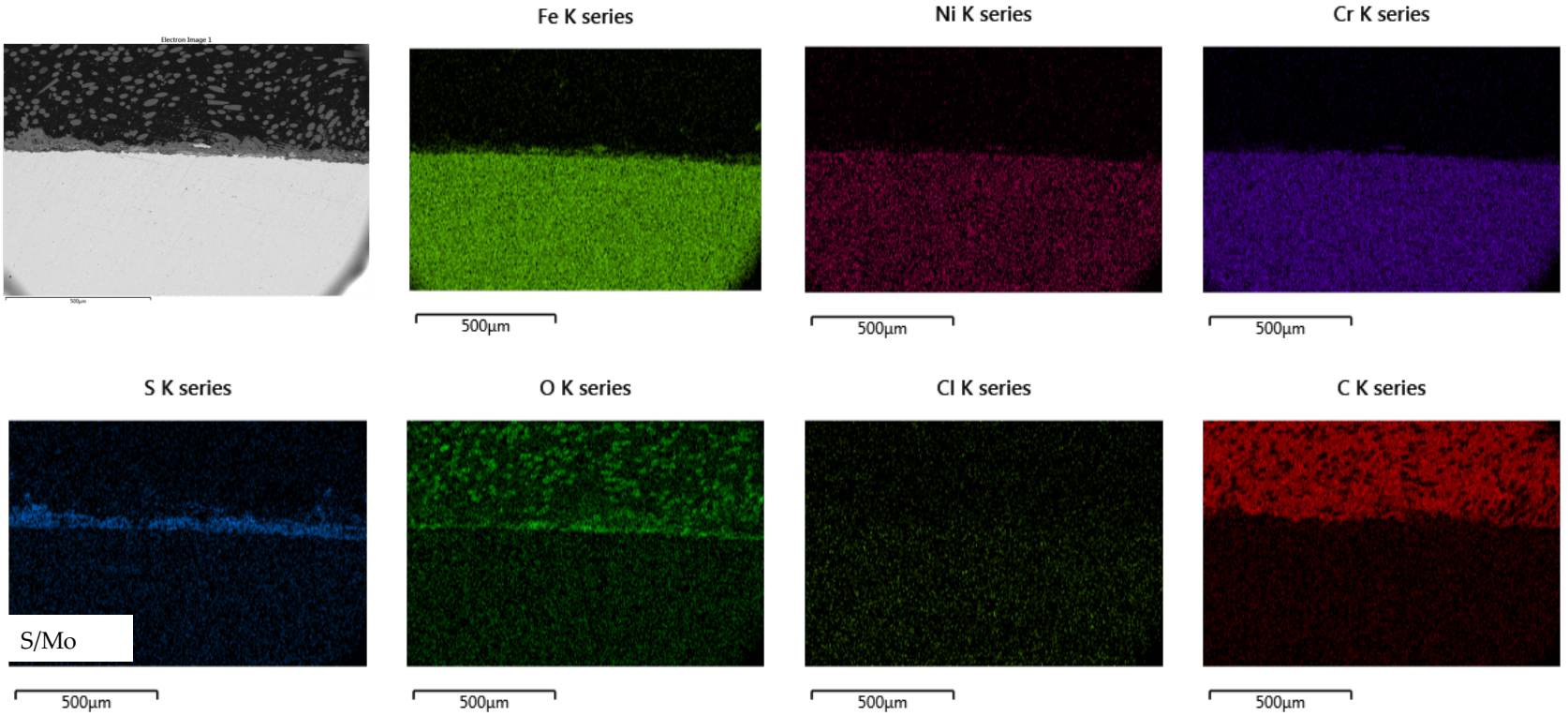

Carbon steel reference (sample removed 2017), (SH HT)

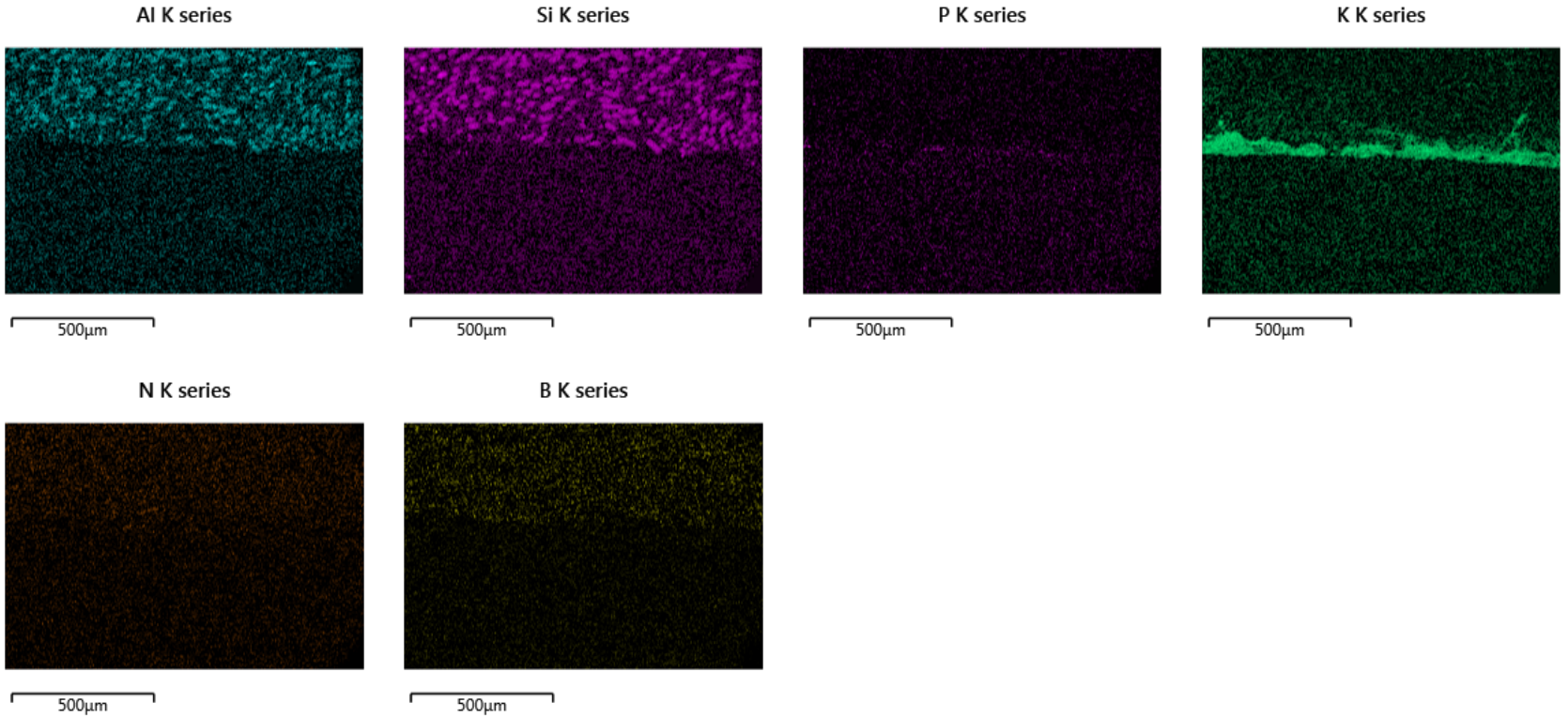

Figure 114. EDS analysis results of carbon steel reference sample after exposure at Ørsted Avedøre in the superheater (SH-HT). Sample removed from site in 2017. Scale bar in SEM image is 500 µm.

Beläggningstyp FMP (BN-silicate), Prov 2B (SH HT) (Mat 4) (sample removed in 2017)

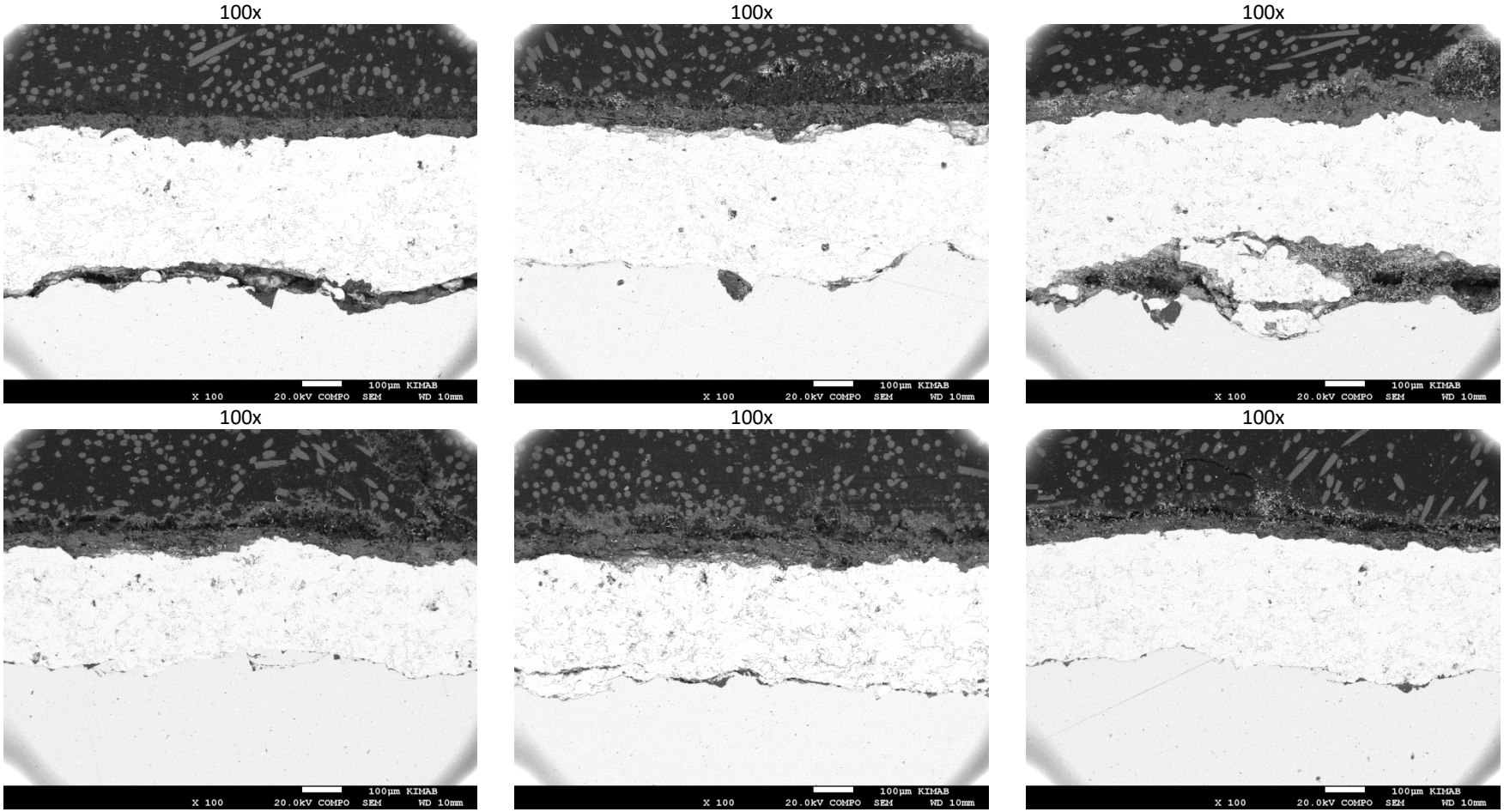

Figure 115. SEM images of material 4 after exposure at Ørsted Avedøre in the superheater (SH-HT). Sample removed from site in 2017. Scale bar is 100 µm at 100x magnification.

Beläggningstyp FMP (BN-silicate), Mat 4, Prov 2B (9.4) (SH HT)

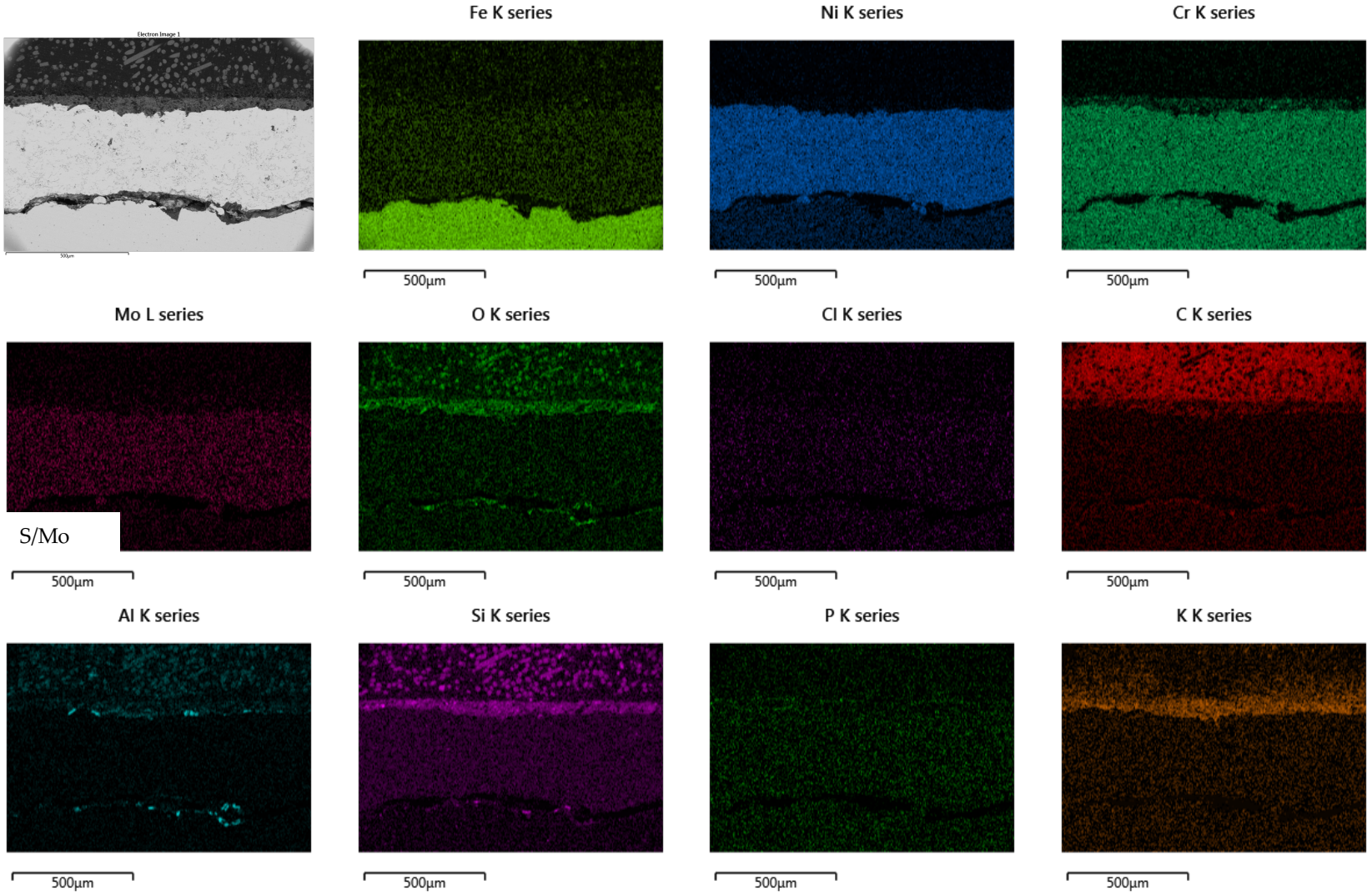

Beläggningstyp FMP (BN-silicate), Mat 4, Prov 2B (9.4) (SH HT)

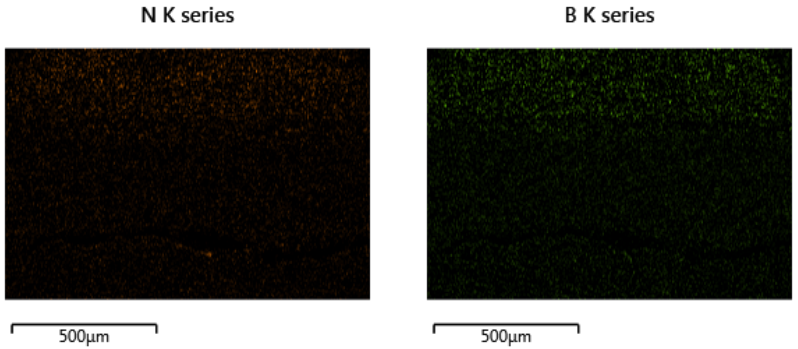

Figure 116. EDS analysis results of material 4 after exposure at Ørsted Avedøre in the superheater (SH-HT). Sample removed from site in 2017. Scale bar in SEM image is 500 µm. The S and Mo maps were identical due to overlap.

Beläggningstyp FMP (BN-silicate), Mat 4, Prov 2B (9.4) (SH HT)

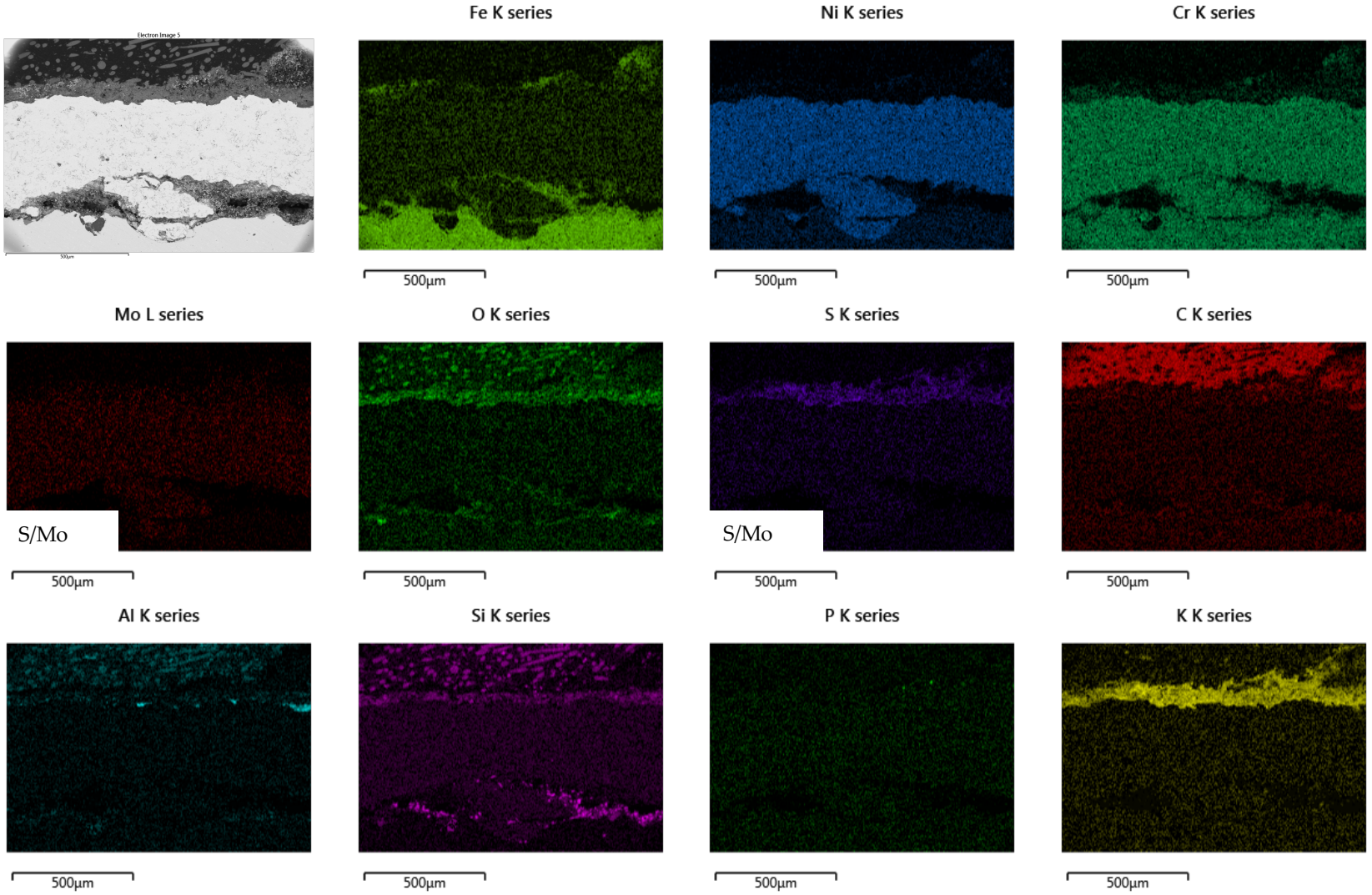

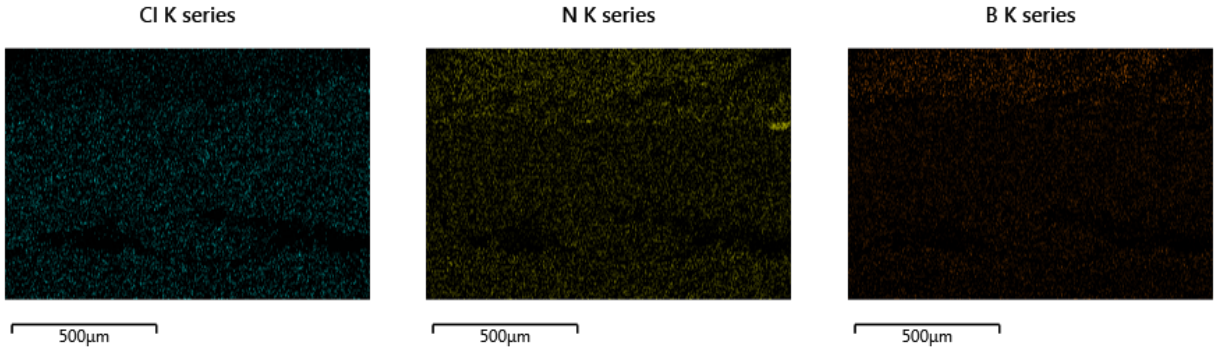

Figure 117. EDS analysis results of material 4 after exposure at Ørsted Avedøre in the superheater (SH-HT). Sample removed from site in 2017. Scale bar in SEM image is 500 µm. Note the difference in sulphur and molybdenum signal despite ordinary EDS analysis. The maps are an indication of sulphur in the deposit layer and Mo in the nickel-base layer, but S and Mo normally overlap.

Beläggningstyp Millidyne, Prov 2a (SH HT) (Mat 7) (sample removed in 2017)

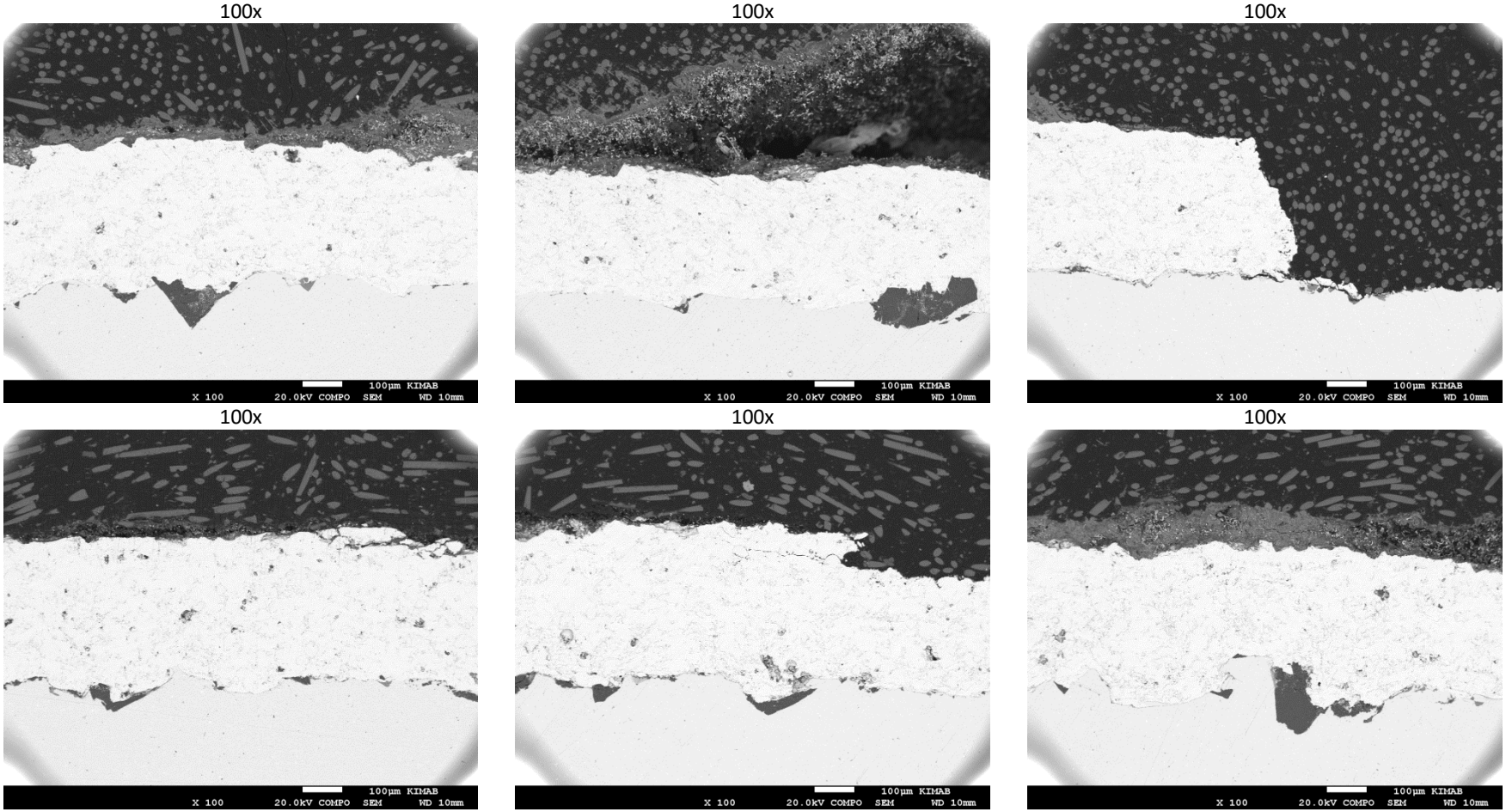

Figure 118. SEM images of material 7 after exposure at Ørsted Avedøre in the superheater (SH-HT). Sample removed from site in 2017. Scale bar is 100 µm at 100x magnification.

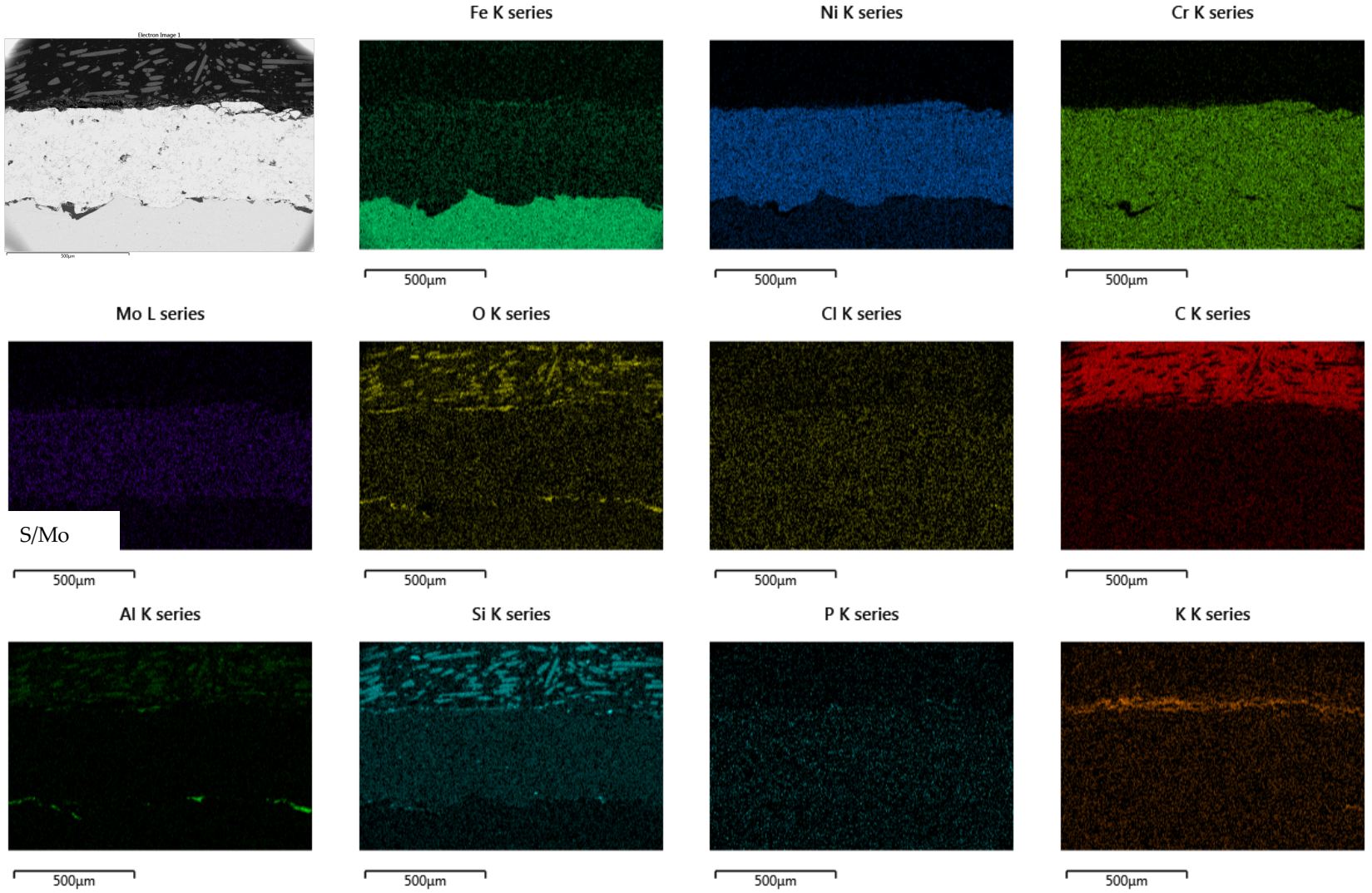

Figure 119. EDS analysis results of material 7 after exposure at Ørsted Avedøre in the superheater (SH-HT). Sample removed from site in 2017. Scale bar in SEM image is 500 µm. The S and Mo maps were identical due to overlap.

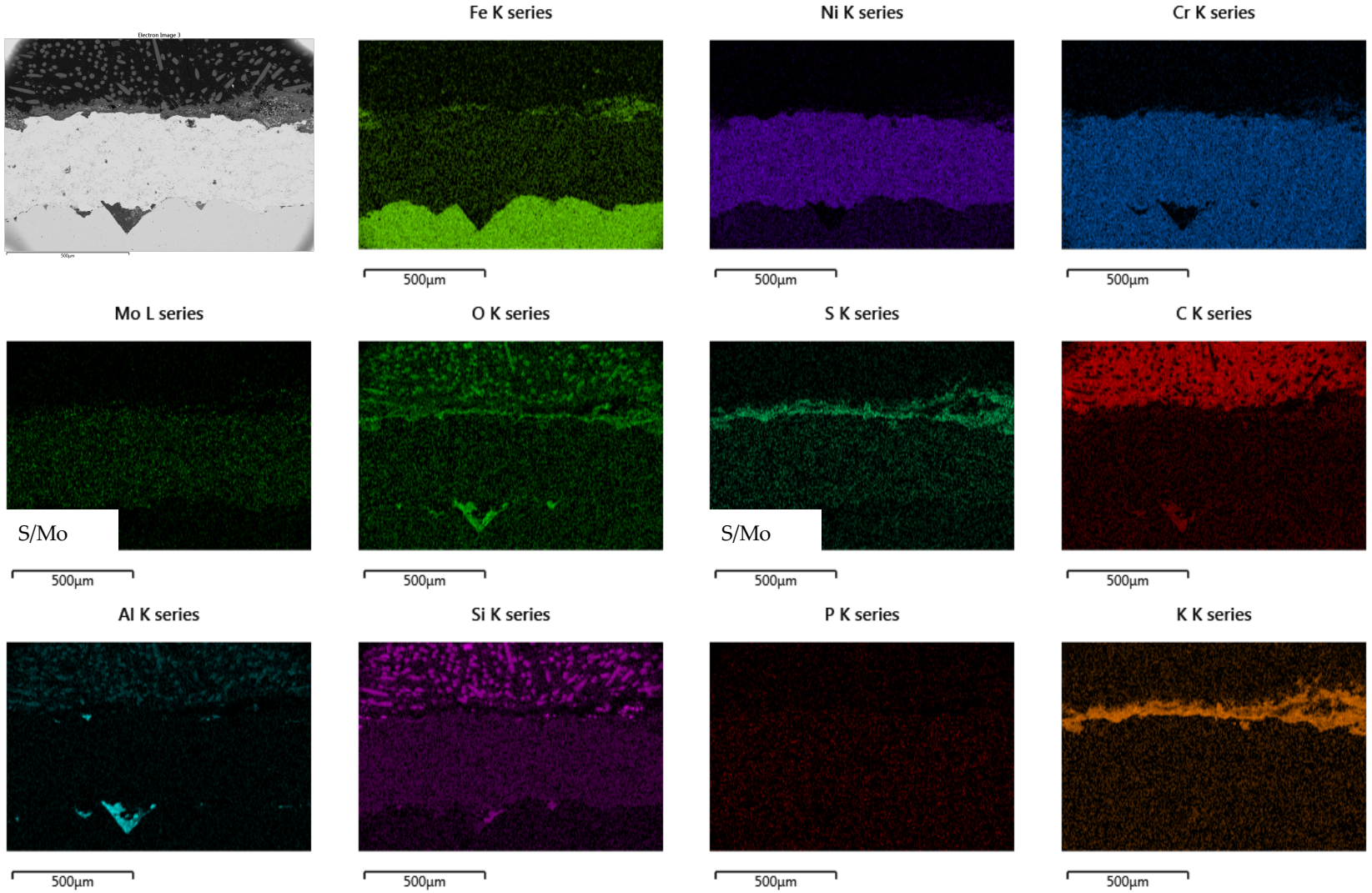
Fe K series
Ni K series
Cr K series
500µm
Mo L series
O K series
S K series
C K series
S/Mo
S/Mo
Al K series
Si K series
P K series
K K series

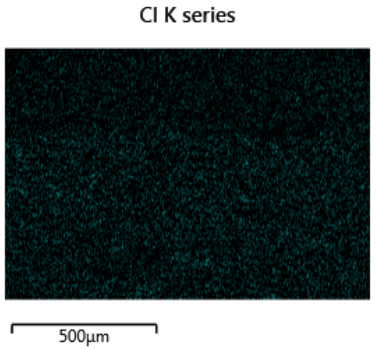

Figure 120. EDS analysis results of material 7 after exposure at Ørsted Avedøre in the superheater (SH-HT). Sample removed from site in 2017. Scale bar in SEM image is 500 µm. Note the difference in sulphur and molybdenum signal despite ordinary EDS analysis. The maps are an indication of sulphur in the deposit layer and Mo in the nickel-base layer, but S and Mo normally overlap as indicated.

Beläggningstyp Aremco, BN, Prov 2D (SH HT) (Mat 9) (sample removed in 2017)

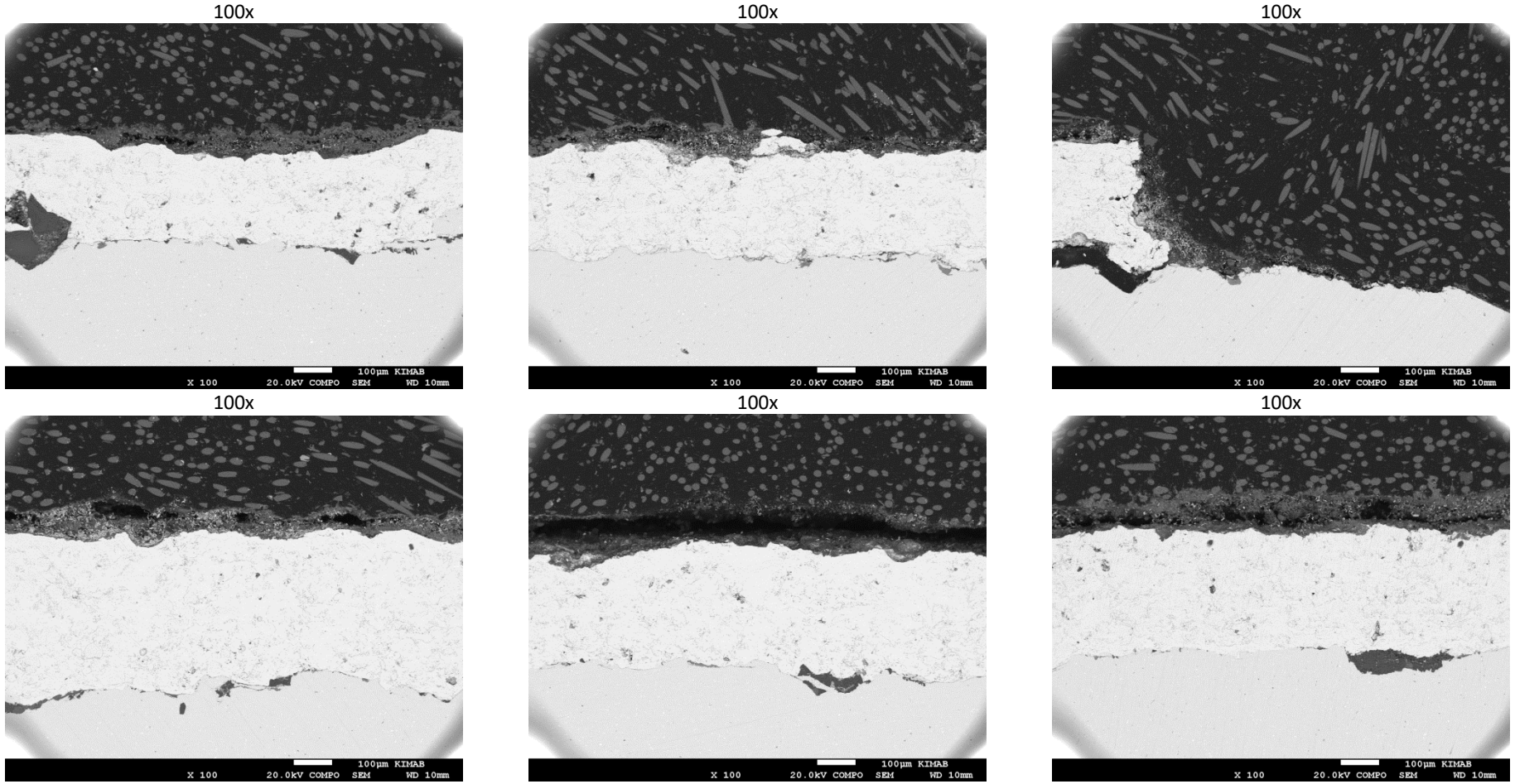

Figure 121. SEM images of material 9 after exposure at Ørsted Avedøre in the superheater (SH-HT). Sample removed from site in 2017. Scale bar is 100 µm at 100x magnification.

Beläggningstyp Aremco, BN, Prov 2D (10.9) (SH HT)

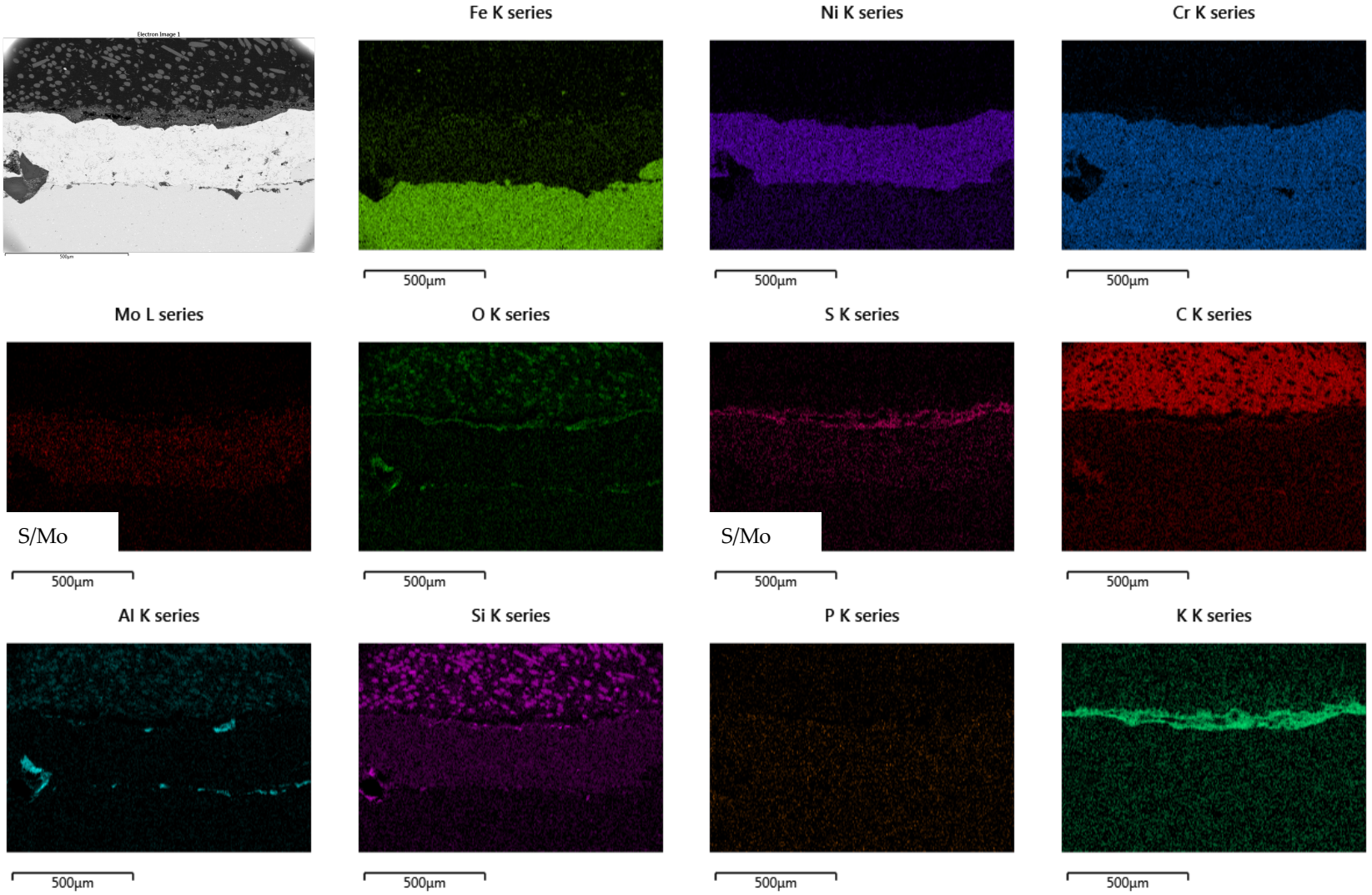

Beläggningstyp Aremco, BN, Prov 2D (10.9) (SH HT)

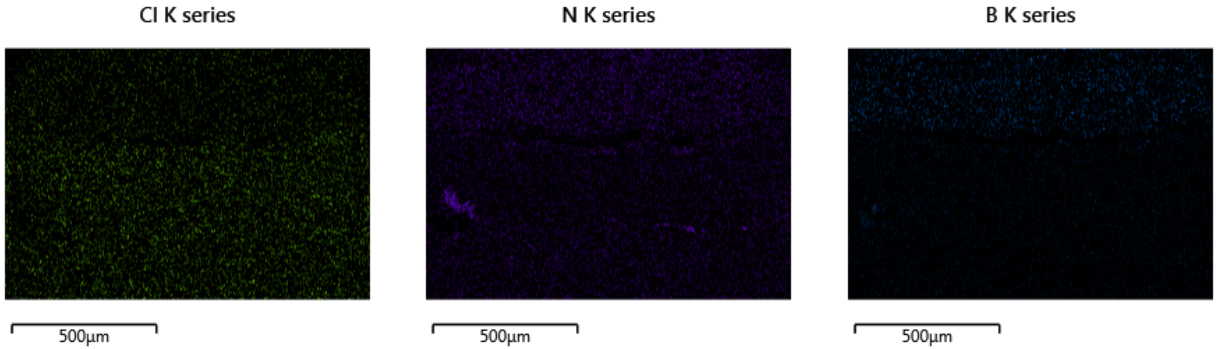

Figure 122. EDS analysis results of material 9 after exposure at Ørsted Avedøre in the superheater (SH-HT). Sample removed from site in 2017. Scale bar in SEM image is 500 µm. The maps are an indication of sulphur in the deposit layer and Mo in the nickel-base layer, but S and Mo normally overlap as indicated.

Beläggningstyp Aremco, BN, Prov 2D (10.9) (SH HT)

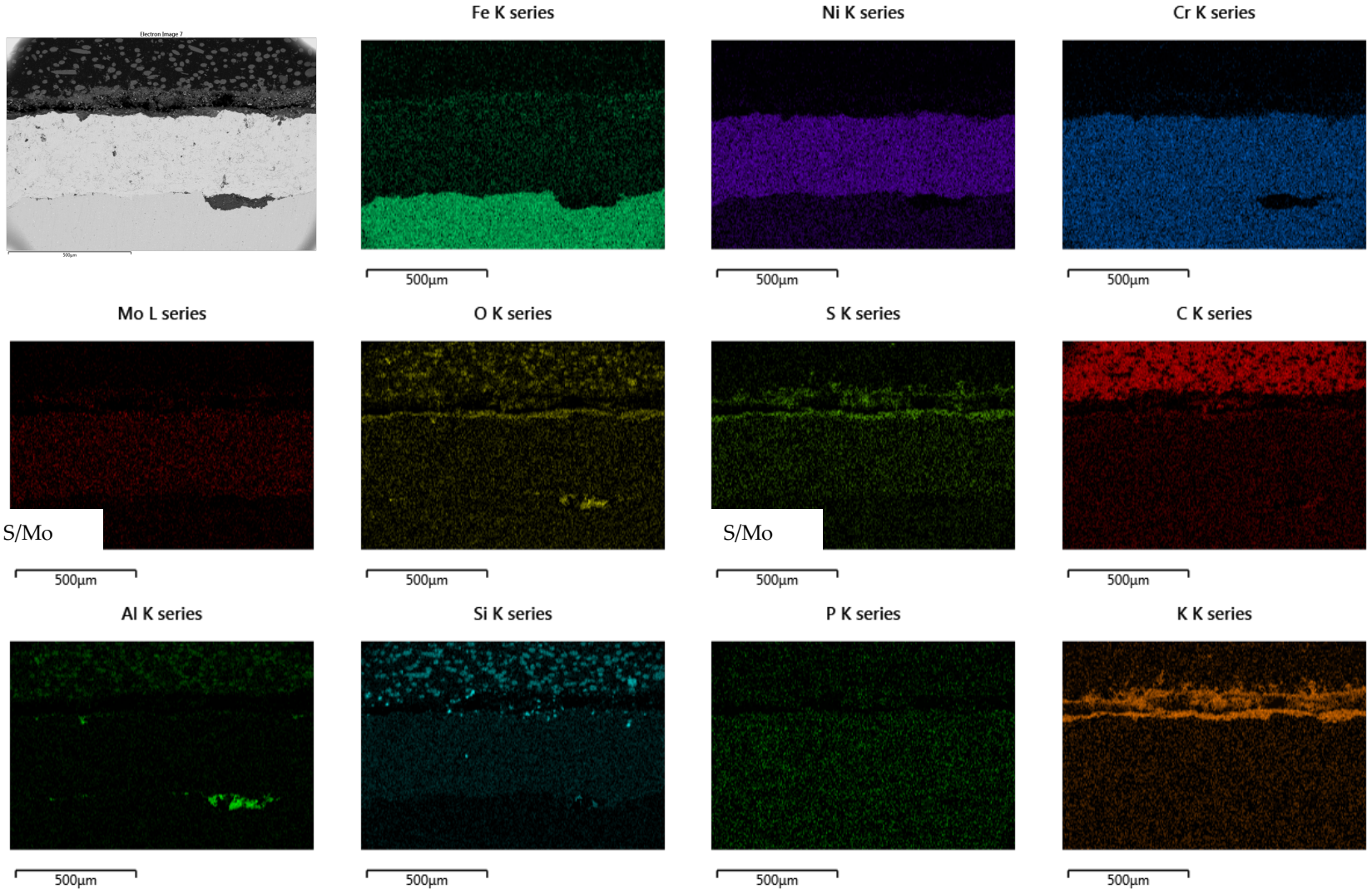

Beläggningstyp Aremco, BN, Prov 2D (10.9) (SH HT)

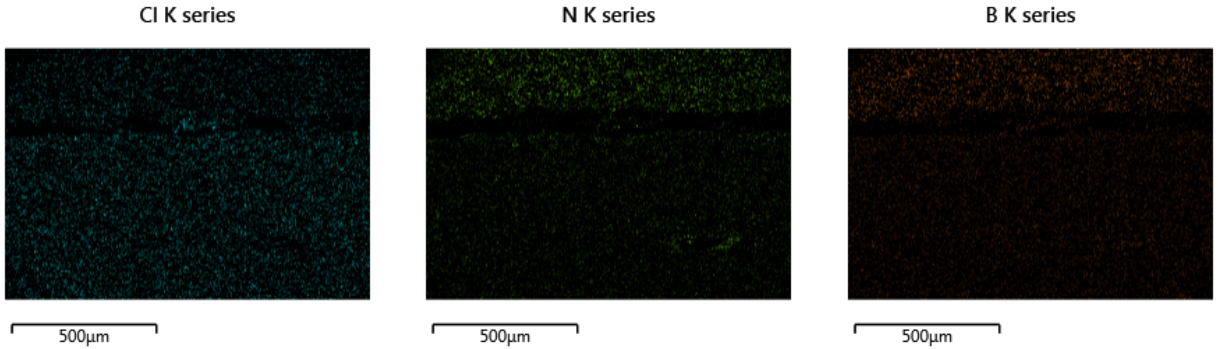

Figure 123. EDS analysis results of material 9 after exposure at Ørsted Avedøre in the superheater (SH-HT). Sample removed from site in 2017. Scale bar in SEM image is 500 µm. The maps are an indication of sulphur in the deposit layer and Mo in the nickel-base layer, but S and Mo normally overlap as indicated.

Beläggningstyp Aremco, Graphite base, Prov 2C (SH HT) (Mat 10) (sample removed in 2017)

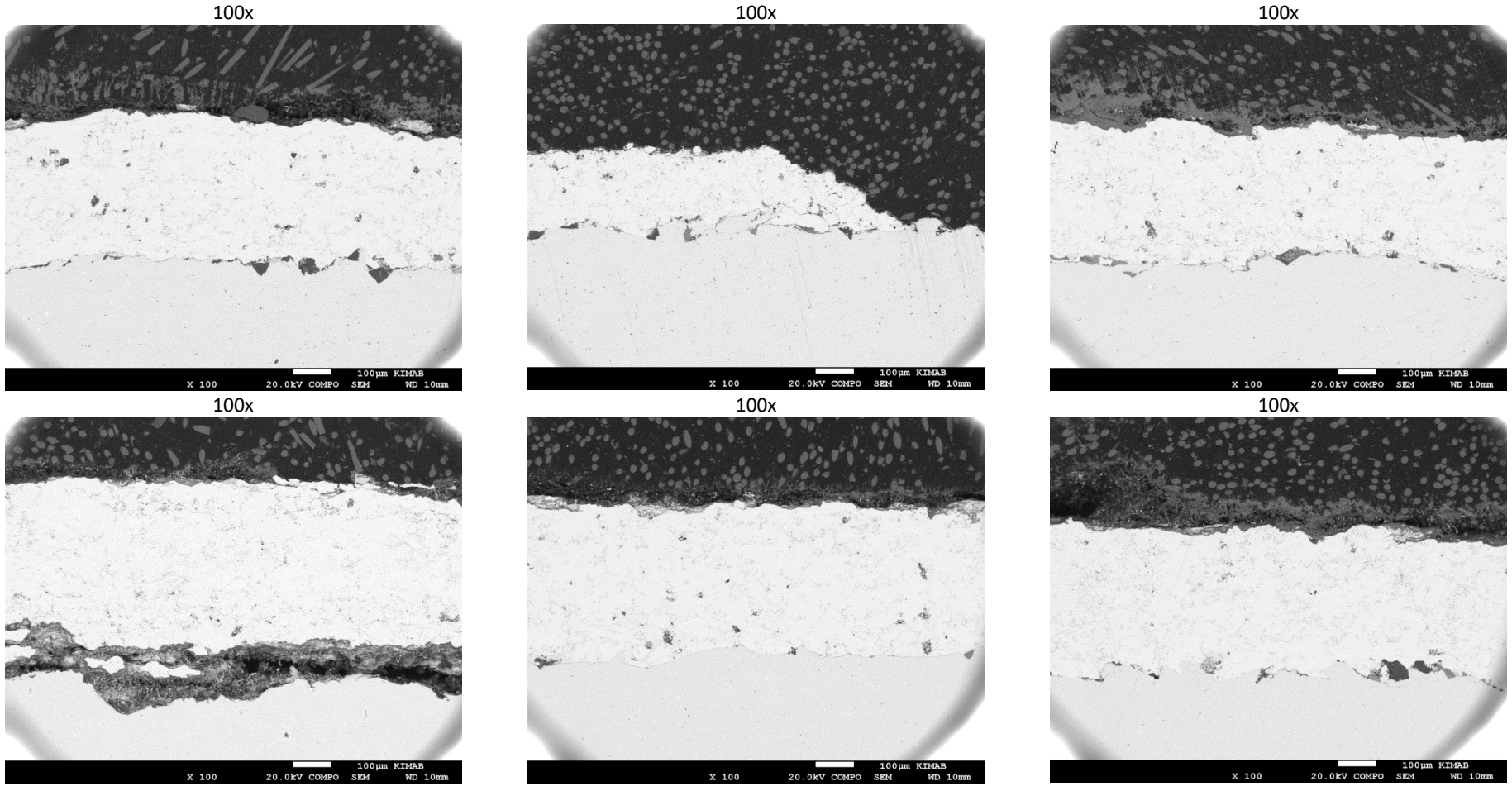

Figure 124. SEM images of material 10 after exposure at Ørsted Avedøre in the superheater (SH-HT). Sample removed from site in 2017. Scale bar is 100 µm at 100x magnification.

Beläggningstyp Aremco, Graphite base, Prov 2C (10.10) (SH HT)

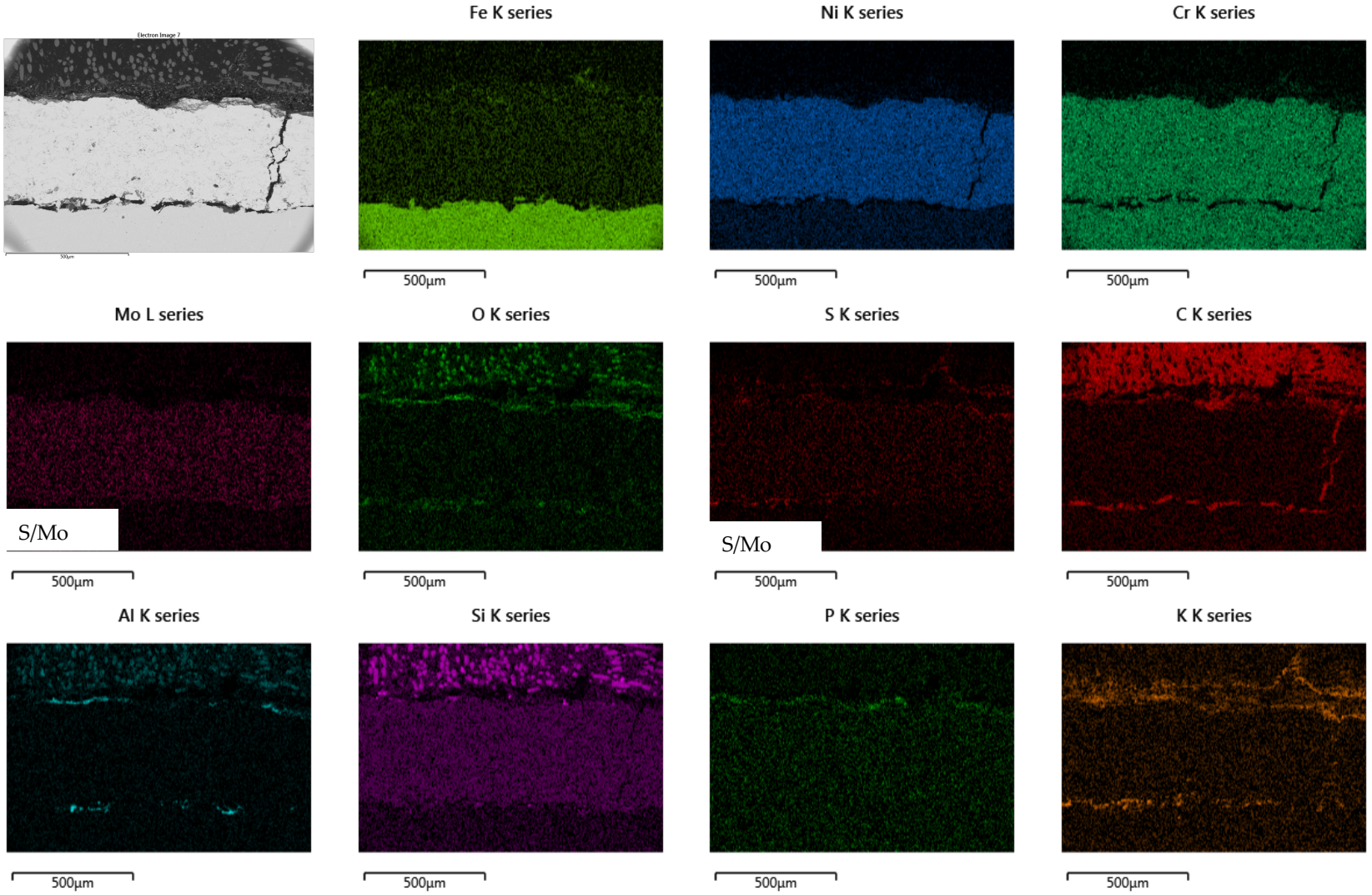

Beläggningstyp Aremco, Graphite base, Prov 2C (10.10) (SH HT)

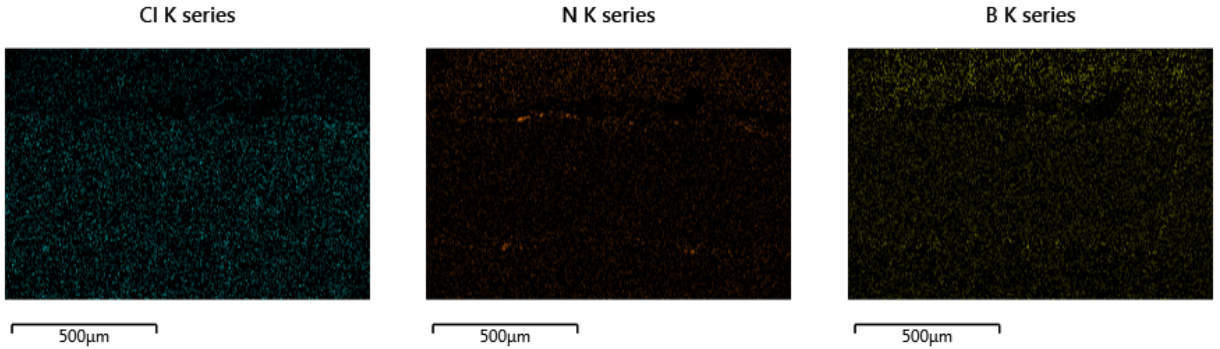

Figure 125. EDS analysis results of material 10 after exposure at Ørsted Avedøre in the superheater (SH-HT). Sample removed from site in 2017. Scale bar in SEM image is 500 µm. The maps are an indication of sulphur in the deposit layer and Mo in the nickel-base layer, but S and Mo normally overlap as indicated.

Beläggningstyp Aremco, Graphite base, Prov 2C (10.10) (SH HT)

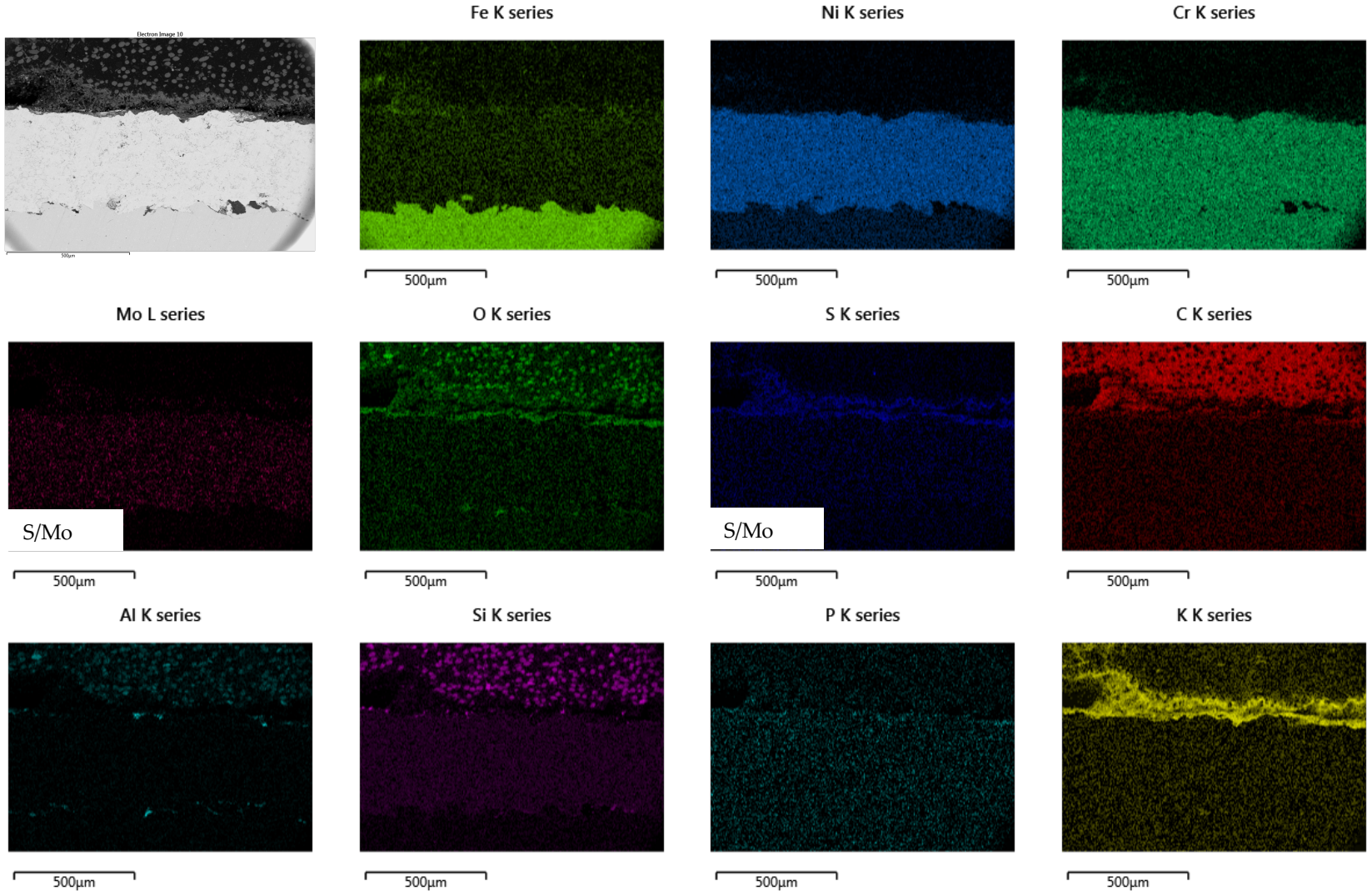

Beläggningstyp Aremco, Graphite base, Prov 2C (10.10) (SH HT)

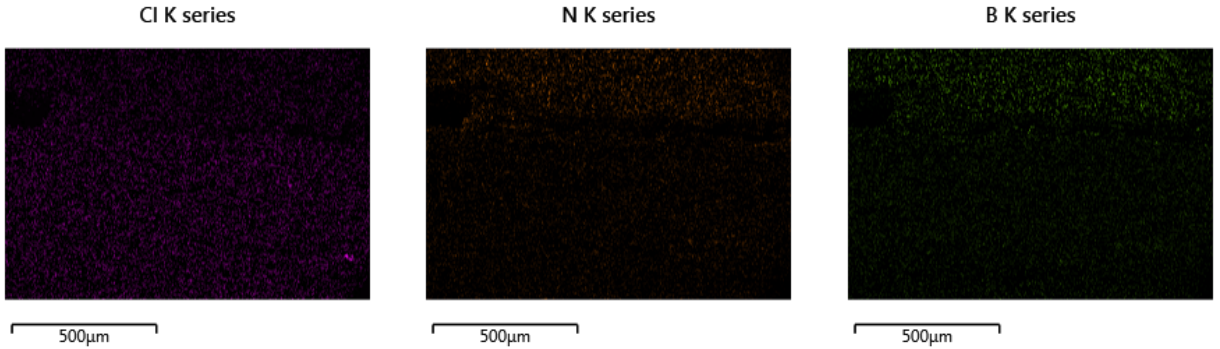

Figure 126. EDS analysis results of material 10 after exposure at Ørsted Avedøre in the superheater (SH-HT). Sample removed from site in 2017. Scale bar in SEM image is 500 µm. The maps are an indication of sulphur in the deposit layer and Mo in the nickel-base layer, but S and Mo normally overlap as indicated.

SH 1 LT

Beläggningstyp Diamant Metallplastic, Dichtol HTR, Prov 1B (7.3) (Mat 3) (sample removed in 2017)

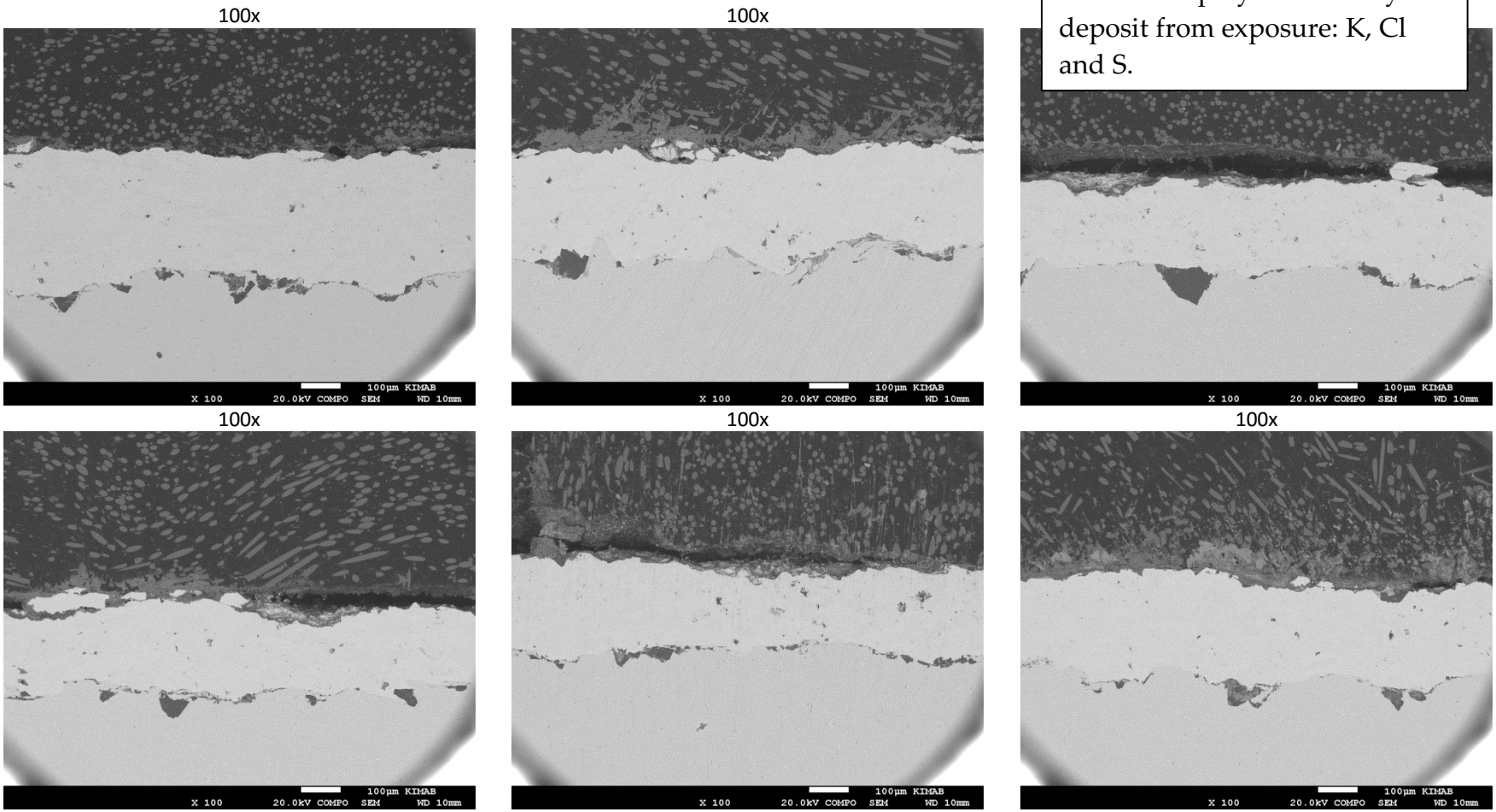

Figure 127. SEM images of material 3 after exposure at Ørsted Avedøre in the superheater (SH-LT). Sample removed from site in 2017. Scale bar is 100 µm at 100x magnification.

Beläggningstyp Diamant, Prov 1B (Sh 1 LT)

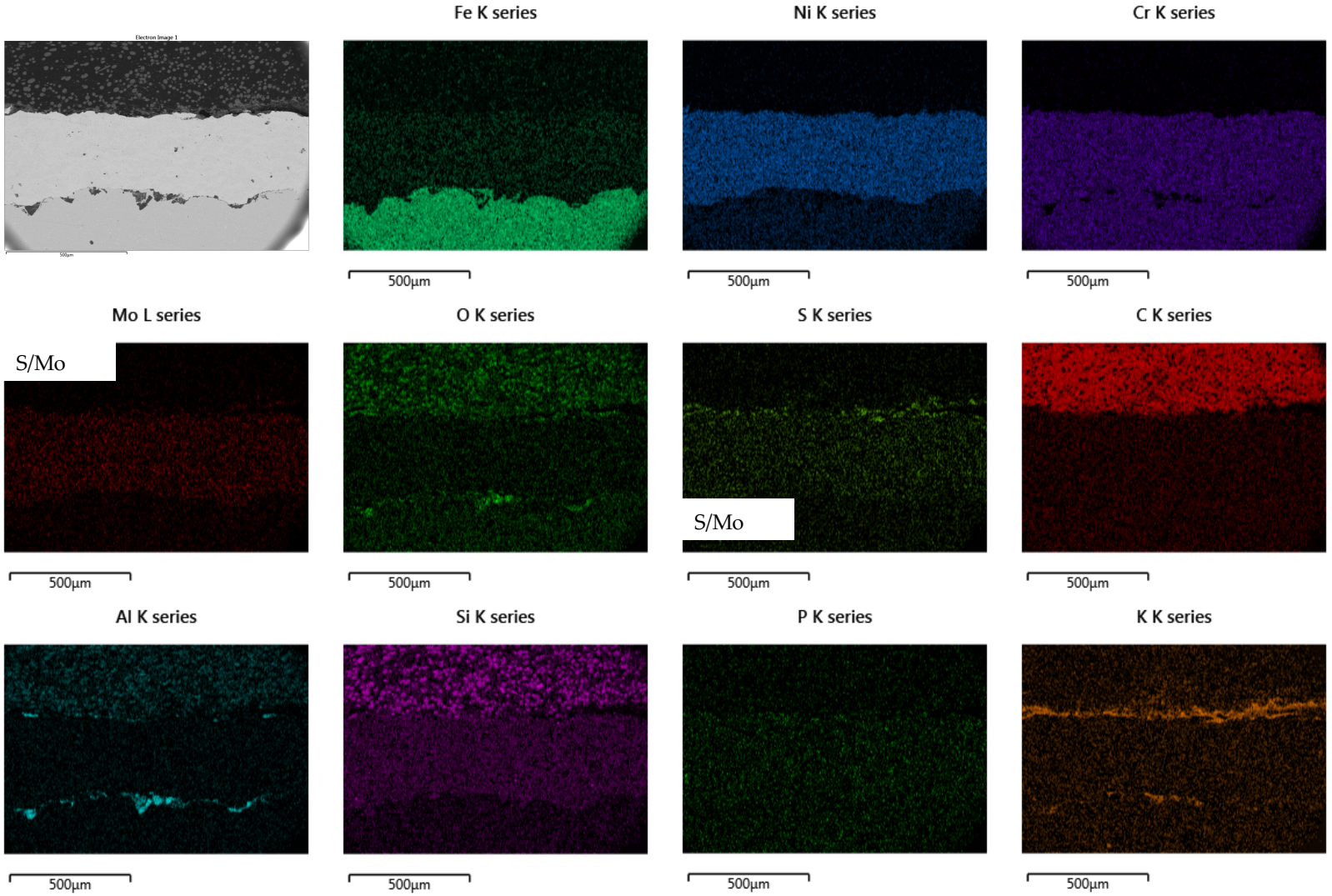

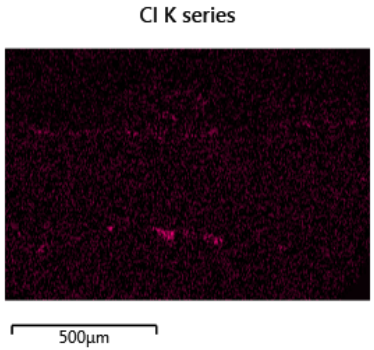

Figure 128. EDS analysis results of material 3 after exposure at Ørsted Avedøre in the superheater (SH-LT). Sample removed from site in 2017. Scale bar in SEM image is 500 µm. The maps are an indication of sulphur in the deposit layer and Mo in the nickel-base layer, but S and Mo normally overlap as indicated.

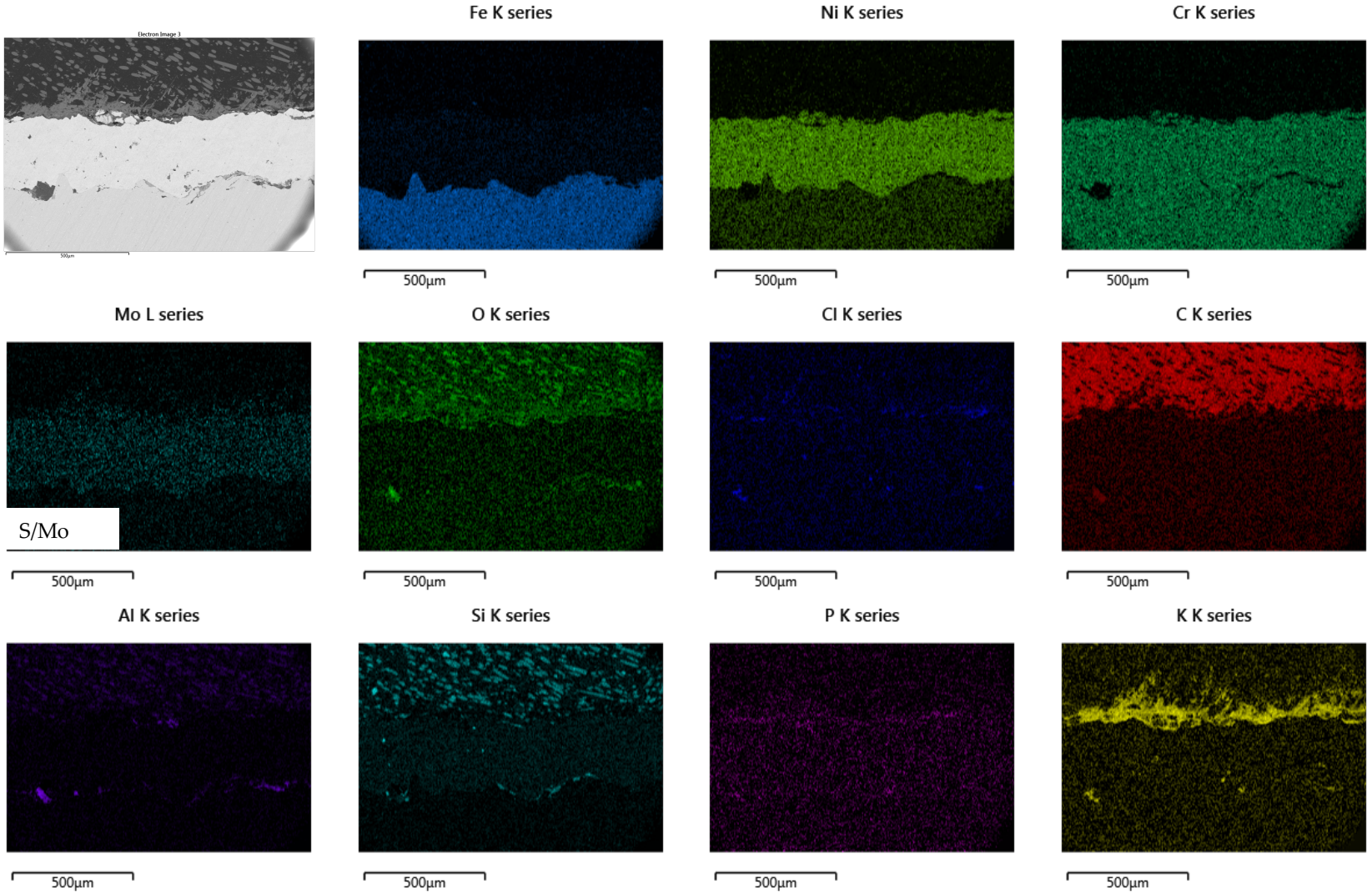

Figure 129. EDS analysis results of material 3 after exposure at Ørsted Avedøre in the superheater (SH-LT). Sample removed from site in 2017. Scale bar in SEM image is 500 µm. S and Mo maps were identical due to overlap and only the Mo map is shown

Beläggningstyp FMP (BN-silicate), Prov 1A (7.4) (Mat 4) (sample removed in 2017)

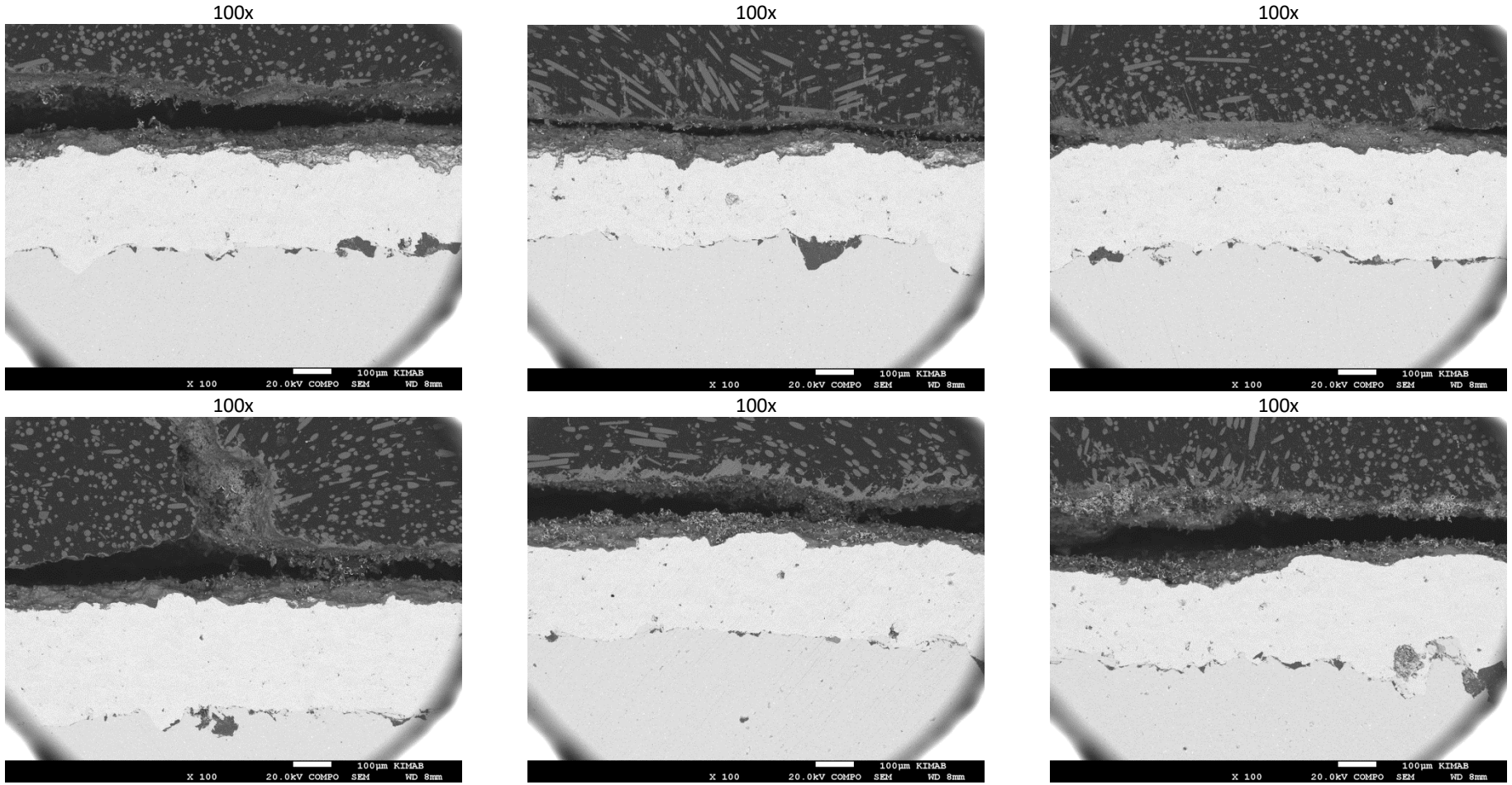

Figure 130. SEM images of material 4 after exposure at Ørsted Avedøre in the superheater (SH-LT). Sample removed from site in 2017. Scale bar is 100 µm at 100x magnification.

Beläggningstyp FMP (BN-silicate), Prov 1A (Sh 1 LT) (Mat 4)

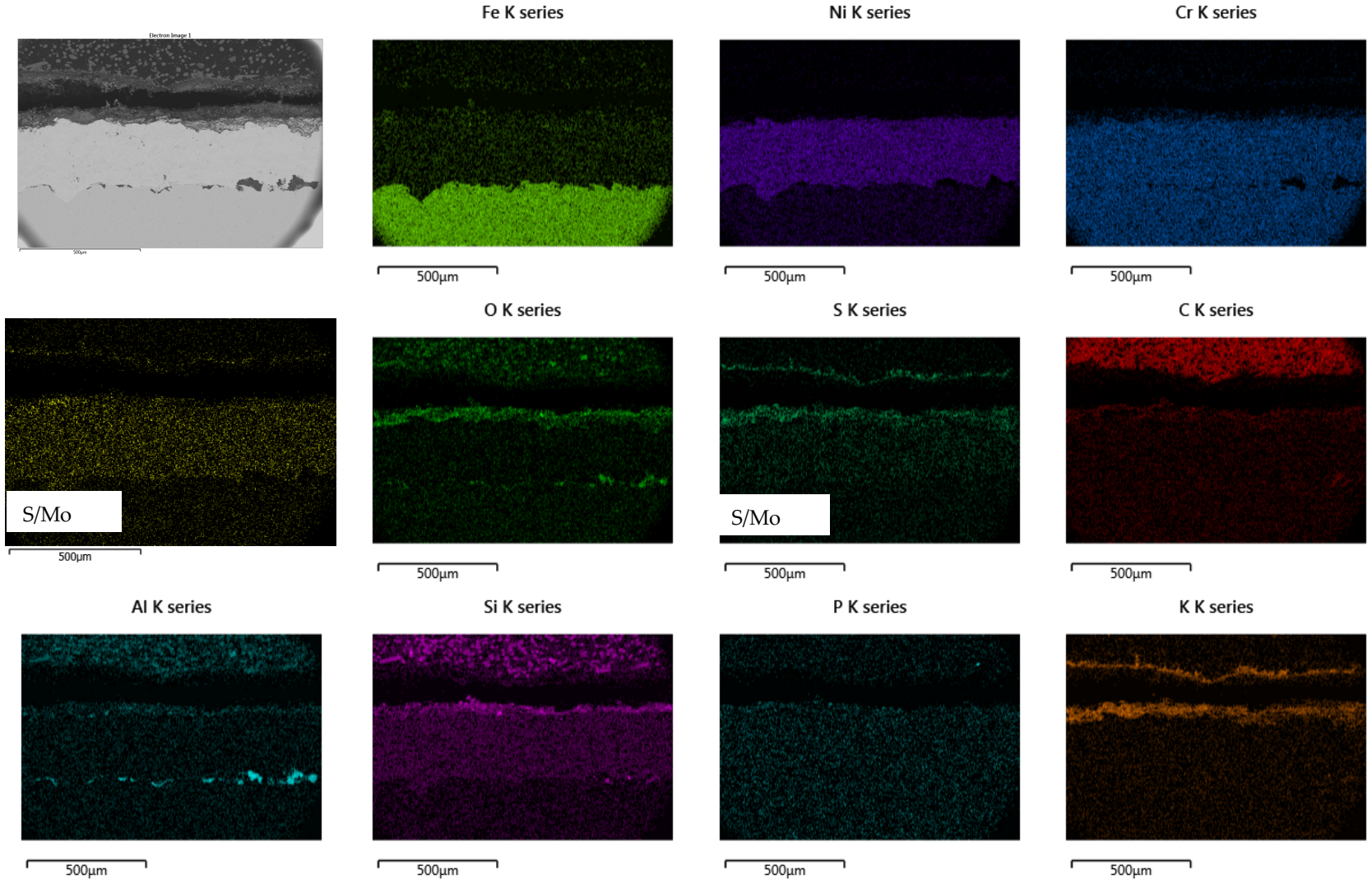

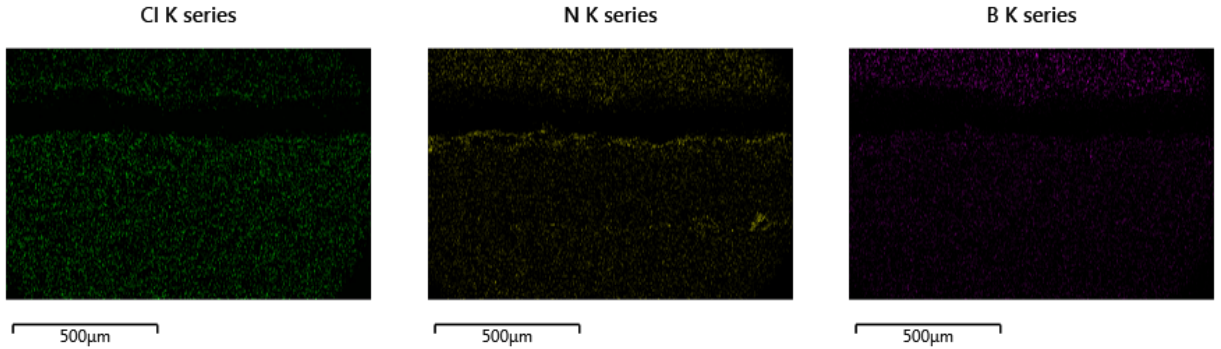

Figure 131. EDS analysis results of material 4 after exposure at Ørsted Avedøre in the superheater (SH-LT). Sample removed from site in 2017. Scale bar in SEM image is 500 µm. . The maps are an indication of sulphur in the deposit layer and Mo in the nickel-base layer, but S and Mo normally overlap as indicated.

Beläggningstyp FMP (BN-silicate), Prov 1A (Sh 1 LT) (Mat 4)

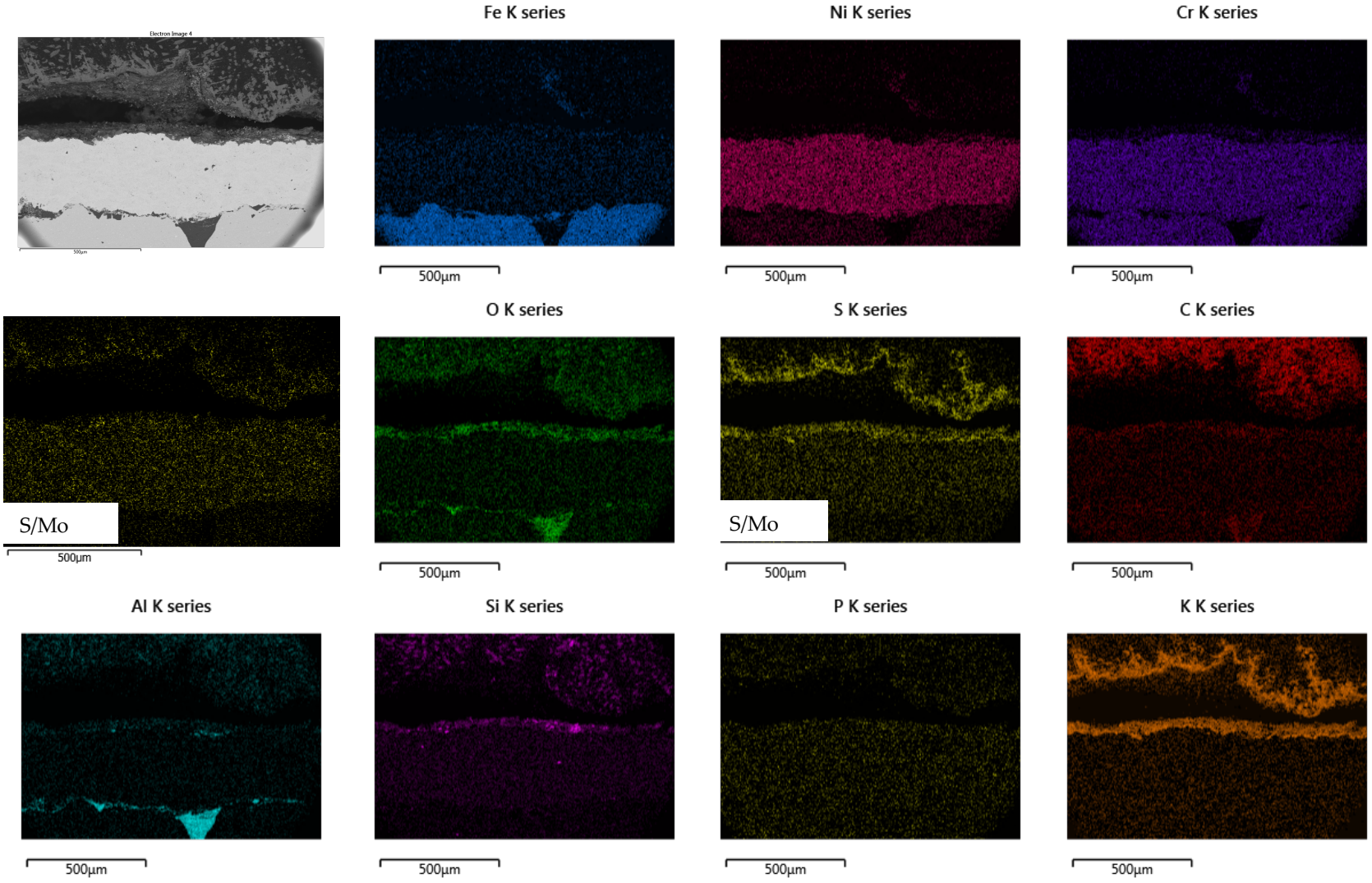

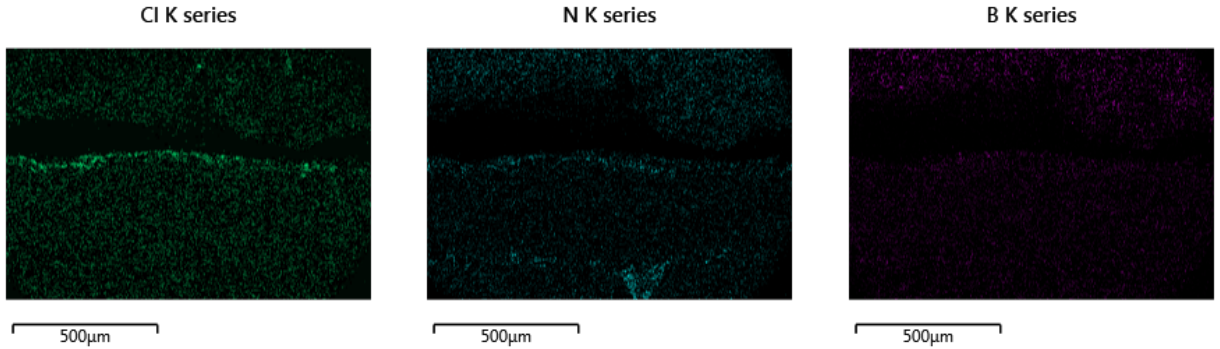

Figure 132. EDS analysis results of material 4 after exposure at Ørsted Avedøre in the superheater (SH-LT). Sample removed from site in 2017. Scale bar in SEM image is 500 µm. . The maps are an indication of sulphur in the deposit layer and Mo in the nickel-base layer, but S and Mo normally overlap as indicated.

Beläggningstyp Millidyne, Prov 1D (8.7) (Mat 7) (sample removed in 2017)

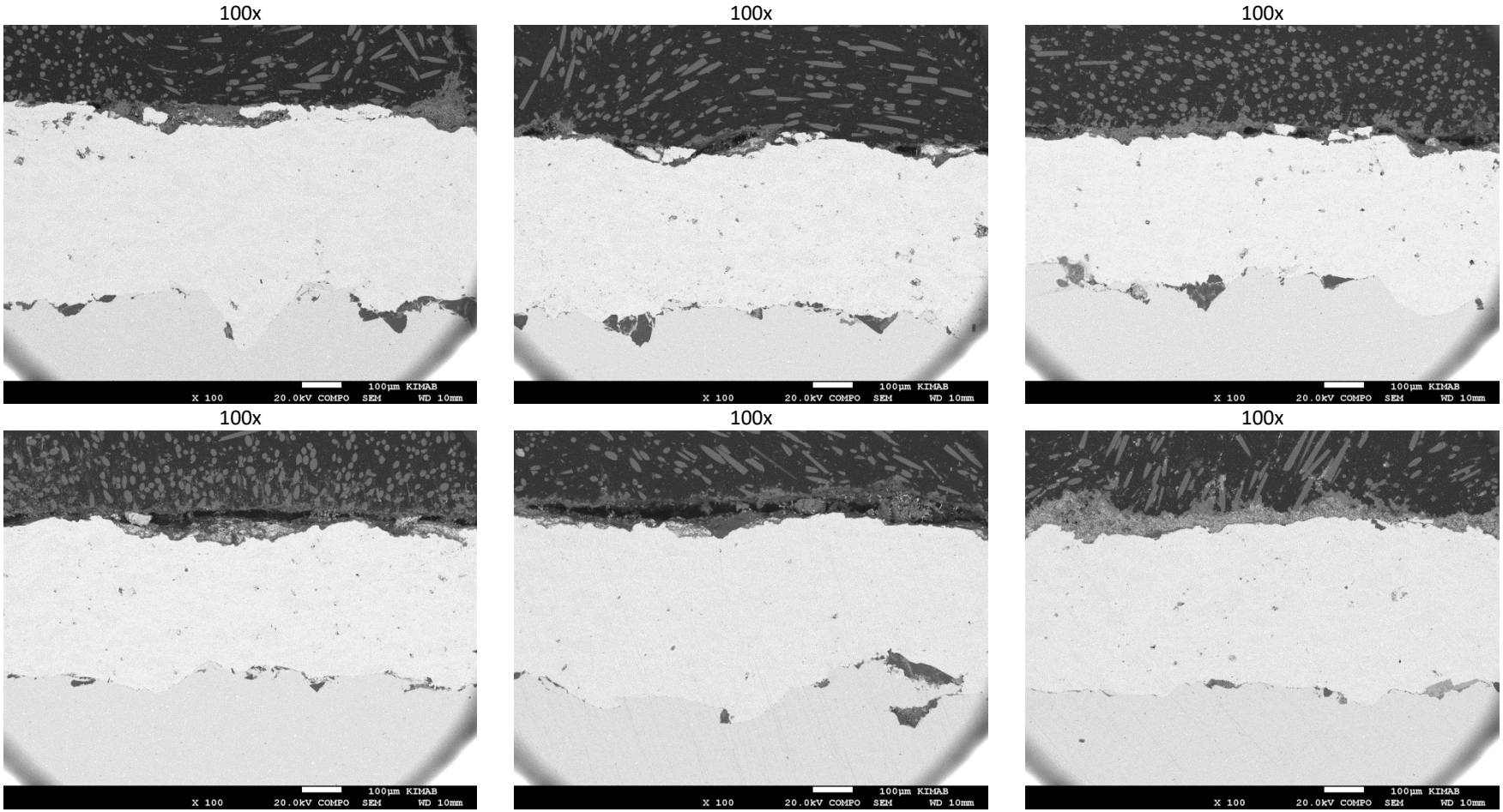

Figure 133. SEM images of material 7 after exposure at Ørsted Avedøre in the superheater (SH-LT). Sample removed from site in 2017. Scale bar is 100 µm at 100x magnification.

Beläggningstyp Millidyne, Prov 1D (SH 1 LT)

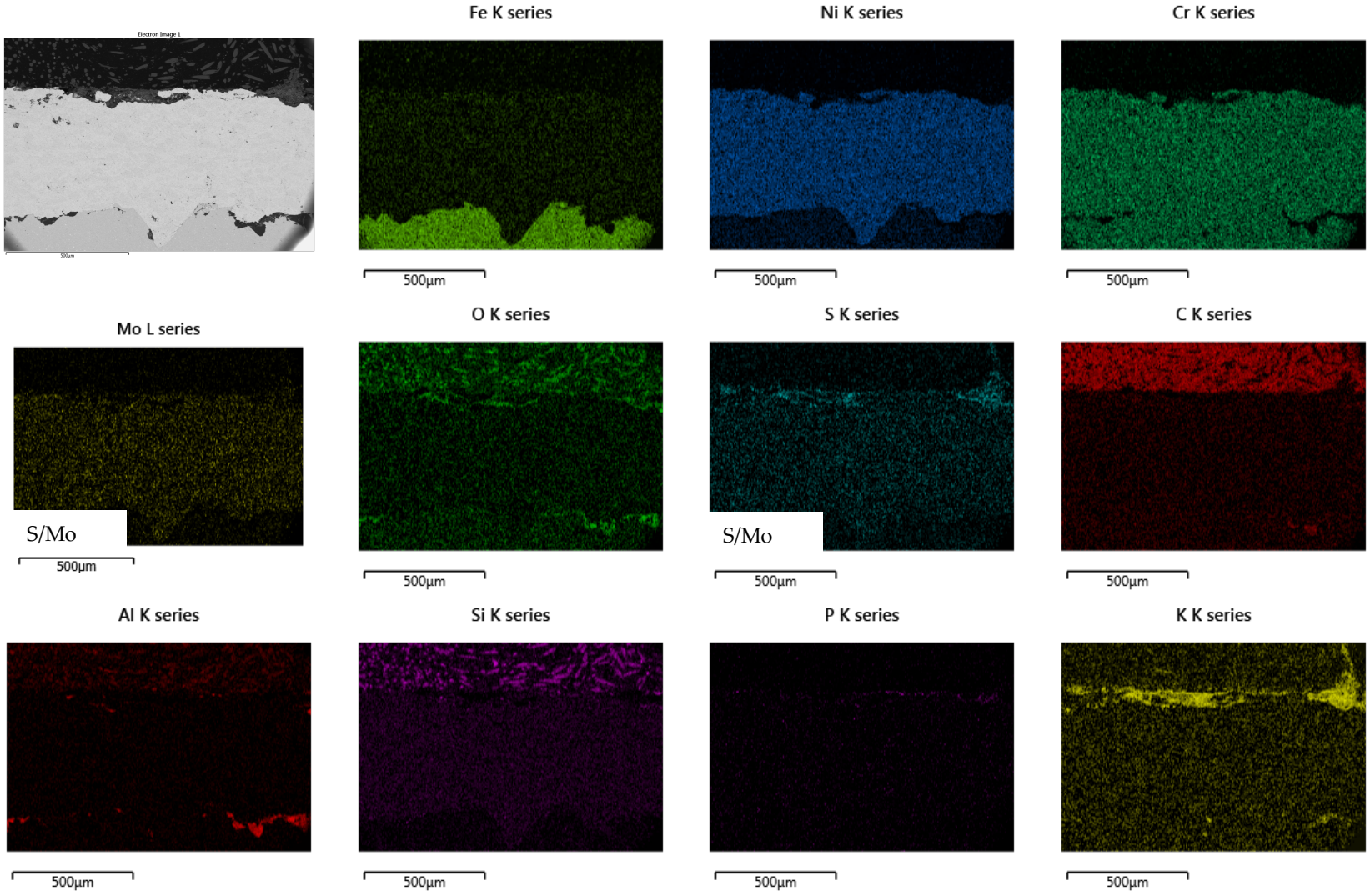

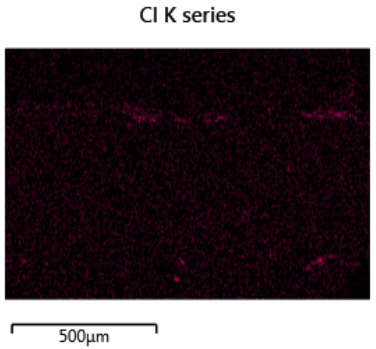

Figure 134. EDS analysis results of material 7 after exposure at Ørsted Avedøre in the superheater (SH-LT). Sample removed from site in 2017. Scale bar in SEM image is 500 µm. . The maps are an indication of sulphur in the deposit layer and Mo in the nickel-base layer, but S and Mo normally overlap as indicated.

Beläggningstyp Millidyne, Prov 1D (SH 1 LT)

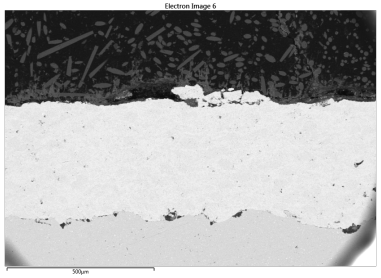

Fe K series

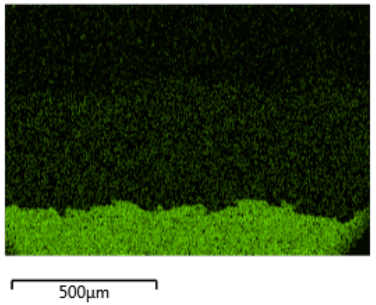

Ni K series

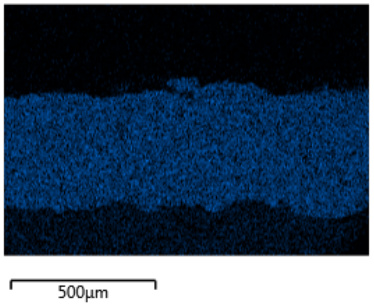

Cr K series

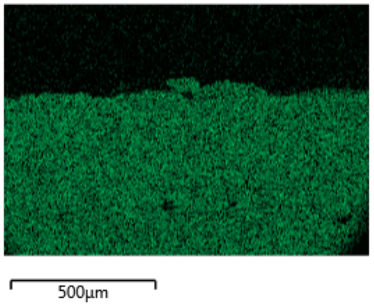

Mo L series

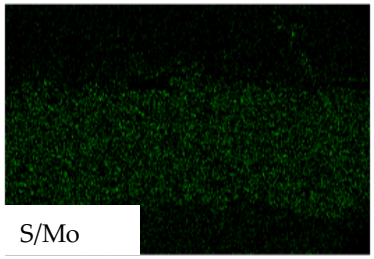

O K series

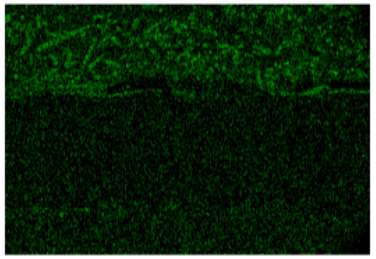

Cl K series

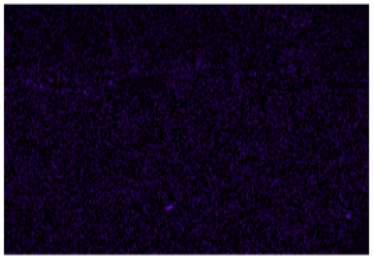

C K series

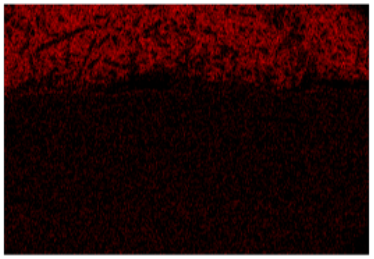

Al K series

Si K series

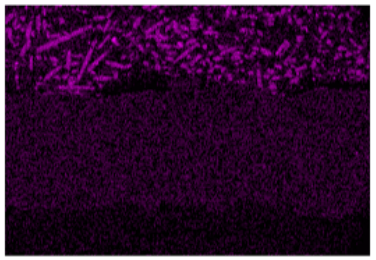

P K series

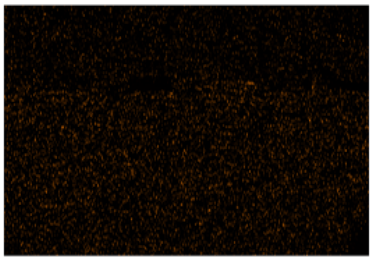

K K series

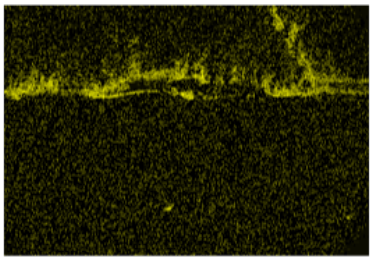

Beläggningstyp Millidyne, Prov 1D (SH 1 LT)

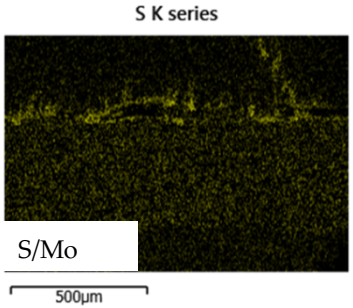

Figure 135. EDS analysis results of material 7 after exposure at Ørsted Avedøre in the superheater (SH-LT). Sample removed from site in 2017. Scale bar in SEM image is 500 µm. . The maps are an indication of sulphur in the deposit layer and Mo in the nickel-base layer, but S and Mo do overlap as indicated.

Economizer 2

Beläggningstyp Diamant Metallplastic, Dichtol HTR, Prov 3A (3.3) (Mat 3) (sample removed in 2017,instead of in 2016)

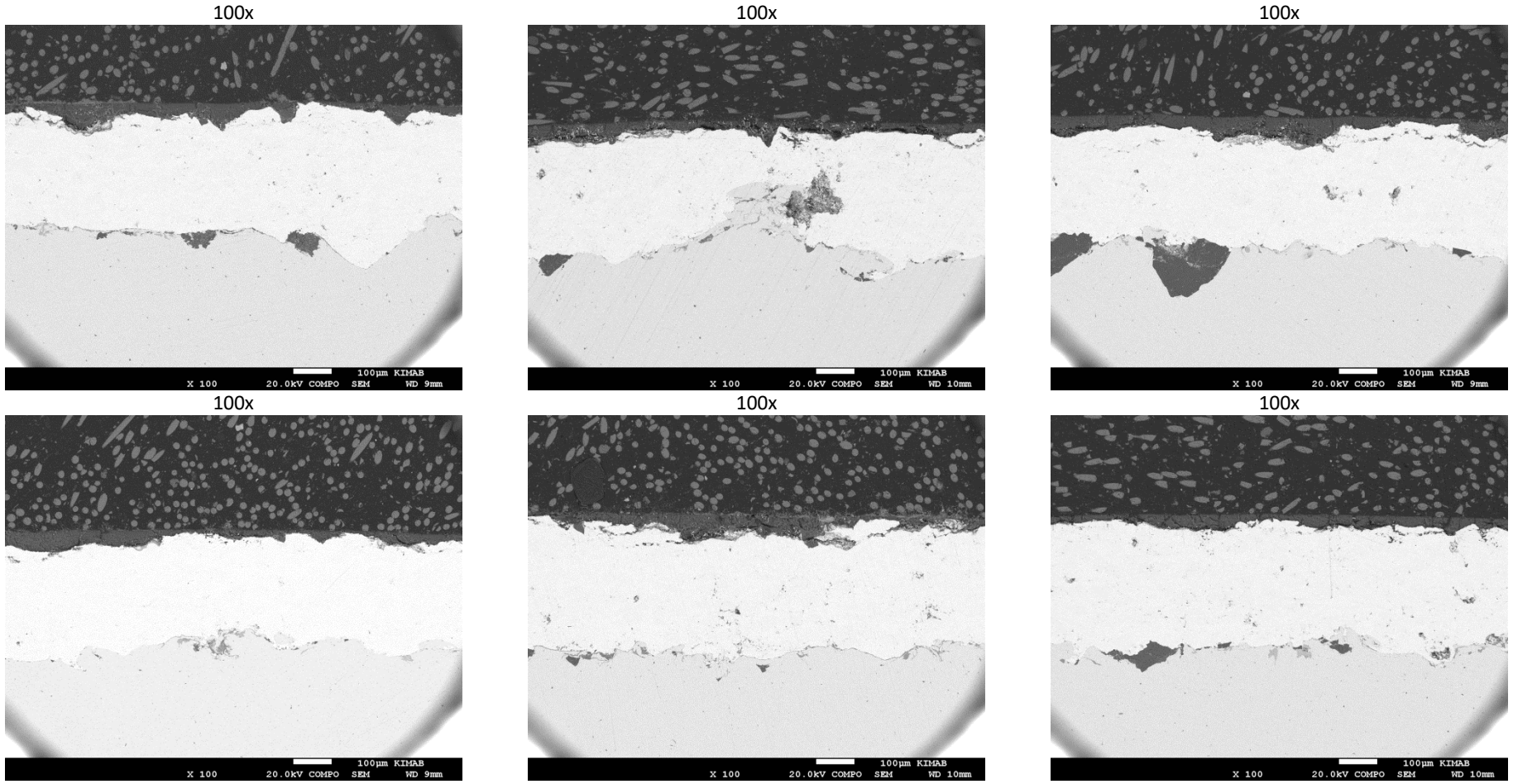

Figure 136. SEM images of material 3 after exposure at Ørsted Avedøre in the economizer. Sample removed from site in 2017. Scale bar is 100 µm at 100x magnification.

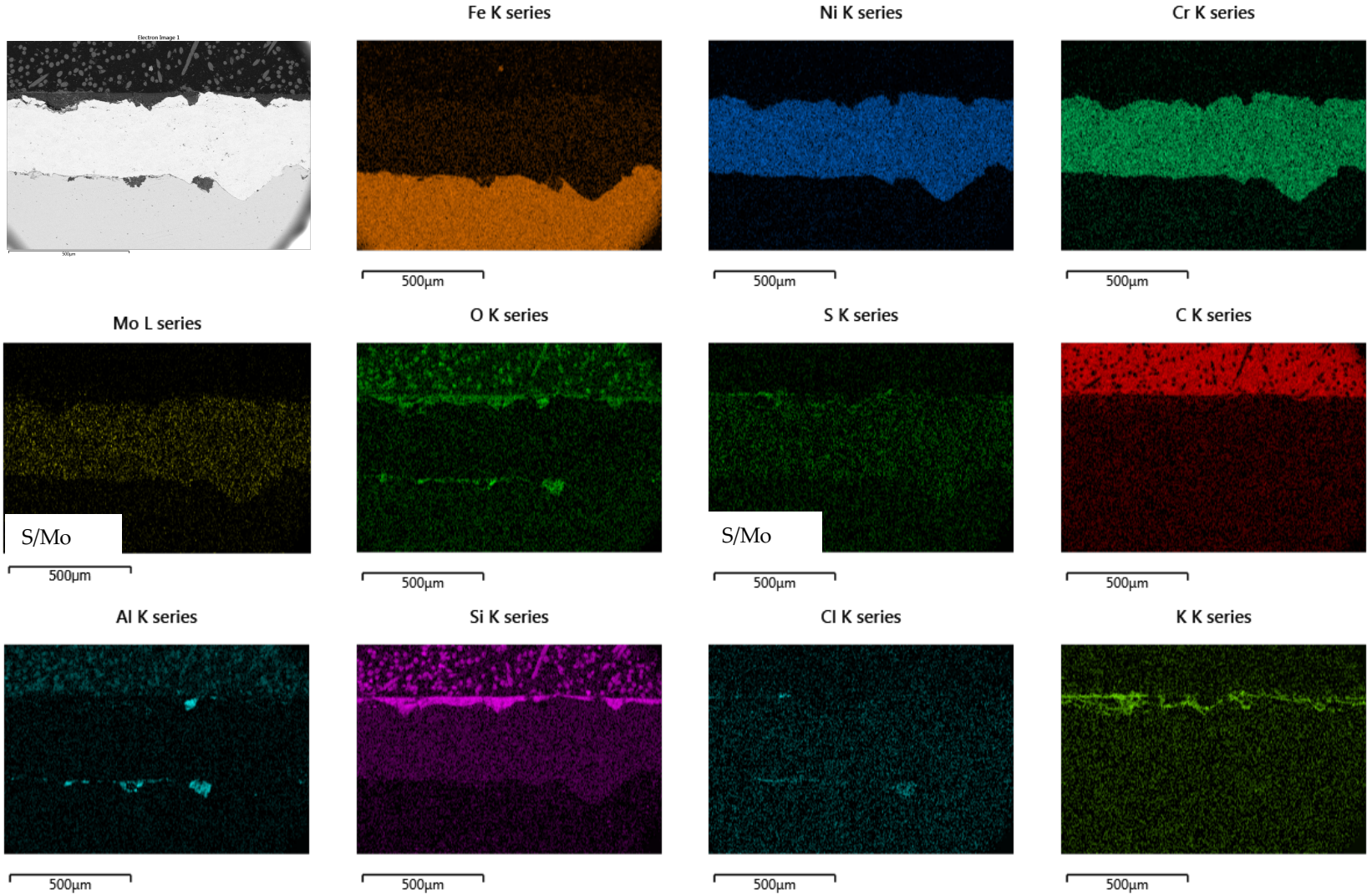

Figure 137. EDS analysis results of material 3 after exposure at Ørsted Avedøre in the economizer. Sample removed from site in 2017. Scale bar in SEM image is 500 µm. . The maps are an indication of sulphur in the deposit layer and Mo in the nickel-base layer, but S and Mo do overlap as indicated.

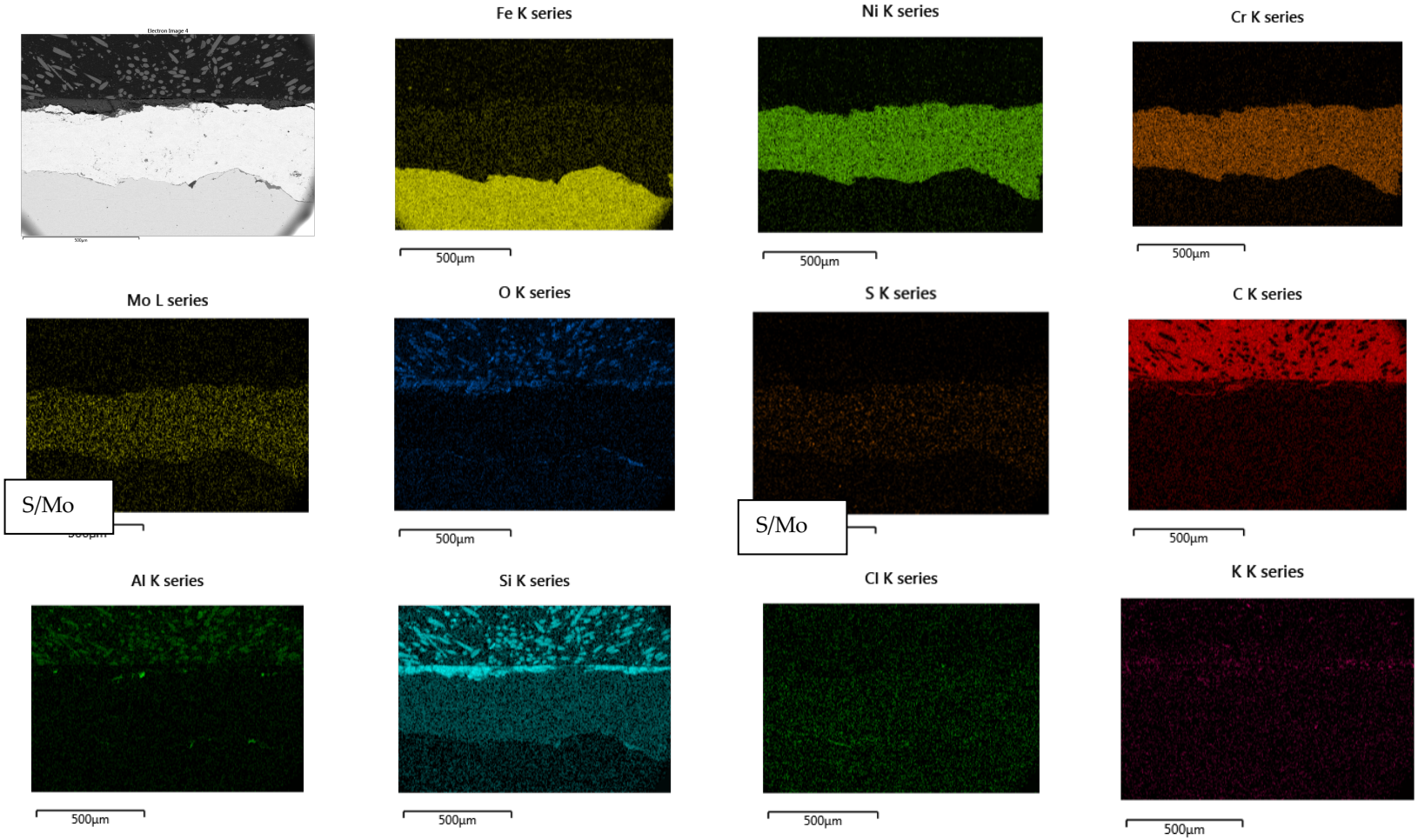

Figure 138. EDS analysis results of material 3 after exposure at Ørsted Avedøre in the economizer. Sample removed from site in 2017. Scale bar in SEM image is 500 µm. S and Mo overlap as indicated.

Beläggningstyp FMP (BN-silicate), Prov 3D (4.4) (Mat 4) (sample removed in 2017,instead of in 2016)

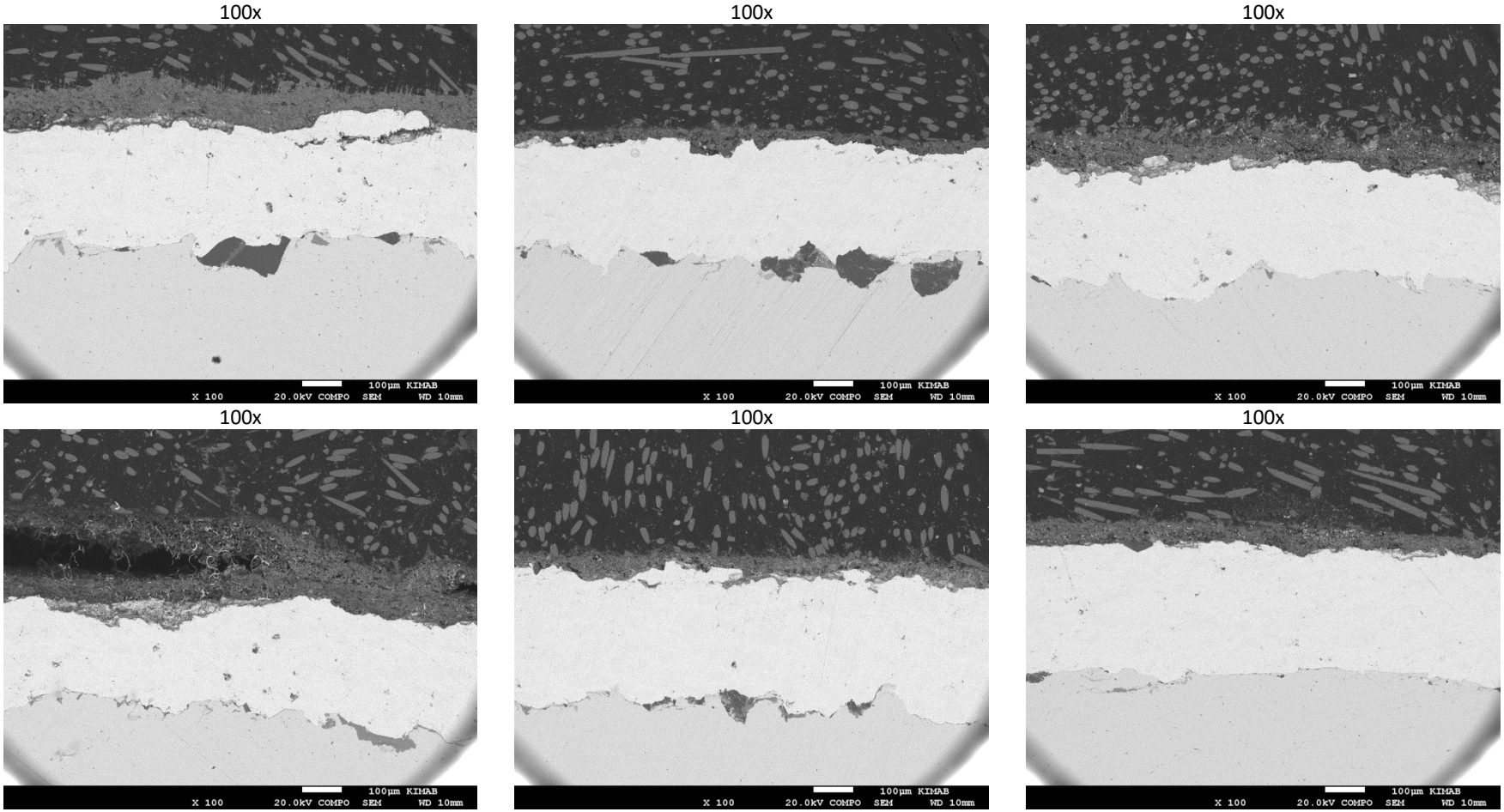

Figure 139. SEM images of material 4 after exposure at Ørsted Avedøre in the economizer. Sample removed from site in 2017 (instead of 2016). Scale bar is 100 µm at 100x magnification.

Beläggningstyp FMP (BN-silicate), Prov 3D (Eco2)

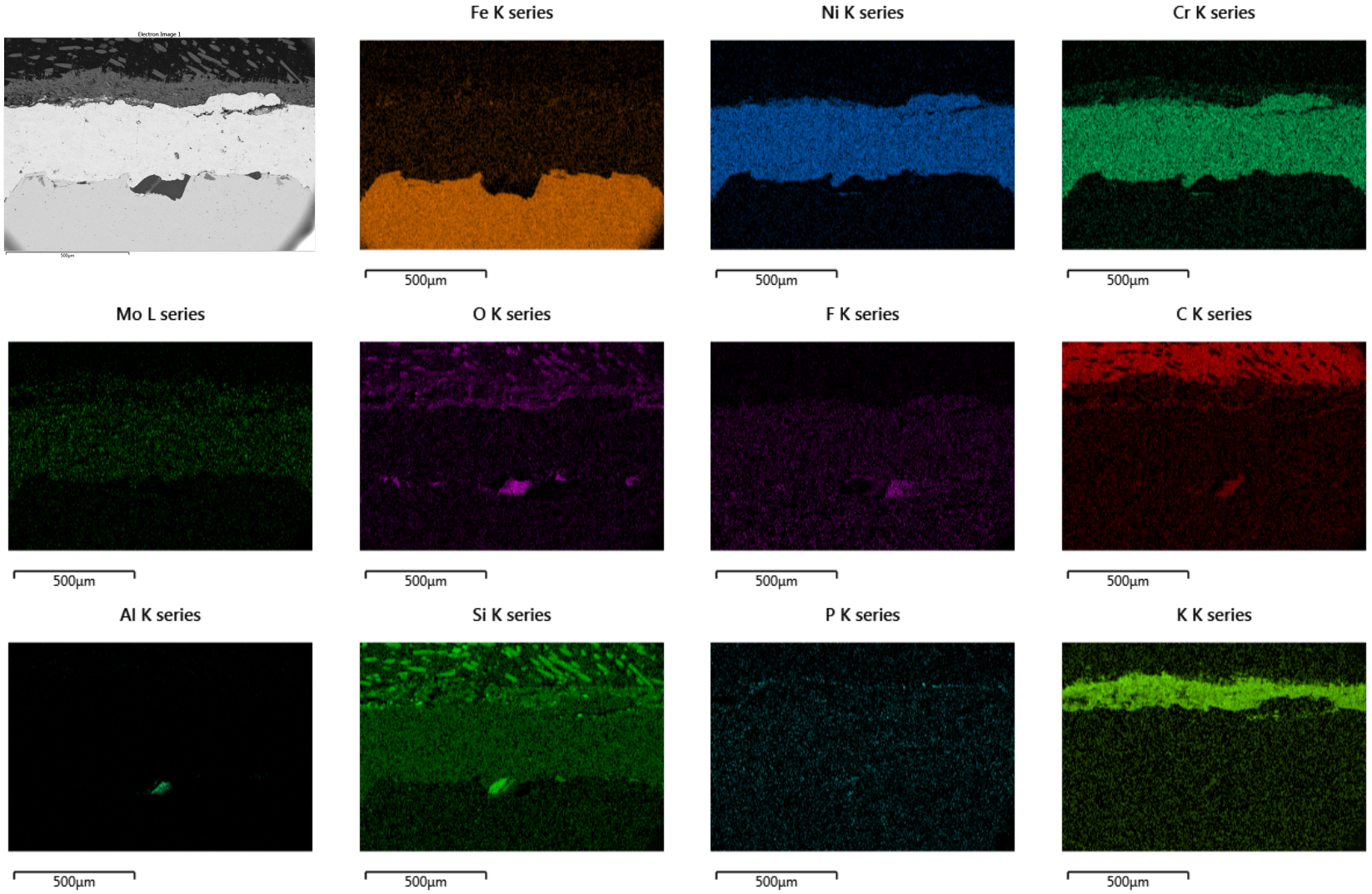

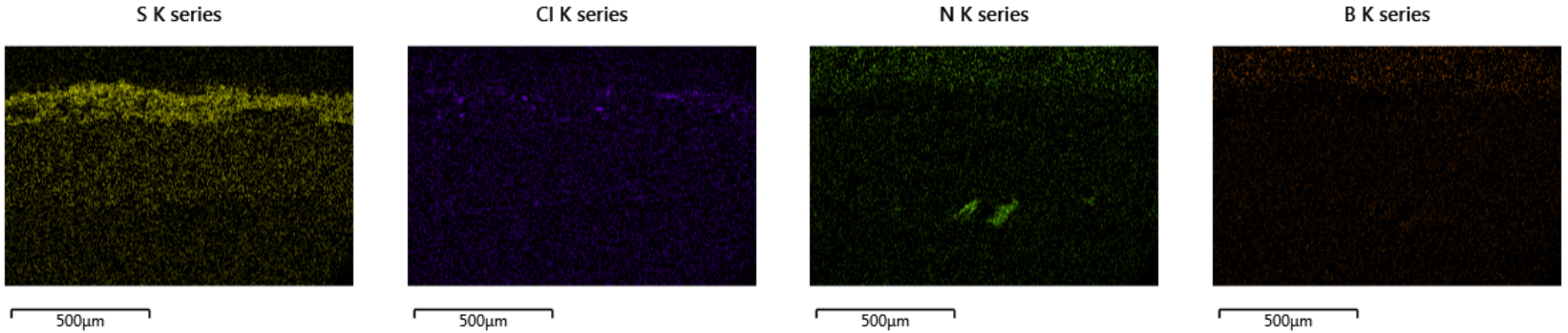

Figure 140. EDS analysis results of material 4 after exposure at Ørsted Avedøre in the economizer. Sample removed from site in 2017. Scale bar in SEM image is 500 µm. . The maps are an indication of sulphur in the deposit layer and Mo in the nickel-base layer, but S and Mo do overlap as indicated. The fluorine signal could be due to an overlap with Fe.

Beläggningstyp FMP (BN-silicate), Prov 3D (Eco2)

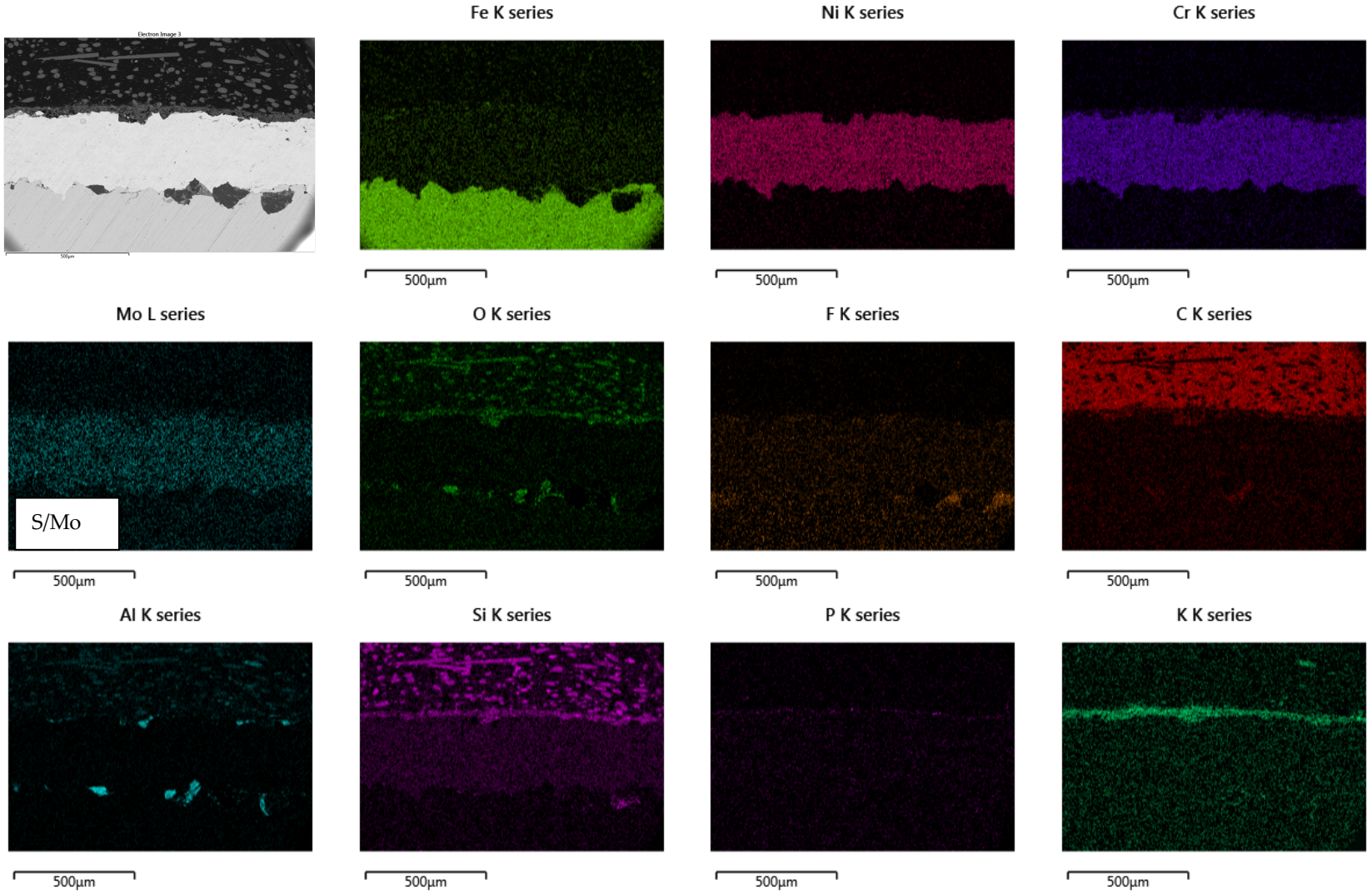

Beläggningstyp FMP (BN-silicate), Prov 3D (Eco2)

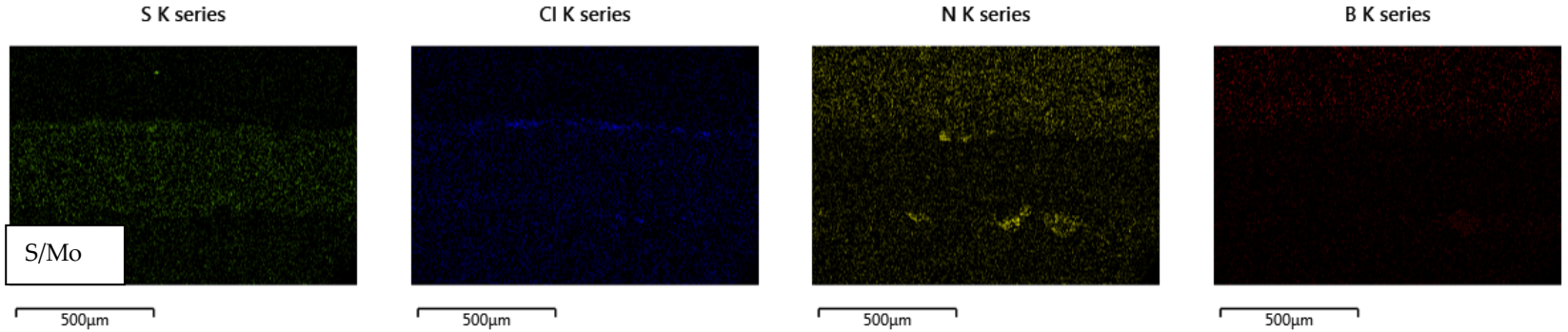

Figure 141. EDS analysis results of material 4 after exposure at Ørsted Avedøre in the economizer. Sample removed from site in 2017. Scale bar in SEM image is 500 µm. S and Mo overlap as indicated.

Beläggningstyp Alu-Releco (Ceramic), Prov 3B (3.2) (Mat 2) (sample removed in 2017,instead of in 2016)

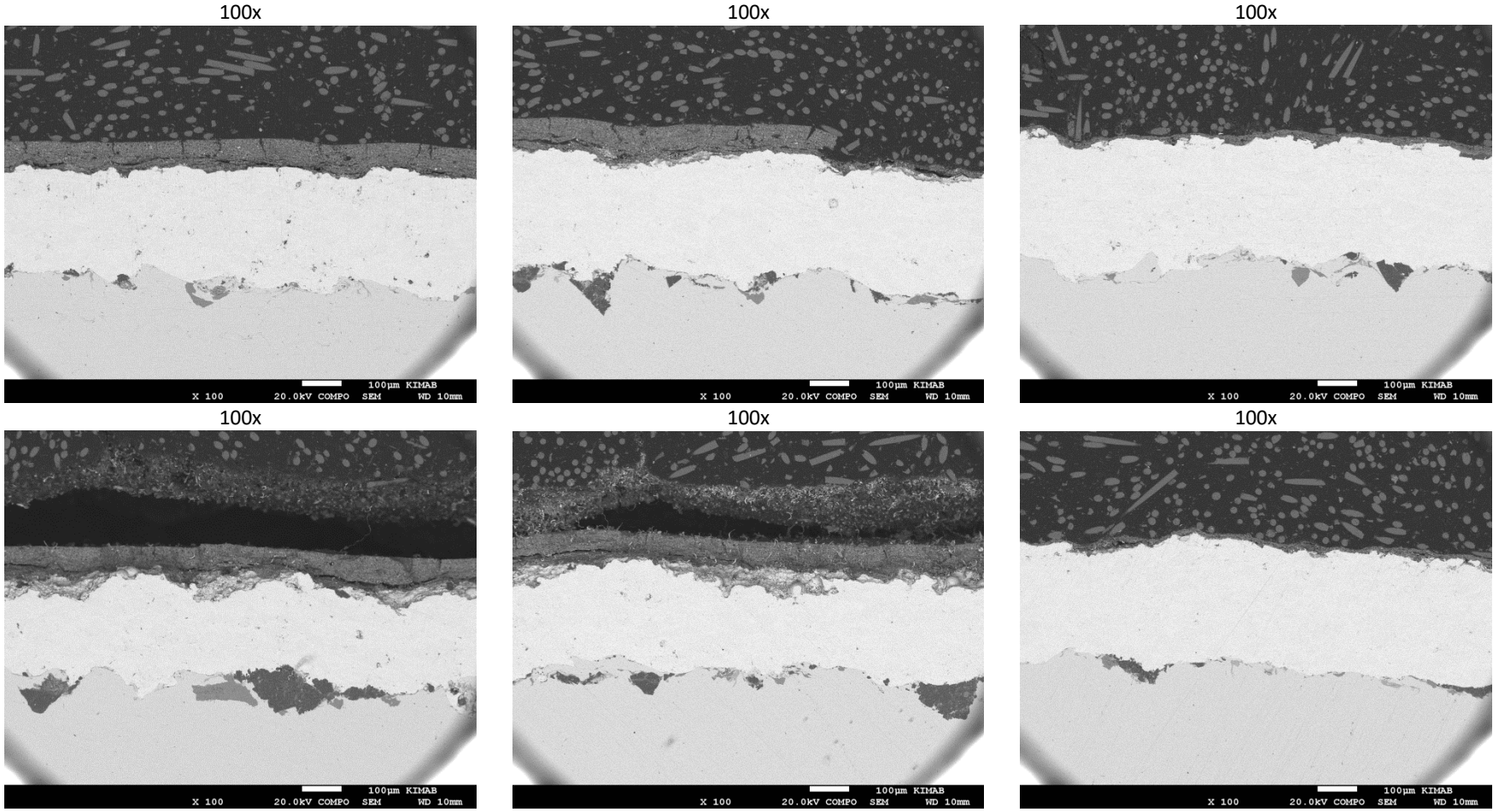

Figure 142. SEM images of material 2 after exposure at Ørsted Avedøre in the economizer. Sample removed from site in 2017 (instead of 2016). Scale bar is 100 µm at 100x magnification.

Beläggningstyp Alu-Releco (Ceramic), Prov 3B (3.2) (Mat 2)

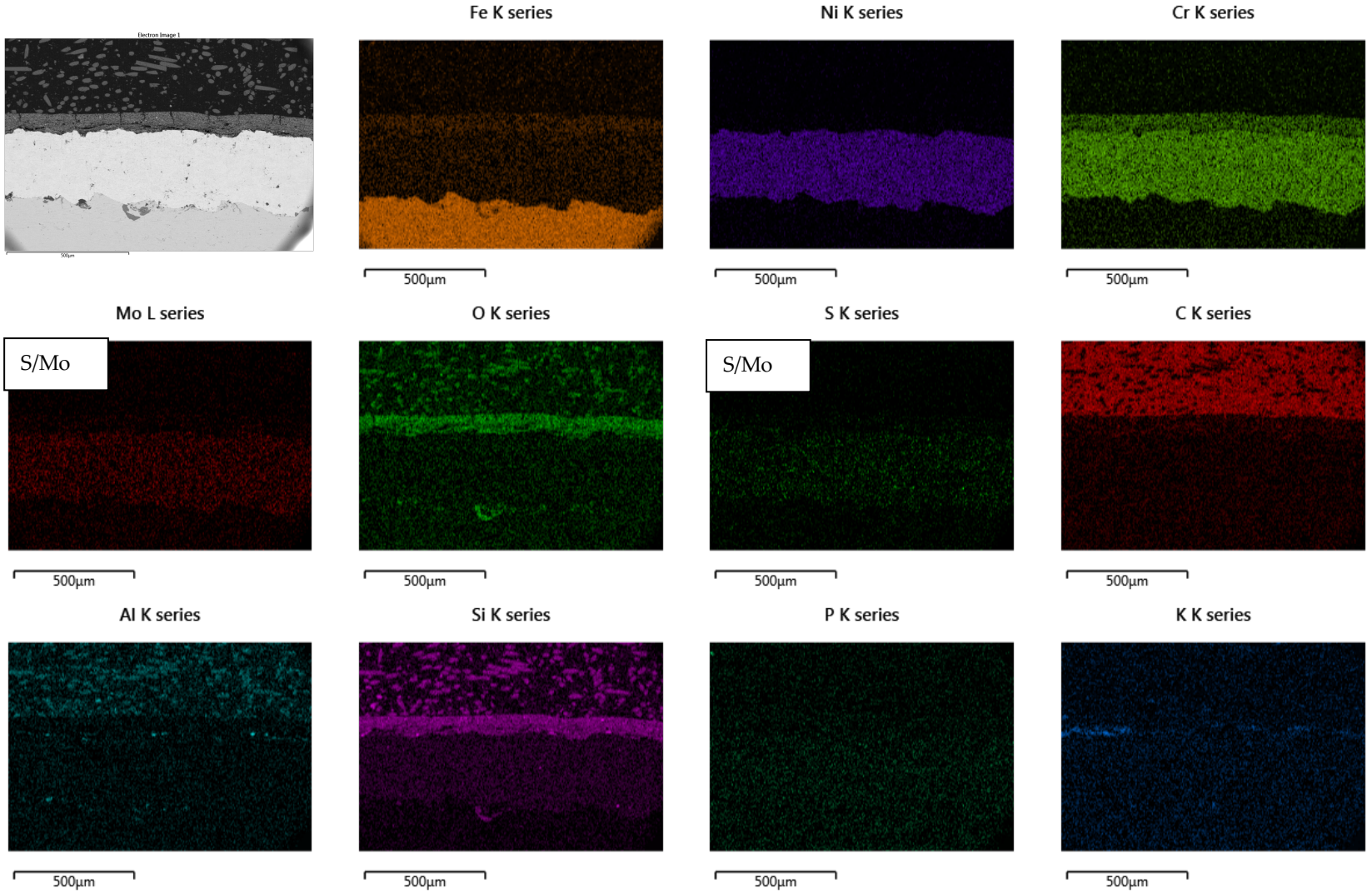

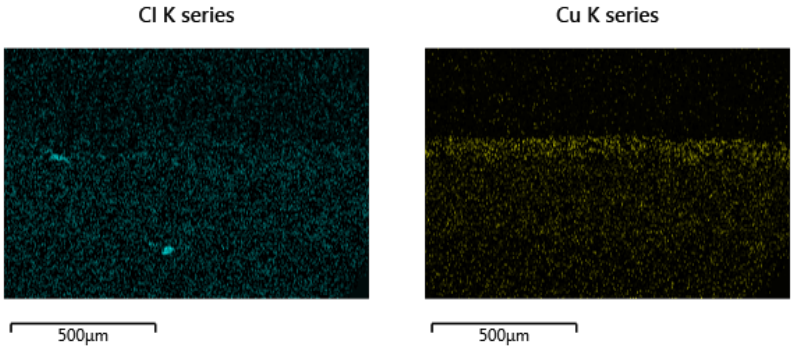

Figure 143. EDS analysis results of material 2 after exposure at Ørsted Avedøre in the economizer. Sample removed from site in 2017. Scale bar in SEM image is 500 µm. S and Mo do overlap as indicated.

Beläggningstyp Alu-Releco (Ceramic), Prov 3B (3.2) (Mat 2)

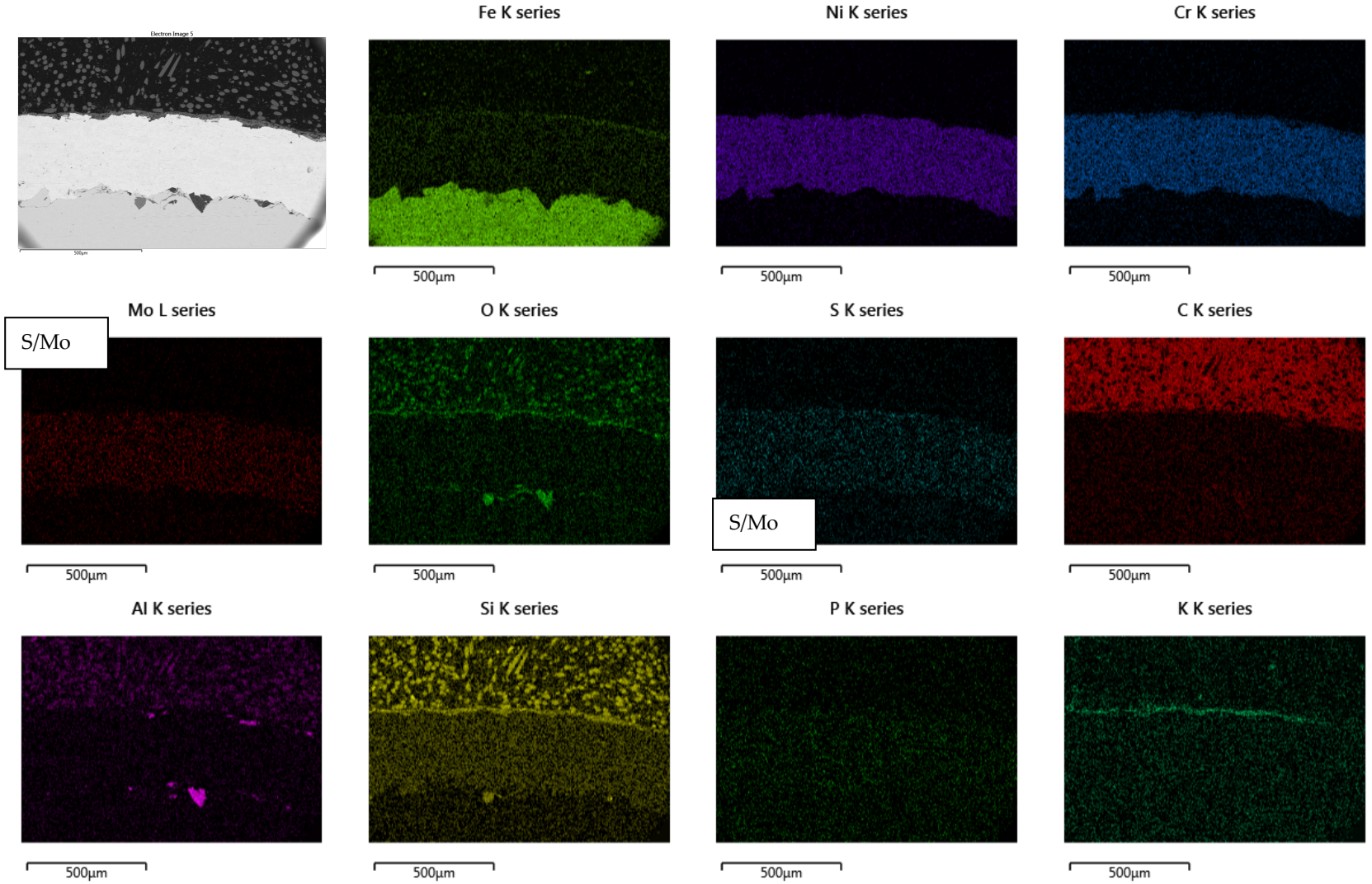

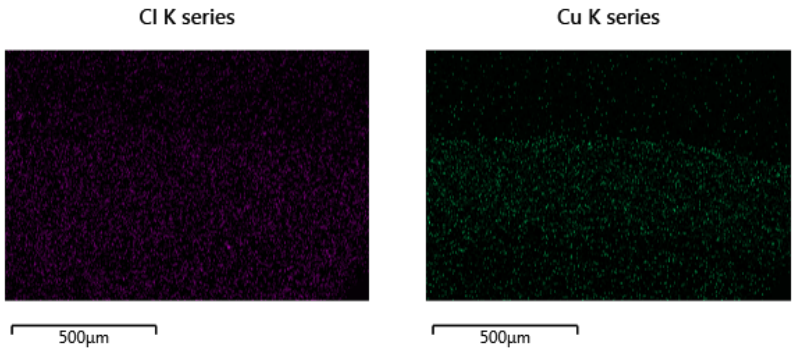

Figure 144. EDS analysis results of material 2 after exposure at Ørsted Avedøre in the economizer. Sample removed from site in 2017. Scale bar in SEM

Appendix D. Late field observations

Öresundskraft/Västhamnsverket

Shortly after the project was finished maintenance work was carried out at Västhamnsverket during which some observations were made that are of importance with respect to the behaviour of tested CMP during field usage.

The following was reported with respect to the furnace:

During 2016 the larger part of the lower part of the furnace was cleaned by sand blasting. This part had earlier been coated by CorEr. The cleaning took 5 days and 12 tonnes of sand was consumed. Before this cleaning ordinary soot blowing had been made by the plant operators. After the sand blasting the whole area was sealed with one of the CMP candidates, Dichtol HTR (Material 3). This material has additives to improve capillary penetration based on polymers that are later decomposed during sintering.

During 2017 there was little operation, because of a mild winter, resulting in that scaffolding was not required to be mounted during the revision stop. Consequently there was no maintenance of the coated area.

During 2018, week 19, the coated area of the furnace was sand blasted once again. This time the procedure took only 2 days and only 5 tonnes of sand was consumed. This winter the boiler had operated had operated for a longer period at full load. Based on previous experience operation at full load for longer periods have always resulted in more deposit build-up.

After cleaning a layer of top-coating was reapplied to the furnace. Figure 145 shows part of the furnace after this procedure. The coating was tinted blue for improved visibility.

The following was reported with respect to the ESP:

Several of the CMP candidates appeared to give improved non-stick properties in the ESP cone. The problem with this cone used to be deposit build-up during longer periods of full load. This is a consequence of the used wood pellets having a high content of alkali metals, in particular potassium. The ash also contains some degree of unburnt particles, which earlier has resulted in fire in the screw after the cone.

Figure 145. The west wall of the lower part of the furnace after it was cleaned and recoated in 2018.

Composite Metal Polymer (CMP) for non-stick improvements in CHP plant

To reduce the amount of deposits in a heat- and power plant, a new concept of a composite surface layer already evaluated in the pulp and paper industry was examined.

The project examined a surface layer consisting of a thermally sprayed layer of a nickel-base material and a top coating with expected good release properties. While the nickel-base material was common for all samples, ten different top coatings were tested. The samples were exposed in wear tests and in plant exposures. As the top coatings had different temperature characteristics, different top coatings were exposed in different positions in the plant.

The wear tests indicate that wear at room temperature leaves a reasonable share of top coating on the surface of the samples. For the polymeric materials, the share was 50-60% after 10 h wear testing.

In furnace exposures, the PTFE-based top coating exposed in lower temperature areas shows the best behaviour in terms of coverage after exposure. No high temperature exposed top coatings could be detected after exposure. In the low-temperature areas, the amount of deposit was generally low. If the samples exposed in the low-temperature areas were compared with reference samples or surrounding tubes, no difference in deposit amount could be observed after exposure. In the high temperature regions, where the amount of deposit is much higher, there were signs that possibly the graphite based material had somewhat less deposit. Unfortunately, these samples were not photographed before demounting and the reduced amount is only an indication.

It is suggested that further research should be focused towards other top coatings especially in the high temperature areas where the deposit amount is substantial.